Irinotecan:

From Clinical Pharmacokinetics

to Pharmacogenetics

Cover design: E.J.M. Mathijssen-Schneijderberg and A.H.J. Mathijssen

Lay-out: A.H.J. Mathijssen
Printed by: [Optima] Grafische Communicatie, Rotterdam

ISBN: 90-9016161-9

Publication of this thesis was financially supported by:
Aventis Pharma BV (main sponsor), and GlaxoSmithKline BV and Ortho Biotech and AstraZeneca BV

Irinotecan: From Clinical Pharmacokinetics to Pharmacogenetics

Irinotecan: van klinische farmacokinetiek naar farmacogenetica

PROEFSCHRIFT

ter verkrijging van de graad van doctor aan
de Erasmus Universiteit Rotterdam
op gezag van de Rector Magnificus
Prof.dr.ir. J.H. van Bemmel
en volgens besluit van het College voor Promoties

De openbare verdediging zal plaatsvinden
op woensdag 6 november 2002 om 15.45 uur

door

Adrianus Henricus Josephus Mathijssen
geboren te Ulvenhout

PROMOTIECOMMISSIE

Promotor:	Prof.dr. J. Verweij
Overige leden:	Prof.dr. G. Stoter
	Prof.dr. H.A.P. Pols
	Prof.dr. J.H.M. Schellens
Copromotor:	Dr. A. Sparreboom

Het begin van mijn laatste dagen
zal stil zijn
en doorzichtig als een bloemblad

Gabriël Smit

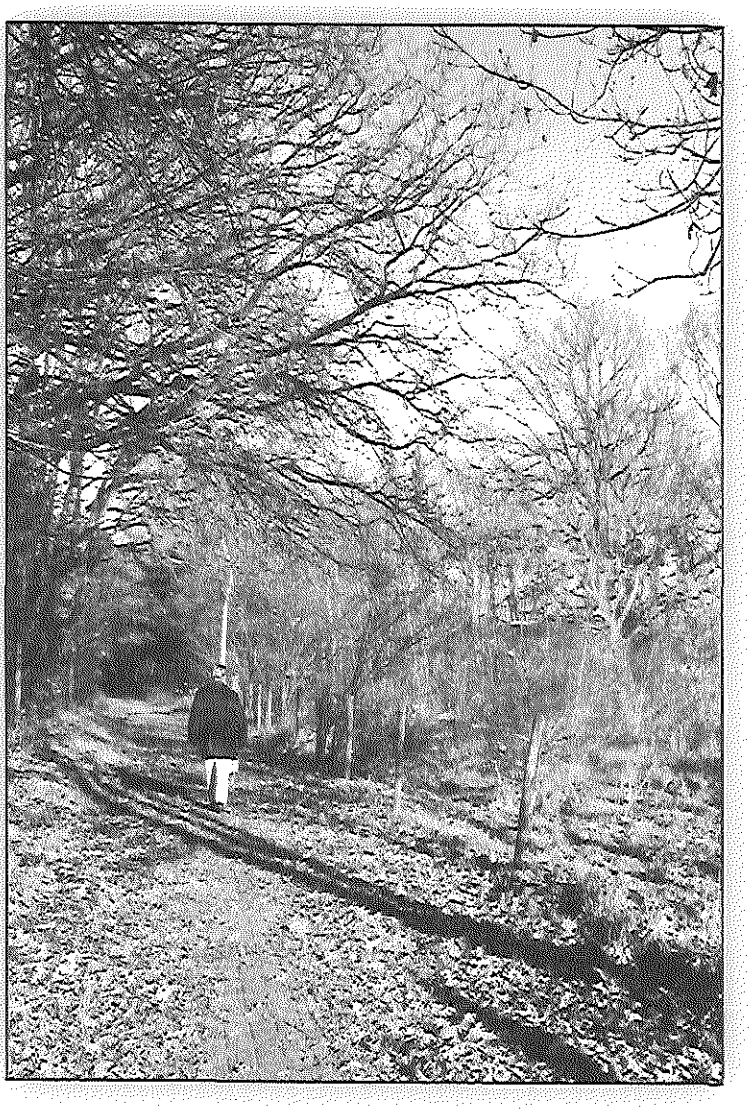

in herinnering aan
Emmy Mathijssen-Schneijderberg

CONTENTS

Chapter One

General Introduction to the Thesis

Four decades ago, a plant alkaloid was isolated from the Chinese tree *Camptotheca acuminata* (Nyssaceae family), which showed promising antitumor activity *in vitro* (1). At that moment, a relatively new class of anticancer agents was born. Unfortunately, during clinical trials, this alkaloid, called camptothecin (CPT), showed severe and unpredictable side effects (myelosuppression, diarrhea, and hemorrhagic cystitis), which were unmanageble during this early chemotherapeutic era (2-4). Later on, the drug's relative lack of hydrophility was found to be the main reason for these adverse events.

Despite this "false start", renewed interest in this compound was found after the elucidation of its mechanism of action during the mid-1980s (i.e the inhibition of topoisomerase I; ref. 5-7). Topoisomerase I is an essential enzyme in DNA replication and RNA transcription and is present in all eukaryotic cells (8). In the physiologic state of the cell nucleus, DNA is double-stranded, super-coiled and fits tightly into a chromosome. To synthesize new DNA, this topological constrained DNA should unwind. To this end, topoisomerase I binds to the DNA, forms a covalent reversible adduct (which is called the cleavable complex), cleaves a phosphodiester bond and a single-strand break occurs (6). Next, the DNA molecule is able to rotate freely around its intact single strand, and relaxation of DNA takes place. After the religation of the cleavage, the enzyme dissociates from DNA. The cleavable complex usually binds for a short period, just to allow the single strand to unwind (9, 10). CPT induces the stabilization of the cleavable complexes (11, 12), what will lead to a disruption of the DNA-strand when the replication fork meets the cleavable complex (7). This double-strand break will lead to the activation of apoptosis pathways and ultimately result in cell-death (7).

In subsequent years, various derivatives of CPT with improved water solubility have been developed, of which irinotecan (CPT-11) was considered to be among the most promising ones (13). It is a semisynthetic water-soluble prodrug, with minor intrinsic cytotoxic activity. After administration, the drug is partially converted into the 100- to 1,000-times more active metabolite SN-38 by the enzyme carboxylesterase (14-17). In the liver, SN-38 is de-toxified by uridine-diphosphate glucuronosyltransferase 1A isoforms, whereby SN-38-glucuronide is formed (18). All these compounds can be secreted into the bile by specific transporters (19). In the intestines, several bacteria produce β-glucuronidase, which enables re-activatation of the glucuronidated form of SN-38 (20). Relatively high concentrations of SN-38 will lead to damage of the bowel mucosa, which results in one of the drug's most prominent side effects: diarrhea (21). In addition, irinotecan can also be oxidated by cytochrome P450 isozymes (22, 23), which will lead to the formation of several inactive metabolites, including APC and NPC.

The pharmacokinetics of irinotecan become even more complex, as CPT analogs exists in two structurally different forms (24). In the lactone form, the pharmacologically active α-hydroxy-δ-lactone ring is closed, while in the carboxylate form this ring is opened and the molecule looses its activity. Between both forms of irinotecan, a pH and protein-dependent equilibrium exists, with the carboxylate form predominating at equilibrium in human plasma.

Although much is known about the way the drug behaves, patients still react very diverse to the therapy. The pharmacokinetics of irinotecan and SN-38 between patients may vary greatly (25). Also, some patients have little or no side effects, while in others these are very severe/ life-threatening (13). In addition, in some patients there is a clearly measurable antitumor effect, while in others therapy with irinotecan will be not effective at all. As irinotecan is currently one of the most important chemotherapeutic drugs in the first-line treatment of colorectal cancer, in combination with 5-fluorouracil and folinic acid (26), it is imperative to identify the causes of the interindividual variability of drug effects. To achieve this, individual patterns in pharmacokinetics and pharmacodynamics should be further investigated, and find the most prominent factors which influence the disposition of irinotecan.

In this thesis, "*Irinotecan: From Clinical Pharmacokinetics to Pharmacogenetics*", we first provide an overview of the pharmacokinetics of irinotecan, then evaluate pharmacokinetic-pharmacodynamic relationships for this agent using different techniques, and finally focus on a variety of factors (including dosing strategies, effects of co-medication, and the influence of genetic constitution of the patient), which may have relevance for future use of irinotecan in clinical practise.

REFERENCES

1. Wall ME, Wani MC, Cook CE, Palmer KH, McPhail AT, Sim GA. Plant antitumor agents. I. The isolation and structure of camptothecine, a novel alkaloidal leukemia and tumor inhibitor from *Camptotheca Acuminata*. J Am Chem Soc 88: 3888-3890, 1966
2. Muggia FM, Creaven PJ, Hansen HH, Cohen MH, Selawry OS. Phase I clinical trial of weekly and daily treatment with camptothecin (NSC-100880): correlation with preclinical studies. Cancer Chemother Rep 56: 515-521, 1972
3. Moertel CG, Schutt AJ, Reitemeier RJ, Hahn RG. Phase II study of camptothecin (NSC-100880) in the treatment of gastrointestinal cancer. Cancer Chemother Rep 56: 95-101, 1972
4. Schaeppi U, Fleischman RW, Cooney DA. Toxicity of camptothecin (NSC-100880). Cancer Chemother Rep 3 5: 25-36, 1974
5. Hsiang YH, Hertzberg R, Hecht S, Liu LF. Camptothecin induces protein-linked DNA breaks via mammalian DNA topoisomerase I. J Biol Chem 260: 14873-14878, 1985
6. Hsiang YH, Liu LF. Identification of mammalian DNA topoisomerase I as an intracellular target of the

anticancer drug camptothecin. Cancer Res 48: 1722-1726, 1988
7. Hsiang YH, Lihou MG, Liu LF. Arrest of replication forks by drug-stabilized topoisomerase I DNA cleavable complexes as a mechanism of cell kiling by camptothecin. Cancer Res 49: 5077-5082, 1989
8. Pommier Y. Eukaryotic DNA topoisomerase I: Genome gatekeeper and its intruders, camptothecins. Sem Oncol 23: 3-10, 1996
9. Takimoto CH, Arbuck SG. The camptothecins. Cancer Chemother and Biother 2nd edition (BL Chabner and DL Longo, editors): 463-484, 1996
10. Rothenberg ML. Topoisomerase I inhibitors: Review and update. Ann Oncol 8: 837-855, 1997
11. Jaxel C, Capranico G, Kerrigan D, Kohn KW, Pommier Y. Effect of local DNA sequence on topoisomerase I cleavage in the presence or absence of camptothecin. J Biol Chem 266: 20418-20423, 1991
12. Tanizawa A, Kohn KW, Pommier Y. Induction of cleavage in topoisomerase I c-DNA by topoisomerase I enzymes from calf thymus and wheat germ in the presence and absence of camptothecin. Nucleic Acids Res 21: 5157-5166, 1993
13. Vanhoefer U, Harstrick A, Achterrath W, Cao S, Seeber S, Rustum YM. Irinotecan in the treatment of colorectal cancer: clinical overview. J Clin Oncol 19: 1501-1518, 2001
14. Rivory LP, Bowles MR, Robert J, Pond SM. Conversion of irinotecan to its active metabolite, 7-ethyl-10-hydroxycamptothecin (SN-38), by human carboxylesterase. Biochem Pharmacol. 52: 1103-1111, 1996
15. Guichard S, Terret C, Hennebelle I, et al. CPT-11 converting carboxylesterase and topoisomerase activities in tumour and normal colon and liver tissues. Br J Cancer 80: 364-370, 1999
16. Humerickhouse R, Lohrbach K, Li L, Bosron WF, Dolan ME. Characterization of CPT-11 hydrolysis by human liver carboxylesterase isoforms hCE-1 and h-CE-2. Cancer Res 60: 1189-1192, 2000
17. Khanna R, Morton CL, Danks MK, Potter PM. Proficient metabolism of CPT-11 by a human intestinal carboxylesterase. Cancer Res 60: 4725-4728, 2000
18. Iyer L, King CD, Whitington PF et al. Genetic predisposition to the metabolism of irinotecan (CPT-11). Role of uridine glucuronosyltransferase isoform 1A1 in the glucuronidation of its active metabolite (SN-38) in human liver microsomes. J Clin Invest 101, 847-854, 1998
19. Chu X-Y, Kato Y, Ueda K, et al. Biliary excretion mechanism of CPT-11 and its metabolites in humans: involvement of primary active transporters. Cancer Res 58: 5137-5143, 1998
20. Sperker B, Backman JT, Kroemer HK. The role of β-glucuronidase in drug disposition and drug targeting in humans. Clin Pharmacokinet 33: 18-31, 1997
21. Abigerges D, Chabot GG, Armand JP, et al. Phase I and pharmacologic studies of the camptothecin analog irinotecan administered every 3 weeks in cancer patients. J Clin Oncol 13: 210-221, 1995
22. Haaz MC, Rivory LP, Riche C, Vernillet L, Robert J. Metabolism of irinotecan (CPT-11) by human hepatic microsomes: participation of cytochrome P-450 3A and drug interactions. Cancer Res 58: 468-472, 1998
23. Santos A, Zanetta S, Cresteil T, et al. Metabolism of irinotecan (CPT-11) by CYP3A4 and CYP3A5 in humans. Clin Cancer Res 6: 2012-2020, 2000
24. Hertzberg RP, Caranfa MJ, Holden KG, et al. Modification of the hydroxy lactone ring of camptothecin: inhibition of mammalian topoisomerase I and biological activity. J Med Chem 32: 715-720, 1989
25. Sparreboom A, de Jonge MJA, de Bruijn P, et al. Irinotecan (CPT-11) metabolism and disposition in cancer patients. Clin Cancer Res 4: 2747-2754, 1998

26. Saltz LB, Cox JV, Blanke C, et al. Irinotecan plus fluorouracil and leucovorin for metastatic colorectal cancer. Irinotecan Study Group. N Engl J Med 343: 905-914, 2000

Chapter Two

Clinical Pharmacokinetics and Metabolism of Irinotecan (CPT-11)

Clinical Cancer Research, 7: 2182-2194, 2001

Ron H.J. Mathijssen
Robbert J. van Alphen
Jaap Verweij
Walter J. Loos
Kees Nooter
Gerrit Stoter
Alex Sparreboom

Department of Medical Oncology, Erasmus MC - Daniel den Hoed
Rotterdam, The Netherlands

ABSTRACT

CPT-11 belongs to the class of topoisomerase I inhibitors, and it acts as a prodrug of SN-38, which is approximately 100 to 1000-fold more cytotoxic than the parent drug. CPT-11 has shown a broad spectrum of antitumor activity in preclinical models as well as clinically, with responses observed in various disease types including colorectal, lung, cervical and ovarian cancer. The pharmacokinetics and metabolism of CPT-11 are extremely complex, and have been the subject of intensive investigation in recent years. Both CPT-11 and SN-38 are known in an active lactone form and an inactive carboxylate form, between which an equilibrium exists that depends on the pH and the presence of binding proteins. CPT-11 is subject to extensive metabolic conversion by various enzyme systems, including esterases to form SN-38, UGT1A1 mediating glucuronidation of SN-38, as well as CYP3A4 which forms several pharmacologically inactive oxidation products. Elimination routes of CPT-11 are also depending on the presence of drug-transporting proteins, notably P-glycoprotein and cMOAT, present on the bile canalicular membrane. The various processes mediating drug elimination, either through metabolic breakdown or excretion, likely impact substantially on interindividual variability in drug handling. Strategies to individualize CPT-11 administration schedules based on patient differences in enzyme or protein expression or by co-administration of specific agents modulating side effects are underway, and may ultimately lead to more selective chemotherapeutic use of this agent.

INTRODUCTION

Camptothecin, a plant alkaloid isolated from *Camptotheca acuminata* (family Nyssaceae), was first discovered in the early 1960s (1). Due to severe and unpredictable side effects of camptothecin in early clinical studies, the clinical development was halted in the 1970s (2-5). It was later revealed that the water-insolubility of camptothecin was an important factor mediating the unpredictable toxic effects (6). The elucidation of the mechanism of action of camptothecin, viz. inhibition of topoisomerase I, a nuclear enzyme which relaxes torsionally strained (super coiled) DNA (7-9), resulted in renewed interest in this agent, and subsequently, numerous derivatives have been synthesized and tested clinically (10-12). Some of these agents, including CPT-11 (13), topotecan (14), 9-aminocamptothecin and 9-nitrocamptothecin (15-17), lurtotecan (GI147211, GG211) (18), and DX-8951f (19), have a broad spectrum of antitumor activity both *in vitro* and *in vivo*, and show more

predictable and clinically-manageable toxicities than the originally isolated structure. Two of these agents, topotecan and CPT-11, have recently been introduced into clinical practice for the treatment of ovarian and colorectal cancer, respectively. Of the currently available camptothecin analogs, CPT-11 has an extremely complex pharmacological profile, which is dependent on a host of enzymes involved in metabolic transformation and active transport proteins, regulating intestinal absorption and hepatobiliary secretion mechanisms (Fig. 1).

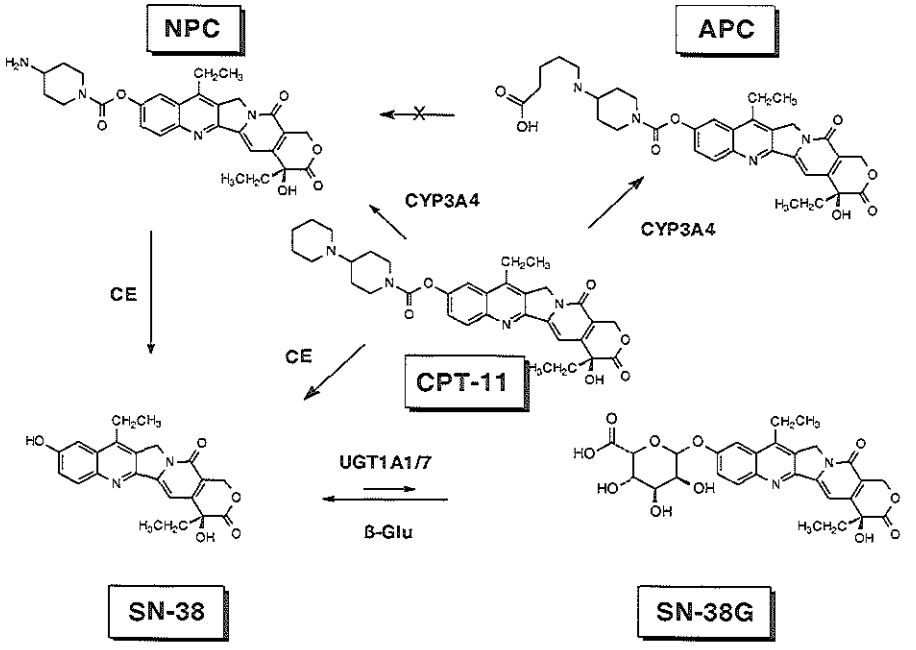

Figure 1. Metabolic pathways of CPT-11 showing carboxylesterase (CE)-mediated formation of the active metabolite SN-38, and its subsequent conversion to a glucuronide derivative (SN-38G) by UGT1A1 and UGT1A7 isoforms, with deglucuronidation by intestinal ß-glucuronidase (ß-Glu). CPT-11 can also undergo CYP3A4-mediated oxidative metabolism to form APC and NPC, of which the latter can be hydrolyzed by CE to release SN-38.

Furthermore, CPT-11 is chemically unique because of the presence of a bulky side chain on the core structure, the enzymatic cleavage of which is a requirement for

pharmacological activity. In addition, CPT-11 is known in two distinguishable forms, an active α-hydroxy-δ-lactone ring form and an inactive carboxylate form, between which a pH-dependent equilibrium exists (12), which significantly impacts on the compound's kinetic profile. In recent years, a wealth of information has become available that has substantially aided in our understanding of the clinical actions of this agent. Here, we will review the clinical pharmacokinetic properties of CPT-11 and its metabolites that appear to be crucial for optimal anticancer chemotherapeutic use.

PHARMACOKINETIC PROPERTIES

Plasma Disposition

The plasma pharmacokinetics of CPT-11 in humans has now been addressed in several studies, and taking into account that these data are from different laboratories, the results are fairly comparable. Most of the initial studies have been performed with the drug administered as a short i.v. infusion (0.5-1.5 h). Following such administration, peak plasma concentrations were reached at the end of infusion (20-36), with a rapid decrease thereafter as a result of multiple distribution and elimination pathways (32, 36). A rebound peak in the concentration-curve has been noticed in some studies (22, 26, 31, 36), and was initially ascribed to enterohepatic recirculation (22, 26). More recently, it has been suggested that this phenomenon is related to substantial uptake of CPT-11 lactone by erythrocytes and its subsequent release followed by accumulation of the carboxylate form in the plasma compartment (37). Equilibrium between the two drug forms is rapidly established and in contrary to CPT-11, the principal metabolite SN-38 predominates in its active lactone form (33, 34). The lactone form of SN-38 accounts for approximately 60-70% of total plasma SN-38 after the end of a CPT-11 infusion, declining to of 33-66% at equilibrium (23, 33). The mean lactone to total AUC ratio of SN-38 is high, being approximately 64%, albeit with large interpatient variability (23, 24, 33, 34, 38). This ratio remains constant for the whole dose range measured. Examples of concentration-time profiles for the lactone and carboxylate forms of CPT-11 and SN-38 are shown in Fig. 2.

The peak concentration of CPT-11 appears to be dose-proportional in a large dose range (100-750 mg/m^2), although substantial interpatient variability has been noted (21-23, 25, 26, 39, 40). This variability increases at later time-points (41). CPT-11 systemic exposure or area under the plasma concentration-time curve (AUC) also increases in a dose-independent way at doses ranging from 33-180 mg/m^2 (24-26, 39, 40, 42), indicating linear pharmacokinetics.

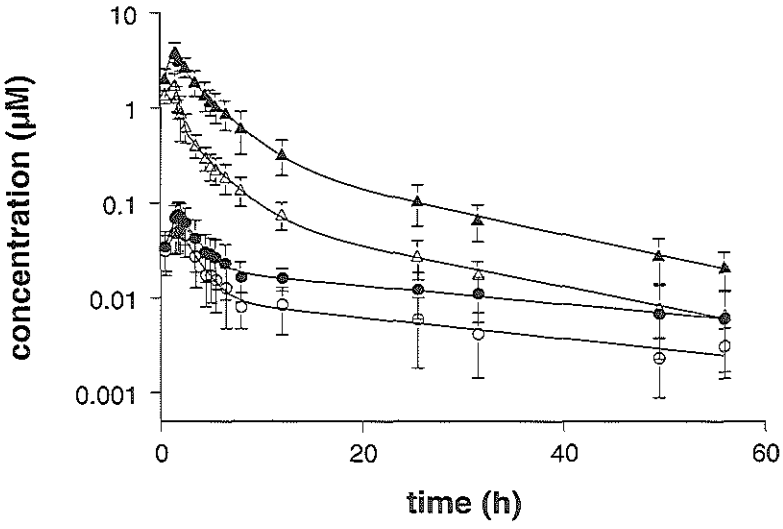

Figure 2. Plasma concentration-time profiles of the lactone (open figures) and total drug (i.e., lactone plus carboxylate, closed figures) forms of CPT-11 (triangles) and SN-38 (circles) in a group of 17 patients receiving CPT-11 at 200 mg/m^2 as a 90-min i.v. infusion. All pharmacokinetic curves were fit to a 3-exponential equation, using Siphar version 4.0 (InnaPhase, Philadelphia, PA), assuming a three-compartmental model for distribution and elimination of the compounds. Data are presented as mean values ± standard deviation. Data were obtained from Mathijssen *et al.* (38).

The ratio of the lactone to total AUC remains relatively constant over the entire dose range of CPT-11, with mean values ranging from 34±5% up to 44±4% (33, 34). The conversion of the lactone into the carboxylate form of CPT-11 is rapid, with a mean half-life of 9.5 min (34). The plasma profiles of the two forms of CPT-11 are comparable, and can best be fitted in a bi- or tri-exponential equation (22, 25, 43), with mean terminal half-life values of about 9.3-14.2 h (22, 25, 35). More recently, it has been suggested that the terminal disposition half-life of CPT-11 is much longer, which may be related to the fact that prolonged sampling schedules were applied in combination with a highly sensitive detection method (20, 43).

The volume of distribution at steady state of CPT-11 is large, suggesting extensive tissue distribution, and remained unchanged with an increase in dose (20, 22, 24, 31). Similarly, the total plasma clearance of CPT-11 was found to be dose-independent, with a value of 13.5±3.5 L/h/m^2 for the total drug (i.e., lactone plus carboxylate forms) and 45.6±10.8 L/h/m^2 for the lactone form (35). The clearance is unaltered during repeated cycles, despite a mean interpatient variability of approximately 30% (21, 35), and an intra-patient variability of approximately 13.5%.

Plasma Protein Binding

An important factor in the pharmacology of drugs is its binding to plasma proteins. In accordance with the hydrophilic nature of CPT-11, in blood, 80% of the drug is mainly bound to, and/or localized in erythrocytes, whereas SN-38 is bound for at least 99%, mainly to albumin and lymphocytes, but also to erythrocytes and neutrophils (44). Although binding to plasma proteins appears to be of subordinate importance for CPT-11, binding of the principal metabolite SN-38 to plasma proteins in adults and pediatric patients is thus substantial, and independent of (pre-therapy) serum albumin levels (~94 to 96%) (44-46). In the presence of albumin, the lactone forms of CPT-11 and SN-38 are more stable (47), with higher percentages of the lactone forms available, compared with the situation without this protein. The protein binding is not significantly different for the lactone and carboxylate form of CPT-11. In contrast, SN-38 lactone binds significantly stronger to albumin than its corresponding carboxylate form, which could explain the better stability of SN-38 in vivo, compared with CPT-11 (47). This, in turn, may play a role in the differential terminal disposition half-lives and volumes of distribution between these molecules. In in vitro incubations in the presence of human serum albumin, the apparent half-life of the interconversion of CPT-11 is more than 3 times higher than that in patients (34). This suggests that there is an early preferential uptake and/or metabolism of the lactone form of CPT-11, thereby altering the ratio of CPT-11 lactone versus carboxylate (34).

METABOLISM

Several studies have shown that hepatic metabolism and biliary secretion are major pathways of CPT-11 elimination in both animals and humans, with major contributions from various classes of enzymes, including CEs, UGTs, CYP3As, and ß-glucuronidases.

Esterases-Mediated Biotransformation

The conversion of CPT-11 to SN-38 through cleavage of the ester-bond at C10 by CEs has been studied extensively in recent years. Two human isozymes of liver CE, viz. hCE-1 and hCE-2, have been characterized that might catalyze this conversion (48, 49). No tumor reduction in SQ20b cells was seen after incubation of CPT-11 with hCE-1, compared with a 60% reduction for hCE-2 (49). Therefore, hCE-2 probably plays the most important role in CPT-11 conversion by CEs in cancer patients. The plasma of several species, including mouse and horse, contains high levels of esterases other than CE and it converts CPT-11 much better into SN-38 than human plasma does. It has been suggested that butyrylcholinesterase, which has CPT-11 converting activity, might be responsible for this phenomenon (50, 51).

SN-38 concentrations have been shown to increase with the CPT-11 dose over the dose range studied (100-750 mg/m^2) (35). The terminal disposition half lives of SN-38 lactone and total drug are significantly longer than those of CPT-11 (38, 43). In an *in vitro* study of human liver microsomes, twice as much SN-38 was formed when CPT-11 was present in its lactone form in comparison with CPT-11 in its carboxylate form (52). As CPT-11 lactone is converted easier, this phenomenon might contribute to the predominance of SN-38 in its lactone form in plasma (52).

A clear relationship between CE levels and the chemosensitivity of proliferating tissues and cell lines in general has been suggested (53-55). CPT-11 was significantly more active in five human small-cell lung cancer cell lines than in four non-small cell lung cancer cell lines, and this was attributed to a higher CE activity in the former case (55). CPT-11-converting CE activity in human tumors has also been studied *in vivo* (56). A wide range of variability in enzyme activity in primary colorectal tumors was seen, with no significant difference between primary and secondary tumors. Relatively high CE activity in these tumors, as compared with normal liver tissue has been noticed, which might suggest a local activation of CPT-11 in tumor tissues (56). There were no significant differences between enzyme activity in human liver and colon tissues.

Selective upgrading of CE levels in tumors, thereby producing tumor-specific activity may clearly have substantial clinical implications; it will maximize the exposure of tumors to SN-38 and limit systemic drug concentrations and therefore also limit adverse effects of CPT-11. This upgrading has been studied for several enzyme/prodrug combinations, using antibodies or viruses to attack tumor cells. For the CE/CPT-11 combination, a recombinant replication deficient adenovirus vector coding for human CE cDNA has been developed (57). This vector effectively suppressed A549 cell growth *in vitro* in the presence of CPT-11 by 7 to 17-fold. As SN-38 diffuses from the tumor cell in which it has been produced to its neighbor cells in

growth suppressive concentrations, only 10% of the A549 cells need to be infected for a cytotoxic effect in 48% of the cells (57). In CPT-11-resistant A549 cells, which had a 6-fold resistance and 42% CE activity compared with normal A549 cells, functional CE expression could be accomplished by infection with this vector (57, 58), and these resistant cells could be suppressed efficiently *in vitro* and *in vivo* (58). This sensitivity has also been described for 2 other human tumor cell lines, although in another 8 human cell lines only a minimal effect was seen (59).

In various studies, the activity of CE isozymes from animal species has been compared with the human enzyme(s), and the latter show consistently lower activity than those of the other species investigated (60, 61). Although the active site amino acids of rabbit and human CE are almost identical, human CE converts CPT-11 100 to 1000-fold less efficiently (59). In Rh30 human rhabdomyosarcoma cells, expression of the rabbit enzyme was associated with more rapid tumor regression and a better prevention of tumor recurrence *in vitro* (59, 62). In addition, immune-deprived mice, carrying rabbit CE expressing Rh30 cells, were more sensitive to CPT-11 than human CE expressing cells or control cells. No recurrent tumors occurred in the rabbit-enzyme group, in contrast to 29% and 100% recurrence in the two other groups, respectively (59). The clinical utility of this approach is currently under further investigation.

UGT-Mediated Biotransformation

SN-38 itself is further metabolized in human liver by UGT1A1 to an inactive compound, SN-38G (63-65). The lactone functionality of SN-38G could also be hydrolyzed following a pH-dependent equilibrium (65). Mostly, the plasma concentrations of SN-38G are related to SN-38 plasma concentrations, with peak values at approximately 1.2 hours (range, 15 min to 4.5 hours) after the end of infusion (31, 43, 66). SN-38G concentrations increase linearly with the administered CPT-11 dose, suggesting that hepatic glucuronidation is not saturated in the dose ranges studied (up to 600 mg/m^2) (36, 42). The AUC of SN-38G is about 7-fold higher than that of SN-38, suggesting extensive glucuronidation of SN-38 into SN-38G (32, 66), with high interpatient variability (41).

Considerable variation in the conversion of SN-38 into SN-38G in human liver cells has also been noticed *in vitro* (63). This may be due to different enzyme activities of the various UGT isoforms. Two distinct gene families of UGT enzymes exist, UGT1 and UGT2, which are both being sub-classified into several isoforms. Results obtained from transfection studies have shown that isoform UGT1A1 is primarily responsible for the SN-38 conversion (63), although it was shown more recently that isoform 1A7 is about 21-fold more efficient at physiological pH than UGT1A1 (67).

A genetic polymorphism has been reported in the TATA box sequences of UGT1A1 (68). Normally, the box contains $(TA)_6TAA$ in its promotor region, and sometimes a box contains an extra TA repeat (68, 69). An extra TA repeat in the TATA box has been associated with Gilbert's syndrome (70). The metabolic ratio (SN-38/SN-38G) for these patients is significantly higher compared with the common genotype, suggesting less SN-38 glucuronidation capacity (69). In addition, it has been reported that in patients with the Crigler-Najjar type I syndrome, UGT1 activity is totally lacking (63, 71, 72). As a result, SN-38 can not be inactivated adequately into SN-38G and therefore patients with these disorders are at increased risk for severe CPT-11-induced toxicity (63). Based on the relative importance of the systemic glucuronidation and the existence of genetic polymorphism, it has been proposed that UGT1A1 genotyping might be an approach to individualize CPT-11 treatment schedules (68, 73).

A significant correlation was recently observed between SN-38 glucuronidation rates and bilirubin glucuronidation by human liver microsomes (63). Interestingly, UGT1A1 is the isozyme that also conjugates bilirubin (72). Also for bilirubin glucuronidation an inverse correlation between glucuronidation rate and number of TA repeats has been reported (68-70). It has been shown subsequently that baseline values of unconjugated bilirubin correlate significantly with both neutropenia and the AUCs of CPT-11 and SN-38, and this relationship might thus be useful in individual dose prescription or adaptation (72). No relationship has been observed between the glucuronidation of SN-38 and that of para-nitrophenol, which is glucuronidated by several UGTs, including UGT1A1 (63). An intriguing observation has been that valproic acid, an inhibitor of glucuronidation, given 5 min before CPT-11 in rats, caused 99% inhibition in SN-38G formation (74), resulting in a mean increase in SN-38 AUC of 270%. Pretreatment with phenobarbital, an inducer of UGT, resulted in a 72% enhancement in the AUC of SN-38G, with a concomitant reduction in the AUCs of CPT-11 and SN-38 of 31% and 59%, respectively (74). These findings are consistent with data indicating that a patient with Gilbert's syndrome could be treated successfully with simultaneous administration of CPT-11 and phenobarbital (31). CPT-11 and SN-38 were formed in concentrations comparable to those achieved in normal patients, although the AUC of SN-38G appeared to be substantially altered (31).

In human lung cancer cell lines, the role of SN-38 glucuronidation in cytotoxicity profiles has been studied extensively (75). PC-7/CPT cell lines showed an increased glucuronidation in comparison to normal PC-7 cells and when UGT activity was inhibited, the cells became more sensitive to SN-38. Thus, an up-regulation of the UGT activity may lead to SN-38 resistance in the tumor (75). BCRP or mitoxantrone-resistance half-transporter (MXR) expression was also found to result in 400 to 1000-fold resistance to SN-38 as compared with parental cell lines (76). As MXR-cells were

highly capable to efflux drugs that are susceptible to glucuronidation, UGT activity in resistant and normal cell lines were compared. In resistant cells higher SN-38G levels were seen than in normal cells. Thus, in cancer cells glucuronidation might contribute to drug resistance, but the lack of high UGT levels in resistant MXR-cells suggests that BCRP alone is sufficient to induce drug resistance patterns (76).

CYP3A-Mediated Biotransformation

Recently, other quantitatively important metabolites of CPT-11 have been identified, the formation of which is dependent of CYP3A. Of these, APC is a major metabolite detectable in plasma, and is formed by a CYP3A-mediated oxidation of the distal piperidine group at C10 of CPT-11 (77-79). NPC is also formed through this pathway, by cleavage of the distal piperidino group of CPT-11 (77, 79-82). APC peaks at about 2 hours after the end of infusion, and AUC values increase linearly with increasing CPT-11 dose, despite important inter-patient variation (36). At equimolar concentrations (as compared to CPT-11), APC did not inhibit the conversion of CPT-11 into SN-38 (83).

Similar to CPT-11, APC shows little cytotoxic activity, although it has some inhibitory effect on acetylcholinesterase, an enzyme involved in the acute cholinergic syndrome observed directly following CPT-11 administration (83). Likely, APC does not contribute directly to the total activity and toxicity following CPT-11 administration *in vivo*, as it shows minor antitumor activity *in vitro* compared to SN-38 and less toxicity compared to CPT-11. NPC is also a poor inhibitor of cell growth and a poor inducer of topoisomerase-I-DNA cleavable complexes, with less antitumor activity in cell lines than CPT-11 (80, 84). In addition, formation of APC and NPC is unlikely to take place in human (colorectal) tumors where CYP3A levels are generally very low (85). It is of particular interest, though, that human liver microsomes and human liver CE are able to hydrolyze NPC into SN-38 though still to a lesser extent than CPT-11 (80, 84), whereas for APC this conversion has not been conclusively demonstrated (80, 86). Nevertheless, patients with high AUCs of SN-38, also had high AUCs of CPT-11 and APC, suggesting that some degree of correlation might be present (36). In addition, NPC can not be formed from APC, in contrast to a formerly suggested conversion (81, 84).

The recognition that CPT-11 is a CYP3A substrate is an important finding, since it makes this agent subject to a host of enzyme-mediated drug interactions, even with commonly prescribed co-medication (81, 87). For example, the prototypical CYP3A inhibitors, ketoconazole and troleandomycine, inhibit the conversion of CPT-11 into APC and NPC almost completely (77-79, 81). In addition, both loperamide and racecadotril inhibit APC and NPC formation by more than 50%, whereas ondansetron

inhibits these formations by 25% and 75% respectively (78, 81). APC and NPC formation correlated significantly with testosterone 6-ß hydroxylation, which is also mediated by CYP3A (78, 81). It has been shown recently, that the subtype CYP3A4 is the main isozyme involved in formation of both APC and NPC (79, 82), although it was suggested previously that cytosolic aldehyde dehydrogenase might also be involved in APC formation (81). CYP3A5 also showed catalytic activity, but neither APC nor NPC were formed in its presence (79, 82). Instead a new (unidentified) metabolite was found (79, 82). As this enzyme is expressed in only 25 to 30% of adult livers, this might explain some of the inter-patient variability in CPT-11 metabolism (82). Preliminary evidence has also been generated indicating that SN-38 might be metabolized by CYP3A4, although the clinical implications of this finding have not yet been evaluated.

ß-glucuronidase-Mediated Biotransformation

When SN-38G is excreted in bile and intestines, several bacteria including *Escherichia coli*, *Bacteroides* species and *Clostridium perfringens* can convert this compound back to the active metabolite SN-38, by producing the enzyme ß-glucuronidase (88-90). Various studies have described (microflora-derived) ß-glucuronidase activity in non-human (91-94) and human intestines (95-97). In rats and athymic mice, within 1 hour after the end of infusion, acute diarrheal symptoms with impaired water absorption and increased PGE_2 levels have been found (92, 93). Histopathological changes in the descending colon, cecum and ileum were observed after the daily administration of CPT-11 (91-93). Recently, these mucosal abnormalities were confirmed in human colon (97). A good correlation between this histological damage and ß-glucuronidase activity in the intestinal lumen has been noticed, while a poor correlation was observed with CE activity (91). The lesser damage found in small intestines compared with damage in colon could be explained by a lower exposure of this tissue to SN-38. This may be due to a smaller amount of ß-glucuronidase in the lumen of small intestines (94).

Because many drugs could affect the functioning of the intestinal bacteria, co-medication may influence the chemotherapeutic treatment of patients with CPT-11 (98). As bacteria producing ß-glucuronidase activity will be killed by antibiotics, it is anticipated that this will lead to a reduction in acute and delayed diarrhea and cecal damage (91). It has been demonstrated that antibiotics had no effects on the plasma concentrations of CPT-11, SN-38 or SN-38G in mice (penicillin/streptomycin) (94), and in humans (neomycin) (99). This combined treatment also resulted in reduced SN-38 concentrations in the intestinal contents with concomitantly increased SN-38G levels (94, 99). A potential approach for modulating CPT-11-induced intestinal toxicity may therefore be to reduce bacterial ß-glucuronidase-mediated deconjugation of SN-38 and

subsequent mucosal destruction. A clinical trial to evaluate the toxicological consequences of pretreatment with neomycin before the administration of CPT-11 is in progress at our institute.

EXCRETION

Several studies have examined the excretion of CPT-11 in bile, feces and urine in animals and humans. In humans, only 52% of the given dose has been recovered using non-radiometric HPLC methods (32, 100), whereas in a recent radiometric study quantitative recovery (95.8±2.7% of radioactivity) was obtained (20). CPT-11 and its 3 most common metabolites (SN-38, SN-38G and APC) were responsible for almost all (~93%) detected material (20).

Urinary Elimination

In urine, CPT-11, APC and SN-38G are the main compounds detected within 24 hours following CPT-11 administration (20, 32), with CPT-11 accounting for about 10-22% of the administered dose, and SN-38 contributing for only 0.18-0.43% (20, 22, 25, 31, 66, 100). Consistent with the highly polar nature of the glucuronic-acid group and increased aqueous solubility, SN-38G may be excreted rapidly by the kidneys (32). The cumulative excretion of APC and NPC was very low, amounting to less than 1% of the dose (32). This suggests that the bulk of CPT-11 and its metabolites is excreted during the first 24 hours after infusion, while assessing urinary recovery of radiolabeled CPT-11 over 196 hours also showed that the excretion was almost complete within 48 hours (Table 1) (20). Similar findings were obtained with daily administration schedules of CPT-11, indicating unchanged urinary excretion profiles (26, 29).

Biliary Secretion

In a few patients CPT-11 and SN-38 concentrations in bile have been measured (20, 24, 25, 100). CPT-11, SN-38 and SN-38G biliary secretion varies between approximately 3-22%, 0.1-0.9% and 0.6-1.1% respectively (100). NPC was also detected in bile at very low concentrations (80). In a female patient, carrying a biliary T-tube and receiving radiolabeled CPT-11, 30.1% of the administered dose was recovered in bile as radioactive compounds (20).

In rats, a cMOAT located on the bile canalicular membrane was shown to be responsible for the transport of CPT-11 carboxylate, SN-38 carboxylate and both SN-38G carboxylate and lactone (101). For CPT-11 carboxylate, cMOAT appeared to be a low affinity transporter, whereas a high affinity transporter is still unknown (102).

Table 1. Cumulative urinary and fecal excretion of CPT-11 and metabolites.

Compound	Urine	Feces	Total
CPT-11	22.4 ± 5.50	32.3 ± 4.47	54.7
SN-38G	3.02 ± 0.77	0.27 ± 0.17	3.29
SN-38	0.43 ± 0.12	8.24 ± 2.51	8.67
APC	2.23 ± 1.53	8.29 ± 2.95	10.5
NPC	0.14 ± 0.08	1.36 ± 0.94	1.50
Total compounds	30.2 ± 6.60	62.0 ± 7.60	92.2
Not extracted	1.25 ± 1.55	9.86 ± 3.77	11.1

Parent drug and metabolite abundance are expressed as percentage of administered dose and were determined by quantitative raiometric high-performance liquid chromatography. Data were obtained from Slatter *et al.* (20).

For SN-38G lactone and carboxylate, cMOAT is the high affinity transporter, while most likely also a low affinity transporter exists, presumably P-glycoprotein. It has also been found that cMOAT transports SN-38G carboxylate more efficiently than its lactone form (102). In humans, the same transport mechanisms by cMOAT of CPT-11 carboxylate, SN-38 carboxylate and SN-38G were found as in rats (see Fig. 3 for a schematic representation) (103).

Cyclosporine, an inhibitor of the biliary secretion (104), and a known substrate and inhibitor of P-glycoprotein (105), significantly increased plasma concentrations of CPT-11, SN-38 and SN-38G in rats (104). At a cyclosporine dose of 60 mg/kg, the AUCs of CPT-11, SN-38 and SN-38G increased 2 to 4-fold. This is most likely the result of reduced renal and non-renal clearance, which simultaneously reduced by 55 and 81%, respectively. Simultaneously, the terminal disposition half-lives of CPT-11 and its metabolites were substantially prolonged. The conversion of CPT-11 into SN-38 was not altered, but the glucuronidation of SN-38 decreased in comparison to CPT-11 infusion without cyclosporine (104). In view of these results, it has been suggested that P-glycoprotein is one of the high affinity transporters of CPT-11 carboxylate (106). However, like P-glycoprotein, also cMOAT function may be inhibited by cyclosporin A, or other substrates and modulators (106). Therefore, inhibition has been studied at various concentrations of CPT-11. As the high affinity component is most active at substrate concentrations of 5 μM, and cMOAT is most active at 250 μM, inhibitors of P-gp and cMOAT were compared at these concentrations. It appeared that

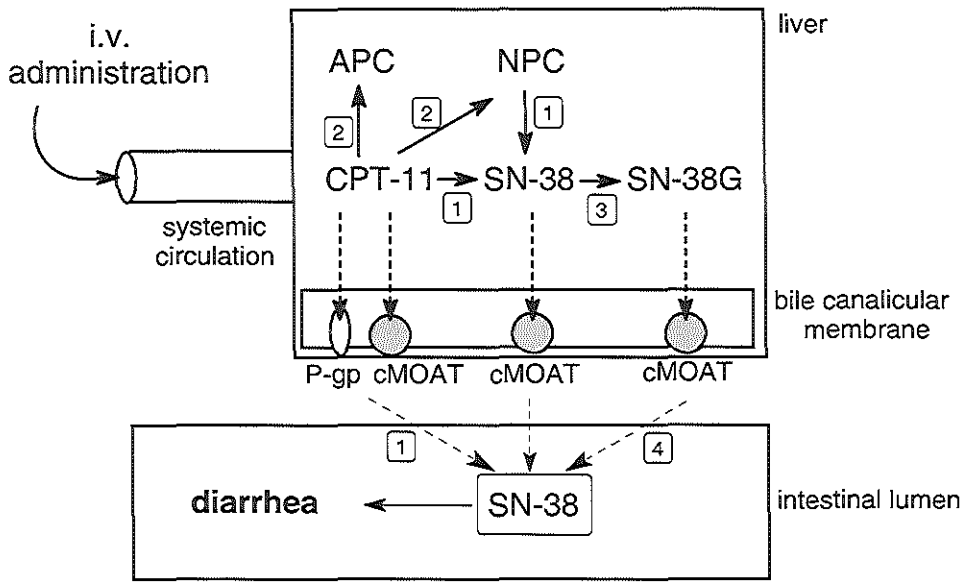

Figure 3. Primary active transport systems for CPT-11 and its metabolites in the bile canalicular membrane of humans indicating the hypothesis for the mechanism of toxicity caused by i.v. administration of CPT-11 [modified from Sugiyama *et al.* (105)].

Abbreviations: **1**, carboxylesterase mediated conversion; **2**, CYP3A-mediated conversion; **3**, UGT1A-mediated conversion; **4**, ß-glucuronidase-mediated conversion.

P-gp substrates or modulators like verapamil, PSC-833 (valspodar) or cyclosporine, inhibited the uptake of CPT-11 carboxylate most at concentrations of 5 µM. This suggests that P-gp might be the high affinity component in CPT-11 carboxylate transport (106).

As an adverse effect, cyclosporine also inhibits bilirubin excretion and this may lead to hyperbilirubinemia (104). In the human Dubin-Johnson syndrome, chronic hyperbilirubinemia is seen as a result of a mutation in the cMOAT gene (107), and variability in the expression of this protein might play a role in the variability in experienced toxicity during CPT-11 treatment (103).

Fecal Excretion

In a mass balance study using radiolabeled CPT-11, fecal excretion was the major route of drug elimination, with 63.7% of the administered drug recovered (20).

The unexpectedly high SN-38 concentrations and relatively low SN-38G concentrations in fecal specimens are suggestive for substantial ß-glucuronidase activity in human intestinal contents, and consequently, the SN-38/SN-38G ratio was relatively high in all patients (20, 32). SN-38, APC and NPC are mainly excreted in feces; 2.5% and 1.7% for SN-38 and NPC, respectively (32).

CONSIDERATIONS OF SCHEDULE AND ROUTE OF ADMINISTRATION

Despite all kinds of dosing schedules, the total CPT-11 dose that can be tolerated in any time period is the same (23-25). Prolonged infusion times might theoretically improve the efficacy of CPT-11, as cytotoxicity of topoisomerase-I inhibitors is S-phase specific (10), although the relevance of this principle for CPT-11, given the prolonged terminal disposition half-life of SN-38, is unclear. From xenograft models it was known that low-dose protracted schedules of CPT-11 administration were more effective and less toxic than the usual higher dosed short infusion periods (108, 109). Chronic low-dose exposure of CPT-11 in patients has been studied recently (29, 39, 45, 110, 111), and revealed that the AUC ratios of lactone to total drug for CPT-11 and SN-38 were in the same range as for the shorter infusion periods (29). The maximal and recommended tolerated doses in these studies, 10 to 30 mg/m^2/day, are much lower for the prolonged infusions than for the shorter durations. Surprisingly, the SN-38 AUC levels reach similar values as compared to those of the shorter infusion periods, presumably reflecting saturation of enzymatic biotransformation with the latter schedules (29, 39, 45, 110).

Oral Administration

Clearly, the availability of a suitable oral formulation of CPT-11 would allow more convenient use of prolonged dosing schedules. When human liver and intestine S9 fractions were incubated with CPT-11, the agent was mostly hydrolyzed into SN-38 by liver, duodenal, jejunal and ileal fractions and less by colonal and rectal fractions (91, 112). Since it has been discovered that CEs are widely expressed in the human liver and gastro-intestinal tract, it may be possible to effectively administer CPT-11 orally (112, 113), with the knowledge that substantial presystemic metabolism could take place. The low pH-value of the stomach may be favorable for the retention of CPT-11 in its lactone form (113).

Oral administration of CPT-11 in mice resulted in peak concentrations of CPT-11 and SN-38 in plasma within 1 hour after administration (114, 115), and the bioavailability of CPT-11 increased with increasing dose and amounted to 10 to 20% (115). In contrast, and of concern, the SN-38 AUC after oral administration did not

correlate linearly with the dose, and in fact even decreased with increasing CPT-11 dose. It has been suggested that saturation of CE might cause this non-linear correlation (115), but the high levels of CE expressed in human intestinal tissues do not render this suggestion very likely (113). The higher SN-38 total to CPT-11 total ratios, compared with i.v. administration, suggest a presystemic CPT-11 conversion (116). Lactone versus carboxylate CPT-11 ratio was comparable with i.v. infusions, but the SN-38 ratio was much higher (113), suggesting a longer persistence of SN-38 lactone when it is given orally. When CPT-11 was given orally to nude mice bearing human tumor xenografts, the agent retained its cytotoxic properties (53). Furthermore, in early clinical trials initial antitumor activity has been observed (113), suggesting that oral CPT-11 might be an attractive therapeutic option for the treatment of several human malignancies.

The uptake rates of [^{14}C]CPT-11 and [^{14}C]SN-38 from hamster intestinal epithelial cells and human colon carcinoma HT29 cells were recently published, providing important insight into the absorption characteristics of these agents (117). The lactone forms of CPT-11 and SN-38 were transported mainly by a passive diffusion, while the carboxylate forms were absorbed as a result of an active transport mechanism. Both compounds were transported significantly more in their lactone form, and the uptake rates showed a clear pH-dependency, as the uptake decreased to 68% when the pH-values were higher than 6.8. Lower SN-38 uptake rates also correlated with lower cytotoxicity (117). It was suggested that raising pH-values in human intestines might decrease the re-absorption of the drug and as a result it will lower the intestinal side effects (117). The clinical utility of this concept is currently under further investigation. Clearly, demonstration of unaltered pharmacokinetics of SN-38 in the presence of intestinal alkalization is of crucial importance. Thus, although these investigators have shown that this concept can reduce CPT-11-induced intestinal toxicity, this may be a pyrrhic victory if a simultaneously altered metabolic clearance (by way of a decreased enterohepatic recirculation of SN-38) results in reduced antitumor activity.

Intraperitoneal Administration

Intraperitoneal (i.p.) administration of CPT-11 has also been studied recently and may have some potential advantages over the i.v. route. It appeared that the therapy was more effective and less toxic in mice bearing C26 colon cancers (118). In mice bearing P388 leukemia ascites, substantially elevated peritoneal AUCs of CPT-11 and SN-38 were found, while the achieved plasma levels were comparable to those after i.v. dosing (118). If the i.p. administration of CPT-11 does not prove to have major local toxicities, this administration pathway might be an asset for the adjuvant therapy of colorectal cancer.

PHARMACOKINETIC-PHARMACODYNAMIC RELATIONSHIPS

Relationships between pharmacokinetic parameters and CPT-11-induced side effects have been studied extensively. For abdominal cramps, nausea, vomiting and anorexia no correlation with any parameter has been found (23). For myelosuppression and diarrhea in relation to the AUCs of CPT-11 and SN-38 respectively, the findings are highly variable and final conclusions can not yet be drawn (Table 2; ref. 21, 29, 45).

The product of the plasma AUC ratio of SN-38 to SN-38G and the plasma CPT-11 AUC (viz., the biliary index) may be an important kinetic variable as it is thought to be correlated with SN-38 bile concentrations (66). Patients with high biliary indices, suggestive of high SN-38 biliary concentrations, in some studies experienced more severe diarrhea (graded 3 and 4 on the National Cancer Institute-Common Toxicity Criteria scale) than those with low biliary indices (31, 66), but this could not be confirmed in other studies (21, 119, 120). It has been hypothesized that consideration of interindividual differences in fecal ß-glucuronidase activity would likely assist in a more accurate prediction of CPT-11-induced intestinal side effects, and may provide a basis to modulate the experienced toxicity (32).

Table 2. Correlation between toxicities and the AUCs of CPT-11 and SN-38.

Observed toxicity	CPT-11 AUC	SN-38 AUC	Refs.
Neutropenia	No	No	26, 29, 40, 45
	No	Yes	23, 39
	Yes	Yes	21, 22, 25, 27
Diarrhea	No	No	21, 23, 29, 45
	No	Yes	40
	Yes	No	26, 39
	Yes	Yes	22, 25, 27

EVALUATION OF DRUG INTERACTIONS

Drug interactions may arise as a result of altered pharmacodynamics or pharmacokinetics of the drugs involved. In the case of pharmacokinetic interactions, this is usually due to modification of tissue disposition and metabolism of the drugs.

These phenomena are of particular importance in cancer chemotherapy when cytotoxic agents are used, because of the increased risks of severe toxicity. Most of the data currently available to evaluate potential drug interactions with CPT-11 come from clinical trials of CPT-11 given in combination with one or more other anticancer agent(s) (Table 3). Although in several cases only limited information is available, some (preliminary) conclusions can be drawn.

Table 3. Evaluation of pharmacokinetic interactions between CPT-11 and anticancer agents.

Combination drug(s)	Dose (CPT-11) (mg/m^2)	Kinetic alterations	Refs.
Carboplatin	5[a] (60)	AUC_{CPT-11} ↓; AUC_{SN-38} ↓	127, 128
Cisplatin	80 (260)	none	32, 119, 120, 124, 125
Cisplatin/Vindesine	100/3.0 (37.5)	none	121, 122
Cisplatin/Ifosfamide	70/1.5 (60)	none	123
Docetaxel	75 (200)	none	135
	70 (250)	none	149
	50 (60)	none	150
Etoposide	80 (80)	none	30
5-Fluorouracil	500(125)	AUC_{CPT-11} ↑; AUC_{SN-38} ↓	130
5-Fluorouracil/ Leucovorin	2600 (80)	none	131, 132, 134
Oxaliplatin	85 (200)	none	148
Paclitaxel	175 (150)	AUC_{CPT-11} ↑; AUC_{SN-38} ↑	136, 137
	75 (50)	none	139
Raltitrexed	3.0 (350)	none	151

[a] Target AUC in mg.min/mL

Pharmacokinetic interaction studies have been performed with cisplatin either given alone or in combination with vindesine (121, 122) or ifosfamide (123), and indicated unaltered disposition profiles of both CPT-11 and its metabolites at any dose level or sequence tested (124-126). Likewise, the pharmacokinetics of carboplatin were not influenced by CPT-11, although in one study, the AUC of both CPT-11 and SN-38 was lower than expected, suggesting increased clearance of CPT-11 when

given together with carboplatin (127, 128). The basis for this apparent change in pharmacokinetic behavior is unknown, although an effect on CYP3A expression due to prior exposure to carboplatin can not be excluded (129).

In a Japanese study, altered pharmacokinetics were also found when 5-fluorouracil was administered immediately after CPT-11 infusion (130). Compared with an earlier CPT-11 monotherapy study conducted by the same group, the AUC of CPT-11 substantially increased while the AUC of SN-38 decreased. An inhibition of CE by 5-FU was suggested to explain these unexpected results (130). Other studies did not find altered pharmacokinetics for this combination therapy or eventually with the further addition of leucovorin (folinic acid) (131-134). The conclusion from the Japanese study has been criticized in view of the large interpatient variation and non-comparable patient populations (134).

Although no comparative pharmacokinetic data are available it has also been suggested that an interaction or sequence-dependent effect is present for the combination of CPT-11 and docetaxel. As both drugs are metabolized by CYP3A, competition might occur when these drugs are given sequentially, and as a result, the clearance of docetaxel might be decreased (135). A significant pharmacokinetic interaction has been observed between CPT-11 and paclitaxel, which is characterized by increased plasma levels of both CPT-11 and SN-38 (136). Similar reactions have also been reported in rats (137), and Cremophor EL, the vehicle used for paclitaxel formulation seems to play a mayor role (104). This type of interaction appears to be related to micellar encapsulation of certain agents in this vehicle, and has also been demonstrated to occur with paclitaxel itself and anthracyclines (138). In any event, because this interaction occurs during the terminal disposition phase of CPT-11, in currently applied dosing schedules the interaction is likely of only minor importance. The combination of weekly administration of CPT-11 with a fixed dose of paclitaxel (75 mg/m^2) indicated that the sequence of drug administration did not affect elimination of CPT-11 (139). There was also no sequence-dependent chemotherapy-related toxicity. To date, no other cytotoxic drug has been shown to affect the pharmacokinetics of CPT-11 or was affected itself by CPT-11.

Anticonvulsants, phenytoin and phenobarbital in particular, are known to induce several metabolic pathways relevant to xenobiotics. CYP3A4, in particular, has increased expression when patients are treated with these compounds. Indeed, a recent study in patients with recurrent or progressive malignant glioma receiving CPT-11 and phenytoin indicated that AUCs of CPT-11, SN-38 and SN-38G were approximately 40%, 25% and 25%, respectively, of those determined previously in patients with metastatic colorectal cancer not receiving antiepileptics (140). Similarly, enzyme-inducing anticonvulsants significantly lowered systemic exposure to CPT-11

importance since it suggests that anticonvulsants thereby largely reduce the potential antitumor effects of CPT-11. In addition to modulation of CYP3A4, another possible explanation for the interaction is the induction of membrane transporters that enhance drug excretion (142).

CONCLUSIONS AND PERSPECTIVES

CPT-11, because of its broad spectrum of antitumor activity, is clearly one of the most important new anticancer drugs developed in the last few decades. The clinical pharmacokinetic behavior of CPT-11 has been explored extensively in recent years, and the generated information has been of fundamental importance in our understanding of the clinical effects of this agent (Table 4).

Table 4. Factors contributing to variability in response to CPT-11.

Parameter	Source of variability	Example(s)
Dose selection	Patient's condition	Performance status
	Host sensitivity	Previous treatments
Systemic exposure	Concomitant drugs	Cyclosporin A (P-glycoprotein inhibitor)
		Valproic acid (UGT1A1 inhibitor)
		Phenobarbital (UGT1A1 inducer)
		Phenytoin (CYP3A4 inducer)
		Ketoconazole (CYP3A4 inhibitor)
	Pharmacogenetics	Gilbert's syndrome (UGT1A1 mutation)
		Crigler-Najjar type 1 syndrome (UGT1A1 deficiency)
		Dubin-Johnson syndrome (cMOAT mutation)
	Altered organ functions	Hepatic dysfunction
Active site levels	Resistance mechanisms	P-glycoprotein
		BCRP
		Topoisomerase I mutations
		CYP3A4 and/or UGT1A1 Overexpression

In addition, a wealth of information has become available that has yielded valuable insight into the mechanism of action, the mechanisms of tumor resistance, toxicities, and considerations of dosage and schedule and route of drug administration. Many of these studies have been made possible by the development of selective analytical methodologies to specifically monitor the parent drug and individual metabolites, with sufficient sensitivity to detect the compounds at levels achieved after therapeutic dosing. However, only through further investigations that may allow better definition of the biochemistry and pharmacokinetics of CPT-11 can the rational optimization of therapy involving this agent be achieved. This need has become even more important in light of the current clinical use of CPT-11 in combination with other antineoplastic drugs or agents specifically administered to modify CPT-11-induced toxicity profiles (143). In this respect, the use of mathematical models to predict systemic exposure measures for CPT-11 and its metabolites by application of limited-sampling strategies (38, 41, 144-147), coupled with continued investigations into the role of individual enzyme-expression levels and detection of enzyme polymorphisms, will allow more rational and selective chemotherapy with this agent.

REFERENCES

1. Wall ME, Wani MC, Cook CE, Palmer KH, Mc Phail AT, Sim GA. Plant antitumor agents: I. The isolation and structure of camptothecine, a novel alkaloidal leukemia and tumor inhibitor from Camptotheca acuminata. J Am Chem Soc 88: 3888-3890, 1966
2. Muggia FM, Creaven PJ, Hansen HH, Cohen MH, Selawry OS. Phase I clinical trail of weekly and daily treatment with camptothecin (NSC-100880): correlation with preclinical studies. Cancer Chemother Rep 56: 515-521, 1972
3. Moertel CG, Schutt AJ, Reitemeier RJ, Hahn RG. Phase II study of camptothecin (NSC-100880) in the treatment of advanced gastrointestinal cancer. Cancer Chemother Rep 56: 95-101, 1972
4. Schaeppi U, Fleischman RW, Cooney DA. Toxicity of camptothecin (NSC-100880). Cancer Chemother Rep 5: 25-36, 1974
5. Creemers GJ, Lund B, Verweij J. Topoisomerase I Inhibitors: topotecan and irinotecan. Cancer Treat Rev 20: 73-96, 1994
6. Rajkumar SV, Adjei AA. A review of the pharmacology and clinical activity of new chemotherapeutic agents in lung cancer. Cancer Treat Rev 24: 35-53, 1998
7. Hsiang Y-H, Hertzberg R, Hecht S, Liu LF. Camptothecin induces protein-linked DNA breaks via mammalian DNA topoisomerase I. J Biol Chem 260: 14873-14878, 1985
8. Hsiang Y-H, Liu LF. Identification of mammalian DNA topoisomerase I as an intracellular target of the anticancer drug camptothecin. Cancer Res 48: 1722-1726, 1988
9. Hsiang Y-H, Lihou MG, Liu LF. Arrest of replication forks by drug-stabilized topoisomerase I-DNA cleavable complexes as a mechanism of cell killing by camptothecin. Cancer Res 49: 5077-5082, 1989
10. Gerrits CJH, de Jonge MJA, Schellens JHM, Stoter G, Verweij J. Topoisomerase I inhibitors: the

relevance of prolonged exposure for clinical development. Br J Cancer 76: 952-962, 1997

11. O' Leary J, Muggia FM. Camptothecins: a review of their development and schedules of administration. Eur J Cancer 34: 1500-1508, 1998
12. Gelderblom HA, de Jonge MJA, Sparreboom A, Verweij J. Oral topoisomerase I inhibitors in adult patients: present and future. Invest New Drugs 17: 401-415, 1999
13. Kunimoto T, Nitta K, Tanaka T, et al. Antitumor activity of 7-ethyl-10-[4-(1-piperidino)-1-piperidino]carbonyloxy-camptothecin, a novel water-soluble derivative of camptothecin, against murine tumors. Cancer Res 47: 5944-5947, 1987
14. Kingsbury WD, Boehm JC, Jakas DR, et al. Synthesis of water-soluble (aminoalkyl)camptothecin analogues: inhibition of topoisomerase I and antitumor activity. J Med Chem 34: 98-107, 1991
15. Pantazis P, Harris N, Mendoza J, Giovanella B. The role of pH and serum albumin in the metabolic conversion of 9-nitrocamptothecin to 9-aminocamptothecin by human hematopoietic and other cells. Eur J Haematol 55: 211-213, 1995
16. Loos WJ, Sparreboom A, Verweij J, Nooter K, Stoter G, Schellens JHM. Determination fo the lactone and lactone plus carboxylate forms of 9-aminocamptothecin in human plasma by senstitive high-performance liquid chromatography with fluorescence detection. J Chromatogr B 694: 435-441, 1997
17. Blaney SM, Takimoto C, Murry DJ, et al. Plasma and cerebrospinal fluid pharmacokinetics of 9-aminocamptothecin (9-AC), irinotecan (CPT-11), and SN-38 in nonhuman primates. Cancer Chemother Pharmacol 41: 464-468, 1998
18. Emerson DL, Besterman JM, Brown HR, et al. In vivo antitumor activity of two new seven-substituted water-soluble camptothecin analogues. Cancer Res 55: 603-609, 1995
19. Vey N, Giles FJ, Kantarjian H, Smith TL, Beran M, Jeha S. The topoisomerase I inhibitor DX-8951f is active in a severe combined immunodeficient mouse model of human acute myelogenous leukemia. Clin Cancer Res 6: 731-736, 2000
20. Slatter JG, Schaaf LJ, Sams JP, et al. Pharmacokinetics, metabolism, and excretion of irinotecan (CPT-11) following I.V. infusion of [(14)C]CPT-11 in cancer patients. Drug Metab Dispos 28: 423-433, 2000
21. Canal P, Gay C, Dezeuze A, et al. Pharmacokinetics and pharmacodynamics of irinotecan during a phase II clinical trail in colorectal cancer. J Clin Oncol 14: 2688-2695, 1996
22. Abigerges D, Chabot GG, Armand J-P, Herait P, Gouyette A, Gandia D. Phase I and pharmacologic studies of the camptothecin analog irinotecan administered every 3 weeks in cancer patients. J Clin Oncol 13: 210-221, 1995
23. Rowinsky EK, Grochow LB, Ettinger DS, et al. Phase I and pharmacological study of the novel topoisomerase I inhibitor 7-ethyl-10-[4-(1-(piperidino)-1-piperidino] carbonyloxycamptothecin (CPT-11) administered as a ninety-minute infusion every 3 weeks. Cancer Res 54: 427-436, 1994
24. Rothenberg ML, Kuhn JG, Burris HA, et al. Phase I and pharmacokinetic trial of weekly CPT-11. J Clin Oncol 11: 2194-2204, 1993
25. De Forni M, Bugat R, Chabot GG, et al. Phase I and pharmacokinetic study of the camptothecin derivate irinotecan, administered on a weekly schedule in cancer patients. Cancer Res 54: 4347-4354, 1994

26. Catimel G, Chabot GG, Guastalla JP, et al. Phase I and pharmacokinetic study of irinotecan (CPT-11) administered daily for three consecutive days every three weeks in patients with advanced solid tumors. Ann Oncol 6: 133-140, 1995
27. Sasaki Y, Hakusui H, Mizuno S, et al. A pharmacokinetic and pharmacodynamic analysis of CPT-11 and its active metabolite SN-38. Jpn J Cancer Res 86: 101-110, 1995
28. Pitot HC, Goldberg RM, Reid JM, et al. Phase I dose-finding and pharmacokinetic trial of irinotecan hydrochloride (CPT-11) using a once-every-three-week dosing schedule for patients with advanced solid tumor malignancy. Clin Cancer Res 6: 2236-2244, 2000
29. Herben VMM, Schellens JHM, Swart M, et al. Phase I and pharmacokinetic study of irinotecan administered as a low-dose, continuous intravenous infusion over 14 days in patients with malignant solid tumors. J Clin Oncol 17: 1897-1905, 1999
30. Masuda N, Fukuoka M, Kudoh S, et al. Phase I and pharmacologic study of irinotecan and etoposide with recombinant human granulocyte colony-stimulating factor support for advanced lung cancer. J Clin Oncol 12: 1833-1841, 1994
31. Gupta E, Mick R, Ramirez J, et al. Pharmacokinetic and pharmacodynamic evaluation of the topoisomerase iInhibitor irinotecan in cancer patients. J Clin Oncol 15: 1502-1510, 1997
32. Sparreboom A, de Jonge MJA, de Bruijn P, et al. Irinotecan (CPT-11) metabolism and disposition in cancer patients. Clin Cancer Res 4: 2747-2754, 1998
33. Sasaki Y, Yoshida Y, Sudoh K, et al. Pharmacological correlation between total drug concentration and lactones of CPT-11 and SN-38 in patients treated with CPT-11. Jpn J Cancer Res 86: 111-116, 1995
34. Rivory LP, Chatelut E, Canal P, Mathieu-Boue A, Robert J. Kinetics of the in vivo interconversion of the carboxylate and lactone forms of irinotecan and of its metabolite SN-38 in patients. Cancer Res 54: 6330-6333, 1994
35. Chabot GG, Abigerges D, Catimel G, et al. Population pharmacokinetics and pharmacodynamics of irinotecan (CPT-11) and active metabolite SN-38 during phase I trails. Ann Oncol 6: 141-151, 1995
36. Rivory LP, Haaz M-C, Canal P, Lokiec F, Armand JP, Robert J. Pharmacokinetic interrelationships of irinotecan (CPT-11) and its three major plasma metabolites in patients enrolled in phase I/II trials. Clin Cancer Res 3: 1261-1266, 1997
37. Loos WJ, Verweij J, Gelderblom HA, et al. Role of erythrocytes and serum proteins in the kinetic profile of total 9-amino-20(S)-camptothecin in humans. Anticancer Drugs 10: 705-710, 1999
38. Mathijssen RHJ, van Alphen RJ, de Jonge MJA, et al. Sparse-data set analysis for irinotecan and SN-38 pharmacokinetics in cancer patients co-treated with cisplatin. Anticancer Drugs 10: 9-16, 1999
39. Ohe Y, Sasaki Y, Shinkai T, et al. Phase I study and pharmacokinetics of CPT-11 with 5-day continuous infusion. J Natl Cancer Inst 84: 972-973, 1992
40. Rothenberg ML, Eckardt JR, Kuhn JG, et al. Phase II trial of irinotecan in patients with progressive or rapidly recurrent colorectal cancer. J Clin Oncol 14: 1128-1135, 1996
41. Mick R, Gupta E, Vokes EE, Ratain MJ. Limited-sampling models for irinotecan pharmacokinetics-pharmacodynamics: prediction of biliary index and intestinal toxicity. J Clin Oncol 14: 2012-2019, 1996
42. Rothenberg ML, Kuhn JG, Schaaf LJ, et al. Phase I and pharmacokinetic study of intravenous irinotecan (CPT-11) administered once every 2 weeks +/- G-CSF. Ann Oncol 10(S): 63, 1998

(abstract)

43. Kehrer DFS, Yamamoto W, Verweij J, de Jonge MJA, de Bruijn P, Sparreboom A. Factors involved in prolongation of the terminal disposition phase of SN-38: clinical and experimental studies. Clin Cancer Res 6: 3451-3458, 2000
44. Combes O, Barré J, Duché J-C, et al. In vitro binding and partitioning of irinotecan (CPT-11) and its metabolite, SN-38, in human blood. Invest New Drugs 18: 1-5, 2000
45. Ma MK, Zamboni WC, Radomski KM, et al. Pharmacokinetics of irinotecan and its metabolites SN-38 and APC in children with recurrent solid tumors after protracted low-dose irinotecan. Clin Cancer Res 6: 813-819, 2000
46. Burke TG, Mi ZH. The structural basis of camptothecin interactions with human serum albumin: impact on drug stability. J Med Chem 37: 40-46, 1994
47. Burke TG, Munshi CB, Mi ZH, Jiang Y. The important role of albumin in determing the relative human blood stabilities of the camptothecin anticancer drugs. J Pharm Sci, 84: 518-519, 1995
48. Slatter JG, Su P, Sams JP, Schaaf LJ, Wienkers LC. Bioactivation of the anticancer agent CPT-11 to SN-38 by human hepatic microsomal carboxylesterases and the in vitro assesment of potential drug interactions. Drug Metab Dispos 25: 1157-1164, 1997
49. Humerickhouse R, Lohrbach K, Li L, Bosron WF, Dolan ME. Characterization of CPT-11 hydrolysis by human liver carboxylesterase isoforms hCE-1 and hCE-2. Cancer Res 60: 1189-1192, 2000
50. Wierdl M, Morton CL, Danks MK, Potter PM. Isolation and characterization of a cDNA encoding a horse liver butyrylcholinesterase: evidence for CPT-11 drug activation. Biochem Pharmacol 59: 773-781, 2000
51. Morton CL, Wadkins RM, Danks MK, Potter PM. The anticancer prodrug CPT-11 is a potent inhibitor of acetylcholinesterase but is rapidly catalyzed to SN-38 by butyrylcholinesterase. Cancer Res 59: 1458-1463, 1999
52. Haaz M-C, Rivory LP, Riché C, Robert J. The transformation of irinotecan (CPT-11) to its active metabolite SN-38 by human liver microsomes. N-S Arch Pharmacol 356: 257-262, 1997
53. Kawato Y, Furuta T, Aonuma M, Yasuoka M, Yokokura T, Matsumoto, K. Antitumor activity of a camptothecin derivative, CPT-11, against human tumor xenografts in nude mice. Cancer Chemother Pharmacol 28: 192-198, 1991
54. Takaoka K, Ohtsuka K, Jin M. Conversion of CPT-11 to its active form SN-38, by carboxylesterase of non-small cell lung cancer. Proc Am Soc Clin Oncol 16: 252a, 1997 (abstract)
55. Van Ark-Otte J, Kedde MA, van der Vijgh WJF, et al. Determinants of CPT-11 and SN-38 activities in human lung cancer cells. Br J Cancer 77: 2171-2176, 1998
56. Guichard S, Terret C, Hennebelle I, et al. CPT-11 converting carboxylesterase and topoisomerase I activities in tumour and normal colon and liver tissues. Br J Cancer 80: 364-370, 1999
57. Kojima A, Hackett NR, Ohwada A, Crystal RG. In vivo human carboxylesterase cDNA gene transfer to activate the prodrug CPT-11 for local treatment of solid tumors. J Clin Invest 101: 1789-1796, 1998
58. Kojima A, Hackett NR, Crystal RG. Reversal of CPT-11 resistance of lung cancer cells by adenovirus-mediated gene transfer of the human carboxylesterase cDNA. Cancer Res 58: 4368-4374, 1998

59. Danks MK, Morton CL, Krull EJ, et al. Comparison of activation of CPT-11 by rabbit and human carboxylesterases for use in enzyme/prodrug therapy. Clin Cancer Res 5: 917-924, 1999
60. Satoh T, Hosokawa M, Atsumi R, Suzuki W, Hakusui H, Nagai E. Metabolic activation of CPT-11, 7-ethyl-10-[4-(1-piperidino)-1-piperidino]carbonyloxycamptothecin, a novel antitumor agent, by carboxylesterase. Biol Pharm Bull 17: 662-664, 1994
61. Inaba M, Ohnishi Y, Ishii H, et al. Pharmacokinetics of CPT-11 in rhesus monkeys. Cancer Chemother Pharmacol 41: 103-108, 1998
62. Danks MK, Morton CL, Pawlik CA, Potter PM. Overexpression of a rabbit liver carboxylesterase sensitizes human tumor cells to CPT-11. Cancer Res 58: 20-22, 1998
63. Iyer L, King CD, Whitington PF, et al. Genetic predisposition to the metabolism of irinotecan (CPT-11). Role of uridine diphosphate glucuronosyltransferase isoform 1A1 in the glucuronidation of its active metabolite (SN-38) in human liver microsomes. J Clin Invest 101: 847-854, 1998
64. Rivory LP, Robert J. Identification and kinetics of a beta-glucuronide metabolite of SN-38 in human plasma after administration of the camptothecin derivative irinotecan. Cancer Chemother Pharmacol 36: 176-179, 1995.
65. Atsumi R, Suzuki W, Hakusui H. Identification of the metabolites of irinotecan, a new derivative of camptothecin, in rat bile and its biliary excretion. Xenobiotica 21: 1159-1169, 1991
66. Gupta E, Lestingi TM, Mick R, Ramirez J, Vokes EE Ratain MJ. Metabolic fate of irinotecan in humans: correlation of glucuronidation with diarrhea. Cancer Res 54: 3723-3725, 1994
67. Ciotti M, Basu N, Brangi M, Owens IS. Glucuronidation of 7-ethyl-10-hydroxycamptothecin (SN-38) by the human UDP-glucuronosyltransferases encoded at the UGT1 locus. Biochem Biophys Res Commun 260: 199-202, 1999
68. Ando Y, Saka H, Asai G, Sugiura S, Shimokata K, Kamataki T. *UGT1A1* genotypes and glucuronidation of SN-38, the active metabolite of irinotecan. Ann Oncol 9: 845-847, 1998
69. Iyer L, Hall D, Das S, et al. Phenotype-genotype correlation of in vitro SN-38 (active metabolite of irinotecan) and bilirubin glucuronidation in human liver tissue with UGT1A1 promotor polymorphism. Clin Pharmacol Ther 65: 576-582, 1999
70. Monaghan G, Ryan M, Seddon R, Hume R, Burchell B. Genetic variation in bilirubin UDP-glucuronosyltransferase gene promotor and Gilbert's syndrome. Lancet 347: 578-581, 1996
71. Wasserman E, Myara A, Lokiec F, et al. Severe CPT-11 toxicity in patients with Gilbert's syndrome: two case reports. Ann Oncol 8: 1049-1051, 1997
72. Wasserman E, Myara A, Lokiec F, et al. Bilirubin (BIL) and SN-38: pharmacokinetic/ pharmacodynamics correlation. Ann Oncol 10(S): 58, 1998 (abstract)
73. Ando Y, Saka H, Ando M, et al. Polymorphisms of UDP-glucuronosyltransferase gene and irinotecan toxicity: a pharmacogenetic analysis. Cancer Res 60: 6921-6926, 2000
74. Gupta E, Wang X, Ramirez J, Ratain MJ. Modulation of glucuronidation of SN-38, the active metabolite of irinotecan, by valproic acid and phenobarbital. Cancer Chemother Pharmacol 39: 440-444, 1997
75. Takahashi T, Fujiwara Y, Yamakido M, Katoh O, Watanabe H, Mackenzie PI. The role of glucuronidation in 7-ethyl-10-hydroxycamptothecin resistance *in vitro*. Jpn J Cancer Res 88: 1211-1217, 1997
76. Brangi M, Litman T, Ciotti M, et al. Camptothecin resistance: role of the ATP-binding cassette (ABC), mitoxantrone-resistance half-transporter (MXR), and potential for glucuronidation in

MXR-expressing cells. Cancer Res 59: 5938-5946, 1999

77. Lokiec F, Monegier du Sorbier B, Sanderink G-J. Irinotecan (CPT-11) metabolites in human bile and urine. Clin Cancer Res 2: 1943-1949, 1996
78. Haaz M-C, Rivory LP, Riché C, Vernillet L, Robert J. Metabolism of irinotecan (CPT-11) by hepatic microsomes: participation of cytochrome P-450 3A and drug interactions. Cancer Res 58: 468-472, 1998
79. Santos A, Zannetta S, Cresteil T, et al. Metabolism of irinotecan (CPT-11) by CYP3A4 and CYP3A5 in humans. Clin Cancer Res 6: 2012-2020, 2000
80. Dodds HM, Haaz M-C, Riou J-F, Robert J, Rivory LP. Identification of a new metabolite of CPT-11 (irinotecan): pharmacological properties and activation to SN-38. J Pharmacol Exp Ther 286: 578-583, 1998
81. Haaz M-C, Riché C, Rivory LP, Robert J. Biosynthesis of an aminopiperidino metabolite of irinotecan [7-ethyl-10-[4-(1-piperidino]carbonyloxycamptothecine] by human hepatic microsomes. Drug Metab Dispos 26: 769-774, 1998
82. Dodds HM, Wunsch RM, Gillam EMJ, Rivory LP. Further elucidation of the pathways involved in the catabolism of the camptothecin analogue irinotecan. Proc Am Assoc Cancer Res 40: 110, 1999 (abstract)
83. Rivory LP, Riou J-F, Haaz M-C, et al. Identification and properties of a major plasma metabolite of irinotecan (CPT-11) isolated from the plasma of patients. Cancer Res 56: 3689-3694, 1996
84. Dodds HM, Haaz M-C, Riou J-F, Robert J, Rivory LP. Identification of a new metabolite of CPT-11 (irinotecan): pharmacological properties and activation to SN-38. J Pharmacol Exp Ther 286: 578-583, 1998
85. Massaad L, de Waziers I, Ribrag V, et al. Comparison of mouse and human colon tumors with regard to phase I and phase II drug-metabolizing enzyme systems. Cancer Res 52: 6567-6575, 1992
86. Rivory LP, Bowles MR, Robert J, Pond SM. Conversion of irinotecan (CPT-11) to its active metabolite, 7-ethyl-10-hydroxycamptothecin (SN-38), by human liver carboxylesterase. Biochem Pharmacol 52: 1103-1111, 1996
87. Dresser GK, Spence JD, Bailey DG. Pharmacokinetic-pharmacodynamic consequences and clinical relevance of cytochrome P450 3A4 inhibition. Clin Pharmacokin 38: 41-57, 2000
88. Skar V, Skar AG, Stromme JH. Beta-glucuronidase activity related to bacterial growth in commen bile duct bile in gallstone patients. Scand J Gastroenterol 23: 83-90, 1988
89. Yokoi T, Narita M, Nagai E, Hagiwara H, Aburada M, Kamataki T. Inhibition of UDP-glucuronosyltransferase by aglycons of natural glucuronides in kampo medicines using SN-38 as a substrate. Jpn J Cancer Res 86: 985-989, 1995
90. Sperker B, Backman JT, Kroemer HK. The role of beta-glucuronidase in drug disposition and drug targeting in humans. Clin Pharmacokin 33: 18-31, 1997
91. Takasuna K, Hagiwara T, Hirohashi M, et al. Involvement of beta-glucuronidase in intestinal microflora in the intestinal toxicity of the antitumor camptotecin derivate irinotecan hydrochloride (CPT-11) in rats. Cancer Res 56: 3752-3757, 1996
92. Kase Y, Hayakawa T, Togashi Y, Kamataki T. Relevance of irinotecan hydrochloride-induced diarrhea to the level of prostaglandin E2 and water absorption of large intestine in rats. Jpn J Pharmacol 75: 399-405, 1997
93. Araki E, Ishikawa M, Iigo M, Koide T, Itabashi M, Hoshi A. Relationship between development of diarrhea and the concentration of SN-38, an active metabolite of CPT-11, in the intestine and the

blood plasma of athymic mice following intraperitoneal administration of CPT-11. Jpn J Cancer Res 84: 697-702, 1993

94. Takasuna K, Hagiwara T, Hirohashi M, et al. Inhibition of intestinal microflora beta-glucuronidase modifies the distribution of the active metabolite of the antitumor agent irinotecan hydrochloride (CPT-11) in rats. Cancer Chemother Pharmacol 42: 280-286, 1998
95. Fujisawa T, Mori M. Influence of various bile salts on beta-glucuronide activity of intestinal bacteria. Appl Microbiol 25: 95-97, 1997
96. Cole CB, Fuller R, Mallet AK, Rowland IR. The influence of the host on expression of intestinal microbial enzyme activities involved in metabolism of foreign compounds. J Appl Bacteriol 59: 549-553, 1985
97. Van Huyen JP, Bloch F, Attar A, et al. Diffuse mucosal damage in the large intestine associated with irinotecan (CPT-11). Dig Dis Sci 43: 2649-2651, 1998
98. Mallett AK, Bearne CA, Rowland IR. The influence of incubation pH on the activity of rat and human gut flora enzymes. J Appl Bacteriol 66: 433-437, 1989
99. Planting AST. Modulation of irinotecan pharmacokinetics/pharmacodynamics by combined treatment with neomycin. Proc Am Soc Clin Oncol 19: 1007, 2000 (abstract)
100. Lokiec F, Canal P, Gay C, et al. Pharmacokinetics of irinotecan and its metabolites in human blood, bile and urine. Cancer Chemother Pharmacol 36: 79-82, 1995
101. Chu X-Y, Kato Y, Niinuma K, Sudo KI, Hakusui H, Sugiyama Y. Multispecific organic anion transporter is responsible for the biliary excretion of the camptothecin derivative irinotecan and its metabolites in rats. J Pharmacol Exp Ther 281: 304-314, 1997
102. Chu X-Y, Kato Y, Sugiyama Y. Multiplicity of biliary excretion mechanisms for irinotecan, CPT-11, and its metabolites in rats. Cancer Res 57: 1934-1938, 1997
103. Chu X-Y, Kato Y, Ueda K, et al. Biliary excretion mechanism of CPT-11 and its metabolites in humans: involvement of primary active transporters. Cancer Res 58: 5137-5143, 1998
104. Gupta E, Safa AR, Wang X, Ratain MJ. Pharmacokinetic modulation of irinotecan and metabolites by cyclosporin A. Cancer Res 56: 1309-1314, 1996
105. Sugiyama Y, Kato Y, Chu X-Y. Multiplicity of biliary excretion mechanisms for the camptothecin derivative irinotecan (CPT-11), its metabolite SN-38, and its glucuronide: role of canalicular multispecific organic anion transporter and P-glycoprotein. Cancer Chemother Pharmacol 42: S44-S49, 1998
106. Chu X-Y, Kato Y, Sugiyama Y. Possible involvement of P-glycoprotein in biliary excretion of CPT-11 in rats. Drug Metab Dispos 27: 440-441, 1999
107. Paulusma CC, Kool M, Bosma PJ, et al. A mutation in the human canalicular multispecific organic anion transporter gene causes the Dubin-Johnson syndrome. Hepatology 25: 1539-1542, 1997
108. Houghton PJ, Cheshire PJ, Hallman JD, et al. Efficacy of topoisomerase I inhibitors, topotecan and irinotecan, administered at low dose levels in protracted schedules to mice bearing xenografts of human tumors. Cancer Chemother Pharmacol 36: 393-403, 1995
109. Thompson J, Zamboni WC, Cheshire PJ, et al. Efficacy of systemic administration of irinotecan against neuroblastoma xenografts. Clin Cancer Res 3: 423-431, 1997
110. Takimoto CH, Morrison G, Harold N, et al. Phase I and pharmacologic study of irinotecan administered as a 96-hour infusion weekly to adult cancer patients. J Clin Oncol 18: 659-667, 2000

111. Furman WL, Stewart CF, Poquette CA, et al. Direct translation of a protracted irinotecan schedule from a xenograft model to a phase I trial in children. J Clin Oncol 17: 1815-1824, 1999
112. Ahmed F, Vyas V, Cornfield A, et al. In vitro activation of irinotecan to SN-38 by human liver and intestine. Anti-Cancer Res 19: 2067-2072, 1999
113. Drengler RL, Kuhn JG, Schaaf LJ, et al. Phase I and pharmacokinetic trial of oral irinotecan administered daily for 5 days every 3 weeks in patients with solid tumors. J Clin Oncol 17: 685-696, 1999
114. Zamboni WC, Houghton PJ, Thompson J, et al. Altered irinotecan and SN-38 disposition after intravenous and oral administration of irinotecan in mice bearing human neuroblastoma xenografts. Clin Cancer Res 4: 455-462, 1998
115. Stewart CF, Zamboni WC, Crom WR, Houghton PJ. Disposition of irinotecan and SN-38 following oral and intravenous irinotecan dosing in mice. Cancer Chemother Pharmacol 41: 259-265, 1997
116. Radomski KM, Stewart CF, Panetta JC, Houghton PJ, Furman WL. Phase I and pharmacokinetic study of oral irinotecan in pediatric patients with solid tumors. Proc Am Soc Clin Oncol 41: 592a, 2000
117. Kobayashi K, Bouscarel B, Matsuzaki Y, Ceryak S, Kudoh S, Fromm H. pH-dependent uptake of irinotecan and its active metabolite, SN-38, by intestinal cells. Int J Cancer 83: 491-496, 1999
118. Guichard S, Chatelut E, Lochon I, Bugat R, Mahjoubi M, Canal P. Comparison of the pharmacokinetics and efficacy of irinotecan after administration by the intravenous versus intraperitoneal route in mice. Cancer Chemother Pharmacol 42: 165-170, 1998
119. De Jonge MJA, Sparreboom A, Planting AST, et al. Phase I study of 3-week schedule of irinotecan combined with cisplatin in patients with advanced solid tumors. J Clin Oncol 18: 187-194, 2000
120. De Jonge MJA, Verweij J, de Bruijn P, et al. Pharmacokinetic, metabolic, and pharmacodynamic profiles in a dose-escalating study of irinotecan and cisplatin. J Clin Oncol 18: 195-203, 2000
121. Shinkai T, Arioka H, Kunikane H, et al. Phase I clinical trail of irinotecan (CPT-11), 7-ethyl-10[4-(1-piperidino)-1-piperidino]carbonyloxy-camptothecin, and cisplatin in combination with fixed dose of vindesine in advanced non-small cell lung cancer. Cancer Res 54: 2636-2642, 1994
122. Mogi H, Hasegawa Y, Watanabe A, Nomura F, Saka H, Shimokata K. Combination effects of cisplatin, vinorelbine and irinotecan in non-small-cell lung cancer cell lines in vitro. Cancer Chemother Pharmacol 39: 199-204, 1997
123. Fujita A, Takabatake H, Tagaki S, Sekine K. Phase I/II study of cisplatin, ifosfamide and irinotecan with rhG-CSF support in patients with stage IIIB and IV non-small-cell lung cancer. Cancer Chemother Pharmacol 45: 279-283, 2000
124. DeVore RF, Johnson DH, Crawford J, et al. Phase II study of irinotecan plus cisplatin in patients with advanced non-small-cell lung cancer. J Clin Oncol 17: 2710-2720, 1999
125. Kudoh S, Fukuoka M, Masuda N, et al. Relationship between the pharmacokinetics of irinotecan and diarrhea during combination chemotherapy with cisplatin. Jpn J Cancer Res 86: 406-413, 1995
126. De Jonge MJA, Verweij J, Planting AST, et al. Drug-administration sequence does not change pharmacodynamics and kinetics of irinotecan and cisplatin. Clin Cancer Res 5: 2012-2017, 1999
127. Okamoto H, Nagatomo A, Kunitoh H, Kunikane H, Watanabe K. A phase I clinical and pharmacologic study of a carboplatin and irinotecan regimen combined with recombinant human

granulocyte-colony stimulating factor in the treatment of patients with advanced nonsmall cell lung carcinoma. Cancer 82: 2166-2172, 1998

128. Fukuda M, Oka M, Soda H, et al. Phase I study of irinotecan combined with carboplatin in previously untreated solid cancers. Clin Cancer Res 5: 3963-3969, 1999
129. LeBlanc GA, Sundseth SS, Weber GF, Waxman DJ. Platinum anticancer drugs modulate P-450 mRNA levels and differentially alter hepatic drug and steroid hormone metabolism in male and female rats. Cancer Res 52: 540-7, 1992
130. Sasaki Y, Ohtsu A, Shimada Y, Ono K, Saijo N. Simultaneous administration of CPT-11 and fluorouracil: alteration of the pharmacokinetics of CPT-11 and SN-38 in patients with advanced colorectal cancer. J Natl Cancer Inst 86: 1096-1097, 1994
131. Saltz LB, Kanowitz J, Kemeny NE, et al. Phase I clinical and pharmacokinetic study of irinotecan, fluorouracil, and leucovorin in patients with advanced solid tumors. J Clin Oncol 14: 2959-2967, 1996
132. Vanhoefer U, Harstrick A, Köhne C-H, et al. Phase I study of a weekly schedule of irinotecan, high-dose leucovorin, and infusional fluorouracil as a first-line chemotherapy in patients with advanced colorectal cancer. J Clin Oncol 17: 907-913, 1999
133. Benhammouda A, Bastian G, Rixe O. A phase I and pharmacokinetic study of CPT-11 and 5-FU (F) combination. Proc Am Soc Clin Oncol 16: 202a, 1997 (abstract)
134. Saltz I, Shimada Y, Khayat D. CPT-11 (Irinotecan) and 5-fluorouracil: a promising combination for therapy of colorectal cancer. Eur J Cancer 32A: S24-S31, 1996
135. Adjei AA, Klein CE, Kastrissios H, et al. Phase I and pharmacokinetic study of irinotecan and docetaxel in patients with advanced solid tumors: preliminary evidence of clinical activity. J Clin Oncol 18: 1116-1123, 2000
136. Asai G, Yamamoto N, Sakai S. Paclitaxel (Taxol) affects pharmacokinetics of irinotecan and its metabolites. Proc Am Soc Clin Oncol 18: 171a, 1999 (abstract)
137. Yamamoto N, Negoro S, Chikazawa H, Shimizu T, Fukuoka M. Pharmacokinetic interaction of the combination of paclitaxel and irinotecan in vivo and clinical study. Proc Am Soc Clin Oncol 18: 186a, 1999 (abstract)
138. Van Zuylen L, Verweij J, Sparreboom A. Role of formulation vehicles in taxane pharmocology. Invest New Drugs 19: 125-141, 2001
139. Murren JR, Peccerillo K, DiStasio SA, et al. Dose escalation and pharmacokinetic study of irinotecan in combination with paclitaxel in patients with advanced cancer. Cancer Chemother Pharmacol 46: 43-50, 2000
140. Friedman HS, Petros WP, Friedman AH, et al. Irinotecan therapy in adults with recurrent or progressive malignant glioma. J Clin Oncol 17: 1516-1525, 1999
141. Gajjar AJ, Radomski KM, Bowers DC, et al. Pharmacokinetics of irinotecan (IRN) and metabolites in pediatric high-grade glioma patients with and without co-administration of enzyme-inducing anticonvulsants. Proc Am Soc Clin Oncol 19: 162a, 2000 (abstract)
142. Grossman SA, Hochberg F, Fisher J, et al. Increased 9-aminocamptothecin dose requirements in patients on anticonsulvants. Cancer Chemother Pharmacol 42: 118-126, 1998
143. Kehrer DFS, Sparreboom A, Verweij J, et al. Modulation of irinotecan-induced diarrhea by cotreatment with neomycin in cancer patients. Clin Cancer Res 7: 1136-1141, 2001
144. Chabot GG. Limited sampling models for simultaneous estimation of the pharmacokinetics of irinotecan and its active metabolite SN-38. Cancer Chemother Pharmacol 36: 463-472, 1995

145. Sasaki Y, Mizuno S, Fujii H, et al. A limited sampling model for estimating pharmacokinetics of CPT-11 and its metabolite SN-38. Jpn J Cancer Res 86: 117-123, 1995
146. Nakashima H, Lieberman R, Karato A, et al. Efficient sampling strategies for forecasting pharmacokinetic parameters of irinotecan (CPT-11): implication for area under the concentration-time curve monitoring. Ther Drug Monit 17: 221-229, 1995
147. Yamamoto N, Tamura T, Karato A, et al. CPT-11: population pharmacokinetic model and estimation of pharmacokinetics using the bayesian method in patients with lung cancer. Jpn J Cancer Res 85: 972-977, 1994
148. Wasserman E, Cuvier C, Lokiec F, et al. Combination of oxaliplatin plus irinotecan in patients with gastrointestinal tumors: results of two independent phase I studies with pharmacokinetics. J Clin Oncol 17: 902-906, 1999
149. Couteau C, Risse ML, Ducreux M, et al. Phase I and pharmacokinetic study of docetaxel and irinotecan in patients with advanced solid tumors. J Clin Oncol 18: 3545-3552, 2000
150. Masuda N, Negoro S, Kudoh S, et al. Phase I and pharmacologic study of docetaxel and irinotecan in advanced non-small-cell lung cancer. J Clin Oncol 18: 2996-3003, 2000
151. Ford HE, Cunningham D, Ross PJ, et al. Phase I study or irinotecan and raltitrexed in patients with advanced gastrointestinal tract adenocarcinoma. Br J Cancer, 83: 146-152, 2000

Chapter Three

Sparse-Data Set Analysis for Irinotecan and SN-38 Pharmacokinetics in Cancer Patients Co-treated with Cisplatin

Anti-Cancer Drugs, 10: 9-16, 1999

Ron H.J. Mathijssen[1]
Robbert J. van Alphen[1]
Maja J.A. de Jonge[1]
Jaap Verweij[1]
Peter de Bruijn[1]
Walter J. Loos[1]
Kees Nooter[1]
Laurent Vernillet[2]
Gerrit Stoter[1]
Alex Sparreboom[1]

[1]Department of Medical Oncology, Erasmus MC - Daniel den Hoed
Rotterdam, The Netherlands

[2]Aventis Pharma, SA
Antony, France

ABSTRACT

The clinical pharmacokinetics of the antineoplastic agent irinotecan (CPT-11) are associated with substantial interpatient variability. The degree to which this variability in CPT-11 exposure impacts upon the response and toxicity of the drug has not yet been properly determined. In general, the area under the plasma concentration-time curve (AUC) is an appropriate indicator of exposure, but requires collection of up to 17 timed blood samples. This presents difficulties if large-scale population samplings are required. The present study involved the development and validation of a strategy to estimate the AUCs of the lactone and total (i.e. lactone *plus* carboxylate) forms of CPT-11 and its active metabolite SN-38 from a limited number of blood samples in patients co-treated with cisplatin. Using data from 24 patients, univariate and multivariate regression analyses were employed to generate the models. The best predictive models for simultaneous estimation of CPT-11 and SN-38 AUCs were obtained with three time points at 0.5, 1.67 and 5.50 h after start of the 90-min i.v. infusion of CPT-11. The models were tested separately in another group of 24 patients receiving the same combination treatment. This validation set demonstrated that CPT-11 and SN-38 AUCs after standard dose administration could be predicted sufficiently unbiased and precise with three timed samples to warrant clinical application.

INTRODUCTION

The antineoplastic agent irinotecan (CPT-11; 7-ethyl-10-[4-(1-piperidino)-1-piperidino] carbonyloxycamptothecin) is a promising water soluble semisynthetic derivative of camptothecine, a plant alkaloid from the Chinese tree *Camptotheca acuminata* (1, 2). The drug displays potent antitumor activity against a variety of tumors, and has recently been approved for the treatment of refractory colorectal and ovarian carcinomas in several countries (3). The mechanism of action of CPT-11 and its structurally related analogues is thought to be related to inhibition of the intranuclear enzyme topoisomerase-I, thereby indirectly impeding DNA-replication and RNA-transcription (4).

CPT-11 and its active metabolite SN-38 (7-ethyl-10-hydroxycamptothecin; Figure 1) are both subject to a rapid, reversible, pH-dependent hydrolysis of a lactone ring moiety in the molecule, generating an open-ring carboxylate (5). At neutral or physiologic pH, e.g. in blood, the equilibrium between the two drug species favors the pharmacologically less active carboxylate for most camptothecines (6). However, the relative importance of the lactone-carboxylate interconversion of CPT-11 and SN-38 with respect to pharmacodynamic outcome is still not completely understood.

Furthermore, the clinical pharmacokinetic behavior of CPT-11 is associated with a substantial degree of interindividual variability. Thus, careful measurement of both drug forms is clearly warranted in order to fully characterize the clinical pharmacology of these agents.

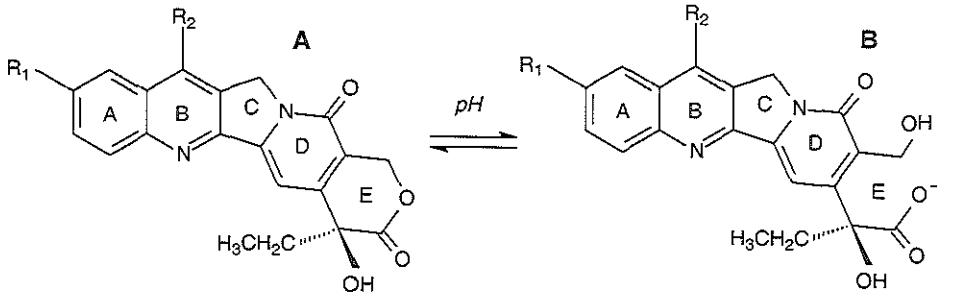

Compound	R_1	R_2
Irinotecan (I)	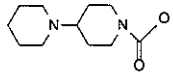	CH_2CH_3
SN-38 (II)	OH	CH_2CH_3
Camptothecin (III)	H	H

Figure 1. Chemical structures of the lactone (A) and carboxylate (B) forms of CPT-11, its active metabolite SN-38, and the related compound camptothecin.

The major dose-limiting toxicities encountered with single agent CPT-11 therapy were neutropenia and diarrhea (7). Relationships for CPT-11 and SN-38 between clinical pharmacokinetics and pharmacodynamic outcome are extremely complex and not thoroughly discerned (reviewed in Takimoto and Arbuck; Ref. 8). Based on the knowledge of camptothecine pharmacology, CPT-11 induced myelosuppression probably occurs due to the inhibition of topoisomerase-I by SN-38 lactone in bone marrow cells. In contrast, acute CPT-11 mediated diarrhea is most likely caused by the anticholinesterase activity of the parent compound. Supporting this theory are reports that the area under the plasma concentration-time curve (AUC) of SN-38 correlated with myelosuppression and the AUC of CPT-11 correlated with diarrhea (8, 9).

However, some studies have not found such associations, indicating that additional studies applying selective analytical methods are essential to help clarify these contrasting results. Such studies will likely involve large numbers of patients and generally require the collection of up to 17 timed blood samples after i.v. drug administration (10). Thus, the objective of the current study was to develop a model for prediction of the AUCs of CPT-11 and SN-38 from a limited blood sampling schedule in patients with advanced solid cancer receiving the drug in combination with cisplatin.

MATERIALS AND METHODS

Patients and Treatment

The pharmacokinetic models were developed and validated in 48 patients with proven malignant solid tumors, participating in a phase I and pharmacokinetic study of combined chemotherapy with CPT-11 and cisplatin (9). Detailed clinical and toxicological profiles will be reported separately. Inclusion criteria included the following: (*a*) no more than one prior combination chemotherapy regimen or two single agent regimens; (*b*) off previous anticancer therapy for at least 4 weeks (6 weeks if nitrosoureas, mitomycin or radiotherapy); (*c*) no prior treatment with topoisomerase-I inhibitors or platinum derivatives; (*d*) age between 18 and 70 years; (*e*) WHO performance status ≤2; (*f*) life expectancy greater than 12 weeks; (*g*) adequate bone-marrow, liver and renal functions and symptomatic peripheral neurotoxicity graded 1 or less (according to National Cancer Institute Common Toxicity Criteria). Written informed consent was obtained from all patients prior to treatment in accordance with the guidelines of the institutional review board.

CPT-11 was provided by Aventis Pharma (Antony, France) as an aqueous formulation containing *d*-sorbitol, lactic acid and sodium hydroxide with a final pH-value of 3.5. The drug was administered at dose levels ranging from 175 to 300 mg/m^2 as a 90-min i.v. infusion. Cisplatin was given as a 3-h intravenous infusion directly after the end of the CPT-11 infusion.

Pharmacokinetic Analysis

For CPT-11 and SN-38 pharmacokinetic analysis heparinized blood samples were drawn from an indwelling cannula at 0.5, 1.5, 1.67, 1.83, 2.0, 2.5, 3.5, 4.5, 5.0, 5.5, 6.5, 8.0, 12.0, 25.5, 32.0, 49.5 and 56.0 h after the start of the infusion. The plasma fraction was obtained by centrifugation and analyzed for CPT-11 and SN-38 using a validated reversed-phase high-performance liquid chromatography system with fluorescence detection (11). The lower limits of quantitation were 0.5 ng/mL for the lactone forms (1-mL samples) and 2.0 ng/mL for the total forms (0.25-mL samples),

respectively. The percentage deviation from the nominal value and the between-run and within-run precision were always less than 15.0%.

CPT-11 and SN-38 (lactone and total) concentration-time data of all patients were fitted to a tri-exponential equation, using Siphar version 4.0 (InnaPhase, Philadelphia, PA), based on discriminating tests described elsewhere (12). All compartmental analyses were obtained by inverse square weighting of the observed concentration. The terminal drug disposition half-life [$t_{1/2}(\gamma)$] and the AUC from time zero to infinity were determined on the basis of the best fitted curves, whereas the peak plasma concentration (C_{max}) was determined graphically from semi-logarithmic concentration-time plots.

Model Development and Validation

Limited sampling models were constructed on a training data set that contained 24 patients, randomly assigned from each separate dose level to avoid bias in the predictive values of one set to another. The models were constructed by assuming that concentration(s) at a fixed time could predict the AUC of each of the compounds of interest simultaneously. Simple linear correlations were initially determined between the concentrations at each time point (independent variables) and the corresponding AUC (dependent variable) by a univariate linear-regression analysis, to find the optimal single-sample time point for each substance measured. Next, forward stepwise multivariate-regression analyses was undertaken to develop the best linear equation describing the association between concentrations at more than one time point and AUC, to increase the precision of the method. The optimal model was eventually identified on the basis of Pearson's correlation coefficient (r), and root mean square residual values as determined from the regression (13).

The pharmacokinetic data from the remaining 24 patients was used to validate the applicability of the constructed models. This was achieved by comparing actual AUCs from the tri-exponential computer fit with estimated AUCs using the best single or multiple time-point models developed from the training set. The predictive performance of the developed models was evaluated using calculations of bias (or percentage mean predictive error; %MPE) and precision (or percentage root mean square error; %RMSE). Due to missing concentrations in this data set at the relevant time points, 3 patients were excluded from validation. Pearson's correlation coefficient was used to rank the concordance between measured and predicted AUCs. Differences in patient demographics and pharmacokinetics between training and validation set patients were evaluated by using Student's t-test. All statistical calculations were performed with the Number Cruncher Statistical System software version 5.X (Dr JL Hintze, East Kaysville, UT, 1992).

RESULTS

Pharmacokinetic studies were completed in 48 patients with various types of solid tumors, treated with a 90-min i.v. infusion of CPT-11, directly followed by a 3-h infusion of cisplatin. The total group of patients was composed of 31 males and 17 females, with a mean age 53 years and a median Eastern Cooperative Oncology Group performance status of 0 (Table 1). Patients were randomly divided in two groups, a training set and a validation set, both containing 24 patients. No significant differences were observed between both groups in patient characteristics (Table 1).

Table 1. Patient demographics.

Characteristic	Training set	Validation set
No. of patients	24	24
Age (years/range)	53 (42-69)	52 (36-68)[a]
Sex (male/female)	16:8	15:9
ECOG performance status (0/1/2)	17:7:0	14:9:1
Primary tumor site		
colorectal	12	9
lung	3	3
pancreas	2	0
mesothelioma	2	0
tonsil	2	1
unknown	2	4
other	1	7

[a]Results expressed as mean value (range).

The mean plasma concentration-time curves for the lactone and total forms of CPT-11 and SN-38 in all patients treated at a dose level of 200 mg/m^2 of CPT-11 are shown in Fig. 2. During the drug infusion, the plasma concentrations of the lactone and total forms of CPT-11 and SN-38 increased steadily, after which a decrease was observed with a decay best described by a tri-exponential equation. Relatively large amounts of CPT-11 and SN-38 were continually present in the lactone forms of these substances, as described for these compounds previously (14). The terminal elimination phases of CPT-11 lactone and total were more rapid than those of the SN-

38 forms, which resulted in prolonged biological half-lives for the active metabolite relative to CPT-11. A summary of the main pharmacokinetic parameters, including AUC, C_{max} and $t_{1/2}(\gamma)$ of CPT-11 and SN-38 between the two patient groups is presented in Tables 2 and 3, respectively.

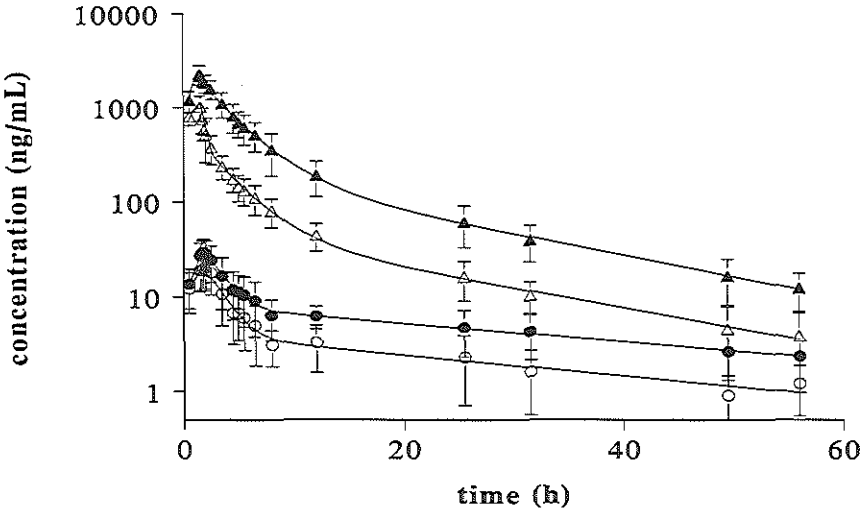

Figure 2. Plasma concentration-time curves of CPT-11 (triangles) lactone and total and of SN-38 (circles) lactone and total in 17 patients given CPT-11 at 200 mg/m² as a 90 min i.v. infusion. The open symbols represent the lactone forms and the closed symbols represent the total forms of CPT-11 and SN-38. All pharmacokinetic curves were fitted to a tri-exponential equation, using Siphar version 4.0 (InnaPhase), assuming a three-compartment model for distribution and elimination of the compounds. Data are presented as mean values (symbols) ± SD (error bars).

There were no significant differences in any pharmacokinetic parameter between the two groups as shown by an unpaired two-sided Student's *t*-test (Tables 2 and 3). Interpatient variability in the concentrations of CPT-11 and SN-38 in the training and validation sets at each of the 17 sample-time points was large (coefficient of variation ranged from 64% (0.5 h) to 96% (1.67 h). The interpatient variability in corresponding AUCs of CPT-11 and SN-38 was slightly dependent on the dose level and ranged from 46% to 64%.

Table 2. Summary of the plasma pharmacokinetic parameters of CPT-11 total and lactone after a 90-min i.v. infusion of CPT-11 in the training (A) and validation (B) sets. Data represent mean values ± SD.

Dose level (mg/m^2)	Set	n	$AUC_{0-\infty}$ total (μg.h/mL)	$AUC_{0-\infty}$ lactone (μg.h/mL)	C_{max} total (μg/mL)
175	A	1	6.53	2.03	1.37
	B	2	7.77, 15.9	2.36, 4.78	2.39, 3.16
200	A	9	11.5±3.75	3.79±0.98	2.49±0.35
	B	7	12.8±3.01	3.66±0.78	2.51±0.41
230	A	3	13.1±2.65	4.32±1.43	2.98±0.72
	B	4	17.7±2.05	5.02±1.11	3.32±0.30
260	A	6	13.5±4.65	4.01±1.07	2.61±0.65
	B	6	13.6±5.88	4.86±2.19	2.70±0.72
300	A	5	22.3±13.3*	6.20±2.96	4.04±1.45*
	B	5	21.2±5.92	7.27±2.61	4.17±1.22

Dose level (mg/m^2)	Set	n	C_{max} lactone (μg/mL)	$t_{1/2}(\gamma)$ total (h)	$t_{1/2}(\gamma)$ lactone (h)
175	A	1	0.60	12.14	12.80
	B	2	1.07, 1.80	8.48, 11.1	5.43, 7.94
200	A	9	1.04±0.22	14.2±7.80	17.3±10.4
	B	7	1.12±0.22	13.6±5.82	12.2±5.65
230	A	3	1.50±0.68	9.21±2.20	13.4±3.72
	B	4	1.39±0.29	11.5±2.22	9.62±2.61
260	A	6	1.31±0.30	12.6±5.86	12.8±4.21
	B	6	1.38±0.43	11.4±1.81	11.2±2.41
300	A	5	1.71±0.59	11.5±2.97*	12.9±3.67
	B	5	1.97±0.59	12.5±1.72	12.0±2.64

All parameters were obtained from a nonlinear three-compartment computer-fitted model with $1/(concentration)^2$ weighting. Results are shown as mean ± SD. *Abbreviations: n*, number of data sets; AUC, area under the plasma-concentration time curve; C_{max}, maximum plasma concentration; $t_{1/2}(\gamma)$, terminal elimination half-life.

*$n = 4$.

Table 3. Summary of the plasma pharmacokinetic parameters of SN-38 total and lactone after a 90-min i.v. infusion of CPT-11 in the training (A) and validation (B) sets. Data represent mean values ± SD.

Dose level (mg/m^2)	Set	n	$AUC_{0-\infty}$ total (μg.h/mL)	$AUC_{0-\infty}$ lactone (μg.h/mL)	C_{max} total (ng/mL)
175	A	1	0.13	0.07	11.43
	B	2	0.29, 0.35	0.16, 0.17	44.6, 47.4
200	A	9	0.43±0.20	0.21±0.08	36.7±10.9
	B	7	0.30±0.08	0.16±0.05	29.2±7.25
230	A	3	0.39±0.16	0.16±0.04	27.4±3.50
	B	4	0.79±0.46	0.27±0.08	57.9±25.8
260	A	6	0.34±0.18	0.22±0.07	40.3±15.8
	B	6	0.51±0.22	0.31±0.13	44.4±14.5
300	A	5	0.43±0.25	0.33±0.21	47.9±27.6
	B	5	0.51±0.22	0.35±0.14	51.2±18.5

Dose level (mg/m^2)	Set	n	C_{max} lactone (ng/mL)	$t_{1/2}(\gamma)$ total (h)	$t_{1/2}(\gamma)$ lactone (h)
175	A	1	6.52	7.72	6.76
	B	2	27.5, 27.7	16.87, 10.3	13.9, 13.2
200	A	9	25.1±7.33	30.4±15.1	24.8±7.61
	B	7	20.8±7.35	20.3±7.64	19.3±5.09
230	A	3	18.4±5.43	42.0±35.2	18.3±7.99
	B	4	42.8±26.5	29.9±14.5	23.4±6.83
260	A	6	25.7±11.3	23.1±10.6	29.8±15.5
	B	6	31.5±8.00	26.9±10.9	23.0±5.80
300	A	5	36.7±27.2	29.9±18.0	39.9±19.3
	B	5	38.4±12.5	29.8±14.6	30.8±11.7

All parameters were obtained from a nonlinear three-compartment computer-fitted model with $1/(concentration)^2$ weighting. Results are shown as mean ± SD. *Abbreviations: n*, number of data sets; AUC, area under the plasma-concentration time curve; C_{max}, maximum plasma concentration; $t_{1/2}(\gamma)$, terminal elimination half-life.

Table 4. Univariate correlation of CPT-11 and SN-38 (lactone and total) concentrations at each sample-time point with the corresponding AUC in the training-data set.

Time point	CPT-11 lactone		CPT-11 total		SN-38 lactone		SN-38 total	
(h)	n	*r*	n	*r*	n	*r*	n	*r*
0.5	23	0.633	23	0.611	17	0.362	24	0.097
1.5	22	0.607	22	0.790	22	0.478	23	0.332
1.67	21	0.422	23	0.841	19	0.823	23	0.523
1.83	22	0.676	23	0.923	22	0.505	24	0.611
2.0	24	0.473	23	0.929	24	0.691	24	0.651
2.5	23	0.766	23	0.942	22	0.477	24	0.686
3.5	22	0.883	23	0.954	20	0.690	24	0.637
4.5	23	0.857	23	0.959	24	0.686	24	0.712
5.0	23	0.886	23	0.968	23	0.742	24	0.636
5.5	23	0.920	23	0.965	24	0.598	23	0.743
6.5	23	0.873	22	0.950	22	0.486	23	0.661
8.0	21	0.938	21	0.946	20	0.621	22	0.586
12.0	21	0.619	21	0.873	20	0.419	20	0.621
25.5	23	0.842	23	0.898	23	0.426	15	0.480
32.0	20	0.756	22	0.894	19	0.477	12	0.528
49.5	23	0.481	22	0.723	20	0.378	8	0.223
56.0	23	0.396	23	0.712	18	0.377	8	0.126

Abbreviations: n, number of data sets at that specific time point; *r*, Pearson's correlation coefficient.

CPT-11 and SN-38 (both lactone and total) concentrations at each sample-time point were correlated with their AUC by using univariate-regression analysis for the training-data set (Table 4). The correlation coefficient ranged from 0.396 to 0.938 for CPT-11 lactone, from 0.611 to 0.968 for CPT-11 total, from 0.362 to 0.823 for SN-38 lactone and from 0.097 to 0.743 for SN-38 total (Table 4). The best correlation was found at the sample-time point of 5.50 h, taken all substances into account simultaneously. Following this univariate-regression, multivariate-regression with a restriction to models with no more than two additional time points was evaluated. In the trivariate models, sample-time point combinations with the highest correlation and precision (lowest %RMSE), were found at different sample-time points for CPT-11 total, CPT-11 lactone, SN-38 total and SN-38 lactone (data not shown). Assuming the

lactone forms being most predictive for toxicities of the given drug, the best sample-time points for the combination of CPT-11 lactone and SN-38 lactone were used for further model development.

The most predictive sample-time points were found at 0.5, 1.67 and 5.5 h after the start of infusion. In the training-data set, the models of all substances demonstrated little bias, with values for the %MPE ranging from 0.22 to 0.85 (Table 5). In this set, the correlation coefficient of SN-38 total was estimated at 0.764 with a %RMSE of 21.1%, suggesting less correlation and lower accuracy than found for the other compounds (correlation coefficients ranging from 0.903 for SN-38 lactone to 0.982 for CPT-11 total and %RMSE ranging from 6.83 for CPT-11 total to 7.94 for SN-38 lactone).

Table 5. Limited-sampling models for the prediction of the AUCs of CPT-11 lactone and total and of SN-38 lactone and total.

Models:

A $AUC_{CPT\text{-}11\ lactone}$ (µg.h/mL) = $1.11*C_{0.5} + 0.0531*C_{1.67} + 16.53*C_{5.5} + 0.439$

B $AUC_{CPT\text{-}11\ total}$ (µg.h/mL) = $1.84*C_{0.5} + 1.19*C_{1.67} + 11.5*C_{5.5} + 0.215$

C $AUC_{SN\text{-}38\ lactone}$ (µg.h/mL) = $2.46*C_{0.5} + 2.36*C_{1.67} + 9.66*C_{5.5} + 0.0521$

D $AUC_{SN\text{-}38\ total}$ (µg.h/mL) = $-6.27*C_{0.5} + 3.72*C_{1.67} + 20.2*C_{5.5} + 0.121$

Model	Training set			Validation set		
	r	%MPE	%RMSE	*r*	%MPE	%RMSE
A	0.953	0.34	7.88	0.936	0.36	11.3
B	0.982	0.22	6.83	0.966	0.10	3.31
C	0.903	0.52	7.94	0.443	1.06	31.7
D	0.764	0.85	21.1	0.869	1.08	29.8

Abbreviations: r, Pearson's correlation coefficient; %MPE, percentage mean predictive error; %RMSE, percentage root mean-squared predictive error; AUC, area under the plasma-concentration time curve; $C_{0.5}$, $C_{1.67}$ and $C_{5.5}$ are the plasma concentrations in µg/mL at 0.5, 1.67 and 5.5 h after start of infusion.

Next, we used the validation-data set, containing the remaining 24 patients to evaluate the predictive performance of the developed models. For CPT-11 lactone and

total, correlation coefficients were 0.936 and 0.966 respectively, with the %MPE (0.36 and 0.10 respectively) and the %RMSE (11.30 and 3.31 respectively) were low, indicating minor bias and excellent precision (Table 5 and Fig. 3).

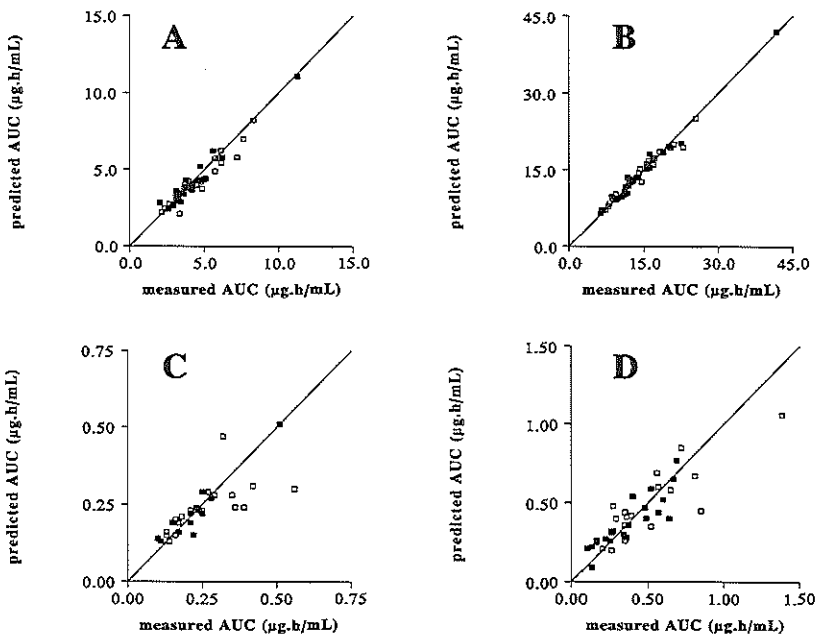

Figure 3. Observed correlations between the measured AUC using a linear three-compartment computer-fitted model with 1/(concentration)^2 weighting and the predicted AUC from the limited sampling models (Table 5) for CPT-11 lactone (**A**), CPT-11 total (**B**), SN-38 lactone (**C**) and SN-38 total (**D**). In all models plasma samples were taken at sample-time points of 0.5, 1.67 and 5.5 h after the start of infusion. Closed symbols represent data from the training set and open symbols data from the validation set. Pearson's correlation coefficients in the training and validation sets were 0.953 and 0.936 for CPT-11 lactone, 0.982 and 0.966 for CPT-11 total, 0.903 and 0.443 for SN-38 lactone, and 0.764 and 0.869 for SN-38 total, respectively. The solid lines represent the lines of identity.

For SN-38 total, similar acceptable data could be obtained using the same model. However, in the validation data-set SN-38 lactone data showed poor results for the correlation coefficient, %MPE and %RMSE, due to a poor correlation between AUC and concentrations at the higher dose levels of CPT-11 (230 to 300 mg/m^2). Hence,

the limited-sampling model was not suitable for prediction of SN-38 lactone AUCs in patients treated at dose levels of CPT-11 higher than 230 mg/m^2.

We also performed an additional analysis to evaluate the use of CPT-11 and SN-38 total concentrations for prediction of the AUCs of the respective lactone drug forms. In general, the best models demonstrated deteriorated correlations and poor accuracy, with values for the %RMSE of up to 42% (data not shown).

DISCUSSION

In recent years, various statistical models have been developed for antineoplastic agents to predict pharmacokinetic parameters from a limited blood sample schedule (15). Previous studies have indicated that such strategies are also feasible for the estimation of CPT-11 and SN-38 pharmacokinetics with the drug given by i.v. infusion, although no differentiation has been made sofar between the lactone and carboxylate forms of the compounds (16-19). In view of the discrepant data published on relationships between drug levels and the observed toxicity, further investigations of CPT-11 kinetics including separate quantitation of the lactone and the total forms of CPT-11 and SN-38 are clearly needed. Previously described limited-sampling models differed considerably in administered dose and infusion duration and are only valid for CPT-11 given as a single agent. In our current study, the follow-up period for sample collection after infusion was much longer as compared to the other studies, resulting in more reliable pharmacokinetic data. Moreover, our limited-sampling models are the first applicable for CPT-11 given in combination with another drug, in this case cisplatin.

To achieve high predictive values for the developed models, i.e. high correlation coefficients and precision with low bias (12), at least three sample-time points were required in all models. Although inclusion of additional samples might have upgraded the predictive performance of the models, fewer samples are more cost-effective and convenient for the patients. In addition, sampling over shorter periods enables pharmacokinetic-pharmacodynamic studies during day-time treatment in an outpatient setting, even in multi-institutional clinical trials.

The pharmacokinetic behavior of SN-38, the principal (active) metabolite of CPT-11, is markedly different from that of the parent drug. The objective of our approach was to accurately predict the AUCs of CPT-11 and SN-38 simultaneously in both lactone and total drug forms, from only three sample-time points. The best compromise for the concurrent determination of the AUCs was found at the sample-time points at 0.5, 1.67 and 5.5 hours after the start of infusion. In selecting these sample-time points, clinical constraints also were taken into consideration. For example, the

samples have to be taken as early as possible after infusion, in view of the potential future usage of CPT-11 in clinical practice with drug-level monitoring for adaptive controlled dosing. In addition, a late sample-time point is not clinically convenient as it makes outpatient treatment difficult or even impossible. For all four limited-sampling models developed, the first sample-time point (at 0.5 h) is critical, for it is part of the ascending part of the concentration-time curves. The second point (at 1.67 h) lies just after the end-of-infusion time-point, and is indicative for near-maximum plasma concentrations of CPT-11 and SN-38. The third sample point (at 5.5 h) is also important for it is part of the descending part of the concentration-time curves. Theoretically, limited-sampling strategies employing other sample-time points which are also predictive, could have been constructed, but would probably lack the above mentioned advantages.

The CPT-11 total AUC is an important pharmacologic parameter, essential for the calculation of the total body clearance and for the calculation of individual metabolic ratios. The active lactone forms, especially that of SN-38, are important as they are assumed to be the real cytotoxic species and responsible for the toxic effects of CPT-11 therapy (8). The proposed models for estimation of the AUCs of CPT-11 lactone and total and SN-38 total were shown to be valid, with excellent predictive utility in a large group of patients given CPT-11 at different dose levels in combination with cisplatin. In case of SN-38 lactone, however, the AUC estimates were slightly biased and less predictable especially at dose levels of >230 mg/m^2. In combination therapy studies, for instance with cisplatin, these high dose levels of CPT-11 may be less relevant for clinical practice, and therefore this model can still be considered useful in a normal clinical setting. Other studies confirmed the variable and less predictive behavior of SN-38 in limited-sampling model development, probably due to the complex pharmacokinetics of this metabolite (20-22).

In future clinical studies, our limited-sampling models will enable prediction of the systemic exposure to CPT-11 and SN-38. Studies to examine the relationships between CPT-11 and SN-38 pharmacokinetics and pharmacodynamics could be explored conveniently using our model and sampling strategy. In our continued investigations, we will be examining these relationships in a future clinical phase II trial with combined CPT-11 and cisplatin chemotherapy.

REFERENCES

1. Creemers GJ, Lund B, Verweij J. Topoisomerase I inhibitors: topotecan and irinotecan. Cancer Treat Rev 20: 73-96, 1994
2. Gerrits CJH, De Jonge MJA, Schellens JHM, Stoter G, Verweij J. Topoisomerase I inhibitors: the relevance of prolonged exposure for present clinical development. Br J Cancer 76: 952-962, 1997

3. De Jonge MJA, Sparreboom A, Verweij J. The development of combination therapy involving camptothecins: a review of preclinical and early clinical studies. Cancer Treatm Rev 24: 205-220, 1998
4. Giovanella BC, Stehlin JS, Wall ME, et al. DNA topoisomerase I-targeted chemotherapy of human colon cancer in xenografts. Science 246: 1046-1048, 1989
5. Hertzberg RP, Caranfa MJ, Holden KG, et al. Modification of the hydroxy-lactone ring of camptothecin: inhibition of mammalian topoisomerase I and biological activity. J Med Chem 32: 715-721, 1989
6. Mi Z, Malak H, Burke TG. Reduced albumin binding promotes the stability and activity of topotecan in human blood. Biochemistry 34: 13722-13728, 1995
7. Bleiberg H, Cvitkovic E. Characterisation and clinical management of CPT-11 (irinotecan)-induced adverse events: the European perspective. Eur J Cancer 32A: S18-S23, 1996
8. Takimoto CH, Arbuck SG. The camptothecins. In: Chabner BA, Longo DL, eds. Cancer Chemotherapy and Biotherapy. Philadelphia: Lippincott-Raven Publishers, 463-484, 1996
9. Rowinsky EK, Grochow LB, Ettinger DS, et al. Phase I and pharmacological study of the novel topoisomerase I inhibitor 7-ethyl-10-[4-(1-piperidino)-1-piperidino] carbonyloxycamptothecin (CPT-11) administered as a ninety-minute infusion every 3 weeks. Cancer Res 54: 427-436, 1994
10. Verweij J, De Jonge MJA, Sparreboom A, et al. Phase I and pharmacokinetic study of irinotecan (CPT-11) and cisplatin in patients with solid tumors. Proc Am Assoc Clin Oncol 17: 188a, 1998 (abstract)
11. De Bruijn P, Verweij J, Loos WJ, Nooter K, Stoter G, Sparreboom A. Determina-tion of irinotecan (CPT-11) and its active metabolite SN-38 in human plasma by reversed-phase high-performance liquid chromatography with fluorescence detection. J Chromatogr 698: 277-285, 1997
12. Sparreboom A, De Jonge MJA, De Bruijn P, et al. Irinotecan (CPT-11) metabolism and disposition in cancer patients. Clin Cancer Res 4: 2747-2754, 1998
13. Sheiner LB, Beal SL. Some suggestions for measuring predictive performance. J Pharmacokin Biopharm 9: 503-512, 1981
14. Rivory LP, Chatelut E, Canal P, Mathieu-Boué A, Robert J. Kinetics of the *in vivo* interconversion of the carboxylate and lactone forms of irinotecan (CPT-11) and of its metabolite SN-38 in patients. Cancer Res 54: 6330-6333, 1994
15. Van Warmerdam LJC, Ten Bokkel Huinink WW, Maes RAA, Beijnen JH. Limited-sampling models for anticancer agents. J Cancer Res Clin Oncol 120: 427-433, 1994
16. Chabot GG. Limited sampling models for simultaneous estimation of the pharmacokinetics of irinotecan and its active metabolite SN-38. Cancer Chemother Pharmacol 36: 463-472, 1995
17. Sasaki Y, Mizuno S, Fujii H, et al. A limited sampling model for estimating pharmacokinetics of CPT-11 and its metabolite SN-38. Jpn J Cancer Res 86: 117-123, 1995
18. Nakashima H, Lieberman R, Karato A, et al. Efficient sampling strategies for forecasting pharmacokinetic parameters of irinotecan (CPT-11): implication for area under the concentration-time curve monitoring. Ther Drug Monit 17: 221-229, 1995
19. Mick R, Gupta E, Vokes EE, Ratain MJ. Limited-sampling models for irinotecan pharmacokinetics-pharmacodynamics: prediction of biliary index and intestinal toxicity. J Clin Oncol 14: 2012-2019, 1996
20. Canal P, Gay C, Dezeuze A, et al. Pharmacokinetics and pharmacodynamics of irinotecan during a phase II clinical trial in colorectal cancer. J Clin Oncol 14: 2688-2695, 1996

21. Chabot GG, Abigerges D, Catimel G, et al. Population pharmacokinetics and pharmacodynamics of irinotecan (CPT-11) and active metabolite SN-38 during phase I trials. Ann Oncol 6: 141-151, 1995
22. Chabot GG. Clinical pharmacokinetics of irinotecan. Clin Pharmacokin 33: 245-259, 1997

Chapter Four

Clinical Pharmacokinetics of Irinotecan and its Metabolites: A Population Analysis

Journal of Clinical Oncology, 20: 3293-3301, 2002

Rujia Xie[1]
Ron H.J. Mathijssen[2]
Alex Sparreboom[2]
Jaap Verweij[2]
Mats O. Karlsson[1]

[1]Department of Pharmaceutical Biosciences, Uppsala University
Uppsala, Sweden

[2]Department of Medical Oncology, Erasmus MC - Daniel den Hoed
Rotterdam, The Netherlands

ABSTRACT

Purpose: To build population pharmacokinetic (PK) models for irinotecan (CPT-11) and its currently identified metabolites.

Patients and Methods: Seventy cancer patients (24 women and 46 men) received 90-minute intravenous infusions of CPT-11 in the dose range of 175 to 300 mg/m^2. The PK models were developed to describe plasma concentration profiles of the lactone and carboxylate forms of CPT-11 and 7-ethyl-10-hydroxy-camptothecin (SN-38) and the total forms of SN-38 glucuronide (SN-38G), 7-ethyl-10-[4-*N*-(5-aminopentanoic acid)-1-piperidino]-carbonyloxycamptothecin (APC) and 7-ethyl-10-[4-amino-1-piperidino]-carbonyloxycamptothecin (NPC) by using NONMEM.

Results: The interconversion between the lactone and carboxylate forms of CPT-11 was relatively rapid, with an equilibration half-life of 14 minutes in the central compartment and hydrolysis occurring at a rate five times faster than lactonization. The same interconversion also occured in peripheral compartments. CPT-11 lactone had extensive tissue distribution (steady-state volume of distribution [V_{ss}], 445 L) compared with the carboxylate form (V_{ss}, 78 L, excluding peripherally formed CPT-11 carboxylate). Clearance (CL) was higher for the lactone form (74.3 L/h), compared with the carboxylate form (12.3 L/h). During metabolite data modeling, goodness of fit indicated a preference of SN-38 and NPC to be formed out of the lactone form of CPT-11, whereas APC could be modeled best by presuming formation from CPT-11 carboxylate. The interconversion between SN-38 lactone and carboxylate was slower than that of CPT-11, with the lactone form dominating at equilibrium. The CLs for SN-38 lactone and carboxylate were similar, but the lactone form had more extensive tissue distribution.

Conclusion: Plasma data of CPT-11 and metabolites could be adequately described by this compartmental model, which may be useful in predicting the time courses, including interindividual variability, of all characterized substances after intravenous administration of CPT-11.

INTRODUCTION

Irinotecan (CPT-11), an inhibitor of DNA topoisomerase I, is widely used in the treatment of several types of tumors, including colorectal cancer (1). CPT-11 is extensively metabolized in the liver to various metabolites. It is cleaved enzymatically by carboxylesterases to form 7-ethyl-10-hydroxycamptothecin (SN-38), which has cytotoxic activity that is 100 to 1,000 times greater than that of the parent drug (2). SN-38 is further conjugated to an inactive glucuronide (SN-38G) by uridine diphosphate

glucuronosyltransferases (3, 4). Other CPT-11 metabolites identified are the major plasma metabolite 7-ethyl-10-[4-*N*-(5-aminopentanoic acid)-1-piperidino]-carbonyloxycamptothecin (APC) and 7-ethyl-10-[4-amino-1-piperidino]-carbonyloxycamptothecin (NPC), resulting from a ring-opening oxidation of the terminal piperidine ring of CPT-11 mediated by cytochrome P450 3A4 enzymes (5, 6).

CPT-11 and its metabolites contain a α-hydroxy-δ-lactone ring, which is chemically unstable and undergoes pH-dependent reversible hydrolysis to a hydroxyl-carboxylate form. An intact lactone group is essential for interaction with the DNA-enzyme complex (7). Therefore, the pharmacokinetics (PK) of CPT-11 lactone and SN-38 lactone are of particular interest. Individual plasma concentrations of CPT-11 and its four currently identified metabolites can be described by three-compartment models (8). Others report that two- or three-compartment models may be used to fit CPT-11 and SN-38 concentration profiles with non-compartmental or compartment approaches (9-12). Ma *et al.* (13) have analyzed individual concentration data of total forms of CPT-11, SN-38, and APC simultaneously by using a four-compartmental model with the assumption of an identical volume of distribution for these substances. The PK of the lactone and carboxylate forms of CPT-11 and SN-38 were investigated previously (9-11, 14), but parameters other then the area under the curve (AUC) of SN-38 were not estimated. The clinical PK, metabolism, and pharmacodynamics of CPT-11 have been widely studied to date (see reviews 9-11). However, for the metabolites, most publications limit the PK analysis to reporting on the AUC ratio of metabolite to parent drug.

In this study, we used nonlinear mixed-effect modeling to analyze data from all patients simultaneously and considered the influence of covariates on the PK parameters. The purposes of this study were to build suitable PK models for CPT-11 and four of its metabolites, including lactone and carboxylate forms, to more clearly understand the PK interrelations between the parent drug and metabolites, and to provide potentially useful information for clinical treatment of CPT-11.

PATIENTS AND METHODS

Patients and study design

Patients with a histologically or cytologically proven malignant solid tumor were treated with CPT-11 intravenously between May 1996 and October 1999 at the Erasmus MC (Rotterdam, the Netherlands). Criteria for eligibility included the following: (*a*) age younger than 75 years; (*b*) an Eastern Cooperative Oncology Group performance status ≤2; (*c*) adequate hematologic function (WBC ≥ 3.0×10^9/L, absolute neutrophil count ≥ 2.0×10^9/L, and platelet count ≥ 100×10^9/L), hepatic

function (total serum bilirubin ≤ 1.25 times the upper limit of normal and AST and ALT levels ≤ 3.0 times the upper limit of normal), and renal function (serum creatinine ≤ 135 μM or creatinine clearance ≥ 60 mL/min); (*d*) no previous anticancer treatment for at least 4 weeks, or 6 weeks in case of nitrosoureas or mitomycin; and (*e*) no previous therapy with other topoisomerase I inhibitors. The clinical protocol was approved by the Erasmus MC Ethical Board, and all patients gave written, informed consent before study entry.

CPT-11 lactone was administered in a 3-weekly regimen as a 90-minute intravenous infusion in the dose range of 175 to 300 mg/m^2, after dilution of the pharmaceutical preparation in 250 mL of isotonic sodium chloride. In all patients, premedication consisted of ondansetron (8 mg intravenously) combined with dexamethasone (10 mg intravenously), both administered 30 minutes before the start of CPT-11 infusion. Delayed-type diarrhea was treated with loperamide (4 mg), followed by 2 mg every 2 hours for a 12-hour time period after the last liquid stool.

Frequent sampling was performed before dosing and at approximately 0, 0.5, 1.5, 1.67, 1.83, 2, 2.5, 3.5, 4.5, 5, 5.5, 6.5, 8, 12, 25.5, 49, and 56 hours. Venous blood was drawn from the arm opposite the one used for infusion, and plasma was separated by centrifugation (3,000 × *g* for 5 minutes at 4°C). Plasma samples were stored at -80°C and analyzed for the lactone and total drug forms of CPT-11 and SN-38 and for the total drug forms only of APC, NPC, and SN-38G by using reversed-phase high-performance liquid chromatography with fluorescence detection, as described previously (15). Because of limited sample supply, concentrations could not be determined for all metabolites in all samples.

PK modeling

The PK models for CPT-11 and four of its metabolites were sequentially built, and the PK analysis was based on multicompartmental models (up to three compartments for each substance). CPT-11 lactone concentrations were first analyzed neglecting any interconversion with the carboxylate form (step 0). This analysis was performed to allow some direct comparison between this analysis and previous analyses that did not consider the pH-dependent lactone-carboxylate interconversion. Thereafter, both lactone and total forms of CPT-11 data were simultaneously analyzed allowing for interconversion and assuming that total CPT-11 was the sum of lactone and carboxylate concentrations (step 1). Models were parameterized in terms of clearances (CLs) and volumes of distribution, whereas rate constants were used for quantifying the interconversion between lactone and carboxylate forms.

For all metabolites except SN-38G, we tested whether the concentration-time data were best described by formation from CPT-11 lactone, CPT-11 carboxylate or a

combination of these two. For SN-38G, models with formation from SN-38 lactone, SN-38 carboxylate, or both were tested. For each model, we tested whether the formation of metabolites was proportional to the dose, which is likely to be the case for a major metabolite, or whether it was proportional to the AUC of CPT-11, which is more likely to be the case for a minor metabolite. For the former, metabolite disposition parameters were expressed as ratios with the fraction of the dose metabolized to the particular metabolite. For the latter, metabolite parameters were expressed as ratios with the CL associated with formation of the metabolite in question (CL_f). The individual CPT-11 lactone or carboxylate concentration-time profile, or both, from step 1 was used as the input for metabolite formation. Models based on lactone and carboxylate interconversion were simultaneously developed for SN-38 lactone and total concentrations (step 2), and then a model for SN-38G was developed, with individual parameters of SN-38 lactone and carboxylate from the final model of step 2 being fixed (step 3). As for CPT-11, the total concentrations of SN-38 were assumed to be the sum of lactone and carboxylate concentrations. Models containing an enterohepatic-cycle component were tested to describe SN-38 and SN-38G data. One strategy to do this was by presuming an extra biliary compartment to store part of the eliminated SN-38G; after a certain (estimated) time period stored SN-38G would be released to another extra compartment (intestine) to be deconjugated to SN-38. Another model, assuming that an oral dose was given to generate rebound concentrations of SN-38, was tested for improvement of the description of the data. Finally, models for APC (step 4) and NPC (step 5) were developed.

Candidate covariate relations for covariate models were built on the basis of individual parameters from the basic model by using generalized additive models (16). The covariates that resulted in a significant decrease in the Akaike information criterion were introduced into the model and tested. The covariates considered were age (median, 54 years; range, 36 to 71 years), sex (24 women and 46 men), and body-surface area (BSA; median, 1.86 m^2; range, 1.35 to 2.5 m^2).

The models were fitted to the data from all individuals simultaneously using NONMEM VI (University of California, San Francisco, CA) with first-order conditional estimation with interaction (17). The parameter for a specific subject (P_i) can be described by equation 1:

$$P_i = P_{pop} * exp(\eta_i) \qquad \text{(eq.1)}$$

where P_{pop} is the parameter for a typical individual and η_i is a symmetrically distributed zero-mean variable with SD ω. Several factors may cause interindividual correlations between all disposition parameters of a metabolite, but a major cause for such

correlations may be interindividual variability in the fraction of the dose forming the metabolite. We chose to parameterize the models so that any such correlation was expressed as variability in the fraction of dose forming the metabolite, because this may aid interpretation and simplify and have no detrimental effects on the fit of the models to the data.

In mixed-effect models, the residual error is the difference between the observed concentration (C_{obs}) and the predicted value (C_{pred}) by P_i. The residual error model was characterized by both additive and proportional components:

$$C_{obs} = C_{pred}^{*} (1 + \varepsilon_1) + \varepsilon_2 \qquad \text{(eq. 2)}$$

where ε_1 and ε_2 are zero-mean normally distributed variables with SDs σ_1 and σ_2, respectively.

The model selection was guided by the decrease in the objection function value (OFV; -2*log likelihood), as well as by using graphical goodness-of-fit analysis with Xpose 3.0 (Uppsala University, Uppsala, Sweden; ref 18). To statistically distinguish between hierarchical models, the difference in the OFV was used because the difference is approximately χ^2 distributed. A significance level of $P < .001$ was used; this corresponded to a difference in OFV of 10.8 for 1 df. Parameter uncertainty was expressed as RSE%, which is the estimate of SE obtained as part of the standard NONMEM output, divided by the parameter value.

RESULTS

Forty-six male and 24 female cancer patients received CPT-11 as a 90-minute intravenous infusion (range, 1.3 to 1.9 h) at doses ranging from 175 to 300 mg/m^2. The predominant tumor types were colorectal cancer (n = 38), adenocarcinoma of unknown primary origin (n = 8), head and neck cancer (n = 5), and non-small-cell lung cancer (n = 4). Sixteen patients were also sampled during a second course, and the median time interval between two doses was 23 days (range, 11 to 38 days).

The observed concentration-time profiles of CPT-11 and its four metabolites are shown in Fig 1, and all concentration units are nanograms per milliliter. The principal components of the model that resulted from the analysis are presented in Fig 2. Overall, CPT-11 carboxylate concentrations were higher than those of CPT-11 lactone, whereas concentrations of SN-38 carboxylate were lower than those of the lactone form. Both SN-38G and APC plasma concentrations were relatively high, whereas those of NPC were low.

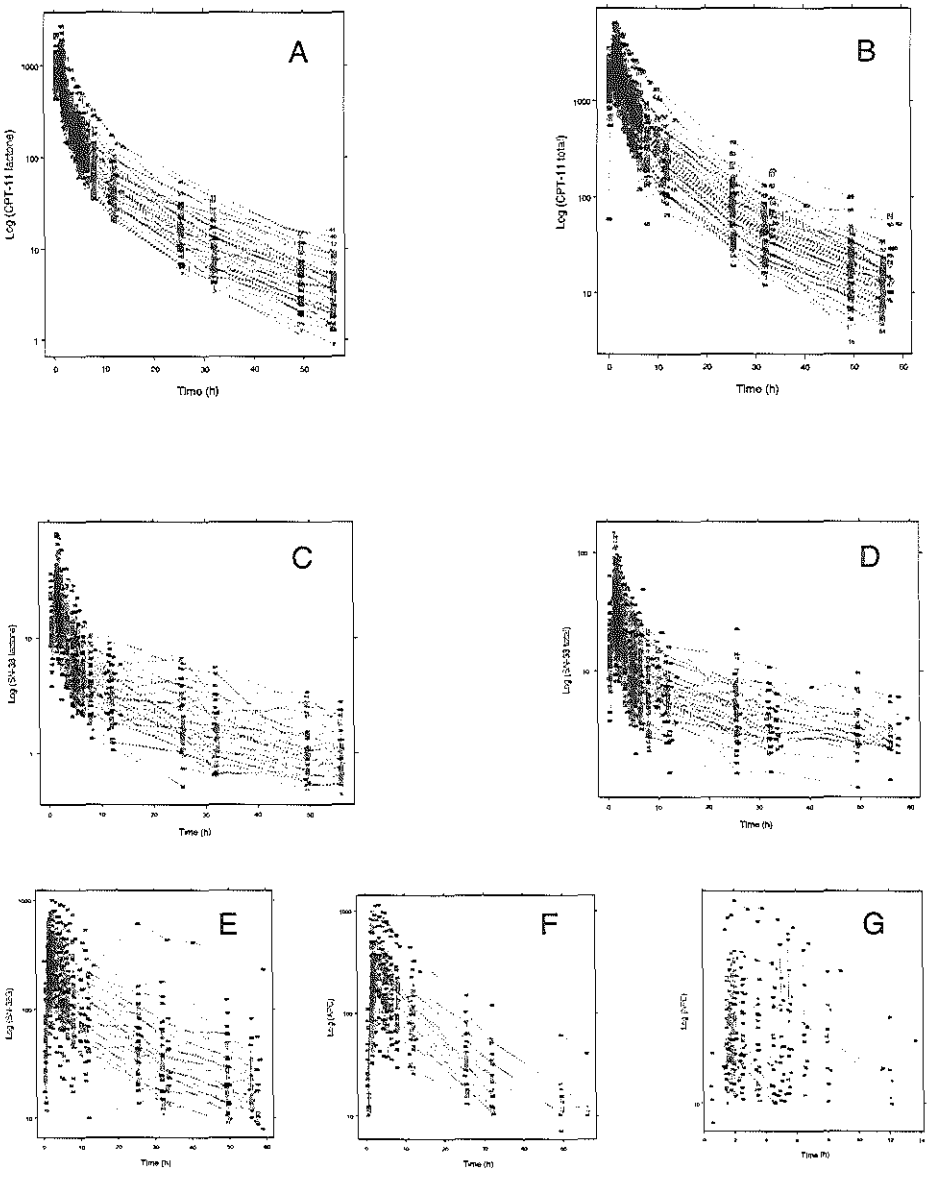

Figure 1. Logarithmic observed concentration-time profiles of (**A**) CPT-11 lactone, (**B**) CPT-11 total, (**C**) SN-38 lactone, (**D**) SN-38 total, (**E**) SN-38G, (**F**) APC, and (**G**) NPC. All concentration units are ng/mL.

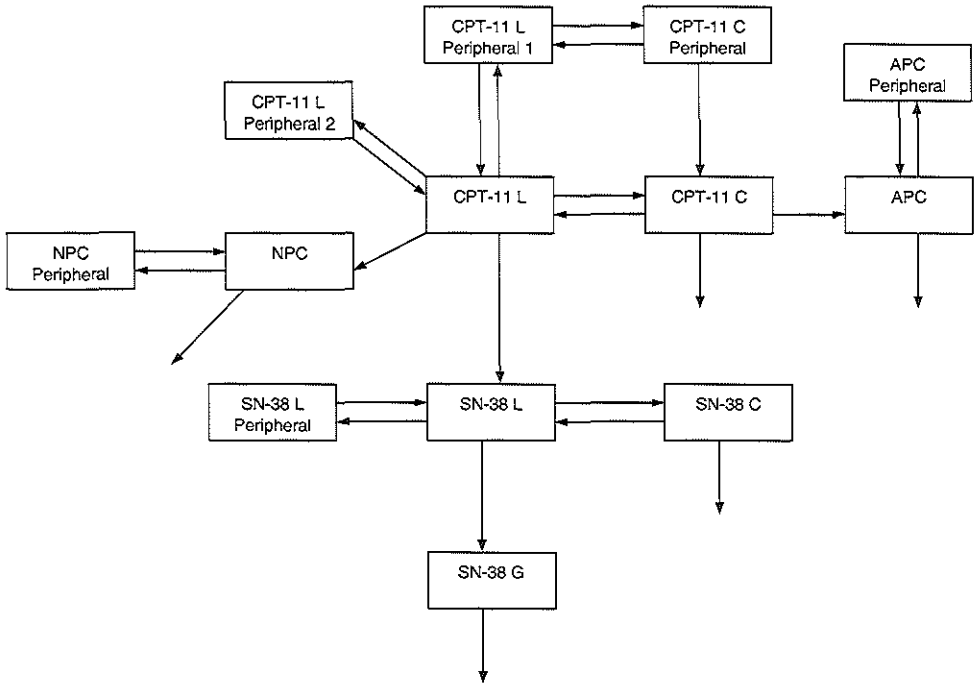

Figure 2. The compartmental pharmacokinetic models for CPT-11 lactone (L) and carboxylate (C), SN-38 L and C, SN-38G, APC, and NPC.

The best model to describe CPT-11 lactone data alone was a three-compartment model with CL estimated to be 107 L/h (57.5 L/h/m^2; step 0). In the joint model for CPT-11 lactone and carboxylate forms (step 1), disposition could be characterized with a three- and two-compartment model for CPT-11 lactone and carboxylate, respectively (Fig 3). The model with interconversion between lactone and carboxylate in the central compartments, as well as in the peripheral compartments, provides the best model for both lactone and total forms of CPT-11. The intercompartmental CL and volume of distribution of the peripheral compartment for CPT-11 carboxylate were estimated to be small (0.0009 L/h and 0.01 L, respectively), but the OFV decreased by more than 1,000 compared with a one-compartment model for CPT-11 carboxylate. A re-parametrization, using rate constants between the central and peripheral compartment of the carboxylate, was applied for the CPT-11 model. The rate constant from central to peripheral of CPT-11 carboxylate was close to 0, according to the estimates of CL and volume of distribution, so this rate constant was fixed at 0, and the volume of distribution in the peripheral compartment was (arbitrarily) fixed to the corresponding value for the lactone in the final model with re-parameterization to the rate constant.

Such a model predicted that CPT-11 carboxylate would not have multicompartmental characteristics were it not formed peripherally from the lactone form. However, because the mass flow of carboxylate is unidirectional from the peripheral compartment to the central, there is no information (or effect on the predictions) on the size of the peripheral carboxylate compartment. The population CL (12.3 L/h) and the steady-state volume of distribution (78 L, excluding peripherally formed carboxylate) of the carboxylate form were six-fold smaller than those of the lactone form (Table 1).

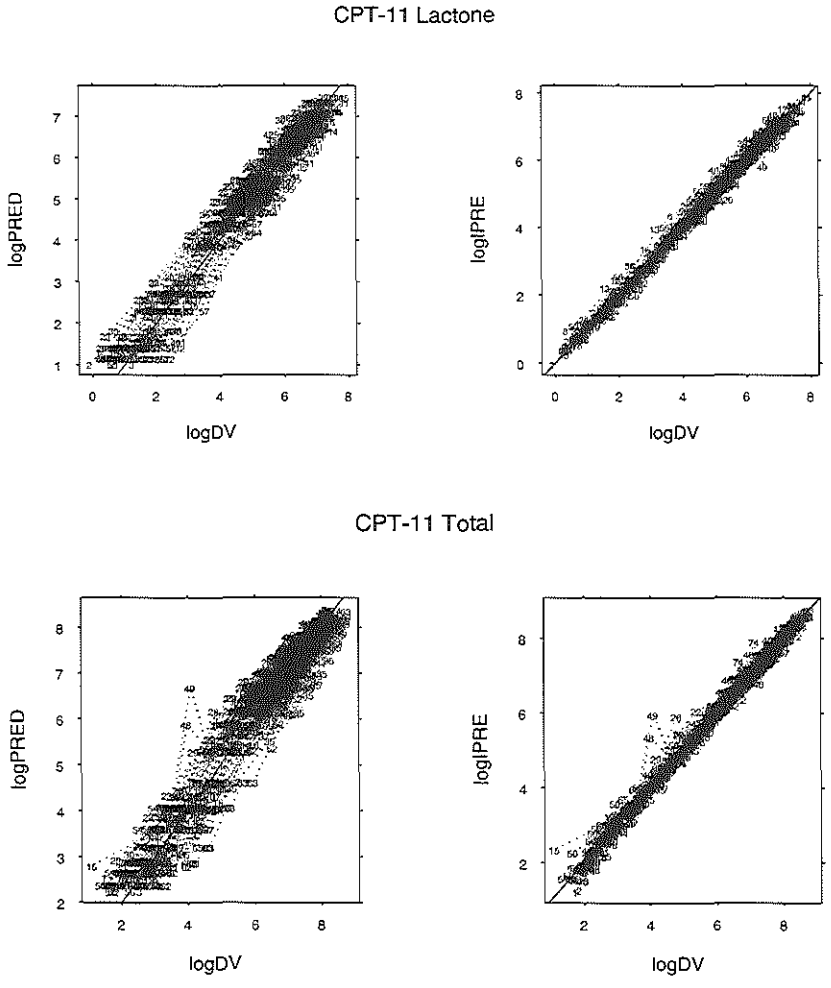

Figure 3. Logarithm of population predictions (logPRED) and individual predictions (logIPRE) versus the logarithm of observations (logDV; DV, dependent variable) of CPT-11 lactone and CPT-11 total. All concentration units are ng/mL.

Table 1. Population PK parameter of estimates and associated interindividual variability of CPT-11 lactone and carboxylate (step 1).

Parameter	Estimate (RSE%)	IIV% (RSE%)
Lactone		
CL_L (L/h/m^2)	39.9 (27)	38 (50)
Q_{L2} (L/h/m^2)	94.1 (22)	95 (43)
Q_{L3} (L/h/m^2)	7.3 (15)	41 (40)
V_{L1} (L/m^2)	20.7 (7.4)	NE
V_{L2} (L/m^2)	47.4 (11)	40 (41)
V_{L3} (L/m^2)	171 (8.2)	41 (40)
k_{L1C1} (h^{-1})	3 (14)	31 (47)
k_{L2C2} (h^{-1})	0.465 (8.2)	NE
Carboxylate		
CL_C (L/h/m^2)	6.6 (54)	19 (62)
k_{C21} (h^{-1})	0.0936 (20)	NE
V_{C1} (L/m^2)	41.8 (15)	22 (37)
V_{C2} (L/m^2)	47.4 (11)*	40 (41)*
k_{C1L1} (h^{-1})	0.64 (14)	19 (62)
k_{C2L2} (h^{-1})	0.0921 (22)	NE

Abbreviations: RSE%, estimate of SE, divided by parameter value; IIV, interindividual variability; CL_L, clearance of CPT-11 lactone; CL_C, clearance of CPT-11 carboxylate; Q, intercompartment clearance; V, volume of distribution; k_{LC}, interconversion rate constant from lactone to carboxylate; k_{CL}, interconversion rate constant from carboxylate to lactone; 1, 2, and 3, denoted to compartment 1, 2, and 3; NE not estimated.

* Value is arbitrary set to the same value as for lactone.

The interindividual variability for parameters of CPT-11 lactone was generally high, with post hoc estimates of CL ranging from 24.8 to 149.9 L/h for the lactone form and 6.6 to 19.5 L/h for the carboxylate form. BSA was the only significant covariate included in the model and had a decrease in OFV of 26.99 compared with the basic model. For a typical individual with a BSA of 1.86 m^2, the CL and steady-state volume of distribution of CPT-11 lactone were 39.9 L/h/m^2 and 239 L/m^2, respectively.

SN-38 concentrations were best described by a two-compartment model for the lactone form and a one-compartmental model for the carboxylate form, where the formation occurred from CPT-11 lactone in the central compartment to SN-38 lactone

in the central compartment (Fig 4). In the model, SN-38 lactone formation was better described as proportional to the dose of CPT-11, rather than proportional to the AUC of CPT-11 lactone. Unlike CPT-11, SN-38 lactone and carboxylate forms had similar CL values, whereas, as for CPT-11, the lactone form had more extensive tissue distribution (Table 2). A one-compartment model, with formation from SN-38 lactone, adequately described the SN-38G data (Fig 5). SN-38G formation was better described as proportional to the dose of CPT-11 than to the AUC of SN-38 lactone. Both SN-38 and SN-38G had substantial formation variability. In the most successful model, SN-38G was formed out of SN-38 lactone (Fig 2 and Table 2).

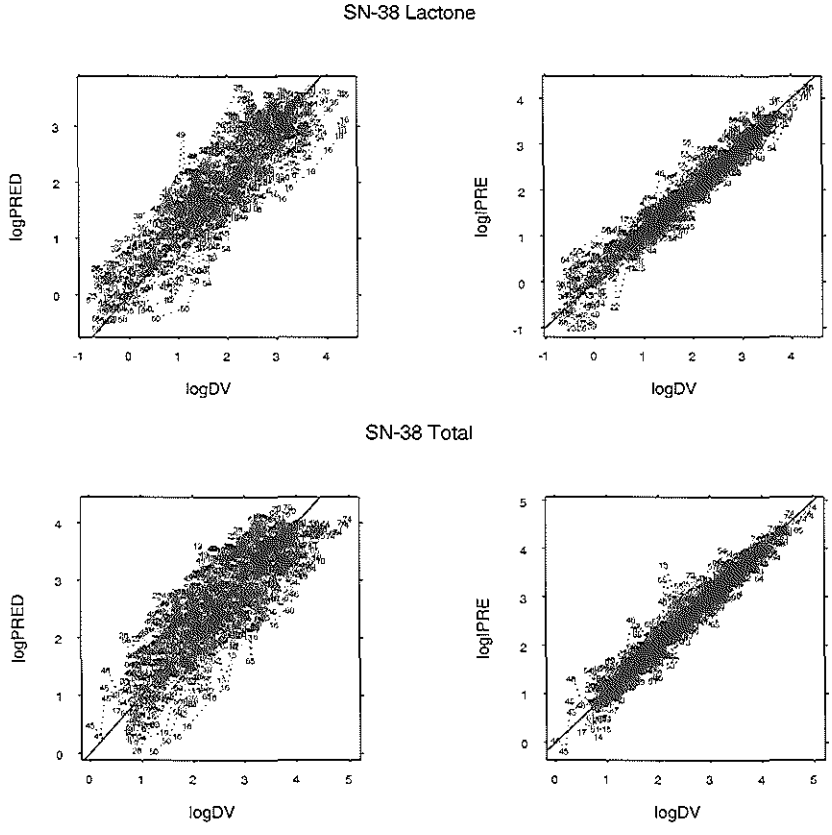

Figure 4. Logarithm of population predictions (logPRED) and individual predictions (logIPRE) versus the logarithm of observations (logDV; DV, dependent variable) of SN-38 lactone and SN-38 total. All concentration units are ng/mL.

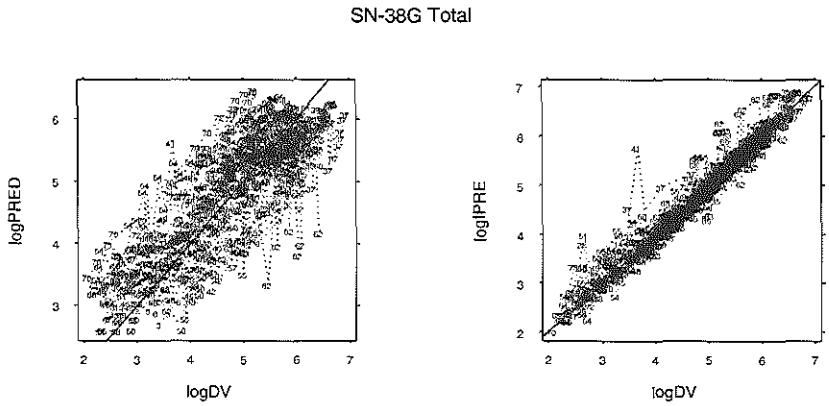

Figure 5. Logarithm of population predictions (logPRED) and individual predictions (logIPRE) versus the logarithm of observations (logDV; DV, dependent variable) of SN-38G total. All concentration units are ng/ml.

Table 2. Population PK parameter of estimates and associated interindividual variability of SN-38 lactone and carboxylate and total SN-38G.

Parameter	Estimate (RSE%)	IIV% (RSE%)
SN-38 lactone		
$CL/F_{m,SNL}$ (L/h)	2,220 (20)	40 (82)
$Q/F_{m,SNL}$ (L/h)	5,480 (7.9)	40 (22)
$V/F_{m,SNL1}$ (L)	10,700 (12)	40 (23)
$V/F_{m,SNL2}$ (L)	66,300 (7.8)	22 (85)
k_{L1C1} (h^{-1})	0.319 (27)	NE
Formation variability		40 (23)
SN-38 carboxylate		
$CL/F_{m,SNC}$ (L/h)	2,030 (40)	29 (110)
$V/F_{m,SNC}$ (L)	4,720 (19)	46 (46)
k_{C1L1} (h^{-1})	0.835 (23)	29 (110)
SN-38G		
$CL/F_{m,SNG}$ (L/h)	115 (9.8)	34 (26)
$V/F_{m,SNG}$ (L)	150 (7.9)	23 (100)
Formation variability		54 (16)

Abbreviations: F_m, formation fraction; SNL, SN-38 lactone; SNC, SN-38 carboxylate.

A relatively high interindividual variability was found for the disposition parameters and formation variability of SN-38 lactone and carboxylate and SN-38G (Table 2). Rebound concentrations of SN-38 and SN-38G were observed in some subjects, but the models with an enterohepatic recycling component were unsuccessful, possibly because of a lack of information of the recycling process. No significant covariate relations were identified for SN-38 or SN-38G.

A 2-compartment model best described the total concentration data of APC with formation from CPT-11 carboxylate (Fig 6). Formation was better described as proportional to the AUC of CPT-11 carboxylate rather than the CPT-11 dose. Age was found to be a statistically significant covariate for the CL of APC. The typical CL ratio (CL/CL_f) was 2.62 at an age of 55 years (Table 3), with a change of 1.4% per year. The only interindividual variability component was in the fraction forming APC, which was estimated to be 48%.

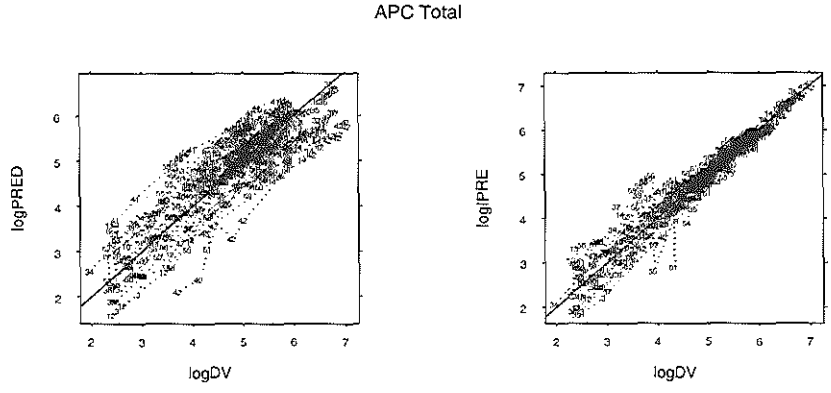

Figure 6. Logarithm of population predictions (logPRED) and individual predictions (logIPRE) versus the logarithm of observations (logDV; DV, dependent variables) of APC total. All concentration units are ng/mL.

A two-compartment model with formation from CPT-11 lactone best described the concentration-time profiles of NPC (Fig 7). Formation was better described as being proportional to the AUC of CPT-11 lactone rather than the CPT-11 dose. The interindividual variability in CL was 110%; this might be due to one individual's having much higher NPC concentrations as compared with other individuals (2.2 to 11.7 times higher). In an analysis without that individual, the variability decreased to 43%. Considering the large effect of this individual on the variability component, final parameters of NPC are listed without this patient (Table 3). No statistically significant covariate relations were found for NPC.

Table 3. Population PK parameter of estimates and associated interindividual variability of total APC and NPC.

Parameter	Estimate (RSE%)	IIV% (RSE%)
APC		
CL_{APC}/CL_f *	2.62 (8)	NE
Q_{APC}/CL_f	1.68 (12)	NE
V_{APC1}/CL_f (h)	2.66 (9.7)	NE
V_{APC2}/CL_f (h)	5.91 (11)	NE
Factor for age	-0.0142 (55)	
Formation variability (%)		48 (22)
NPC**		
CL_{NPC}/CL_f	8.85 (16)	43 (62)
Q_{NPC}/CL_f	1.77 (24)	120 (28)
V_{NPC1}/CL_f (h)	5.41 (8.1)	43 (62)
V_{NPC2}/CL_f (h)	197 (6)	NE

* CL included age, expressed as: $CL= \theta_1*[1+\theta_2*(age-55)]*exp(\eta_1)$.

** One individual was excluded from the data set.

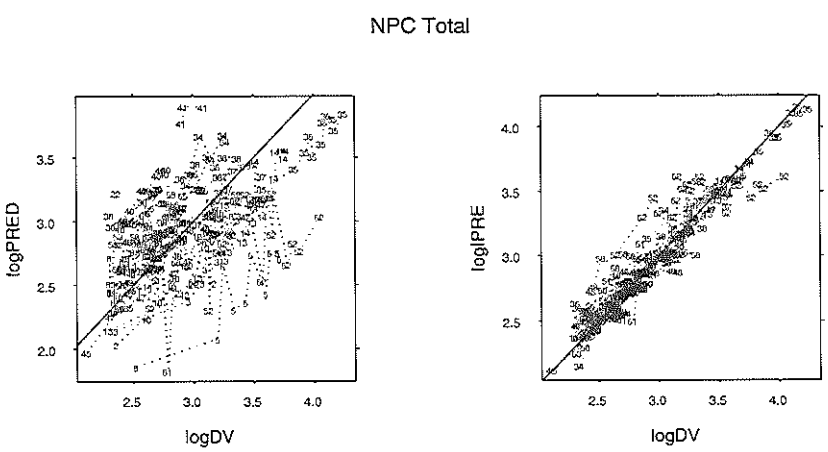

Figure 7. Logarithm of population predictions (logPRED) and individual predictions (logIPRE) versus the logarithm of observations (logDV) of NPC total. All concentration units are ng/mL.

Finally, the typical values of parameters for CPT-11, SN-38, SN-38G, APC or NPC (Tables 1 to 3) were used in a simulation for a typical individual with a BSA of 1.86 m^2, receiving a 1-hour infusion at a standard dose of 350 mg/m^2. The simulated concentration-time profiles are presented in Fig 8. The terminal half-lives based on this simulation were 18.3, 18.1, 24.2, 24.2, 24.2, 18.3, and 33.3 hours for CPT-11 lactone, CPT-11 total, SN-38 lactone, SN-38 total, SN-38G, APC, and NPC, respectively. Of the dose administered, 74% was eliminated as CPT-11 lactone and 26% as CPT-11 carboxylate.

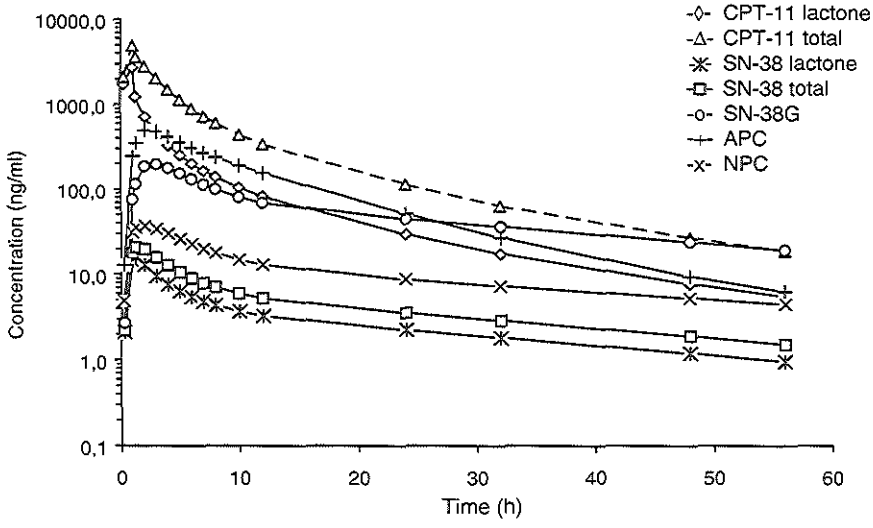

Figure 8. Simulated concentration-time profiles: CPT-11 lactone and total, SN-38 lactone and total, SN-38G, APC and NPC for a typical individual with a BSA of 1.86 m^2, receiving CPT-11 lactone infusion for 1 hour at a dose of 350 mg/m^2, based on population estimates of corresponding compounds.

DISCUSSION

The clinical PK of CPT-11 has been extensively reported on in the literature (9, 10, 14). The current investigation may add to that knowledge because (i) it is the first model-based analysis that takes into account the interconversion between lactone and

carboxylate forms, (ii) it reports more extensively on the PK of CPT-11 metabolites, and (iii) the database is substantially larger than the ones used in previous reports. In addition, we introduce parameterizations of population PK models that allow additional information compared with standard models to be extracted from metabolite data.

The CL estimate of 107 L/h (57.5 L/h/m^2) in the analysis of the lactone form of CPT-11 that ignores the carboxylate interconversion (step 0) is in good agreement with previously reported values from similar analyses (39 to 75.1 L/h/m^2; ref. 8, 12, 19). Similarly, the steady-state volume of distribution estimate of 722 L (388 L/m^2) is in good agreement with previously reported values (8) of 601 to 871 L but is somewhat larger than a reported value (12) of 263 L/m^2. Also, the full model, including conversion between lactone and carboxylate, predicts similar value of CL (100 L/h; see Appendix).

As mentioned previously, CPT-11 and its metabolites contain a lactone ring, which undergoes a pH-dependent equilibrium with the carboxylate form (20). At physiologic pH, the carboxylate form of CPT-11 dominates in plasma. However, only the lactone form has antitumor activity (7). Therefore, it is of interest to differentiate the PK of the lactone form from the total drug form (i.e., lactone plus carboxylate) of CPT-11. From the model that considers the lactone-carboxylate interconversion, a relatively rapid interconversion of CPT-11 lactone to carboxylate was found with a half-life of 14 minutes, which is close to the previously published value of 9.4 minutes (12). Population estimates of CL and steady-state volume of distribution of CPT-11 lactone were 39.9 L/h/m^2 and 239 L/m^2. The CL of CPT-11 lactone was six times higher than that of the carboxylate form. Published CL values of CPT-11 total are in the range of 12 to 24 L/h/m^2 during short time infusions (30 to 90 minutes; ref. 8, 9, 21). Our model predicts a CL of 18 L/h/m^2 for total CPT-11 (see Appendix). The difference between lactone and total forms in CL may partly be explained by a lower distribution of the carboxylate form into the liver. The analysis also suggests a different metabolic pathway for CPT-11 carboxylate, with formation of APC while SN-38 and NPC are formed from CPT-11 lactone. CPT-11 lactone displayed extensive tissue distribution, and it was found that rate constants between the central and peripheral compartments of CPT-11 carboxylate were much smaller than the interconversion rate constants from lactone to carboxylate between peripheral compartments, implying local conversion of CPT-11.

CPT-11 is extensively metabolized to its active metabolite SN-38 by the carboxylesterase enzyme system (14, 22), and the anticancer efficacy of SN-38 is far greater than the parent drug *in vitro* (23). Therefore, it is important to understand the PK of SN-38, especially for its active lactone form. During the model building for SN-38, the model with hydrolysis from CPT-11 lactone and carboxylate forms to the corresponding forms of SN-38 was tested, and it seemed that the model with only

transformation between lactone forms performed best (final model). When the values of parameters were compared, the interconversion rate constant from SN-38 lactone to carboxylate (0.319/h; Table 2) was larger than the elimination rate constant of CPT-11 carboxylate (0.158/h, calculated from CL of CPT-11 carboxylate and the volume of distribution of CPT-11 carboxylate in compartment one, Table 1). This lends further support to the supposition that SN-38 carboxylate is formed by hydrolysis (lactone to carboxylate) and not through carboxylesterase-mediated metabolism from CPT-11 carboxylate. It has been reported that *in vitro* the steady-state formation rates of SN-38 by CPT-11 lactone are two times higher than those through CPT-11 carboxylate (24). Similarly, the parameter estimates from this modeling analysis indicated that the interconversion rate constant for lactonization (carboxylate to lactone) was 2.6-fold higher than that of hydrolysis (Table 2). The reason might be that SN-38 lactone is more tightly bound to human serum albumin than the carboxylate form, so the dynamic equilibrium is preferential towards the lactone form (25). This could explain the *in vivo* observations that the lactone form of SN-38 was the dominant form in patient plasma in our study and the earlier investigation by Rivory *et al.* (12). From modeling, it was found that SN-38 formation was proportional to the dose of CPT-11, suggesting that SN-38 is a major metabolite. The fact that SN-38 disposition parameters were relatively high may suggest otherwise, but these high values could also be a consequence of a sequential metabolism of SN-38 to SN-38G in the liver.

SN-38 can be further converted into SN-38G by hepatic uridine diphosphate glucuronyltransferase (3, 4), and the plasma concentrations of this glucuronide compound were relatively high. It has been shown that the AUC ratio of SN-38G to SN-38 ranges from 4.5 to 32 (8). SN-38G had the highest plasma concentrations of all metabolites. Evidence that SN-38G is the result of a major pathway of CPT-11 elimination was also indicated by the fact that the model assuming SN-38 and SN-38G was best related to dose.

Large interindividual variability for parameters of CPT-11 lactone and SN-38 lactone was found in this study. This probably indicates that a large variability in carboxylesterase expression and activity exists between individuals and also indicates that variability in interconversion between lactone and carboxylate forms may partly contribute to the overall interindividual variability of these parameters (14, 26).

During the modeling, no significant covariates were found, except for BSA in the case of CPT-11 and age in the case of APC. This is consistent with previous observations from phase I and II clinical trials indicating that the CL of CPT-11 or the formation ratio of SN-38 and SN-38G is not significantly correlated with age, sex, serum creatinine level, transaminase level, alkaline phosphatase level, or the presence of liver metastases (27).

Both APC and NPC total concentration-time profiles could be best described by two-compartment models. The model predicted that the metabolic pathway of CPT-11 to APC was through the carboxylate form. The interindividual variability in exposure to APC suggests that the differences in metabolism and formation between patients are the main source of variability for APC PK. Unlike APC, NPC was predicted to be mainly formed from CPT-11 lactone, and no formation variability was needed. It has been found *in vivo* (8) that NPC is a minor plasma metabolite of the parent drug, which contrasts with *in vitro* results in which NPC was a major metabolite (6). An explanation for this apparent contradiction could be the fact that NPC is subject to conversion to SN-38 by plasma carboxylesterases (6, 14, 28). This alternative metabolic pathway might partly explain the high interindividual variability in NPC PK.

In summary, we built population PK models to adequately describe plasma data of CPT-11 and its currently known metabolites, including the lactone-carboxylate interconversion. These data not only increase our knowledge to better understand the clinical PK of this drug but also may prove useful in predicting the PK of all characterized metabolites and interconversion products after various administration regimens of CPT-11.

REFERENCES

1. Wiseman LR, Markham A. Irinotecan. A review of its pharmacological properties and clinical efficacy in the management of advanced colorectal cancer. Drugs 52: 606-623, 1996
2. Kawato Y, Aonuma M, Hirota Y, Kuga H, Sato K. Intercellular roles of SN-38, a metabolite of the camptothecin derivative CPT-11, in the antitumor effect of CPT-11. Cancer Res 51: 4187-4191, 1991
3. Rivory LP, Robert J. Identification and kinetics of a beta-glucuronide metabolite of SN-38 in human plasma after administration of the camptothecin derivative irinotecan. Cancer Chemother Pharmacol 36: 176-179, 1995
4. Haaz MC, Rivory L, Jantet S, Ratanasavanh D, Robert J. Glucuronidation of SN-38, the active metabolite of irinotecan, by human hepatic microsomes. Pharmacol Toxicol 80: 91-96, 1997
5. Rivory LP, Riou JF, Haaz MC, et al. Identification and properties of a major plasma metabolite of irinotecan (CPT-11) isolated from the plasma of patients. Cancer Res 56: 3689-3694, 1996
6. Dodds HM, Haaz MC, Riou JF, Robert J, Rivory LP. Identification of a new metabolite of CPT-11 (irinotecan): pharmacological properties and activation to SN-38. J Pharmacol Exp Ther 286: 578-583, 1998
7. Hertzberg RP, Caranfa MJ, Holden KG, et al. Modification of the hydroxy lactone ring of camptothecin: inhibition of mammalian topoisomerase I and biological activity. J Med Chem 32: 715-720, 1989
8. De Jonge MJ, Verweij J, de Bruijn P, et al. Pharmacokinetic, metabolic, and pharmacodynamic profiles in a dose- escalating study of irinotecan and cisplatin. J Clin Oncol 18: 195-203, 2000
9. Chabot GG. Clinical pharmacokinetics of irinotecan. Clin Pharmacokinet 33: 245-259, 1997

10. Herben VM, Ten Bokkel Huinink WW, Schellens JH, Beijnen JH. Clinical pharmacokinetics of camptothecin topoisomerase I inhibitors. Pharm World Sci 20: 161-172, 1998
11. Iyer L, Ratain MJ. Clinical pharmacology of camptothecins. Cancer Chemother Pharmacol 42: S31-S43, 1998
12. Rivory LP, Chatelut E, Canal P, Mathieu-Boue A, Robert J. Kinetics of the in vivo interconversion of the carboxylate and lactone forms of irinotecan (CPT-11) and of its metabolite SN-38 in patients. Cancer Res 54: 6330-6333, 1994
13. Ma MK, Zamboni WC, Radomski KM, et al. Pharmacokinetics of irinotecan and its metabolites SN-38 and APC in children with recurrent solid tumors after protracted low-dose irinotecan. Clin Cancer Res 6: 813-819, 2000
14. Mathijssen RH, van Alphen RJ, Verweij J, et al. Clinical pharmacokinetics and metabolism of irinotecan (CPT-11). Clin Cancer Res 7: 2182-2194, 2001
15. De Bruijn P, Verweij J, Loos WJ, Nooter K, Stoter G, Sparreboom A. Determination of irinotecan (CPT-11) and its active metabolite SN-38 in human plasma by reversed-phase high-performance liquid chromatography with fluorescence detection. J Chromatogr B Biomed Sci Appl 698: 277-285, 1997
16. Mandema JW, Verotta D, Sheiner LB. Building population pharmacokinetic-pharmacodynamic models. 1. Models for covariate effects. J Pharmacokinet Biopharm 20: 511-528, 1992
17. Beal SL, Sheiner LB. NONMEM Users' Guides. San Francisco, CA, NONMEM Project Group, University of California at San Fransisco, 1992
18. Jonsson EN, Karlsson MO. Xpose: An S-PLUS based population pharmacokinetic/ pharmacodynamic model building aid for NONMEM. Comput Methods Programs Biomed 58: 51-64, 1999
19. Rowinsky EK, Grochow LB, Ettinger DS, Sartorius SE, Lubejko BG, Chen TL, et al. Phase I and pharmacological study of the novel topoisomerase I inhibitor 7-ethyl-10-[4-(1-piperidino)-1-piperidino]carbonyloxycamptothecin (CPT-11) administered as a ninety- minute infusion every 3 weeks. Cancer Res 54: 427-436, 1994
20. Fassberg J, Stella VJ. A kinetic and mechanistic study of the hydrolysis of camptothecin and some analogues. J Pharm Sci 81: 676-684, 1992
21. Kehrer DF, Sparreboom A, Verweij J, et al. Modulation of irinotecan-induced diarrhea by cotreatment with neomycin in cancer patients. Clin Cancer Res 7: 1136-1141, 2001
22. Tsuji T, Kaneda N, Kado K, Yokokura T, Yoshimoto T, Tsuru D. CPT-11 converting enzyme from rat serum: purification and some properties. J Pharmacobiodyn 14: 341-349, 1991
23. Tanizawa A, Fujimori A, Fujimori Y, Pommier Y. Comparison of topoisomerase I inhibition, DNA damage, and cytotoxicity of camptothecin derivatives presently in clinical trials. J Natl Cancer Inst 86: 836-842, 1994
24. Haaz MC, Rivory LP, Riche C, Robert J. The transformation of irinotecan (CPT-11) to its active metabolite SN- 38 by human liver microsomes. Differential hydrolysis for the lactone and carboxylate forms. Naunyn Schmiedebergs Arch Pharmacol 356: 257-262, 1997
25. Burke TG, Mi Z. The structural basis of camptothecin interactions with human serum albumin: impact on drug stability. J Med Chem 37: 40-46, 1994
26. Canal P, Gay C, Dezeuze A, et al. Pharmacokinetics and pharmacodynamics of irinotecan during a phase II clinical trial in colorectal cancer. Pharmacology and Molecular Mechanisms Group of the European Organization for Research and Treatment of Cancer. J Clin Oncol 14:

2688-2695, 1996

27. Herben VM, Schellens JH, Swart M, et al. Phase I and pharmacokinetic study of irinotecan administered as a low- dose, continuous intravenous infusion over 14 days in patients with malignant solid tumors. J Clin Oncol 17: 1897-1905, 1999

28. Kehrer DF, Yamamoto W, Verweij J, de Jonge MJ, de Bruijn P, Sparreboom A. Factors involved in prolongation of the terminal disposition phase of SN-38: clinical and experimental studies. Clin Cancer Res 6: 3451-3458, 2000

ACKNOWLEDGEMENT

We thank the Swedish Cancer Society.

APPENDIX

Compartments are numbered from 1 to 5 in the following order with regards to CPT-11: lactone central; lactone peripheral 1; carboxylate central; carboxylate peripheral; and lactone peripheral 2. Deriving the equation to calculate CPT-11 lactone clearance (CL_L) considering interconversion between lactone and carboxylate forms. The relationship between these two forms is present in Fig 2. The amount (A) of change in each compartment is described by equations 1 to 5:

$$dA_{(1)}/dt = R_o+k_{21}*A_{(2)}+k_{31}*A_{(3)}+k_{51}*A_{(5)}-(k_{10}+k_{12}+k_{13}+k_{15})*A_{(1)} \quad \text{(eq. 1)}$$

$$dA_{(2)}/dt = k_{12}* A_{(1)}+k_{42}*A_{(4)}-(k_{21}+k_{24})*A_{(2)} \quad \text{(eq. 2)}$$

$$dA_{(3)}/dt = k_{13}*A_{(1)}+k_{43}*A_{(4)}-(k_{30}+k_{31})* A_{(3)} \quad \text{(eq. 3)}$$

$$dA_{(4)}/dt = k_{24}*A_{(2)}-(k_{42}+k_{43})*A_{(4)} \quad \text{(eq. 4)}$$

$$dA_{(5)}/dt = k_{15}*A_{(1)}- k_{51}*A_{(5)} \quad \text{(eq. 5)}$$

where, R_o is the infusion rate and k is the rate constant. The Arabic numbers represent the compartmental numbers. At steady-state (ss), the amount in each compartment is derived according to equations 6-10:

$$A_{(1)ss} = \frac{R_0 + k_{12} * A_{(2)ss} + k_{31} * A_{(3)ss}}{k_{10} + k_{12} + k_{13}} \quad \text{(eq. 6)}$$

$$A_{(2)ss} = \frac{k_{12} * (k_{42} + k_{43})}{k_{21} * (k_{42} + k_{43}) + k_{24} * k_{43}} * A_{(1)ss} \quad \text{(eq. 7)}$$

$$A_{(3)ss} = \left[\frac{k_{13}}{k_{30} + k_{31}} + \frac{k_{12} * k_{24} * k_{43}}{(k_{30} + k_{31}) * (k_{21} * (k_{42} + k_{43}) + k_{24} * k_{43})} \right] * A_{(1)ss} \quad \text{(eq. 8)}$$

$$A_{(4)ss} = \frac{k_{12} * k_{24}}{k_{21} * (k_{42} + k_{43}) + k_{24} * k_{43}} * A_{(1)ss} \quad \text{(eq. 9)}$$

$$A_{(5)ss} = \frac{k_{15}}{k_{51}} * A_{(1)ss} \quad \text{(eq.10)}$$

If equations 6, 7, 8, 9, and 10 are rearranged, lactone concentration at steady-state can be expressed as

$$C_{(1)ss} = \frac{R_0}{V_1 * \left[k_{10} + k_{12} + k_{13} - \frac{k_{13} * k_{31}}{k_{30} + k_{31}} - \frac{k_{12} * k_{21} * (k_{30} + k_{31}) * (k_{42} + k_{43}) + k_{12} * k_{13} * k_{24} * k_{43}}{(k_{30} + k_{31}) * (k_{21} * (k_{42} + k_{43}) + k_{24} * k_{43})} \right]} \quad \text{(eq. 11)}$$

The CL_L is expressed as the ratio of R_0 and $C_{(1)ss}$. Therefore, CL_L (taking into consideration the equilibrium with the carboxylate form) can be calculated by using equation 12, where V_1 is the volume of distribution in the central compartment of the lactone form (compartment 1):

$$CL_L = \frac{R_0}{C_{(1)ss}} = V_1 * \left[k_{10} + k_{12} + k_{13} - \frac{k_{13} * k_{31}}{k_{30} + k_{31}} - \frac{k_{12} * k_{21} * (k_{30} + k_{31}) * (k_{42} + k_{43}) + k_{12} * k_{13} * k_{24} * k_{43}}{(k_{30} + k_{31}) * (k_{21} * (k_{42} + k_{43}) + k_{24} * k_{43})} \right] \quad \text{(eq. 12)}$$

Deriving the equation to estimate the clearance of CPT-11 total forms (CL_T), considering the interconversions between lactone and carboxylate forms. The steady-state plasma concentration of CPT-11 total ($C_{T,ss}$) is the sum of lactone ($C_{(1)ss}$) and carboxylate ($C_{(3)ss}$) forms. Combined with equation 8, $C_{T,ss}$ can be expressed as

$$C_{T,ss} = C_{(1)ss} * \left[1 + \left(\frac{k_{13}}{k_{30} + k_{31}} + \frac{k_{12} * k_{24} * k_{43}}{(k_{30} + k_{31}) * (k_{21} * (k_{42} + k_{43}) + k_{24} * k_{43})} \right) * \frac{V_1}{V_3} \right] \quad \text{(eq. 13)}$$

where V_3 is the volume of distribution in the central compartment of the carboxylate form (compartment 3). The total clearance of CPT-11 lactone is the ratio of infusion rate and $C_{T,ss}$. Therefore, CL_T can be derived from equations 12 and 13:

$$CL_T = \frac{R_0}{C_{T,ss}} = \frac{CL_L * V_3}{V_3 + \left(\frac{k_{13}}{k_{30} + k_{31}} + \frac{k_{12} * k_{24} * k_{43}}{(k_{30} + k_{31}) * (k_{21} * (k_{42} + k_{43}) + k_{24} * k_{43})} \right) * V_1} \quad \text{(eq. 14)}$$

Chapter Five

Clinical Pharmacokinetics of Irinotecan and its Metabolites in Relation with Diarrhea

Clinical Pharmacology & Therapeutics, 72: 265-275, 2002

Rujia Xie[1]
Ron H.J. Mathijssen[2]
Alex Sparreboom[2]
Jaap Verweij[2]
Mats O. Karlsson[1]

[1]Department of Pharmaceutical Biosciences, Uppsala University
Uppsala, Sweden

[2]Department of Medical Oncology, Erasmus MC - Daniel den Hoed
Rotterdam, The Netherlands

ABSTRACT

Objectives: Our objective was to build population pharmacokinetic models that describe plasma concentrations of irinotecan (CPT-11) and its metabolites SN-38 and SN-38 glucuronide (SN-38G) and to investigate pharmacokinetic-pharmacodynamic relationships between drug exposure and diarrhea, the major dose-limiting toxicity.

Methods: Data were obtained from 109 patients (65 men and 44 women) who received 1.5-hour (range, 0.75- to 2.25-hour) intravenous infusions of irinotecan at doses that ranged from 100 to 350 mg/m^2; 44 patients had a second course. The population pharmacokinetic models were developed to describe plasma concentration-time profiles. The area under the concentration-time curve from time zero to 60 hours [$AUC_{0\text{-}60h}$] was used as a measure of drug exposure to model the probabilities of diarrhea with use of a logistic regression model.

Results: A 3-compartment pharmacokinetic model best described the disposition of irinotecan, whereas SN-38 and SN-38G showed 2-compartmental characteristics. The population estimate of clearance for irinotecan was 31.6 L/h, and the volume of distribution at steady-state (V_{ss}) was 263 L. The clearance devided by formation fraction (F_m) was 712 L/h and 66.8 L/h for SN-38 and SN-38G, respectively. The V_{ss}/F_m was 72,000 L for SN-38 and 85.4 L for SN-38G. The frequencies of diarrhea scores in this study were 46% (grade 0), 28% (grade 1), 20% (grade 2), 4% (grade 3), and 2% (grade 4). Significant correlations between $AUC_{0\text{-}60h}$ and diarrhea scores were found for irinotecan (P <.05) and SN-38G (P <.01) but not for SN-38 or the biliary index.

Conclusions: In this population analysis, irinotecan and SN-38G AUC values were appropriate predictors of the risk for diarrhea, and SN-38G AUC showed the stronger relationship of the two. The developed population models may be useful in further clinical development of this agent.

INTRODUCTION

The anticancer agent irinotecan (CPT-11) has proven activity in a wide range of tumors and is registered for treatment of colorectal cancer (1). It is extensively metabolized, and it is reported that cytotoxic activity of one of its metabolites, SN-38 (7-ethyl-10-hydroxycamptothecin), is 100 to 1000 times greater than that of irinotecan itself (2). SN-38 is further conjugated to an inactive glucuronic acid conjugate (SN-38G) by UDP glucuronosyltransferase 1A1 (3, 4). Pharmacokinetic parameters of irinotecan and its metabolites reported are mostly based on individual analyses. Individual plasma concentrations of irinotecan and its metabolites have

been described previously by use of 2- or 3-compartment models (5-9). For population pharmacokinetic analysis purposes, Yamamoto *et al.* (10) used a 2-compartment model to characterize concentration profiles of irinotecan.

The major dose-limiting nonhematologic toxicity of irinotecan is diarrhea (11). Although the pharmacokinetic-pharmacodynamic relationship between exposure and toxicity has been widely studied, the results have been discrepant because of its complex and incompletely understood relationship and because of different study designs (12). Although most investigations have reported that area under the concentration-time curve (AUC) values for both irinotecan and SN-38 significantly correlated with the severity of diarrhea (6, 7, 13), others have detected that correlation only for irinotecan AUC (14). Similarly, although several studies have suggested that there is a correlation between the biliary index and diarrhea (15, 16), other studies could not confirm that correlation (17, 18). Finally, some trials failed to find any relationship between diarrhea and any of the studied pharmacokinetic parameters (5, 18-20). All of these previous pharmacodynamic analyses have been based on statistical analysis, such as analysis of variance (ANOVA), correlation analysis, or *t*-tests.

The purpose of this study was to create appropriate population pharmacokinetic models to describe plasma concentrations of irinotecan, SN-38, and SN-38G. In addition, we wanted to build pharmacokinetic-pharmacodynamic models for any potential relationship between drug or metabolite exposure (AUC) and diarrhea, the major dose-limiting toxicity.

PATIENTS AND METHODS

Patients and treatment

Patients with a histologically or cytologically proven malignant solid tumor that stipulated an irinotecan-based chemotherapeutic regimen were eligible for the trials that formed the basis of the present study. All patients were treated between May 1996 and February 2001 at the Erasmus MC (Rotterdam, the Netherlands). Additional criteria for eligibility included the following: (*a*) age between 18 and 75 years, (*b*) an Eastern Cooperative Oncology Group performance status $\leq$ 2, (*c*) adequate hematopoietic (absolute neutrophil count $\geq$ 1.5×10^9 per liter and platelet count $\geq$ 100×10^9 per liter), liver and kidney function at the time of study entry, (*d*) no previous anticancer treatment for at least 4 weeks, and (*e*) no previous therapy with irinotecan or other topoisomerase I inhibitors. Written informed consent was obtained from each patient before study entry in accordance with federal and institutional guidelines.

Irinotecan was provided by Aventis Pharma (Hoevelaken, the Netherlands) as

the hydrochloride trihydrate salt in 40- or 100-mL vials that contained 20 mg/mL irinotecan in sorbitol and a lactic acid-sodium hydroxide buffer system (pH 3.5 – 4.5). The drug was administered once every 21 days as a 1.5-hour (range, 0.75 – 2.25 hour) intravenous infusion at doses ranging from 100 to 350 mg/m^2. Intestinal toxicity was graded as a diarrhea score measured on a point scale from 0 to 4 in accordance with the National Cancer Institute Common Toxicity Criteria.

For the pharmacodynamic evaluation, the grade assigned to a patient was the worst grade of diarrhea experienced during the 3-week period after drug administration. The strategy for treatment of diarrhea was the same for all patients. For delayed diarrhea the patient received 4 mg oral loperamide, followed by a dose of 2 mg loperamide administered every 2 hours for up to 12 hours after the last liquid stool, without exceeding 48 hours of treatment. If diarrhea persisted for more than 24 hours, the patient received a 7-day prophylactic oral antibiotic course with ciprofloxacin. This treatment was considered to be adequate for all patients, and no problems were encountered with the antidiarrheal medication (e.g. vomiting) in this group of patients.

Sampling and analysis

Serial blood samples were obtained from each patient before drug administration and at approximately 0.5, 1.5, 1.67, 1.83, 2, 2.5, 3.5, 4.5, 5, 5.5, 6.5, 8, 12, 25.5, 49, and 56 hours after administration. The samples (approximately 7 mL) were drawn from a vein in the patient's arm that was opposite to the one used for infusion, and the plasma was immediately separated by centrifugation (3000 × *g* for 5 minutes at 4°C) and then stored frozen until analysis. Plasma samples were analyzed for the presence of irinotecan and metabolites by use of a validated reversed-phase high-performance liquid chromatography system with fluorescence detection as described previously (5). It has previously been shown that the total drug levels (i.e., the total of lactone and carboxylate forms) of irinotecan, SN-38 and SN-38G provide a consistent and accurate reflection of the respective lactone concentrations with little variability (12). We therefore monitored total drug concentrations for all analytes in this study because it serves as an appropriate surrogate of the lactone forms. In brief, the sample pre-treatment procedure involved a protein-precipitation step of 250-µL aliquots with a mixture of methanol and 5% (wt/vol) of aqueous perchloric acid (1:1, vol/vol). Separation of the various analytes and endogenous compounds was achieved on a analytical column packed with Hypersil octadecylsilane material (internal diameter, 100 x 4.6 mm; particle size, 5-µm; LC Service, Emmen, the Netherlands), and isocratic elution was accomplished with a mixture of methanol and 0.1 M ammonium acetate that contained 10 mM tetrabutylammonium sulphate (30:70, vol/vol), with the pH

adjusted to 5.3 (hydrochloric acid). The column effluent was monitored at excitation and emission wavelengths of 355 and 515 nm, respectively. The lower limit of quantitation of this method is 2.0 ng/mL for each of the analytes of interest. Because of the limited sample supply, concentrations could not be determined for all metabolites in all samples.

Pharmacokinetic analysis

Pharmacokinetic analysis was based on multi-compartmental models (up to 3 compartments), and the pharmacokinetic models were built sequentially for irinotecan, SN-38, and SN-38G. Irinotecan concentrations were analyzed first, and then individual (post hoc) parameters for irinotecan were fixed in the further analysis of SN-38 and SN-38G. Similarly, individual parameter estimates of SN-38 were fixed in the analysis of SN-38G. It was assumed that SN-38 was formed from irinotecan according to a first-order process and that SN-38G was formed from SN-38 by means of a first-order process.

Covariate models were built on the basis of generalized additive models (21, 22). The covariate that resulted in the largest decrease in the Akaike information criterion was introduced into the model and tested. The covariates considered were age, sex, body surface area and concomitant medication with cisplatin or tipifarnib (R115777).

The area under the concentration-time curve from time zero to 60 hours ($AUC_{0\text{-}60h}$) values for irinotecan, SN-38, and SN-38G were estimated according to their concentrations and the estimates of parameters from the final models. The models were fitted to the data for all individuals simultaneously by use of NONMEM (version VI) with a first-order conditional estimation method with interaction (23). Interindividual variability in exponential expression was included in the pharmacokinetic parameters. The residual error model was characterized by both additive and proportional components. If one of the terms was estimated to be negligible, it was excluded from the model. Model selection was guided by the decrease in the objection function value (-2log likelihood) and by graphical goodness-of-fit analyses with Xpose 3.0 (22). To differentiate between hierarchic models, $P < .05$ was chosen for an additional parameter or covariate, corresponding to a difference in the objective function value (OFV) of 3.84, with the OFV approximately χ^2 distributed.

Pharmacokinetic-pharmacodynamic analysis

The pharmacokinetic-pharmacodynamic relationship between exposure and toxicity (diarrhea) was established with $AUC_{0\text{-}60h}$, which was obtained from the

pharmacokinetic analysis. Because nonhematologic toxicity of diarrhea score is a categoric variable (taking integer values of 0 to 4), the probability (P) of each diarrhea score was modeled with logistic regression, similar as used for dry mouth score (24). If $Y_n = (Y_0, Y_1, ...)$ is the vector of the diarrhea scores for individual patients, the probability for Y_n larger than or equal to the score m (m = 0, 1, 2, 3, and 4) can be expressed as follows:

$$g\{P(Y_n \geq m)\} = \text{logit}(p) = \text{Int} + f_d$$

in which:

$$\text{logit}(p) = \text{Log}[p/(1-p)]$$

and:

$$p = \exp(\text{Int} + f_d)/[1 + \exp(\text{Int} + f_d)]$$

$$\text{Int} = \sum_{L=0}^{m} \mu_{Li}$$

$$f_d = \text{Slop} * AUC_{0\text{-}60h}$$

in which g is the logit function of a probability (p is the short notation for $P(Y_n \geq m)$), $\mu_{Li} \geq 0$ specifies the baseline probabilities of diarrhea scores which are summed to Int, and f_d is representing the drug or metabolite effect introduced in the model as a function of the $AUC_{0\text{-}60h}$ values of irinotecan, SN-38 or SN-38G and the parameter Slop. The biliary index (14), calculated as the product of the $AUC_{0\text{-}60h}$ ratio of SN-38 to SN-38G and irinotecan $AUC_{0\text{-}60h}$, was tested in the model in a manner similar to that of the other exposure measures. Note that $P(Y_n \geq 0) = 1$, so that in the model it was necessary only to estimate the cumulative probabilities for the diarrhea scores 1 to 4. The probability for each individual score could thereafter be calculated from the estimated cumulative probabilities.

For each treatment course, the individual course-specific exposure was used. Some patients received 2 courses, which was taken into account through 2 different approaches (separately and in combination) as follows: (i) We investigated whether there was a different relation between exposure and diarrhea at the second visit; (ii) we included a random effect, which indicated interindividual variability in the exposure-diarrhea score relation. The effects of covariates (concomitant medication (cisplatin or R115777), and tumor type) on diarrhea were tested for incorporation into the pharmacokinetic-pharmacodynamic model. As in the pharmacokinetic analysis, the significance criteria ($P < .05$) with a difference in OFV of more than 3.84 was used to assess drug effect on the diarrhea score probability, and the model was analyzed with the NONMEM program.

RESULTS

Patients

Sixty-five male and 44 female patients between 34 and 75 years old were enrolled in this study (Table 1). The predominant tumor type in this group of patients was colorectal cancer (n=69). Eighty-two patients were treated in combination with other chemotherapy (i.e. 56 patients also received cisplatin, and 26 patients also received R115777) (5, 25). Forty-four of the 109 patients were also evaluated during a second treatment course. Plasma samples were analyzed for the presence of irinotecan and SN-38 in all 109 patients, whereas data for SN-38G were available from 56 patients. One hundred and four of 109 patients having irinotecan and SN-38 concentrations had diarrhea scores, and 51 of 56 patients had both diarrhea scores and SN-38G concentrations.

Table 1. Patient demographics.

Characteristic		
No. of patients studied		109
No. of evaluable courses		153
Sex (man/ women)		65/ 44
Age (y)		54[a] (34-75)
Length (m)		1.73[a] (1.51-1.92)
Weight (kg)		74[a] (38-115)
Body-surface area (m^2)		1.87[b] (1.29-2.40)
Infusion duration (h)		1.50[a] (0.75-2.25)
Irinotecan dose (mg/m^2)		300[b] (100-350)
Combination therapy:	None	27
	Cisplatin	56
	R115777	26
Tumor type:	(A)CUP	12
	Colorectal	69
	Miscellaneous	28[c]

[a] mean values with range in parenthesis; [b] median values with range in parenthesis;
[c] gastro-intestinal (nine), lung (six), head or neck (six), pancreatic (three), penile (one), kidney (one), bladder (one), thorax (one).

Pharmacokinetic analysis

The observed total plasma concentration-time profiles of irinotecan, SN-38 and SN-38G are presented in Figure 1, and all concentrations are given in nanograms per milliliter. A 3-compartment model, including body-surface area as a covariate for all pharmacokinetic parameters (direct proportionality), best described the plasma concentration-time profiles of irinotecan (Fig. 2) which, compared to the basic model without body-surface area, resulted in a decrease in OFV of 81.3. Coadministration with cisplatin was found to have no significant effect on irinotecan pharmacokinetics, and the influence of R115777 on irinotecan clearance was less than 15%. Plasma concentrations of the SN-38 and SN-38G metabolites could be adequately described by 2-compartment models (Fig. 2). The population estimate of total body clearance (CL) for irinotecan was 31.6 L/h, and the volume of distribution at steady-state (V_{ss}) was 263 L (Table 2). Pharmacokinetic parameters for SN-38 and SN-38G were estimated and expressed as parameter divided by formation fraction (F_m). Values for CL/F_m and V_{ss}/F_m of SN-38 were much larger than those of irinotecan and SN-38G, and SN-38G had the smallest steady-state volume (Table 2). $AUC_{0\text{-}60h}$ values for all individuals were estimated from the models using individual-specific parameters. The mean (± SD) estimated $AUC_{0\text{-}60h}$ was 17,226 ± 8,016 ng/ml*h (range, 4,043 – 46,164 ng/ml*h) for irinotecan, 403 ± 214 ng/ml*h (range, 126 – 1,229 ng/ml*h) for SN-38, and 4,416 ± 3,816 ng/ml*h (range, 197 – 22,734 ng/ml*h) for SN-38G. Sex and age were not significantly correlated to any pharmacokinetic parameter.

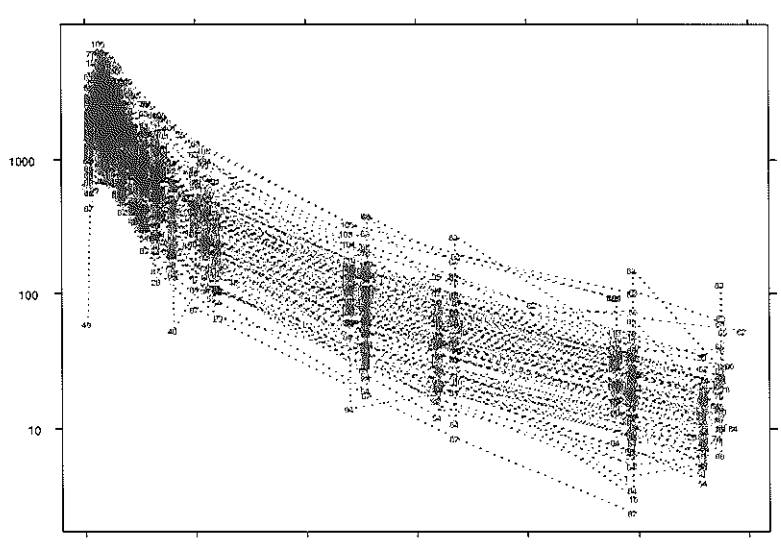

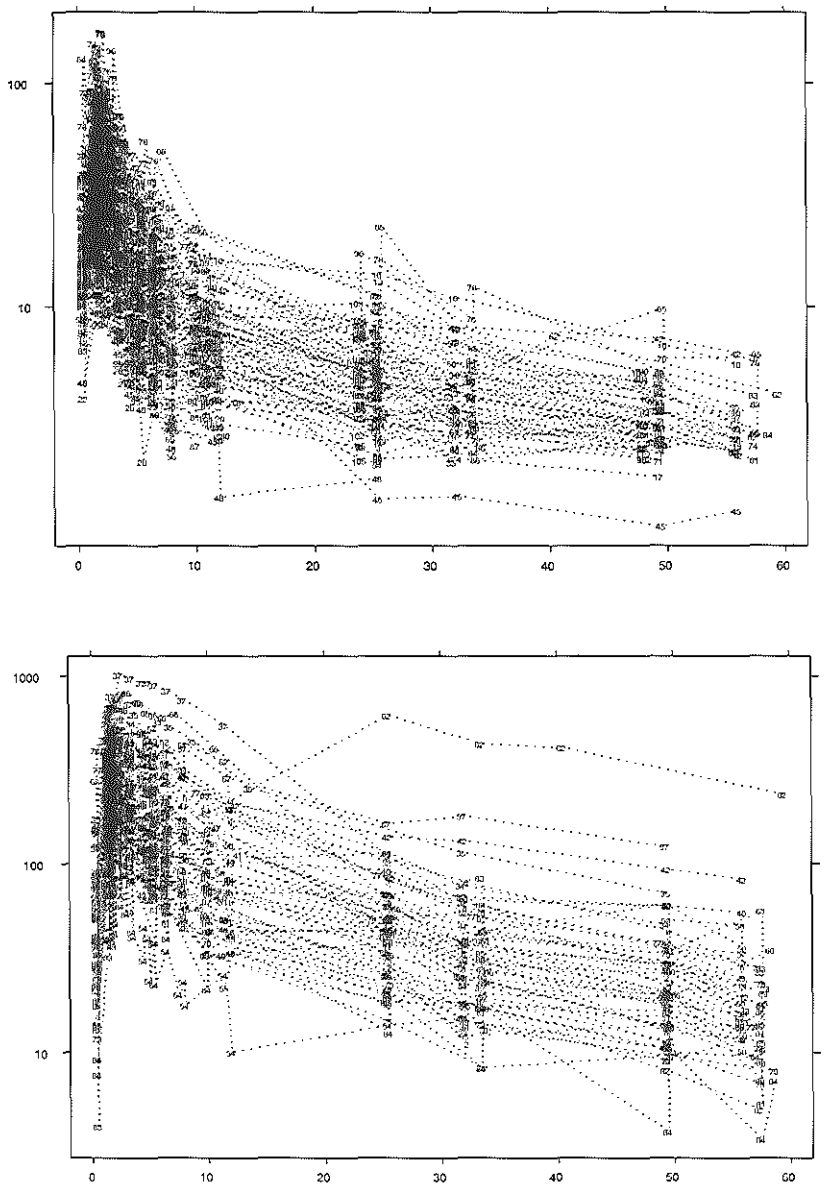

Figure 1. Observed total plasma concentration-time profiles of irinotecan (previous page), SN-38 (top panel), and SN-38G (bottom panel) after intravenous infusion of irinotecan. All concentrations are mentioned in ng/mL, and time is mentioned in hours. The dotted lines indicate connected individual data points.

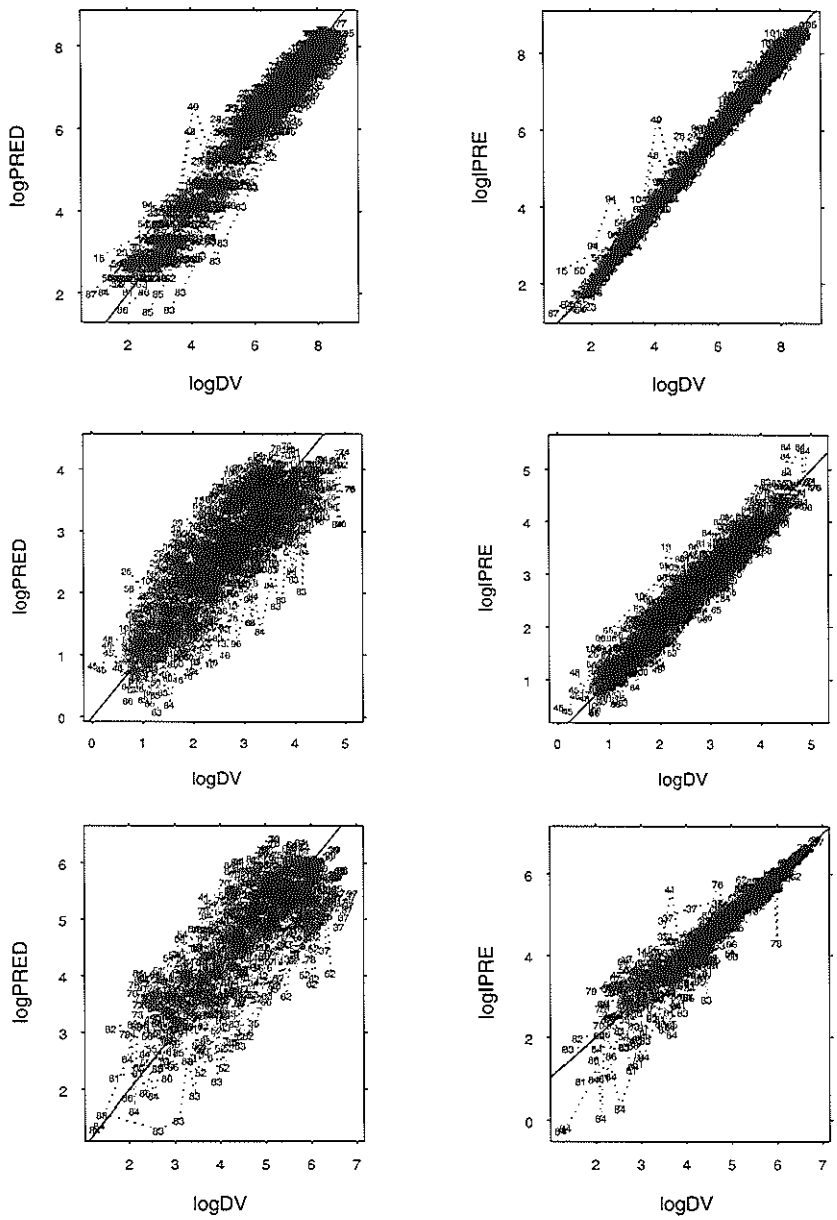

Figure 2. Population predicted (logPRED; left panels) and individual predicted (logIPRE; right panels) versus observed plasma concentrations (logDV) for irinotecan (top panels), SN-38 (middle panels) and SN-38G (bottom panels). Concentration is given in nanograms/milliliter. The dotted lines indicate connected individual data points, and the solid lines indicate the lines of identity.

Table 2. Summary of population pharmacokinetic estimates for irinotecan and metabolites.

Parameters	CPT-11 Estim.	RSE (%)	SN-38 Estim.	RSE (%)	SN-38G Estim.	RSE(%)
CL, L/h/m^2	16.9	3.5				
CL/F_m, L/h			712	11	66.8	10
Q_2, L/h/m^2	61.0	58				
Q_2/F_m, L/h			1530	7.8	23.9	18
Q_3, L/h/m^2	4.75	17				
V_1, L/m^2	36.7	12				
V_1/F_m, L			408	9.9	37	10
V_2, L/m^2	35.9	9.9				
V_2/F_m, L			71600	16	48.4	14
V_3, L/m^2	67.9	13				
V_{ss}, L/m^2	140.4	-				
V_{ss}/F_m, L			72008	-	85.4	-
IIV (CL), %	32	19				
IIV (CL/F_m), %			58	64	80	17
IIV (Q_2), %	74	39				
IIV (Q_2/F_m), %			56	35	97	49
IIV (Q_3), %	47	71				
IIV (V_1), %	26	13				
IIV (V_1/F_m), %			89	29	75	43
IIV (V_2), %	27	21				
IIV (V_2/F_m), %			59	31	59	42
IIV (V_3), %	45	16				
ε_1, ng/mL	1.3	40	0.56	26	34.5	12
ε_2, %	16.7	4.2	26.8	4.5	-	-

Abbreviations: Estim., Estimation; RSE, relative standard error; V_1, V_2, and V_3, the volume of distribution in the central and peripheral compartments; V_{ss}, volume of distribution at steady-state; Q_2 and Q_3, inter-compartment clearances; F_m, formation fraction for metabolite; IIV, inter-individual variability; ε_1 and ε_2, SD of additive and CV of proportional residual errors.

Pharmacokinetic-pharmacodynamic analysis

The probabilities of diarrhea scores from 0 to 4 for all patients were 46% for grade 0, 28% for grade 1, 20% for grade 2, 4% for grade 3 and 2% for grade 4. The

frequencies of scores in the SN-38G data set were 46% for grade 0, 24% for grade 1, 20% for grade 2, 5% for grade 3 and 5% for grade 4. No correlation between diarrhea scores and tumor types was found. Coadministeration with cisplatin or R115777 did not show any influence in the effect of irinotecan or SN-38G on diarrhea. For irinotecan, SN-38 and SN-38G separately, models with and without a relationship between diarrhea score and exposure ($AUC_{0\text{-}60h}$) were tested to assess drug effect (Table 3).

Table 3. Difference in objective function value (ΔOFV).

Drug	ΔOFV for full data set (n=104)	ΔOFV for reduced data set (n=51)
Irinotecan	-4.29*	-3.514
SN-38	-2.468	-1.672
SN-38G	-	-8.43**
Biliary Index	-	-0.522

*P = .04, **P = .0038.

The model that included irinotecan $AUC_{0\text{-}60h}$ was significantly better than the model that excluded $AUC_{0\text{-}60h}$, with a ΔOFV of 4.29 (P <.05). Although SN-38 $AUC_{0\text{-}60h}$ did not show any significant effect (P >.1), SN-38G $AUC_{0\text{-}60h}$ was correlated with the diarrhea scores (P <.005). No significant improvement was observed in any of the models when the linear relation (on a logit scale) was replaced by a maximum effect (E_{max}) model (not shown). No significant improvements were observed when a component for interindividual variability in the exposure-diarrhea score relation or a difference between the first and second course were incorporated into the model. Figure 3 shows the goodness of fit of the final models, and Figure 4 shows predictions of probabilities of different diarrhea scores versus their corresponding $AUC_{0\text{-}60h}$ values for irinotecan and SN-38G, respectively. The population estimates of these parameters are listed in Table 4. The biliary index showed no correlation with diarrhea score.

For about half of all subjects, the SN-38G plasma concentrations were not available because of a limiting sample supply; therefore a reduced data set that contained data only from the subjects with observations for irinotecan, SN-38, and SN-38G was also used to compare the effect of irinotecan, SN-38 and SN-38G in the same situation. The correlations between either irinotecan or SN-38 $AUC_{0\text{-}60h}$ and diarrhea were not significant in this reduced data set (Tables 3 and 4).

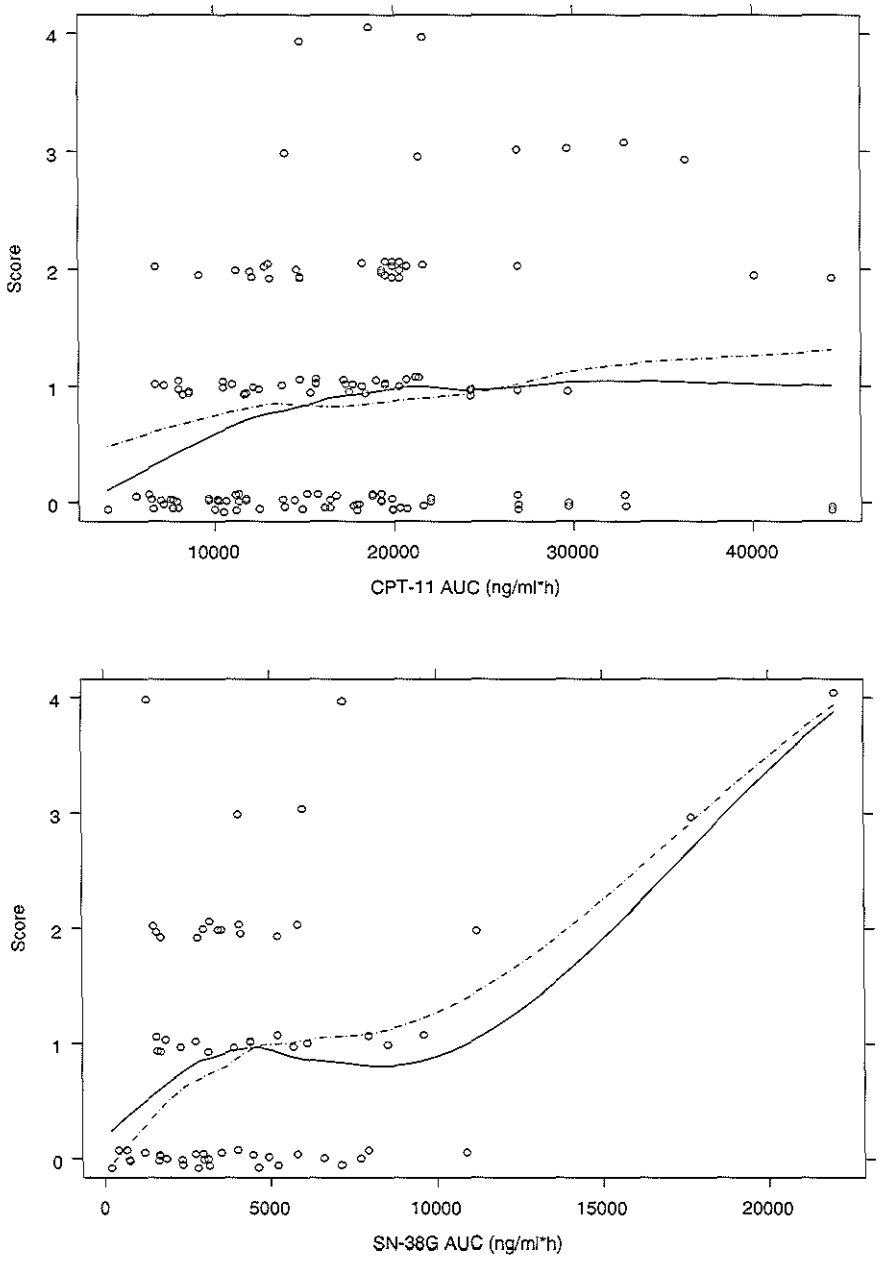

Figure 3. Diarrhea scores versus the $AUC_{0\text{-}60h}$ (ng/ml*h) for irinotecan (top panel) and SN-38G (bottom panel). The solid lines are the smoothed lines for observed scores; the broken lines are the smoothed lines for the predicted scores, which are simulated from the final pharmacokinetic-pharmacodynamic models.

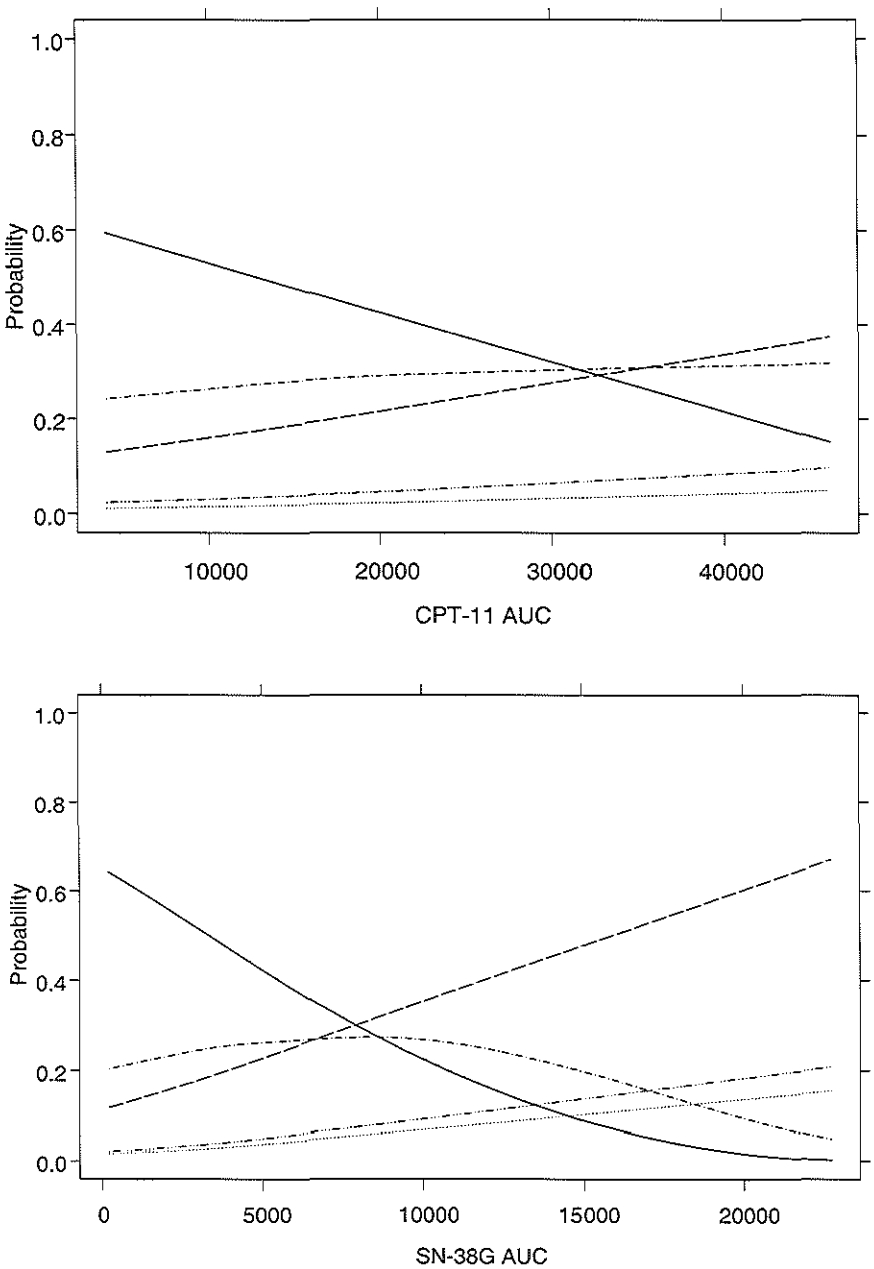

Figure 4. Predicted probabilities for diarrhea score 0 (solid lines [—]), diarrhea score 1 (dashed-dotted lines[-.-.]), diarrhea score 2 (dashed lines [---]) , diarrhea score 3 (lines with sequence of dash, 3 dots, dash, 3 dots [-...-...]), and diarrhea score 4 (dotted lines [...]) versus irinotecan $AUC_{0\text{-}60h}$ (ng/ml*h; top panel) and SN-38G $AUC_{0\text{-}60h}$ (ng/ml*h; bottom panel).

Table 4. Summary of population pharmacodynamic estimates.

Parameter	Irinotecan (n=104)		SN-38 (n=104)		SN-38G (n=51)	
	Estimate	SE	Estimate	SE	Estimate	SE
Intercept, m=1	-0.55	0.42	-0.31	0.35	-0.62	0.37
Intercept, m=2	-1.23	0.19	-1.22	0.19	-1.10	0.26
Intercept, m=3	-1.69	0.31	-1.68	0.31	-1.58	0.39
Intercept, m=4	-1.16	0.49	-1.15	0.49	-0.90	0.53
Slope *10^{-5}	4.26	2.0	120	79	18.7	6.0

*Slope for linear drug effect on the logit scale.

DISCUSSION

Population pharmacokinetic models were established for irinotecan, SN-38, and SN-38G, in which pharmacokinetic parameters for all 3 substances were well estimated with a low relative standard error, except for one intercompartmental clearance of irinotecan. The total body clearance of irinotecan was estimated to be 31.6 L/h, which is close to previously published results (18, 26). The V_{ss} of irinotecan was 263 L, indicating extensive distribution into the peripheral compartments. We found no significant effect of coadministration with cisplatin on irinotecan pharmacokinetics, and the influence of the farnesyltransferase inhibitor R115777 on irinotecan systemic clearance was less than 15% and was not considered to be clinical significant. Pharmacokinetic parameters for SN-38 and SN-38G were estimated as the true parameter value divided by the metabolite formation fraction (F_m). The estimated CL/F_m and V_{ss}/F_m for SN-38 were 712 L/h and 72,000 L, respectively, which may suggest that SN-38 is excreted or metabolized quickly or is distributed extensively into tissues, but it could also reflect a low value of F_m for SN-38. We found that SN-38G CL/F_m had a large variability compared with irinotecan and SN-38, probably reflecting a large interindividual variability in glucuronidation rate.

The pharmacokinetic-pharmacodynamic analysis showed that the diarrhea score had the strongest correlation with SN-38G $AUC_{0\text{-}60h}$, whereas it failed to identify a relationship with SN-38 exposure. Although SN-38 is the active metabolite of irinotecan and SN-38G is inactive, these results may not be so surprising. It can be hypothesized that diarrhea was related mainly to local intestinal concentrations of

SN-38 formed from intestinal SN-38G by bacterial glucuronidases. If that were the case, intestinal SN-38G concentrations might have been closely related to plasma concentrations of SN-38G, whereas high plasma concentrations of SN-38 might have been (partly) a consequence of poor glucuronidation capacity and therefore associated with low local intestinal levels of SN-38G. Support for this hypothesis comes from a recently presented trial in which pretreatment of patients with neomycin (27), which presumably killed the bacteria in question, was shown to result in a markedly lower frequency and severity of irinotecan-induced diarrhea.

Certain genetic polymorphisms in the promotor area and exons of the UDP glucuronosyltransferase *UGT1A1* gene have a dramatic effect on the functionality of the enzyme, leading to an altered glucuronidation of drugs (12). It has recently been shown that a mutation named *UGT1A1*28* is correlated with the main toxicities of irinotecan (i.e. leukopenia and diarrhea) (28, 29). In addition, a correlation with the irinotecan pharmacokinetics in American white patients and in Japanese patients has been detected (29, 30), although those data could not be confirmed in a large group of European patients (31). Pharmacogenetic screening may be attractive as a means to determine pharmacodynamic and therapeutic outcome in the (near) future.

A relation was also found between diarrhea and exposure of irinotecan, although it was weaker than that for SN-38G and no statistically significant relation was found for the reduced data set, which was used to derive the SN-38G relationship. This difference in significance for irinotecan can be explained by the different sample sizes as already with the larger data set, the irinotecan relation was of borderline significance.

The same significant results were obtained when diarrhea scores of 3 and 4 were merged (data not shown). If diarrhea scores were treated as dichotomous outcome ("diarrhea" or "no diarrhea"), no significant correlations were observed between irinotecan $AUC_{0\text{-}60h}$ or SN-38G $AUC_{0\text{-}60h}$ and the diarrhea score. This analysis of relations between exposure and diarrhea therefore has two main advantages over previous reports. First, it is based on a larger number of patients and it uses a graded diarrhea score, not just characterization of the toxicity as present or absent. The latter is important because bivariate outcome variables lack the information provided by graded scales. The relation between the diarrhea score and SN-38G exposure supports clinical strategies to reduce diarrhea frequency that are based on a reduction in the amount of SN-38G formed. In addition, it gives a mechanistic support for treatment that limits intestinal glucoronidase activity to decrease the probability of diarrhea (12). Although no difference in the relation between exposure and diarrhea was found between the first and second courses, our analysis was limited because data after more than 2 courses of treatment were

not available.

To investigate the influence of sample size on pharmacokinetic-pharmacodynamic output, the reduced data sets for irinotecan and SN-38 (which included the same patients as SN-38G) were analyzed. A significant correlation between irinotecan $AUC_{0\text{-}60h}$ and severity of diarrhea score could not be established for that data set (Table 3). This suggests that the relationship between irinotecan exposure and diarrhea can be established only in a relatively large sample size and that it is not as strong an indicator as SN-38G. This could also partly explain the conflicting published results for these correlations, as mentioned earlier. For example, the biliary index (the product of the AUC ratio of SN-38/SN-38G and irinotecan AUC) has previously been reported to be an important pharmacokinetic parameter correlated with diarrhea (15, 16), but we did not find that relationship in this study. Various factors, including the study design, the particular patient population being studied, the number of subjects, or the differences in sampling times, are crucial for accurate determination of pharmacokinetic-pharmacodynamic relationships.

In conclusion, we have developed population pharmacokinetic models for irinotecan, its pharmacologically active metabolite SN-38, and its glucuronic acid conjugate SN-38G. We used those models to establish a positive pharmacokinetic-pharmacodynamic relationship between SN-38G AUC and the severity of diarrhea. The population modeling we have described continues to refine our knowledge of this clinically important drug and, where appropriate, will lead to more easily exportable and optimized dosing strategies. We are currently involved in the development of a population pharmacokinetic model to correlate irinotecan disposition with drug-induced hematologic toxicity.

REFERENCES

1. Vanhoefer U, Harstrick A, Achterrath W, Cao S, Seeber S, Rustum YM. Irinotecan in the treatment of colorectal cancer: clinical overview. J Clin Oncol 19:1501-1518, 2001
2. Kawato Y, Aonuma M, Hirota Y, Kuga H, Sato K. Intracellular roles of SN-38, a metabolite of the camptothecin derivative CPT-11, in the antitumor effect of CPT-11. Cancer Res 51:4187-4191, 1991
3. Iyer L, King CD, Whitington PF, et al. Genetic predisposition to the metabolism of irinotecan (CPT-11). J Clin Invest 101:847-854, 1998
4. Haaz MC, Rivory L, Jantet S, Ratanasavanh D, Robert J. Glucuronidation of SN-38, the active metabolite of irinotecan, by human hepatic microsomes. Pharmacol Toxicol 80:91-96, 1997
5. De Jonge MJA, Verweij J, de Bruijn P et al. Pharmacokinetic, metabolic, and pharmacodynamic profiles in a dose- escalating study of irinotecan and cisplatin. J Clin Oncol 18:195-203, 2000
6. Chabot GG, Abigerges D, Catimel G, et al. Population pharmacokinetics and

pharmacodynamics of irinotecan (CPT-11) and active metabolite SN-38 during phase I trials. Ann Oncol 6:141-151, 1995

7. De Forni M, Bugat R, Chabot GG, et al. Phase I and pharmacokinetic study of the camptothecin derivative irinotecan, administered on a weekly schedule in cancer patients. Cancer Res 54:4347-4354, 1994
8. Herben VM, Ten Bokkel Huinink WW, Schellens JH, Beijnen JH. Clinical pharmacokinetics of camptothecin topoisomerase I inhibitors. Pharm World Sci 20:161-172, 1998
9. Iyer L, Ratain MJ. Clinical pharmacology of camptothecins. Cancer Chemother Pharmacol 42:S31-43, 1998
10. Yamamoto N, Tamura T, Karato A, et al. CPT-11: population pharmacokinetic model and estimation of pharmacokinetics using the Bayesian method in patients with lung cancer. Jpn J Cancer Res 85:972-977, 1994
11. Bleiberg H, Cvitkovic E. Characterisation and clinical management of CPT-11 (irinotecan)-induced adverse events: the European perspective. Eur J Cancer 32A:S18-23, 1996
12. Mathijssen RHJ, van Alphen RJ, Verweij J, et al. Clinical pharmacokinetics and metabolism of irinotecan (CPT-11). Clin Cancer Res 7:2182-2194, 2001
13. Sasaki Y, Hakusui H, Mizuno S, et al. A pharmacokinetic and pharmacodynamic analysis of CPT-11 and its active metabolite SN-38. Jpn J Cancer Res 86:101-110, 1995
14. Catimel G, Chabot GG, Guastalla JP, et al. Phase I and pharmacokinetic study of irinotecan (CPT-11) administered daily for three consecutive days every three weeks in patients with advanced solid tumors. Ann Oncol 6:133-140, 1995
15. Gupta E, Lestingi TM, Mick R, Ramirez J, Vokes EE, Ratain MJ. Metabolic fate of irinotecan in humans: correlation of glucuronidation with diarrhea. Cancer Res 54:3723-3725, 1994
16. Gupta E, Mick R, Ramirez J, et al. Pharmacokinetic and pharmacodynamic evaluation of the topoisomerase inhibitor irinotecan in cancer patients. J Clin Oncol 15:1502-1510, 1997
17. De Jonge MJA, Sparreboom A, Planting AST, et al. Phase I study of 3-week schedule of irinotecan combined with cisplatin in patients with advanced solid tumors. J Clin Oncol 18:187-194, 2000
18. Herben VM, Schellens JH, Swart M, et al. Phase I and pharmacokinetic study of irinotecan administered as a low-dose, continuous intravenous infusion over 14 days in patients with malignant solid tumors. J Clin Oncol 17:1897-1905, 1999
19. Canal P, Gay C, Dezeuze A, et al. Pharmacokinetics and pharmacodynamics of irinotecan during a phase II clinical trial in colorectal cancer. J Clin Oncol 14:2688-2695, 1996
20. Rowinsky EK, Grochow LB, Ettinger DS, et al. Phase I and pharmacological study of the novel topoisomerase I inhibitor 7-ethyl-10-[4-(1-piperidino)-1-piperidino] carbonyloxycamptothecin (CPT-11) administered as a ninety-minute infusion every 3 weeks. Cancer Res 54:427-436, 1994
21. Mandema JW, Verotta D, Sheiner LW. Building population pharmacokinetic-pharmacodynamic models. I. Models for covariate effects. J Pharmacokinet Biopharm 20:511-528, 1992
22. Jonsson EN, Karlsson MO. Xpose--an S-PLUS based population pharmacokinetic/ pharmacodynamic model building aid for NONMEM. Comput Methods Programs Biomed 58:51-64, 1999
23. Beal SL, Sheiner LB. NONMEM Users' Guides, NONMEM Project Group, University of California at San Fransisco, 1992
24. Gupta SK, Sathyan G, Lindemulder EA, Ho PL, Sheiner LB, Aarons L. Quantitative

characterization of therapeutic index: application of mixed-effects modeling to evaluate oxybutynin dose-efficacy and dose-side effect relationships. Clin Pharmacol Ther 65:672-684, 1999

25. Kehrer DFS, Sparreboom A, de Jonge MJA, et al. Clinical pharmacokinetics of irinotecan given in combination with the farnesyl transferase inhibitor Zarnestra™. Clin Cancer Res 7:3744s, 2001 (abstract)
26. Chabot GG. Clinical pharmacokinetics of irinotecan. Clin Pharmacokinet 33:245-259, 1997
27. Kehrer DFS, Sparreboom A, Verweij J, et al. Modulation of irinotecan-induced diarrhea by cotreatment with neomycin in cancer patients. Clin Cancer Res 7:1136-1141, 2001
28. Ando Y, Saka H, Ando M, et al. Polymorphisms of UDP-glucuronosyltransferase gene and irinotecan toxicity: a pharmacogenetic analysis. Cancer Res 60:6921-6926, 2000
29. Iyer L, Das S, Janisch L, et al. *UGT1A1*28* polymorphism as a determinant of irinotecan disposition and toxicity. Pharmacogenom J 2:43-47, 2002
30. Ando Y, Ueoka H, Sugiyama T, Ichiki M, Shimokata K, Hasegawa Y. Polymorphisms of UDP-glucuronosyltransferase and pharmacokinetics of irinotecan. Ther Drug Monit 24:111-116, 2002.
31. Sparreboom A, Marsh S, Mathijssen RHJ, Verweij J, McLeod HL. Irinotecan (CPT-11) disposition in relation to single-nucleotide polymorphisms (SNPs) of ABC transporters and drug-metabolizing enzymes. Proc Am Soc Clin Oncol 21, 83a, 2002 (abstract)

ACKNOWLEDGEMENT

We gratefully acknowledge the expert technical assistance of Peter de Bruijn (Erasmus MC – Daniel den Hoed, Rotterdam, the Netherlands).

Chapter Six

Irinotecan Pharmacokinetics-Pharmacodynamics: the Clinical Relevance of Prolonged Exposure to SN-38

British Journal of Cancer, 87: 144-150, 2002

Ron H.J. Mathijssen
Jaap Verweij
Walter J. Loos
Peter de Bruijn
Kees Nooter
Alex Sparreboom

Department of Medical Oncology, Erasmus MC - Daniel den Hoed
Rotterdam, The Netherlands

SUMMARY

We have shown previously that the terminal disposition half-life of SN-38, the active metabolite of CPT-11, is much longer than earlier thought (Kehrer *et al.*, Clin. Cancer Res., 6: 3451-3458, 2000). Currently, it is not known whether this prolonged exposure has any relevance toward SN-38-induced toxicity. Here, we found that SN-38 concentrations present in human plasma for up to 3 weeks after a single CPT-11 infusion induce significant cytotoxicity *in vitro*. Using pharmacokinetic data from 26 patients, with sampling up to 500 hours, relationships were evaluated between systemic exposure (AUC) to SN-38 and the per cent decrease in absolute neutrophil count (ANC) at nadir, or by taking the entire time course of ANC into account (AOC). The time course of SN-38 concentrations (AUC_{500h}) was significantly related to this AOC ($P < .001$). Based on this findings, a new limited-sampling model (LSM) was developed for SN-38 AUC_{500h} using only 2 timed samples: $AUC_{500h} = (6.588 \times C_{2.5h}) + (146.4 \times C_{49.5h}) + 15.53$, where $C_{2.5h}$ and $C_{49.5h}$ are plasma concentrations at 2.5 and 49.5 hours after start of infusion, respectively. The use of this LSM may open up historic databases to retrospectively obtain information about SN-38-induced toxicity in patients treated with CPT-11.

INTRODUCTION

Irinotecan (CPT-11) belongs to the family of camptothecins, and is a member of the class of topoisomerase I inhibitors. A broad spectrum of anti-tumor activity was seen in preclinical models as well as in patients, with responses observed in various disease types, including colorectal, lung, cervical, and ovarian cancers (1, 2). CPT-11 is a prodrug that requires activation to the active metabolite, 7-ethyl-10-hydroxycamptothecin (SN-38), which is approximately 100 to 1000-fold more active than the parent drug (3). A host of enzymes, including carboxylesterases to form SN-38 (4), UDP glucuronosyltransferases mediating SN-38 glucuronidation to form the β-glucuronic acid conjugate, SN-38G, (5), intestinal and endogenous β-glucuronidases causing deconjugation of SN-38G (6, 7), as well as cytochrome P-450 isoforms (8, 9) to form APC and NPC are involved in CPT-11 metabolism. In addition, several drug-transporting proteins, notably a canalicular multispecific organic anion transporter (cMOAT) located on the bile canalicular membrane (10), and P-glycoprotein (11), can influence CPT-11 elimination through hepatobiliary secretion and intestinal (re-) absorption.

As a result of these (and probably also other presently unknown) mechanisms, CPT-11 and its metabolites are subject to large interindividual kinetic variability (12), and show relatively long disposition half-lives. We have recently shown that by

applying an extended sampling-time period of 500 hours, the circulation time of SN-38 in cancer patients was found to be substantially longer than held previously (13). We hypothesized that, because of the poorly defined relationships between pharmacokinetic parameters and pharmacodynamic outcome of CPT-11 treatment (2), the prolonged terminal-disposition phase of SN-38 should be taken into consideration in future studies to identify kinetic correlates that would assist in prediction of the dose-limiting myelosuppression. Here, we examined the impact of this prolonged SN-38 exposure using an *in vitro* approach with a panel of human cancer cell lines, and re-examined exposure-toxicity relationships in a group of 26 cancer patients treated with CPT-11 administered as a 90-minute intravenous infusion in a 3-weekly regimen at a dose of 350 mg/m^2.

MATERIALS AND METHODS

Growth-inhibition studies

Exponentially growing cells obtained from the IGROV (ovarian cancer), Caco-2 (colon cancer) and H226 (lung cancer) cell lines were cultured in 4 mL of RPMI-1640 medium, and plated in 25 cm^2 T-flasks (Corning Costar), at a density of 10,000 cells/flask. Hereafter, plates were incubated in a controlled environment at 37°C and 95% air/5% CO_2, and 24 hours after the start of incubation, the medium was replaced by medium containing SN-38 at final concentrations of 100 pM (39.2 pg/mL), 1.00 nM (392 pg/mL), or 10.0 nM (3,920 pg/mL). These concentrations were chosen because they adequately simulated the median SN-38 plasma concentrations circulating in patients after 3 weeks, 10 days, and 2 days, respectively, after infusion of the standard dose of CPT-11 (350 mg/m^2, given as a 90-minute infusion once every three weeks; see Figure 1). As a control, flasks containing cells in the absence of SN-38 were used. At 48-hour intervals, and for a maximum period of about 3 weeks (i.e., 500 hours), the culture medium was replaced with fresh medium to minimize possibly confounding effects caused by chemical instability of SN-38. At the same intervals, culture flasks were treated with trypsin for 30 minutes, and subsequently the cell suspension was centrifuged for 2 minutes at 500 x *g* (4°C). Next, the supernatant was discarded, and the cells were re-suspended in 50 µL of buffer and counted in a Bürker-cell chamber. Each experiment was repeated twice, with each counting performed in quadruplicate.

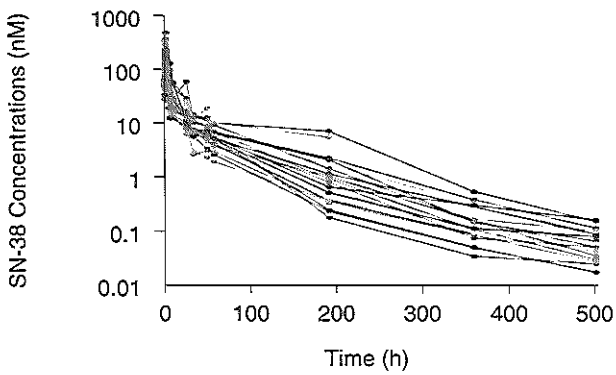

Figure 1. Plasma concentration-time profiles of SN-38 in patients treated with a 90-min i.v. infusion of CPT-11 (dose level 350 mg/m^2).

Patients and treatment

We retrospectively studied records from patients participating to various prospective clinical trials of CPT-11 in which pharmacokinetic monitoring was involved; the full clinical profiles are documented elsewhere (13-15). All patients had a histologically or cytologically confirmed malignant solid tumor for which CPT-11 was considered to be a treatment option. An adequate haematopoietic (white blood cell count (WBC) $\geq 3.0 \times 10^9$/liter; absolute neutrophil count (ANC) $\geq 1.5 \times 10^9$/liter; and platelet count (PLT) $\geq 100 \times 10^9$/liter), hepatic and renal function at the time of study entry was required. Eligibility criteria also included a World Health Organization performance status of 0 or 1, and age between 18 and 70 years. Before study entry, written informed consent was obtained from all patients.

CPT-11 was provided by Aventis Pharma (Antony Cedex, France) as a hydrochloride trihydrate salt in vials containing 40 or 100 mg, dissolved in d-sorbitol and a lactic acid-sodium hydroxide buffer system (pH 3.5-4.5) at a concentration of 20 mg/mL. This solution was further diluted in 250 mL of sterile, isotonic sodium chloride, prior to dosing. The drug was administered as a 90-minute continuous intravenous infusion at a dose of 350 mg/m^2, and each patient received prophylactic antiemetics including ondansetron (8 mg) or granisetron (1 mg) and dexamethasone (10 mg). In the first course of treatment, patients did not receive any other medication known to interfere with CPT-11 pharmacokinetics.

Pharmacokinetic analysis

Blood samples for pharmacokinetic analysis were drawn from an indwelling cannula from the arm opposite to that used for drug infusion. These samples were collected in glass tubes containing lithium heparin prior to infusion, at 0.5, and 1.5 hours (end of infusion) during infusion, and at 10, 20, and 30 minutes, and 1, 1.5, 2, 4, 5, 8.5, 24, 32, 48, 56, 190, 360, and 500 hours after the end of infusion. Blood samples were immediately centrifuged at 3000 × *g* for 10 minutes after collection to separate the blood cells and the plasma fraction was stored at -80°C until analysis.

Concentrations of CPT-11 and it metabolite SN-38 were determined by reversed-phase high-performance liquid chromatography with fluorescence detection, as described in detail elsewhere (16). To determine SN-38 at low femtomole levels, a more specific analytical method was used (17). Earlier pharmacokinetic findings showed that total drug levels (i.e., the total of lactone and carboxylate forms) of CPT-11 and SN-38 provided a consistent and accurate reflection of the pharmacologically active lactone concentration of both compounds with little variability (18). Therefore, it was concluded that total drug monitoring of CPT-11 and SN-38 could serve as an appropriate surrogate of the respective lactone forms. For practical reasons, we only used total drug forms for further analysis. Plasma concentration-time data of CPT-11 and SN-38 were fitted to a tri-exponential equation using the software package Siphar v4.0 (InnaPhase, Philadelphia, PA), based on previously described considerations for model discrimination (6). Calculation of the area under the plasma concentration-time curve (AUC) was based on integration from the tri-exponential curve with extrapolation to infinity. Extrapolated AUC values of SN-38 were either based on a 56-hour (AUC_{56h}) or a 500-hour sampling-time period (AUC_{500h}).

Exposure-toxicity relationships

Hematological parameters of interest (i.e., those derived from ANC, WBC and PLT) were determined before CPT-11 infusion and on a twice weekly basis during the entire pharmacokinetic sampling-time period, to enable a pharmacokinetic/ pharmacodynamic (PK/PD) evaluation. The pharmacodynamic endpoint for establishment of the PK/PD relationships was determined in 2 different ways. First, prior to the PK/PD analysis, individual toxicity data expressed as blood cell counts were plotted for each patient in a concentration versus time profile. The estimated area over these curves (AOC_{tox}), as well as the area under the curves (AUC_{tox}), was calculated by the linear-trapezoid method (Figure 2).

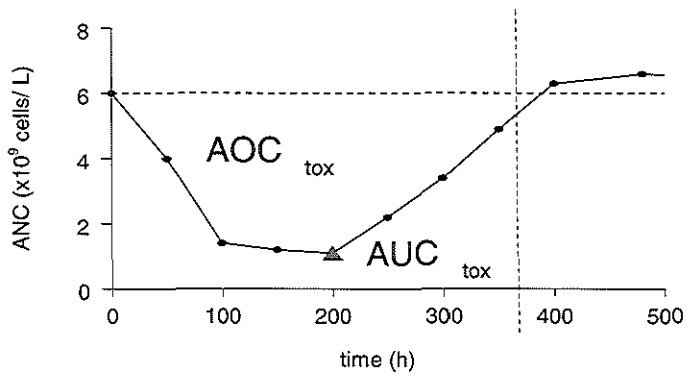

Figure 2. Example of an ANC-time pattern. The triangle represents the nadir count. The horizontal line represents the baseline value of ANC.

The ratio $AOC_{tox}/(AOC_{tox}+AUC_{tox})$, referred to as AOC, in which the denominator represents the area described by the pre-therapy toxicity value times the maximum pharmacokinetic sampling time, was hypothesized to be a simple and accurate function of drug-related hematological toxicity (19). Second, drug-related hematological toxicities were evaluated by using the nadir count, which was measured to determine the percent decrease in hematopoietic cells as:

Percent decrease = (pre-therapy value – nadir count) / (pre-therapy value) × 100

To avoid confounding bias due to changes in hematological data unrelated to treatment, patients showing extreme pre-infusion hematological numbers (i.e., with ANC > 13.0×10^9/liter) were excluded in these calculations. Each of these two relative hematological-toxicity functions were fitted to the AUC of SN-38 using a sigmoidal maximum effect (E_{max}) model, based on a modified Hill equation, as follows:

$$E = E_0 + E_{max} \times [(AUC_{SN\text{-}38}{}^{\gamma}) / (AUC_{SN\text{-}38}{}^{\gamma} + CE_{50}{}^{\gamma})]$$

In this equation, E_0 is the minimum reduction possible, E_{max} is the maximum response, CE_{50} is the AUC value of SN-38 predicted to result in 50% of the maximum response, and γ is the Hill constant, which describes the sigmoidicity of the curve (20).

Pharmacokinetic-pharmacodynamic analysis was performed using the software package Siphar version 4.0, and weighted and extended least squares techniques

were used to estimate model parameters. Model selection was guided by the decrease in the objective function value (-2xlog likelihood). The criteria to assess the goodness of fit of the models was based on (i) computation of the coefficient of variation, defined as the ratio of the standard deviation computed using the variance-covariance matrix and the parameter value, (ii) the Akaike information criterion, and (iii) the correlation coefficient and *P*-value of the relationship.

Statistical considerations

All statistical calculations were performed using the Number Cruncher Statistical System package version 5.X (J.L. Hintze, East Kaysville, UT, 1992) and/or the Siphar package. The level of significance was set at $P < .05$.

Limited sampling models (LSMs)

Patients were randomly entered in 2 groups, a training-data set and a validation-data set containing up to 20 samples for each individual patient, as has been described before (21). A restricted block randomisation was performed as described elsewhere (22) to keep the number of patients close for both groups, and only one course of each patient was taken to avoid bias as a result of potential cumulative effects and to keep the observations independent.

Our goal was to predict the AUC of SN-38 adequately with a minimum number of samples (1 to 3). Moreover, these samples should be taken at the most convenient time-points for practical reasons. The first step in the model development consisted of univariate linear-regression analysis to determine the best single-sample time points from the training data set. Next, we performed a stepwise (forward) multivariate linear-regression analysis using the optimal single sampling-time points to describe the association between SN-38 concentrations at multiple time points and its corresponding AUC. The Pearson's coefficient (r), root mean-square error (RMSE), and mean-predictive error (MPE), which describe correlation, precision and bias, respectively, were calculated to determine the best LSMs. The usefulness of the models was evaluated in the training data set, by comparing AUC values determined using the full data with AUC values predicted by the LSMs.

RESULTS

In vitro analysis of SN-38–induced cytotoxicity

The growth-inhibitory potential of low SN-38 concentrations was evaluated in vitro against several cell lines using a 3-week continuous-exposure period. Clear

manifestation of growth-inhibiting effects were seen at SN-38 concentrations of 100 pM, 1.00 nM and 10.0 nM in the IGROV cell lines, with the number of remaining viable cells being reduced by 46 ± 8.7%, 77 ± 10.4%, and > 99.9%, respectively, as compared to untreated controls (Figure 3). At these concentrations, 34 ± 5.9%, 73 ± 4.0% and 98 ± 0.2% growth inhibition, respectively, was seen in the H226 cells, relative to their controls. As the doubling time of the Caco-2 was shorter than that of the IGROV cells, data could not be obtained for the entire 3-week period in the Caco-2 cell line. Nonetheless, the data suggest overall that the low circulating concentrations of SN-38 determined previously in patients receiving CPT-11 at a dose of 350 mg/m^2 induce substantial inhibition of cancer cell growth, in spite of evident concerns in extrapolating data from in vitro experiments to the clinical situation.

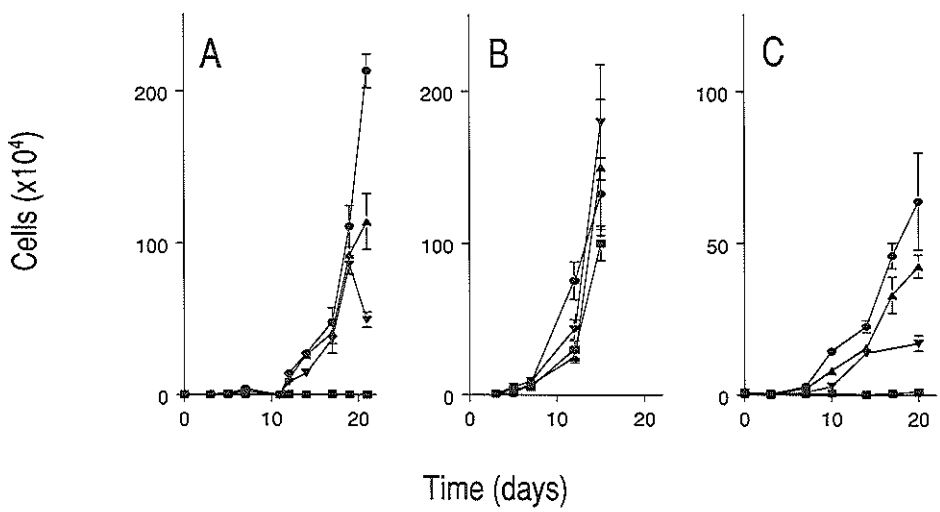

Figure 3. Cell-growth versus time curves for the IGROV (**A**), Caco-2 (**B**), and H226 (**C**) cell lines, incubated with medium containing 100 pM (▲), 1.00 nM (▼) or 10.0 nM (■) of SN-38 or medium without SN-38 (●) (reference) for a 500-hour incubation time period. Data indicate mean values (symbol) with SD (error bars), which are shown when larger than symbol.

Patient population

A total of 26 patients, predominantly suffering from colorectal cancer, were entered onto the current trial (Table 1). All patients received a single-agent regimen with CPT-11 in the first treatment course at a dose of 350 mg/m^2. One course was excluded because of extreme pre-treatment values for hematological parameters (i.e., ANC value greater than 13.0×10^9/liter), making a total of 25 courses assessable for PK/PD analysis.

Table 1. Patient characteristics for PK/PD evaluation.

Characteristic	
Total number of patients	26
Total number of courses	38
Assessable courses	25
Age [years (range)]	54[a] (37-71)
Sex (male/ female)[b]	12/ 14
Primary tumour site[b]:	
Colorectal	24
Cervix	1
Unknown primary site	1

[a] Results expressed as median value; [b] Results expressed as number of patients

Pharmacokinetics and pharmacodynamics

The two groups of SN-38 AUCs based on short (56 hours) and prolonged sampling (500 hours), respectively, were highly correlated (r^2 = 0.79). However, as shown in Figure 4, all AUC values calculated using the short sampling-time period substantially underestimated the true AUC, albeit with huge variation (7 up to 81%). The mean dose over AUC ratio for SN-38 based on prolonged sampling was 860 ± 410 L/h in this group of patients, and was 1400 ± 890 L/h when based on short sampling.

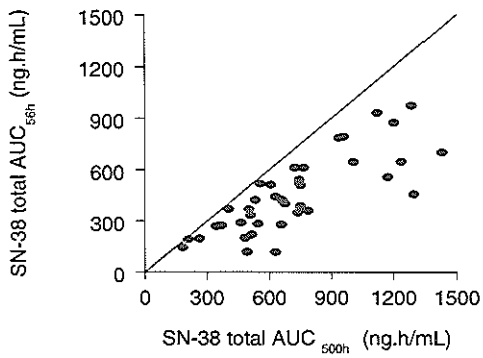

Figure 4. Relationship between calculated SN-38 AUCs, based on 500-h sampling and 56-h sampling respectively. (n=38). The solid line represents the line of identity (y=x).

The parameter estimates for the different pharmacodynamic models, using data from 25 patients, are shown in Figure 5. Preliminary results demonstrated that separate estimation of the observed maximum effect did improve the fits, and that optimal results were obtained with a model fitted to the data using weighted least squares (weighting factor, 1/y) and the Powell minimization algorithm. Data sets based on short and prolonged sampling were both plotted separately against individual values of ANC, WBC and PLT applying the ratio AOC_{tox} / (AOC_{tox} + AUC_{tox}) and the percent decrease in blood cell counts, using the E_{max}-model (23, 24). The kinetic parameters predicted to result in half of the maximum response showed a substantial degree of interindividual variability, and were poorly estimated in some models, presumably because of the small number of patients. The exposure-neutropenia relationship was best described with the model based on the 500-hour sampling-time period and the ratio AOC_{tox}/(AOC_{tox}+AUC_{tox}) (Figure 5B), although no significant improvement of the fit was obtained as compared to the relationship based on the short sampling time period (Figure 5A). In the optimal model, the following model parameters were observed: CE_{50} = 460 ± 82.9 ng.h/mL, γ = 2.22 ± 1.55, P = .0001 and r = 0.77. With the use of the percent decrease in ANC at nadir as pharmacodynamic measure, the fits were worse than those based on AOC. The disparity in the data of ratio AOC_{ANC} / (AOC_{ANC} + AUC_{ANC}) and percent decrease in ANC suggests that PD analysis based on percent decrease in ANC is not sufficiently accurate to be used as a measure for prediction of hematological toxicity. In contrast to ANC, no correlations with PK were observed for WBC and PLT.

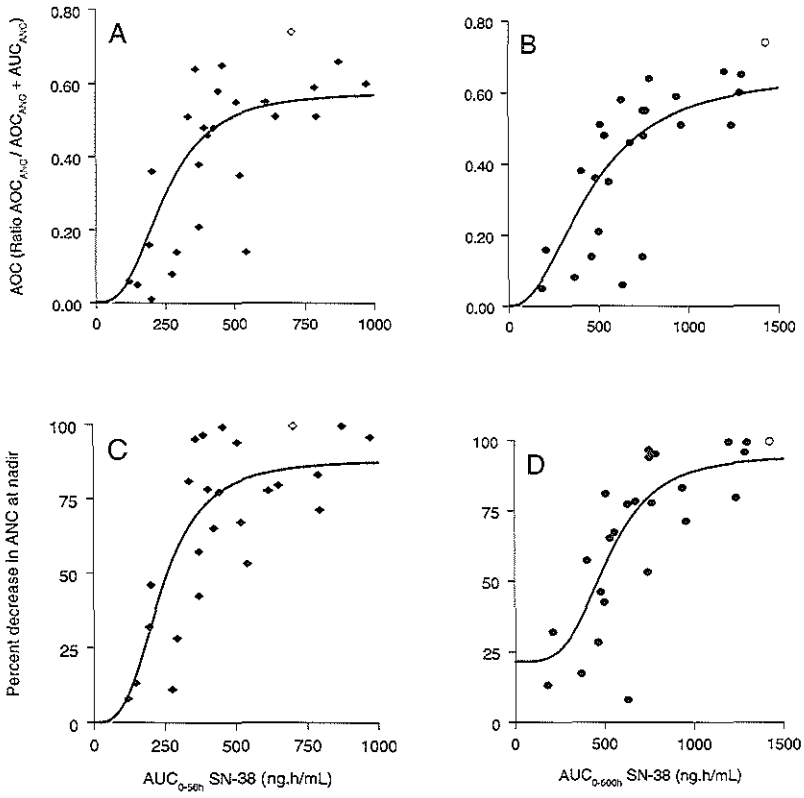

Figure 5. Relationship between ratio $AOC_{ANC}/(AOC_{ANC}+AUC_{ANC})$ and SN-38 AUC based on a 56-h sampling time period (**A**), or SN-38 AUC based on a 500-h sampling time period (**B**). Relationship between percent decrease in ANC at nadir versus SN-38 AUC based on a 56-h sampling time period (**C**), or SN-38 AUC based on a 500-h sampling time period (**D**). (*n*=25). Open symbols represent excluded data as a result of a baseline ANC > 13.0×10^9/liter.

Limited-sampling models

We developed a new limited-sampling model (LSM) for determination of SN-38 AUC_{500h} using one to three samples taken after drug administration, taking into account feasibility and usefulness in a routine clinical setting. There were no significant differences in patient characteristics between the training and validation data set. The

same 26 patients were included in this analysis, and in both groups 13 patients were entered (6 females and 7 males in both cases). The median age in the training set was 53 years (range, 37 to 71 years), versus 54 years (range, 42 to 71 years) in the validation set. Results of a univariate linear-regression analysis of SN-38 concentrations at each sample time points and the corresponding AUC showed correlation coefficients ranging from 0.08 to 0.82 in the training set (Table 2).

Table 2. Univariate correlation between SN-38 total concentrations at each sampled time point (after the start of infusion) and its corresponding AUC in training-data set patients.

Time point (h)	r[a]	Number of patients
0.50	0.25	13
1.50	0.14	13
1.67	0.14	13
1.83	0.08	12
2.00	0.22	13
2.50	0.35	13
3.00	0.22	12
3.50	0.09	10
5.50	0.25	13
6.50	0.15	12
10.0	0.24	13
25.5	0.48	13
33.5	0.49	11
49.5	0.68	11
57.5	0.82	7
191.5	0.54	13
361.5	0.54	10
501.5	0.34	10

[a] r: Pearson's correlation coefficient

Multiple-regression analysis, based on one or two additional time points led to significantly improved correlation coefficients. Based on a variety of considerations, including, low values for RMSE and MPE with high correlation coefficients, the optimal LSM was a bivariate model containing concentration data at 2 time points:

$$AUC_{SN\text{-}38}\ (ng.h/mL) = (6.588 \times C_{2.5h}) + (146.4 \times C_{49.5h}) + 15.53$$

where $C_{2.5h}$ and $C_{49.5h}$ represent plasma concentrations of SN-38 (in ng/mL) at 2.5 hours after the start of infusion (1 hour post-infusion) and 49.5 hours (48 hours post-infusion), respectively. In both the training set and validation sets, this model showed little bias (MPE, 0.33% and 0.76%) and excellent precision (RMSE, 4.9% and 9.1%), with correlation coefficients of 0.99 and 0.96, respectively (Figure 6).

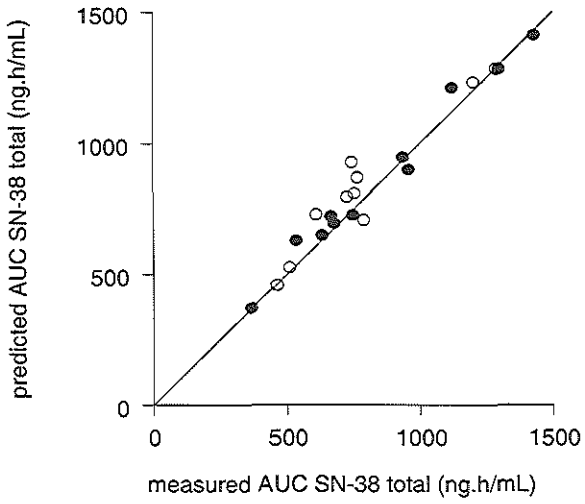

Figure 6. Correlation between the observed AUC from a linear three-compartment model and the predicted AUC from the LSM for SN-38 total. Closed symbols represent training set data; open symbols represent validation set data. The solid line represents the line of identity (y=x).

Trivariate models were also evaluated using the clinically most optimal sample-time points (i.e 1, 190 and 360 hours post-infusion). Unfortunately, the predictive performance of this model appeared to be worse (validation set: MPE = 1.6%; RMSE = 18%; r^2= 0.83), despite acceptable training set statistics (MPE = 0.62%; RMSE = 9.5%; r^2= 0.95).

DISCUSSION

This study shows that the prolonged exposure at low circulating concentrations of the pharmacologically active CPT-11 metabolite, SN-38, in plasma of cancer patients after a single dose has important cytotoxic potential *in vitro* and therewith may have clinical relevance toward SN-38-induced toxicity and antitumor activity. In our *in vitro* experiments we exposed several cancer cell lines to SN-38 concentrations, which were known to be circulating in plasma for up to 3 weeks after a 90-minute i.v. infusion of CPT-11 at a dose of 350 mg/m^2. After a 3-week incubation period in the presence of SN-38 at concentrations of 100 pM, 1.00 nM and 10.0 nM, significantly reduced tumour growth was observed as compared to untreated cells, suggesting significant cytotoxic activity, even at these low drug levels. Using pharmacokinetic data from 26 patients treated with CPT-11, with sampling up to 500 hours after drug administration, PK/PD relationships were evaluated between systemic exposure (AUC) to SN-38 and the percent decrease in ANC at nadir or by taking the entire time course of ANC into account (AOC), using a modified Hill function (sigmoidal E_{max} model). Taking into consideration the entire time course of SN-38 concentrations (AUC_{500h}), the most optimal relationships were observed for the AOCs. These data not only emphasise the need to apply appropriate PK/PD models with sufficient sampling-time points for the accurate estimation of complete concentration-time profiles, but also has direct clinical relevance in view of the fact that relationships between drug exposure and effect (i.e., toxicity and efficacy) were poorly defined previously (2).

We have shown earlier that the use of an extended sample-collection period of 500 hours led to terminal disposition half-life and AUC estimates for SN-38 after CPT-11 administration of 47 ± 7.9 hours and 2.0 ± 0.79 μM.h, respectively (13), both representing a 2-fold increase as compared to earlier reported estimates. As an explanation for this phenomenon, we previously observed a substantial formation of SN-38 from CPT-11 and the cytochrome P-450 3A4-mediated metabolite, NPC, by plasma carboxylesterases. In addition, transport studies in Caco-2 cell monolayers indicated that SN-38 could cross the membrane from the apical to the basolateral side, indicating the potential for re-circulation processes that can prolong circulation times (13). More recently, we also noted extensive partitioning of CPT-11 in erythrocytes resulting in prolonged association of the parent drug in the central blood compartment (25). Regardless of the exact underlying causes for the prolonged SN-38 circulation, the fact that low circulating levels of SN-38 demonstrate profound cytotoxic potential indicates the need to not take an oversimplified view when modelling drug-induced hematological toxicity.

Pharmacokinetic information on the concentration-time profiles has previously been combined with efficacy-toxicity data to form PK/PD models for drugs in a wide

variety of therapeutic areas. The most common type of this kind of PK/PD model is one in which a summary measure of exposure, such as AUC, is related to the principal side effect of the treatment, in this case hematological toxicity, for which singly measured nadir counts are usually employed. However, experimental evidence suggests that information on an entire time course of changes in blood cell counts is more important than the nadir count. For example, it has been demonstrated that patients with prolonged neutropenia have a greater risk of infection than patients who have the same nadir count with rapid recovery. Therefore, we hypothesised that using data from the entire time course of neutropenia after CPT-11 treatment would provide useful information. Thus, we analysed our data using two different types of analysis (percent decrease in toxicity at nadir and a measure of time course (AOC)) using two different variables based on AUC calculated using 56-hour or 500-hour sampling periods, with those based on AOC showing superiority for prediction of hematological toxicity. For both PD parameters, the quantity of available data is positively correlated with the quality (accuracy) of the determined outcome variables. Thus, at least several data points are required for an accurate estimate of the nadir count. In our current study, a rich data set was available with hematological toxicity data, which might explain the moderate predictive performance of the PK/PD relationship using (assumed) nadir counts. Clinically even more important PD parameters than the just mentioned parameters may be (i) the time period during which the neutrophil count remains below a certain level (for instance $4x10^9$ cells/L) or (ii) the area between the curve of time versus leukocyte count and the line representing a cell count of $4x10^9$ cells/L (26). Also in our current study, this area was shown to be demonstrated the best correlation of all tested PK/PD combinations. In order to further optimise PK/PD relationships, a population model for CPT-11-induced neutropenia by modelling the full time course of hematological toxicity is currently being developed, as done previously for paclitaxel and etoposide (26-28).

Some clinical implications from the data presented in this study, particularly with respect to considerations of treatment schedule, are easily envisaged. Regarding administration regimens of CPT-11 used in cancer patients, it is particularly noteworthy that different schedules are being used in Europe (350 mg/m^2 once every 3 weeks), the USA (125 mg/m^2 weekly for 4 or 6 weeks) and Japan (100 mg/m^2 every week). Furthermore, there is a current trend for the use of protracted intravenous or oral dosing regimens of CPT-11 using daily drug administration (29), based on earlier clinical experience with camptothecin analogues with relatively short terminal disposition half-lives, such as topotecan. However, the unique pharmacokinetic behavior of SN-38, coupled to our current pharmacodynamic observations, suggests

that a single administration of CPT-11 repeated every third week is the preferred regimen, and that increased frequency of administration may result in drug accumulation.

Obviously, the clinical applicability of SN-38 AUC as a PK parameter predicting toxicity would increase by the availability of accurate and predictive limited sampling models (LSM). Earlier developed models for the determination of SN-38 total AUC were only useful for the estimation of AUC models up to 24 or 56 hours (21). Therefore, a new LSM was developed for determination of SN-38 AUC_{500h} using only 2 timed samples: AUC_{500h} (ng.h/ml) = $(6.588 \times C_{2.5\ h}) + (146.4 \times C_{49.5\ h}) + 15.53$, where $C_{2.5\ h}$ and $C_{49.5\ h}$ are plasma concentrations at 2.5 and 49.5 hours after start of CPT-11 infusion, respectively. The model was shown to be precise (RMSE = 4.9%) with no demonstration of any bias (MPE = 0.33%). This model enables us to perform PK studies in a very efficient manner, and it is less expensive and might therefore be applicable to large-scale investigations. For example, PK sampling might be performed easily in an outpatient setting. In addition, the use of this LSM may open up historic databases for a re-evaluation, or at least provide prospective studies to obtain information about SN-38-mediated (hematological) toxicity in cancer patients treated with CPT-11. For the determination of SN-38 AUC, this model is currently being implemented in a multi-institutional clinical trial with CPT-11 administered at a dose level of 350 mg/m^2 in the presence or absence of the aminoglycoside antibiotic, neomycin.

In conclusion, we have shown that the prolonged circulation of SN-38 at low concentrations following CPT-11 administration has clinical implications, and resulted in altered exposure-toxicity relationships. This information, coupled to the prospective implementation of the newly developed LSM, may be of importance for future individualization of drug therapy in order to avoid excessive toxicity.

REFERENCES

1. Vanhoefer U, Harstrick A, Achterrath W, Cao S, Seeber S, Rustum YM. Irinotecan in the treatment of colorectal cancer: clinical overview. J Clin Oncol 19: 1501-1518, 2001
2. Mathijssen RHJ, van Alphen RJ, Verweij J, et al. Clinical pharmacokinetics and metabolism of irinotecan (CPT-11). Clin Cancer Res 7: 2182-2194, 2001
3. Hertzberg RP, Caranfa MJ, Holden KG, et al. Modification of the hydroxy lactone ring of camptothecin: inhibition of mammalian topoisomerase I and biological activity. J Med Chem 32: 715-720, 1989
4. Humerickhouse R, Lohrbach K, Li L, Bosron WF, Dolan ME Characterization of CPT-11 hydrolysis by human liver carboxylesterase isoforms hCE-1 and h-CE-2. Cancer Res 60: 1189-1192, 2000
5. Iyer L, King CD, Whitington PF, et al. Genetic predisposition to the metabolism of irinotecan (CPT-11). Role of uridine diphosphate glucuronosyltransferase isoform 1A1 in the

glucuronidation of its active metabolite (SN-38) in human liver microsomes. J Clin Invest 101: 847-854, 1998

6. Sparreboom A, de Jonge MJA, de Bruijn P, et al. Irinotecan (CPT-11) metabolism and disposition in cancer patients. Clin Cancer Res 4: 2747-2754, 1998
7. Slatter JG, Schaaf LJ, Sams JP, et al. Pharmacokinetics, metabolism, and excretion of irinotecan (CPT-11) following I.V. infusion of [(14)C]CPT-11 in cancer patients. Drug Metab Dispos 28: 423-433, 2000
8. Haaz MC, Rivory L, Riche C, Vernillet L, Robert J. Metabolism of irinotecan (CPT-11) by human hepatic microsomes: participation of cytochrome P-450 3A and drug interactions. Cancer Res 58: 468-472, 1999
9. Santos A, Zanetta S, Cresteil T, et al. Metabolism of irinotecan (CPT-11) by CYP3A4 and CYP3A5 in humans. Clin Cancer Res 6: 2012-2020, 2000
10. Chu XY, Kato Y, Ueda K, et al. Biliary excretion mechanism of CPT-11 and its metabolites in humans: involvement of primary active transporters. Cancer Res 58: 5137-5143, 1998
11. Chu XY, Kato Y, Sugiyama Y. Possible involvement of P-glycoprotein in biliary excretion of CPT-11 in rats. Drug Metab Dispos 27: 440-441, 1999
12. Mathijssen RHJ, Verweij J, de Jonge MJA, Nooter K, Stoter G, Sparreboom A. Impact of body-size measures on irinotecan clearance: Alternative dosing recommendations. J Clin Oncol 20: 81-87, 2002
13. Kehrer DFS, Yamamoto W, Verweij J, de Jonge MJA, de Bruijn P, Sparreboom A. Factors involved in prolongation of the terminal disposition phase of SN-38: Clinical and experimental studies. Clin Cancer Res 6: 3451-3458, 2000
14. Kehrer DFS, Sparreboom A, Verweij J, et al. Modulation of irinotecan-induced diarrhea by co-treatment with neomycin in patients with metastatic colorectal cancer. Clin Cancer Res 7: 1136-1141, 2001
15. Kehrer DFS, Mathijssen RHJ, Verweij J, de Bruijn P, Sparreboom A. Modulation of irinotecan metabolism by ketoconazole. J Clin Oncol 20: 3122-3129, 2002
16. De Bruijn P, Verweij J, Loos WJ, Nooter K, Stoter G, Sparreboom A. Determination of irinotecan (CPT-11) and its active metabolite SN-38 in human plasma by reversed-phase high-performance liquid chromatography with fluorescence detection. J Chromatogr 698: 277-285, 1997
17. De Bruijn P, de Jonge MJA, Verweij J, et al. Femtomole quantitation of 7-ethyl-10-hydroxycamptothecine (SN-38) in plasma samples by reversed-phase high-performance liquid chromatography. Anal Biochem 269: 174-178, 1999
18. Sasaki Y, Yoshida Y, Sudoh K, et al. Pharmacological correlation between total drug concentration and lactones of CPT-11 and SN-38 in patients treated with CPT-11. Jpn J Cancer Res 86: 111-116, 1995
19. Gurney HP, Ackland S, Gebski V, Farrell G. Factors affecting epirubicin pharmacokinetics and toxicity: evidence against using body-surface area for dose calculation. J Clin Oncol 16: 2299-2304, 1998
20. Holford NH, Sheiner LB. Understanding the dose-effect relationship: clinical application of pharmacokinetic-pharmacodynamic models. Clin Pharmacokinet 6: 429-453, 1981
21. Mathijssen RHJ, van Alphen RJ, de Jonge MJA, et al. Sparse-data set analysis for irinotecan and SN-38 pharmacokinetics in cancer patients co-treated with cisplatin. Anticancer Drugs 10:

9-16, 1999

22. Altman DG. Practical statistics for medical research. Chapman & Hall: London, 1991
23. Gianni L, Kearns CM, Giani A, et al. Nonlinear pharmacokinetics and metabolism of paclitaxel and its pharmacokinetic/ pharmacodynamic relationships in humans. J Clin Oncol 13: 180-190, 1995
24. Ohtsu T, Sasaki Y, Tamura T, et al. Clinical pharmacokinetics and pharmacodynamics of paclitaxel: a 3-hour infusion *versus* a 24-hour infusion. Clin Cancer Res 1: 599-606, 1995
25. Mathijssen RHJ, Loos WJ, Verweij J, De Bruijn P, Sparreboom A. Differential distribution and red-cell partitioning of irinotecan (CPT-11) and SN-38 in cancer patients. Proc Am Assoc Cancer Res 43: 209, 2002 (abstract)
26. Minami H, Sasaki Y, Watanabe T, Ogawa M. Pharmacodynamic modeling of the entire time course of leukopenia after a 3-hour infusion of paclitaxel. Jpn J Cancer Res 92: 231-238, 2001
27. Karlsson MO, Molnar V, Bergh J, Freijs A, Larsson R. A general model for time-dissociated pharmacokinetic-pharmacodynamic relationships exemplified by paclitaxel myelosuppression. Clin Pharmacol Ther 63: 11-25, 1998
28. Minami H, Sasaki Y, Saijo N, et al. Indirect-response model for the time course of leukopenia with anticancer drugs. Clin Pharmacol Ther 64: 511-521, 1998
29. Kehrer DFS, Soepenberg O, Loos WJ, Verweij J, Sparreboom A. Modulation of camptothecin analogues in the treatment of cancer, a review. Anticancer Drugs 12: 89-106, 2001

Chapter Seven

Impact of Body-Size Measures on Irinotecan Clearance: Alternative Dosing Recommendations

Journal of Clinical Oncology, 20: 81-87, 2002

Ron H.J. Mathijssen
Jaap Verweij
Maja J.A. de Jonge
Kees Nooter
Gerrit Stoter
Alex Sparreboom

Department of Medical Oncology, Erasmus MC - Daniel den Hoed
Rotterdam, The Netherlands

ABSTRACT

Purpose: To evaluate relationships between various body-size measures and irinotecan (CPT-11) clearance and metabolism in cancer patients, and to provide future dosing recommendations for this agent.

Patients and Methods: Pharmacokinetic data were obtained from 82 adult patients (50 men, 32 women; median age, 54 years) receiving CPT-11 as a 90-minute intravenous infusion (dose range, 175 to 350 mg/m^2). In each patient, plasma samples were collected at timed intervals in the first administration of a 3-week schedule, and CPT-11 and its metabolite, SN-38, were measured by a liquid chromatographic assay.

Results: The mean (±SD) CPT-11 clearance was 33.6 ± 10.8 L/h, with an interindividual variability (IIV) of 32.1%. When clearance was adjusted for body-surface area (BSA), the IIV was similar (34.0%). In addition, in a multiple linear-regression analysis, none of the studied measures (BSA, lean-body mass, [adjusted] ideal body weight, and body-mass index) was a significant covariate ($P > .13$; $r^2 < .014$) in our population. Similarly, BSA did not significantly contribute to variability in the relative extent of conversion to SN-38 ($P = .26$).

Conclusion: BSA is not a predictor of CPT-11 clearance or SN-38 pharmacokinetics and does not contribute to reducing kinetic variability. These findings provide a rationale for the conduct of a comparative phase III study between BSA-based dosing and flat or fixed dosing of CPT-11.

INTRODUCTION

Irinotecan (7-ethyl-10-[4-(1-piperidino)-1-piperidino]carbonyloxycamptothecin; CPT-11) belongs to the class of topoisomerase I inhibitors, and it acts as a prodrug of SN-38, which is approximately 100- to 1,000-fold more cytotoxic than the parent drug (1). CPT-11 has shown a broad spectrum of antitumor activity in preclinical models as well as clinically, with responses observed in various disease types, including colorectal, lung, cervical and ovarian cancer (2). The pharmacokinetics and metabolism of CPT-11 are extremely complex and have been the subject of intensive investigation in recent years. Both CPT-11 and SN-38 are known in an active lactone form and an inactive carboxylate form, between which equilibrium exists that depends on the pH and the presence of binding proteins. In addition, CPT-11 is subject to extensive metabolic conversion by both phase I and phase II enzyme systems, including carboxylesterases to form SN-38 (3), uridine diphosphoglucuronate glucuronosyltransferases (UGT1A1) mediating

glucuronidation of SN-38 (4), as well as cytochrome P-450 isoforms (mainly CYP3A4) which form several pharmacologically inactive oxidation products (5, 6). Elimination routes of CPT-11 also depend on the presence of drug-transporting proteins, notably P-glycoprotein (7) and a canalicular multispecific organic anion transporter (cMOAT; ref. 8), present on the bile canalicular membrane.

The various processes that mediate drug elimination, either through metabolic breakdown or excretion, likely have a substantial impact on interindividual variability in drug handling. Strategies are now underway to individualize CPT-11 administration schedules based on patient differences in enzyme or protein expression or by coadministration of specific agents modulating side effects (9). These strategies may ultimately lead to more selective chemotherapeutic use of this agent. In contrast, the prescribed dose of CPT-11 is currently calculated using body-surface area (BSA) as the only independent variable, and it has been shown that this approach still results in large interindividual variability in exposure. Although this has been widely recognized for some agents, until recently its significance has not been fully appreciated and remains unstudied for most anticancer drugs used in today's clinical practice. The purpose of this report was to assess CPT-11 clearance and metabolism as a function of commonly used body-size measures in adult cancer patients to provide a pharmacokinetic rationale for the appropriate dosing of CPT-11.

PATIENTS AND METHODS

Patients population

Records collected as part of clinical CPT-11 monitoring at the Erasmus MC were examined retrospectively; the full clinical profiles have been documented elsewhere (10-13). All patients had a malignant solid tumor that stipulated a CPT-11-based regimen and had adequate hematopoietic (absolute neutrophil count $\geq 1.5 \times 10^9$/L; platelet count $\geq 100 \times 10^9$/L), hepatic, and renal function at the time of study entry. Inclusion also required an Eastern Cooperative Oncology Group performance status of 2 or less and age between 18 and 75 years. All patients with complete information (consisting of age, disease, height, weight, and first-dose pharmacokinetic data) were included in the current analysis. No other agents known to interfere with CPT-11 disposition were administered immediately before or concomitantly with CPT-11. All patients provided informed consent for the pharmacologic analysis.

Drug administration

CPT-11 was provided as the hydrochloride trihydrate salt by Aventis Pharma (Antony Cedex, France) in 40- or 100-mL vials containing 20 mg CPT-11/mL in *d*-sorbitol and a lactic acid-sodium hydroxide buffer system (pH 3.5 to 4.5). Before dosing, the pharmaceutical preparation was diluted in 250 mL of sterile, isotonic sodium chloride. The drug was administered every 3 weeks as a 90-minute continuous intravenous infusion at a dose level between 175 and 350 mg/m^2, and each patient received an intravenous premedication schedule that included ondansetron (8 mg) and dexamethasone (10 mg). The pharmacokinetic behavior of CPT-11 at these dose levels is linear and dose-independent (14).

Pharmacokinetic analysis

Heparinized blood samples for pharmacokinetic analysis were drawn from an indwelling cannula. These samples were collected before infusion, at 0.5 and 1.5 h during infusion, and 10, 20, and 30 minutes and 1, 2, 3, 3.5, 4, 5, 6.5, 10.5, 24, 30.5, 48, and 54.5 hours after the end of infusion. Plasma fractions were obtained immediately after collection by centrifugation (3000 × *g* for 10 minutes). Concentrations of CPT-11 and SN-38 were determined by a validated reversed-phase high-performance liquid chromatography system with fluorescence detection (15). A preliminary analysis of the initial raw data indicated that CPT-11 and SN-38 total drug levels (i.e., the total of lactone and carboxylate forms) provided a consistent and accurate reflection of the lactone concentration with little variability (not shown). This is in agreement with previous findings (16) and suggests that total drug monitoring serves as an appropriate surrogate of the lactone forms. Therefore, we decided, for practical purposes, to use only total drug forms in further analysis.

Concentration-time data of CPT-11 and SN-38 were fitted to a tri-exponential equation, using the software package Siphar, version 4.0 (InnaPhase, Philadelphia, PA), on the basis of a previously described model discrimination (17). Inverse square weighting of the measured concentrations was used for all compartmental analyses. The absolute clearance of CPT-11 (in L/h) was calculated by dividing the dose administered (in mg) by the observed AUC values. The apparent clearance (in L/h/m^2) was also calculated by dividing the absolute clearance of irinotecan by a patient's individual BSA value. For SN-38, the apparent metabolic clearance and the relative extent of conversion, defined as the area under the curve (AUC; in M×h) ratio of SN-38 and CPT-11, were calculated.

The various body size measures, including BSA (in m^2; ref. 18), lean body mass (LBM; in kg; ref. 19), ideal body weight (IBW; in kg; ref. 20), adjusted ideal body weight

(AIBW; in kg; ref. 20), and body mass index (BMI; ref. 20), were calculated using the following equations, with length expressed in meters and weight in kg:

$$BSA = \sqrt{((lenght \times weight) / 36)} \text{ or } 0.007184 \times weight^{0.425} \times length^{0.725} \quad \text{(eq. 1)}$$

$$LBM\ (men) = 1.10 \times weight - 120 \times (weight/ (length \times 100))^2 \quad \text{(eq. 2)}$$

$$LBM\ (women) = 1.07 \times weight - 148 \times (weight/ (length \times 100))^2 \quad \text{(eq. 3)}$$

$$IBW\ (men) = 50 + 0.91 \times ((length \times 100) - 152) \quad \text{(eq. 4)}$$

$$IBW\ (women) = 45 + 0.91 \times ((length \times 100) - 152) \quad \text{(eq. 5)}$$

$$AIBW = IBW + 0.25 \times (weight - IBW) \quad \text{(eq. 6)}$$

$$BMI = weight / (length)^2 \quad \text{(eq. 7)}$$

After studying the whole included population, patients were divided in several groups. First, sex was studied separately. Second, patients were classified into three BSA-groups: BSA less than 1.7 m^2, BSA between 1.7 and 2.0 m^2, and BSA more than 2.0 m^2, respectively.

Statistical analysis

All pharmacokinetic parameters are reported as mean values±SD. Interindividual variability in parameters was evaluated by the coefficient of variation, defined as the ratio of SD and the observed mean. Univariate and multivariate linear-regression analysis were performed to evaluate potential relationships between CPT-11 clearance or relative extent of conversion to SN-38 and each of the studied body-size measures, sex, tumor type, and age. After tests for normality in parameter variability, absolute clearance (dependent variable) was plotted to BSA, LBM, IBW, AIBW, BMI, weight, and length (independent variables). Probability values and adjusted r^2 were calculated as measurements for correlation. One-way analysis of variance was used to compare difference in body-size normalized clearance among different BSA categories with the Bonferroni correction for multiple comparisons. All statistical calculations were performed using the NCSS package version 5.X (J.L. Hintze, East Kaysville, UT). Probability values of less than .05 were regarded as statistically significant.

RESULTS

Patient population

The entire population studied consisted of 82 patients, of whom 50 were male and 32 were females (Table 1). The median age was 54 years (range, 36 to 71 years), and the majority of patients suffered from a colorectal carcinoma. Administered CPT-11 dose levels varied from 175 to 350 mg/m^2.

Table 1. Demographics.

Patient characteristic	Number of patients
Total number of patients	82
Age [years (range)]	54[a] (36-71)
Sex (male/ female)	50:32
Length [m (range)]	1.73[a] (1.51-1.92)
Weight [kg (range)]	75[a] (47-115)
BSA [m^2 (range)]	1.90[a] (1.47-2.40)
LBM [kg (range)]	57[a] (38-80)
IBW [kg (range)]	67[a] (44-86)
AIBW [kg (range)]	69[a] (49-90)
BMI (range)	25[a] (16-37)
Primary tumor site	
Colorectal	52
Gastrointestinal	4
Lung	6
Head and neck	6
Miscellaneous	6
Unknown	8
Irinotecan dose (mg/m^2)	
175	6
200	22
230	7
260	12
300	9
350	26

[a] Results expressed as mean value.

CPT-11 clearance

The mean plasma clearance of CPT-11 was 33.6 ± 10.8 L/h (range, 13.5 to 64.8 L/h), with an interindividual variability of 32.1% (Table 2). After correction of the clearance for BSA, a mean value of 17.9 ± 6.1 $L/h/m^2$ was found, along with a similar degree of variability (i.e., 34.0%). Similarly, after adjustments of CPT-11 clearance for LBM, IBW, AIBW, BMI, weight, or length, the interpatient variability was not reduced (Table 2).

Table 2. Mean CPT-11 clearance as a function of body-size measures.

Body-size measure	CV (%)	Clearance (mean ± SD)
None	32.1	33.6 ± 10.8 L/ h
BSA	34.0	17.9 ± 6.1 L/ h/ m^2
LBM	35.3	1.37 ± 0.48 L/ h/ kg
IBW	36.7	0.51 ± 0.19 L/ h/ kg
AIBW	36.0	0.49 ± 0.18 L/ h/ kg
BMI	35.3	1.37 ± 0.48
Weight	38.3	0.46 ± 0.18 L/ h/ kg
Length	32.6	19.4 ± 6.3 L/ h/ m

Abbreviation: CV, coefficient of variation

Using linear-regression analysis, we found that CPT-11 was not significantly related to any of the studied body-size estimates (Figs 1 and 2). In a univariate analysis, which included weight, length, dose, sex, age, and tumor type as independent variables, no significant covariates were identified (*P*-values between .09 and .58; adjusted r^2 between < .0001 and .023) (Table 3). Multiple regression analysis also did not result in any significant correlation with CPT-11 clearance ($P = .21$, $r^2 = .032$). The interindividual variability in CPT-11 clearance was similar between men (33.4%) and women (34.6%), whereas variabilities in absolute clearance were 32.0% and 32.3 % for these two groups, respectively. No differences in clearance for the three studied BSA groups (i.e., < 1.7 m^2, between 1.7 and 2.0 m^2, and > 2.0 m^2) were found ($P = .06$), with mean values of 33.8, 31.0 and 37.4 L/h respectively. Neither BSA nor any other body-size estimate could reduce interpatient variability (not shown).

SN-38 pharmacokinetics

The overall apparent metabolic clearance of SN-38 was 1,490 ± 934 L/h, with an interindividual variability as high as 63%. Similar to the CPT-11 clearance data, this value remained in the same order (approximately 65%) after correction for patients' individual BSA values. As expected, the metabolic clearance of SN-38 and the relative extent of conversion to SN-38 were not related to BSA using linear-regression analysis ($P = .26$, adjusted $r^2 = .0032$ and $P = .55$, adjusted $r^2 < .0001$, respectively) (Fig. 1).

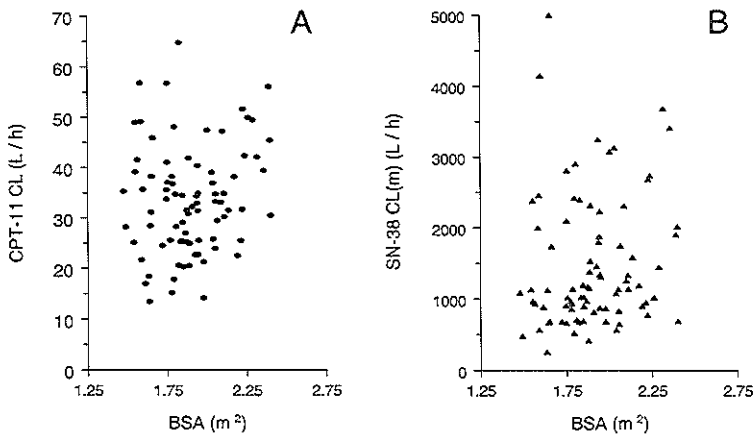

Figure 1. Relationship between absolute CPT-11 clearance (**A**) or metabolic clearance of SN-38 (**B**) and BSA (n=82).

Table 3. Relationships between CPT-11 clearance and patient characteristics.

Variable	*P*	r^2
BSA	.14	.014
LBM	.20	.0081
IBW	.52	<.0001
AIBW	.28	.0026
BMI	.13	.016
Weight	.09	.023
Length	.58	<.0001
Dose	.27	.0030
Gender	.43	<.0001
Age	.15	.013
Tumortype	.52	<.0001

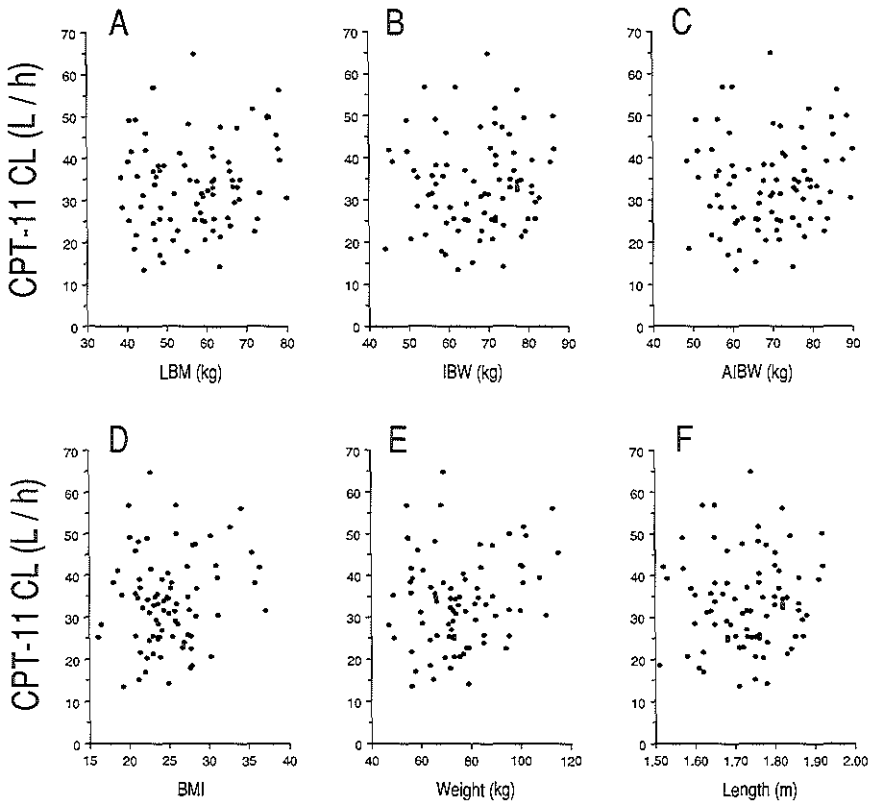

Figure 2. Relationship between absolute CPT-11 clearance and LBM (**A**), IBW (**B**), AIBW (**C**), BMI (**D**), weight (**E**), and length (**F**) (n=82).

DISCUSSION

A common practice in clinical oncology is to dose anticancer drugs on the basis of a patient's BSA with the aim of reducing interindividual pharmacokinetic variability. Despite the lack of evidence of the clinical relevance for this dose selection in adults, the use of BSA for this purpose is widespread (21, 22). The most commonly used formula to estimate BSA originates from 1916 (18), and during the last decade, several critical notes concerning this BSA-based dosing concept have been published (21-29). With the possible exception of docetaxel (30), it has been demonstrated that the clearance of most agents, including epirubicin (25-27), topotecan (28), cisplatin (29) and busulfan (20), is not related to BSA. Various alternative body-size measures have

been proposed in recent years, e.g. IBW, AIBW, BMI, and LBM, that might be better predictors of drug clearance, but no clear rationale for their use has yet been found (18, 25).

In the present study, we evaluated the relationship between CPT-11 clearance and metabolism with BSA and several other body-size measures in a group of 82 cancer patients. The interindividual variability in CPT-11 clearance is large and is an important determinant of toxicity (14). The coefficients of variation for the absolute CPT-11 clearance or that expressed relative to BSA when including all patients in this study were 32.1% and 34.0%, respectively. Thus, we found that, similar to the case with most other chemotherapeutic agents, dose calculations based on BSA did not reduce interpatient variability in CPT-11 clearance. In addition, in a multiple regression analysis with body-size measures as the independent variable, no significant covariate on clearance could be identified. In contrast, some estimates of body size (i.e., LBM, IBW, and AIBW) were shown to be even worse predictors of CPT-11 clearance and metabolism than BSA. Interestingly, it was reported by Miya *et al* (31) that BMI was an independent predictor of peak plasma concentrations of CPT-11 in a group of 36 patients who received the drug as a 90-minute intravenous infusion at a dose of 100 mg/m^2 ($P = .01$, $r^2 = .40$). These authors speculated that water-soluble drugs such as CPT-11, with drug doses calculated on the basis of BSA, are poorly distributed to adipose tissue and might produce elevated peak concentrations in plasma as compared to hydrophobic agents in obese patients (31). In our current data set, such a correlation between peak levels and BMI could not be established. The basis for these discrepant findings is presently unknown, although they may relate, for example, to patient-specific (ethnic) differences in the studied patient populations.

Much controversy has also arisen with respect to potential sex-dependent differences in the pharmacokinetic behavior of camptothecin anticancer agents. At least one recent observation indicated that whole blood and plasma concentrations of unchanged CPT-11 were generally lower in males as compared to females (32). In addition, sex has been identified recently as an important independent variable for the occurrence of severe CPT-11-induced leukocytopenia (grade 4) and/or diarrhea (grade 3 or worse) (33). However, because of substantial interindividual variability and the small sample size, differences in pharmacokinetic parameters or the effects of sex on severe toxicity were not statistically significant. In our patient population, sex was unrelated to (variability in) CPT-11 clearance, which finding is supported by earlier pharmacokinetic data (34). In addition, in a recent population pharmacokinetic model developed using NONMEM (S.L. Beal and L.B. Sheiner, San Francisco, CA), sex was not a significant covariate on CPT-11 clearance and formation ratio of SN-

38 (35). In contrast, for the related agent topotecan, a sex-dependent difference in clinical pharmacokinetics was noticed recently resulting from physiologic differences in hematocrit between males and females (36). These differences in kinetic behavior as a function of hematocrit between the various camptothecin analogs are not completely understood but may involve a variable degree in binding affinity for plasma proteins mediating erythrocyte partitioning and sequestration.

Using univariate and multivariate-regression analyses, we also found that various additional demographic variables, including disease type, drug dose, and age, were unrelated to CPT-11 clearance. This is in agreement with previous data (37, 38), suggesting that reduced starting doses are not required for elderly patients. The results of this study also suggest that CPT-11 clearance is similar in lean and obese subjects, whereas the metabolic clearance of SN-38 is slightly higher, although not significantly different, in obese patients as compared with lean controls. These findings with CPT-11 and SN-38 are consistent with data indicating that the absolute clearance of xenobiotics eliminated by hepatic P450 oxidase metabolism is similar in obese and lean patients, whereas the absolute clearance of drugs eliminated primarily by phase II enzymes is higher in the obese (20).

The only current factor routinely taken into consideration in clinical practice to predict toxicity following CPT-11 administration and to optimize or alter the dosage is a pathologic condition indicating hepatic dysfunction. It has been demonstrated that (elevated) bilirubin and alkaline phosphatase levels in plasma samples taken before treatment correlate positively with CPT-11 clearance, which may (partly) be explained by cMOAT activity (39). Also, correlations between CPT-11 clearance and γ-glutamyl transferase (negative), γ-glutamyl transpeptidase (negative), aspartate aminotransferase (positive) and alanine aminotransferase (positive), respectively, were recently observed (40, 41). In addition, it has been documented that interindividual variability in cMOAT-expression, as for instance in the Dubin-Johnson syndrome (42), can result in hyperbilirubinemia, and require dose modifications. Importantly, however, it is increasingly recognized that bilirubin level is not an appropriate parameter *per se* to predict severe CPT-11-induced toxicity, and it seems clinically negligible as a tool to predict toxicity (33), unless patients abstain from drug and alcohol and are strictly fasted. Thus, at present, bilirubin measurements have low predictability and are highly impractical. In addition, in view of the multiple enzyme systems and drug transporters involved in CPT-11 elimination, it seems that pharmacogenetic analysis such as that described for UGT1A1 (43-47), CYP3A4 (48), and P-glycoprotein (49, 50) polymorphism is unlikely to be the sole factor contributing to interindividual variability in CPT-11 clearance. We

believe that this inherent uncertainty, as well as a host of logistic problems associated with its implementation in routine clinical practice for the near future, presents significant limitations of pharmacogenetic analyses to individualization of CPT-11 dosage. In contrast, the concept of fixed rather than BSA-normalized dosing should be an area for fruitful clinical pharmacologic studies with CPT-11. We intend to conduct a study to prospectively evaluate the feasibility of delivering a fixed dose of CPT-11 as a 90-minute intravenous infusion every 3 weeks, based on the known flat dose (mg)-area under the plasma concentration-versus-time curve and systemic exposure-toxicity relationships of the compound (14), rather than following the standard practice of administering the drug on a mg/m^2 basis. Clearly, implementation of such concepts would have significant economic implications. The ability to manufacture a unit dose has obvious benefits for the pharmaceutical company involved. Similarly, reconstituting a fixed dose without subsequent individualization for different patients is more efficient and cost-effective than preparing individualized doses, and it would eliminate a significant source of error in attempting to obtain precise dosing (51).

In conclusion, we have shown that BSA as well as all other tested body-size measures are unrelated to CPT-11 clearance and metabolism. In view of the significant degree of interindividual variability in systemic exposure to CPT-11 and SN-38 and the small range in observed BSA within the studied population, CPT-11 can be added to the list of anticancer agents where BSA-based dosing does not seem to be more accurate and might suggest a (harmful) false sense of accuracy. Better individual predictors of CPT-11 elimination and pharmacodynamics might be available in the future. However, further research into the exact relationships between these key factors and pharmacologic endpoints is clearly required before they can be implemented in routine clinical practice. Therefore, the findings of this study provide a rationale for the conduct of a comparative phase III study between BSA-based dosing and fixed dosing of CPT-11. In case of fixed dosing, variability in drug clearance will still be approximately five-fold, and many patients will still be over- or underdosed. Since CPT-11 clearance and SN-38 pharmacokinetics correlate with toxicity, adjusting the dose for subsequent cycles based on toxicity induced by the drug is clearly recommended. The economic advantage may not be lost, since a range of fixed doses could be made available. As better methods of dose calculation become available in the future, these same doses could still be used as starting doses.

REFERENCES

1. Loos WJ, de Bruijn P, Verweij J, Sparreboom A. Determination of camptothecin analogs in biological matrices by high-performance liquid chromatography. Anticancer Drugs 11: 315-324, 2000
2. Vanhoefer U, Harstrick A, Achterrath W, Cao S, Seeber S, Rustum YM. Irinotecan in the treatment of colorectal cancer: clinical overview. J Clin Oncol 19: 1501-1518, 2001
3. Humerickhouse R, Lohrbach K, Li L, Bosron WF, Dolan ME. Characterization of CPT-11 hydrolysis by human liver carboxylesterase isoforms hCE-1 and h-CE-2. Cancer Res 60: 1189-1192, 2000
4. Iyer L, King CD, Whitington PF, et al. Genetic predisposition to the metabolism of irinotecan (CPT-11). Role of uridine diphosphate glucuronosyltransferase isoform 1A1 in the glucuronidation of its active metabolite (SN-38) in human liver microsomes. J Clin Invest 101: 847-854, 1998
5. Haaz MC, Rivory L, Riche C, Vernillet L, Robert J. Metabolism of irinotecan (CPT-11) by human hepatic microsomes: participation of cytochrome P-450 3A and drug interactions. Cancer Res 58: 468-472, 1998
6. Santos A, Zanetta S, Cresteil T, et al. Metabolism of irinotecan (CPT-11) by CYP3A4 and CYP3A5 in humans. Clin Cancer Res 6: 2012-2020, 2000
7. Chu XY, Kato Y, Sugiyama Y. Possible involvement of P-glycoprotein in biliary excretion of CPT-11 in rats. Drug Metab Dispos 27: 440-441, 1999
8. Chu XY, Kato Y, Ueda K, et al. Biliary excretion mechanism of CPT-11 and its metabolites in humans: involvement of primary active transporters. Cancer Res 58: 5137-5143, 1998
9. Kehrer DFS, Soepenberg O, Loos WJ, Verweij J, Sparreboom A. Modulation of camptothecin analogs in the treatment of cancer: a review. Anticancer Drugs 12: 89-105, 2001
10. De Jonge MJA, Verweij J, Planting AST, et al. Drug-administration sequence does not change pharmacokinetics and –dynamics of irinotecan and cisplatin. Clin Cancer Res 5: 2012-2017, 1999
11. De Jonge MJA, Sparreboom A, Planting AST, et al. Phase I study of 3-weekly irinotecan combined with cisplatin in patients with advanced solid tumors. J Clin Oncol 18: 187-194, 2000
12. De Jonge MJA, Verweij J, de Bruijn P, et al. Pharmacokinetic, metabolic, and pharmacodynamic profiles in a dose-escalating study of irinotecan and cisplatin. J Clin Oncol 18: 195-203, 2000
13. Kehrer DFS, Sparreboom A, Verweij J, et al. Modulation of irinotecan-induced diarrhea by co-treatment with neomycin in patients with metastatic colorectal cancer. Clin Cancer Res, 7: 1136-1141, 2001
14. Mathijssen RHJ, van Alphen RJ, Verweij J, et al. Clinical pharmacokinetics and metabolism of irinotecan. Clin Cancer Res, 2182-2194, 2001
15. De Bruijn P, Verweij J, Loos WJ, Nooter K, Stoter G, Sparreboom A. Determination of irinotecan (CPT-11) and its active metabolite SN-38 in human plasma by reversed-phase high-performance liquid chromatography with fluorescence detection. J Chromatogr 698: 277-285, 1997
16. Sasaki Y, Yoshida Y, Sudoh K, et al. Pharmacological correlation between total drug concentration and lactones of CPT-11 and SN-38 in patients treated with CPT-11. Jpn J Cancer Res 86: 111-116, 1995

17. Sparreboom A, de Jonge MJA, de Bruijn P, et al. Irinotecan metabolism and disposition in cancer patients. Clin Cancer Res 4: 2747-2754, 1998
18. Du Bois D, du Bois EF. A formula to estimate the approximate surface area if height and weight be known. Arch Intern Med 17: 863-871, 1916
19. Morgan DJ, Bray KM. Lean body mass as a predictor of drug dosage. Clin Pharmacokinet 26: 292-307, 1994
20. Gibbs JP, Gooley T, Corneau B, et al. The impact of obesity and disease on busulfan oral clearance in adults. Blood 93: 4436-4440, 1999
21. Gurney HP. Dose calculation of anticancer drugs: a review of the current practice and introduction of an alternative. J Clin Oncol 14: 2590-2611, 1996
22. Ratain MJ. Body-surface area as a basis for dosing anticancer agents: science, myth or habit? J Clin Oncol 16: 2297-2298, 1998
23. Sawyer M, Ratain MJ. Body surface area as a determinant of pharmacokinetics and drug dosing, Invest New Drugs 19: 171-177, 2001
24. Grochow LB, Baraldi C, Noe D. Is dose normalization to weight or body surface area useful in adults? J Natl Cancer Inst 82: 323-325, 1990
25. Gurney HP, Ackland S, Gebski V, Farrell G. Factors affecting epirubicin pharmacokinetics and toxicity: evidence against using body-surface area for dose calculation. J Clin Oncol 16: 2299-2304, 1998
26. Cosolo WC, Morgan DJ, Seeman E, Zimet AS, McKendrick JJ, Zalcberg JR. Lean body mass, body surface area and epirubicin kinetics. Anticancer Drugs 5: 293-297, 1994
27. Dobbs NA, Twelves CJ. What is the effect of adjusting epirubicin doses for body surface area? Br J Cancer 78: 662-666, 1998
28. Loos WJ, Gelderblom H, Sparreboom A, Verweij J, de Jonge MJA. Inter- and intrapatient variability in oral topotecan pharmacokinetics: implications for body-surface area dosage regimens. Clin Cancer Res 6: 2685-2689, 2000
29. De Jongh FE, Verweij J, Loos WJ, et al. Body-surface area based dosing does not increase accuracy of predicting cisplatin exposure. J Clin Oncol, 19: 3733-3739, 2001
30. Bruno R, Vivier N, Vergniol JC, De Philips SL, Montay G, Sheiner LB. A population pharmacokinetic model for docetaxel (Taxotere): model building and validation. J Pharmacokinet Biopharm 24: 153-172, 1996
31. Miya T, Goya T, Fujii H, et al. Body mass index (BMI) is an independent predictor of peak plasma concentration (Cmax) of irinotecan (CPT-11). Proc Am Soc Clin Oncol 18: 220a, 1999 (abstract)
32. Slatter JG, Schaaf LJ, Sams JP, et al. Pharmacokinetics, metabolism, and excretion of irinotecan (CPT-11) following I.V. infusion of [(14)C]CPT-11 in cancer patients. Drug Metab Dispos 28: 423-433, 2000
33. Ando Y, Saka H, Ando M, et al. Polymorphisms of UDP-glucuronosyltransferase gene and irinotecan toxicity: a pharmacogenetic analysis. Cancer Res 60: 6921-6926, 2000
34. Gupta E, Mick R, Ramirez J, et al. Pharmacokinetic and pharmacodynamic evaluation of the topoisomerase inhibitor irinotecan in cancer patients. J Clin Oncol 15: 1502-1510, 1997
35. Xie R, Mathijssen RHJ, Sparreboom A, Verweij J, Karlsson MO. Clinical pharmacokinetics of irinotecan and its metabolites: A population analysis. J Clin Oncol 20: 3293-3301, 2002
36. Loos WJ, Gelderblom H, Verweij J, Brouwer E, de Jonge MJA, Sparreboom A. Gender-dependent pharmacokinetics of topotecan in adult patients. Anticancer Drugs 11: 673-680, 2000

37. Schaaf LJ, Ichhpurani N, Elfring GL, Wolf DL, Rothenberg ML, Von Hoff DD. Influence of age on the pharmacokinetics of irinotecan (CPT-11) and its metabolites, SN-38 and SN-38 glucuronide (SN-38G), in patients with previously treated colorectal cancer. Proc Am Soc Clin Oncol 16: 202, 1997 (abstract)
38. Pazdur R, Zinner R, Rothenberg ML, et al. Age as a risk factor in irinotecan (CPT-11) treatment of 5-FU-refractory colorectal cancer. Proc Am Soc Clin Oncol 16: 260, 1997 (abstract)
39. Boige V, Vernillet L, Hua A, et al. Total plasma clearance of irinotecan (CPT-11) correlates with both alkaline phosphatase and bilirubin levels in patients with tumoral hepatic involvement. Proc Am Ass Cancer Res 41: 608, 2000 (abstract)
40. Van Groeningen CJ, van der Vijgh WJF, Baars JJ, Stieltjes H, Huibregtse K, Pinedo HM. Altered pharmacokinetics and metabolism of CPT-11 in liver dysfunction: a need for guidelines. Clin Cancer Res 6: 1342-1346, 2000
41. Chabot GG, Abigerges D, Catimel G, et al. Population pharmacokinetics and pharmacodynamics of irinotecan (CPT-11) and active metabolite SN-38 during phase I trials. Ann Oncol 6: 141-151, 1995
42. Borst P, Evers R, Kool M, Wijnholds J. A family of drug transporters: the multidrug resistance-associated proteins. J Natl Cancer Inst 92: 1295-1302, 2000
43. Hall D, Ybazeta G, Destro-Bisol G, Petzl-Erler ML, di Rienzo A. Variability at the uridine diphosphate glucuronosyltransferase 1A1 promotor in human populations and primates. Pharmacogenetics 9: 591-599, 1999
44. Iyer L, Hall D, Das S, et al. Phenotype-genotype correlation of in vitro SN-38 (active metabolite of irinotecan) and bilirubin glucuronidation in human liver tissue with UGT1A1 promoter polymorphism. Clin Pharmacol Ther 65: 576-582, 1999
45. Kaplan M, Hammerman C, Renbaum P, Klein G, Levy-Lahad E. Gilbert's syndrome and hyperbilirubinaemia in ABO-incompatible neonates. Lancet 356: 652-653, 2000
46. De Wildt SN, Kearns GL, Leeder JS, van den Anker JN. Glucuronidation in humans. Pharmacogenetic and developmental aspects. Clin Pharmacokinet 36: 439-452, 1999
47. Kadakol A, Ghosh SS, Sappal BS, Sharma G, Chowdhury JR, Chowdhury NR. Genetic lesions of bilirubin uridine-diphosphoglucuronate glucuronosyltransferase (UGT1A1) causing Crigler-Najjar and Gilbert syndromes: correlation of genotype to phenotype. Hum Mutat 16: 297-306, 2000
48. Wandel C, Witte JS, Hall JM, Stein CM, Wood AJ, Wilkinson GR. CYP3A activity in African American and European American men: population differences and functional effect of the CYP3A4*1B5'-promotor region polymorphism. Clin Pharmacol Ther 68: 82-91, 2000
49. Hoffmeyer S, Burk O, von Richter O, et al. Functional polymorphisms of the human multidrug-resistance gene: multiple sequence variations and correlation of one allele with P-glycoprotein expression and activity in vivo. Proc Natl Acad Sci USA 97: 3473-3478, 2000
50. Cascorbi I, Gerloff T, Johne A, et al. Frequency of single nucleotide polymorphisms in the P-glycoprotein drug transporter MDR1 gene in white subjects. Clin Pharmacol Ther 69: 169-174, 2001
51. Egorin MJ. Overview of recent topics in clinical pharmacology of anticancer agents. Cancer Chemother Pharmacol 42: S22-30, 1998

Chapter Eight

Modulation of Irinotecan Metabolism by Ketoconazole

Journal of Clinical Oncology, 20: 3122-3129, 2002

Diederik F.S. Kehrer
Ron H.J. Mathijssen
Jaap Verweij
Peter de Bruijn
Alex Sparreboom

Department of Medical Oncology, Erasmus MC - Daniel den Hoed
Rotterdam, The Netherlands

ABSTRACT

Purpose: Irinotecan (CPT-11) is a prodrug of SN-38 and has been registered for the treatment of advanced colorectal cancer. It is converted by the cytochrome P450 3A4 isozyme (CYP3A4) into several inactive metabolites, including APC. To investigate the role of CYP3A4 in irinotecan pharmacology, we evaluated the consequences of simultaneous treatment of irinotecan with a potent enzyme inhibitor, ketoconazole, in a group of cancer patients.

Patients and Methods: A total of 7 evaluable patients was treated in a randomized cross-over design with irinotecan (350 mg/m^2 i.v. over 90 min) given alone and followed 3 weeks later by irinotecan (100 mg/m^2) in combination with ketoconazole (200 mg orally for 2 days), or vice versa. Serial plasma, urine and feces samples were obtained up to 500 hours after dosing and analyzed for irinotecan, metabolites (SN-38, SN-38 glucuronide [SN-38G], APC), and ketoconazole by high performance liquid chromatography.

Results: With ketoconazole co-administration, the relative formation of APC was reduced by 87% (P = .002), whereas the relative exposure to the carboxylesterase-mediated SN-38 as expected on the basis of dose (area under the plasma-concentration-time curve normalized to dose) was increased by 109% (P = .004). These metabolic alterations occurred without substantial changes in irinotecan clearance (P = .90) and formation of SN-38G (P = .93).

Conclusion: Inhibition of CYP3A4 in cancer patients treated with CPT-11 leads to significantly increased formation of SN-38. Simultaneous administration of various commonly prescribed inhibitors of CYP3A4 can potentially result in fatal outcomes, and up to four-fold reductions in CPT-11 dose are indicated.

INTRODUCTION

There is considerable motivation for understanding adverse drug interactions with anticancer agents because of their narrow therapeutic index and the numerous concomitant medications that are administered routinely or intermittently (1). Indeed, drug interactions, including those with anticancer agents are a major cause of morbidity and mortality in modern medical practice (2), causing more than 100,000 deaths per year in the United States, and making it between the fourth and sixth leading cause of death in 1994 (1). Usually such interactions arise as a result of altered pharmacodynamics or pharmacokinetics of the drugs involved (3). In the latter case, this is usually due to changes in metabolic routes, and several mechanisms contributing to clinically important interactions have been identified, including expression of cytochrome P450 (CYP) isozymes. This class of enzymes,

particularly the CYP3A4 isozyme, is responsible for the oxidation of more than 50% of all drugs currently administered to humans (4), resulting in more polar and usually pharmacologically inactive metabolites, which can be excreted efficiently by the kidneys and the liver. It is evident that anticancer substrate drugs given in combination with drugs that are efficiently metabolized by CYP3A4 are likely to result in serious toxicity. However, most of the data currently available to evaluate possible drug interactions with anticancer agents have been addressed by animal experiments or the use of test systems in vitro (4).

In this study, we investigated the effect of CYP3A4 inhibition, using the model inhibitor ketoconazole (5), on the pharmacokinetics and toxicity profile of irinotecan (CPT-11), which is an important drug used in the treatment of colorectal cancer (6), and a partial substrate of the CYP3A4 isozyme (7).

MATERIALS AND METHODS

Patients and Treatment

Patients were eligible if they had a histologically confirmed diagnosis of metastatic colorectal cancer and proven progressive disease after first line chemotherapy (with fluorouracil) or a malignancy for which there was no effective standard regimen. Additional eligibility criteria were identical as documented elsewhere (8, 9). The original primary end point of the study was a measurable effect of ketoconazole on SN-38 and APC pharmacokinetics. Based on the standard deviation (SD) of the changes expected in irinotecan disposition (s_d), a power (1-β) of 0.8 (80%), a clinically relevant difference (δ; standardized difference, $2\delta/s_d$) of 30%, and a two-sided significance level (α) of 0.01 (1%), a patient sample size of seven was required in a paired, two-sided analysis. The s_d was estimated from an unpublished data set of 26 patients treated with irinotecan at 350 mg/m^2 and the assumption of no variance increase as a result of ketoconazole coadministration. The Ethics Board of the Erasmus MC approved the protocol, and all patients signed informed consent before study entry.

Patients screened and meeting study entry criteria were randomly assigned to receive either irinotecan alone (as a 90-minute intravenous infusion) at a dose of 350 mg/m^2 and followed 3 weeks later by irinotecan at a dose of 100 mg/m^2 given in combination with ketoconazole (200 mg) orally 1 hour before and 23 hours after the infusion of irinotecan, or both treatment cycles were given vice versa. A restricted randomization was performed to avoid bias in cycle sequence and to keep the number of patients close for both arms. This was achieved by choosing a randomized block at random using a table of random numbers to create the

allocation sequence. Before drug administration, the clinical irinotecan formulation (Aventis Pharma, Hoevelaken, the Netherlands) was diluted in 250 mL of isotonic sodium chloride.

Patients received a standard regimen of ondansetron and dexamethasone therapy, both given 30 minutes prior to chemotherapy. Atropine (0.25 mg) was administered subcutaneously as a prophylaxis for irinotecan-induced acute cholinergic syndrome in case the patient experienced this side effect in the previous cycle. Physical examination and toxicity assessment was performed on a weekly basis, as were clinical chemistry tests, for both treatment cycles.

Pharmacologic Analysis

Irinotecan, SN-38, SN-38-glucuronide (SN-38G), and APC pharmacokinetics were performed during both cycles. Blood samples (approximately 5 mL) were collected immediately before irinotecan infusion, at 30 minutes after the start of the infusion, at 5 minutes before the end of infusion, at 10, 20 and 30 minutes, and at 1, 1.5, 2, 4, 5, 8.5, 24, 32, 48, 56, 196 (day 8), 360 (day 15), and 500 (day 21) hours after the end of infusion. Complete urine and stool was collected in 24-hour intervals for 3 days after the start of treatment in both cycles. All biologic matrices were handled as outlined (10), and irinotecan and metabolite (SN-38, SN-38G, and APC) concentrations were determined by validated assays based on reversed-phase high-performance liquid chromatography (HPLC) with fluorescence detection, as described (11, 12).

Pertinent pharmacokinetic parameters, including peak concentration, area under the plasma concentration-time curve (AUC), total plasma clearance (defined as the ratio of dose administered in mg/m^2 and AUC), the rate constant of the terminal disposition phase, and the half-life of the terminal disposition phase were calculated using a linear three-compartment model running on Siphar version 4.0 (InnaPhase, Philadelphia, PA) (13). Metabolic ratios were calculated from plasma AUCs as well as urinary and fecal excretion data, as described previously (14). Previously, it has been shown that the AUC of irinotecan is dose-proportional over a large dose range (100 to 750 mg/m^2) in the tested 3-week regimen with the drug administered as a 90-minute intravenous infusion, indicating a linear pharmacokinetic behavior (7). Similarly, irinotecan metabolite concentrations increase linearly with the dose, and metabolic ratios are dose-independent in this dose range (7). Therefore, values for total plasma clearance of irinotecan and the various metabolic ratios between the treatment courses with and without ketoconazole co-administration were compared directly without any correction. Plasma concentrations of ketoconazole were measured by reversed-phase HPLC

with UV detection (15).

Pharmacodynamic evaluation involved analysis of pretherapy and nadir values of white blood cell counts and absolute neutrophil counts as a function of treatment course, expressed in absolute values (in 10^9/L) and in percent decrease relative to pretherapy values (eg, [(pretherapy value – nadir value) / pretherapy value] × 100%).

Enzyme Activity in Plasma

Total esterase activity in plasma samples was determined by a spectrophotometric assay using *o*-nitrophenyl acetate as a substrate (16), using purified esterase from porcine liver (EC3.1.1.1; Sigma, St Louis, MO) as a reference. Briefly, extracts prepared by sonication in 50 mM HEPES buffer (pH value of 7.4) were incubated in 3 mM of *o*-nitrophenyl acetate, and the absorbance at 420 nm was measured at 1-minute intervals for 10 minutes. Protein concentrations in extracts were determined using a Coomassie brilliant blue G250 dye-binding assay (17), using bovine serum albumin as a reference standard. Esterase activity is reported as micromoles of *o*-nitrophenyl acetate converted per minute per milligram of protein (μmol/min/mg).

Hepatic Metabolism In Vitro

Pooled human liver microsomes (Gentest Corp., Woburn, MA) containing 1 mg of protein per mL were incubated with irinotecan or SN-38 (both at a final concentration of 1 μM) in the presence and absence of ketoconazole (1 μM) as described (18). Reactions were incubated for 60 min at 37°C in the presence or absence of an NADPH-regenerating system. The decrease in substrate concentration as well as the formation of potential metabolites was measured at serial time points by HPLC as described (19).

Drug Transport Assays

Caco-2 cells were cultured and treated as described earlier (20). Transport studies of CPT-11 and SN-38 across complete monolayers in 12-well Transwell clusters (Costar, Cambridge, MA) with 1-cm^2 polycarbonate membrane filters (0.4-μm pore size) were conducted in a controlled environment at a temperature of 37°C. The integrity of the cell monolayers was evaluated by measuring transepithelial transport of [^{14}C]mannitol as described elsewhere (21). The experiments were initiated with the addition of the lactone forms of irinotecan and SN-38 at an initial concentration of 10 μM, both diluted from metanolic stock solutions diluted in Dulbecco's minimum-essential medium to avoid precipitation due to the limited

solubility in physiological buffers. This drug concentration was used to allow sufficiently accurate determination of transport rates of both irinotecan and SN-38 across the Caco-2 cell monolayers given the sensitivity limit of the available analytical method (11). Transport inhibition experiments were also performed under identical conditions in the presence of ketoconazole or the P-glycoprotein/breast cancer-resistance protein (BCRP) inhibitor GF120918 (Glaxo Wellcome, Research Triangle Park, NC) added to the apical or basolateral side of the monolayer (22). At various continuous exposure durations of 1, 1.5, 2, 2.5, and 3 hours, aliquots of the apical and basolateral solutions were collected, centrifuged for 5 min at 24,000 × *g* (4°C), and immediately stored at –80°C until analysis for total drug concentrations (lactone plus carboxylate forms) by a liquid chromatographic assay (11). For each experiment, performed in triplicate on three separate occasions, the mean transport rate was calculated from the linear part of the plot of the total amount of drug transported versus time. The apparent permeability coefficient (P_{app}), expressed in centimeters per second was calculated as $\Delta Q/\Delta t \times 1/60 \times 1/A \times 1/C_0$, where $\Delta Q/\Delta t$ is the permeability rate (in µg/min), A is the surface area of the membrane (in cm^2), and C_0 is the initial concentration in the donor chamber (in µg/mL) (21).

Statistical Considerations

All data are presented as mean values ± SD, unless stated otherwise. The statistical significance of differences in data between treatments was evaluated using two-tailed, paired *t* tests after testing for approximate normality or a modification for the case with unequal variances detected using a variance-ratio test, assuming weak period and/or sequence effects (7). The significance level was set at $P < .05$. Statistical calculations were performed on NCSS version 5.X (J.L. Hintze, East Kaysville, UT; 1992) or SISA binomial (D.G. Uitenbroek, Hilversum, the Netherlands; 2001; http://home.clara.net/sisa/binomial.htm).

RESULTS

Patients and Toxicity Profiles

To determine the influence of CYP3A4 inhibition by ketoconazole on CPT-11 pharmacokinetics and toxicity, a total of nine patients was accrued to the study. In two of nine patients, ketoconazole was only administered on day 1 in the combined schedule, and these patients were considered not evaluable. Of the seven remaining patients, three were male and four were female with a median age of 54 years (range, 42 to 71 years) and a median performance score of 1 (range, 0 to 2). All patients completed the study within the scheduled time without delay. The predominant disease type was colorectal cancer (n = 5), and the principal toxicity

consisted of neutropenia. Paired analysis of hematological pharmacodynamic parameters indicated that the degree of myelosuppression, including the percent decrease in absolute neutrophil count, was similar between the courses, in spite of a 3.5-fold reduced irinotecan dose when given in combination with ketoconazole (Table 1). Non-hematological toxicities (nausea, vomiting and diarrhea) were observed on both arms, but were also not substantially different in severity or incidence.

Table 1. Summary of Hematological Pharmacodynamics*

Parameter	CPT-11	CPT-11/ketoconazole
Leukocytes		
%decrease WBC	67.1 ± 27.2 (29.9 – 98.0)	55.4 ± 29.8 (17.0 – 91.7)
Nadir ($\times 10^9$/L)	2.33 ± 1.70 (0.55 – 4.70)	3.29 ± 1.61 (0.97 – 4.90)
Neutrophils		
%decrease ANC	74.5 ± 22.5 (42.4 – 99.6)	56.9 ± 23.3 (46.0 – 96.5)
Nadir ($\times 10^9$/L)	1.11 ± 0.87 (0.10 – 2.30)	1.93 ± 1.19 (0.34 – 3.40)

Abbreviations: WBC, white blood cell count; ANC, absolute neutrophil count.
*Data are expressed as mean values ± SD, with range in parenthesis.

Irinotecan Disposition and Effects of Ketoconazole

Since ketoconazole is a known potent inhibitor of CYP3A4, and given the prominent role of this enzyme in irinotecan metabolism, we assessed the influence of ketoconazole on disposition profiles (Table 2). The peak concentration of ketoconazole was 4.72 ± 2.53 μg/mL, and the AUC amounted to 15.4 ± 9.80 μg.h/mL, which is similar to previous findings (5). In the presence of ketoconazole, the relative exposure to the CYP3A4-mediated metabolite APC was reduced by 87% ($P = .002$), while the relative exposure to the pharmacologically active metabolite SN-38 increased by 109% ($P = .004$). The opposing effects of these metabolic routes on drug elimination left the systemic clearance of irinotecan almost unaffected ($P = .90$). Similarly, ketoconazole had no effect on circulating levels of SN-38G ($P = .93$), suggesting no effect on β-glucuronidation pathways. The cumulative exposure to the total of all metabolites, on a molar basis and normalized to a 350 mg/m^2 dose, was also not dependent on the presence of ketoconazole (13.7 ± 5.00 vs 11.5 ± 4.50

μM.h; $P = .65$). In addition, the cumulative fecal excretion of CPT-11, expressed as the percentage of the absolute dose excreted in feces within the first 56 hours after drug administration, was not different in the presence or absence of ketoconazole (13.8% ± 15.9% vs 19.5% ± 13.9%; $P = .48$). However, the fecal recovery of SN-38 was increased by 207% and that of APC was reduced by 78.0%. The similarity of the terminal disposition phases in plasma of these metabolites (Fig. 1) between treatment courses indicate that the altered fecal excretion in the presence of ketoconazole is related to altered formation rather than diminished biliary secretion.

Table 2. Summary of Pharmacokinetic Parameter Estimates*

Parameter	CPT-11	CPT-11/keto	Difference (%)
CPT-11 dose (mg)†	650 (600 – 875)	180 (175 – 230)	
Infusion time (h)†	1.50 (1.45 – 1.60)	1.50 (1.30 – 1.50)	
Irinotecan			
C_{max} (μM)	7.65 ± 1.53	2.13 ± 1.02	
AUC (μM.h)	46.9 ± 16.0	12.1 ± 2.73	
CL (L/h)	30.6 ± 12.3	29.8 ± 8.90	-0.13 ± 15.1 ($P = .90$)
SN-38			
C_{max} (μM)	0.164 ± 0.063	0.088 ± 0.043	
AUC (μM.h)	1.11 ± 0.476	0.597 ± 0.245	
REC	0.023 ± 0.005	0.049 ± 0.013	109 ± 36.6 ($P = .004$)
SN-38G			
C_{max} (μM)	0.312 ± 0.083	0.138 ± 0.012	
AUC (μM.h)	4.53 ± 1.64	2.45 ± 1.04	
REG	4.18 ± 0.372	4.14 ± 1.17	-1.56±22.6 ($P = .93$)
APC			
C_{max} (μM)	0.627 ± 0.283	0.040 ± 0.014	
AUC (μM.h)	8.03 ± 3.80	0.241 ± 0.125	
REM	0.177 ± 0.092	0.020 ± 0.012	-86.9±7.14 ($P = .002$)

Abbreviations: C_{max}, peak plasma concentration; AUC, area under the plasma concentration versus time curve; CL, apparent plasma clearance; REC, relative extent of conversion (AUC ratio of SN-38 to CPT-11); REG, relative extent of glucuronidation (AUC ratio of SN-38G to SN-38); REM, relative extent of metabolism (AUC ratio of APC to CPT-11).

*Data are expressed as mean values ± SD.

†Median with range.

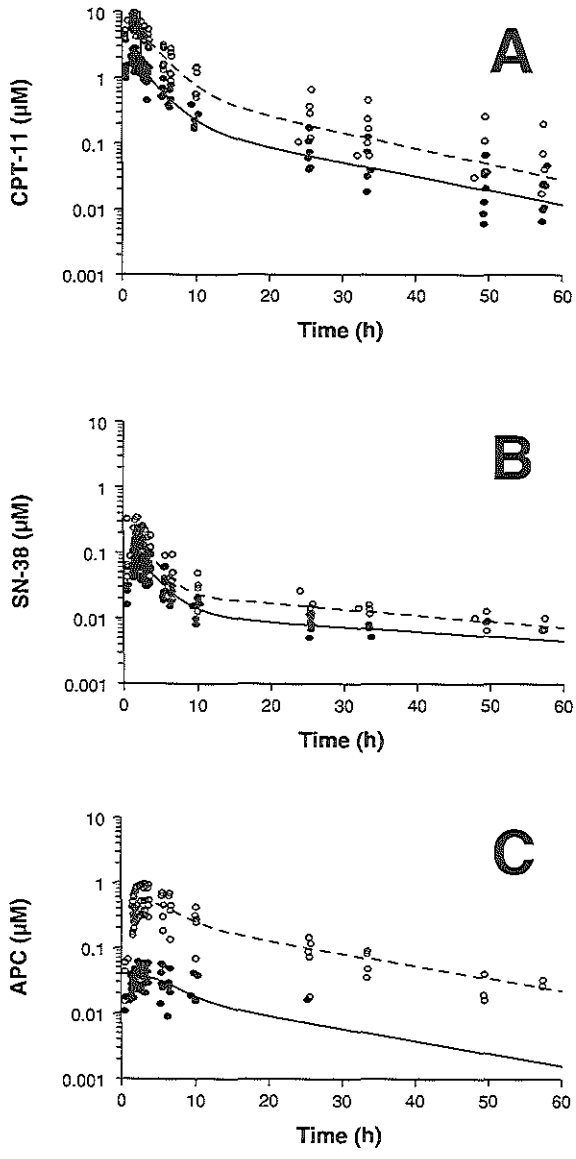

Figure 1. Plasma concentration-time curves of irinotecan (**A**), SN-38 (**B**) and APC (**C**) in the presence (irinotecan 100 mg/m^2, solid line, closed symbols) and absence (irinotecan 350 mg/m^2, dashed line, open symbols) of ketoconazole.

Ex Vivo Analysis of Esterase Activity in Patient Plasma

To gain insight into the observed altered pharmacokinetic behavior of irinotecan in the presence of ketoconazole, various in vitro experiments were performed. The esterase activity in patient plasma, measured for 50 hours after irinotecan administration using the artificial substrate *o*-nitrophenyl acetate, was relatively consistent and independent of sampling time points, with mean values of 20.7 ± 1.58 and 20.9 ± 2.40 μmol/min/mg in the absence and presence of ketoconazole, respectively (P = .89).

Effect of Ketoconazole on SN-38 Metabolism by Human Liver Microsomes

To assess a possible effect of ketoconazole on metabolism of SN-38 by human liver microsomes, we incubated microsomal preparations with irinotecan and SN-38 for 60 min at 37°C. In line with previous findings, we found that irinotecan was extensively metabolized to various polar compounds, including APC, but not in the presence of ketoconazole (99-100% inhibition) (18). In contrast to previous data published in abstract form (23), no metabolic degradation by liver microsomes to a very polar, CYP3A-mediated peak was observed for SN-38, and no additional effects of ketoconazole were noted (data not shown).

Polarized Transport of SN-38 in Human Intestinal Cells

We next studied the transepithelial flux of irinotecan and SN-38 in Caco-2 cell monolayers, a well-established model of human intestinal absorption (24), to further define the potential role of active transport mechanisms in SN-38 pharmacokinetics and the influence on these processes by ketoconazole. Previously, we showed that Caco-2 cells demonstrate significant expression of P-glycoprotein, multidrug-resistance associated protein (MRP-1), and the canalicular multispecific organic anion transporter (cMOAT or MRP-2) (20). We also recently observed pronounced staining using immunoprecipitation at the apical side of Caco-2 cells with an antibody to BCRP (Sparreboom et al, unpublished data), a recently identified member of the ATP-binding cassette transporter family, for which SN-38 is one of the best known substrates (25).

The flux of irinotecan and SN-38 across Caco-2 cell monolayers, when drug was loaded on the apical side of the cells was essentially linear for up to 3 hours (Fig. 2). In the presence of the P-glycoprotein/BCRP inhibitor GF120918, the P_{app} for the apical to basolateral transport increased from 3.6×10^{-6} to 7.0×10^{-6} cm/sec and from 3.6×10^{-6} to 9.7×10^{-6} cm/sec for irinotecan and SN-38, respectively, consistent with the known prominent role of P-glycoprotein and BCRP activity in SN-38 transport (26). With ketoconazole, the flux of irinotecan and SN-38 was increased by

47.2% (P_{app} = 5.3 × 10^{-6} cm/sec) and 55.6% (P_{app} = 5.6 × 10^{-6} cm/sec), respectively, whereas addition of ketoconazole to GF120918 had essentially no additional effect as compared to GF120918 alone (CPT-11, P_{app} = 6.2 × 10^{-6} cm/sec; SN-38, P_{app} = 8.0 × 10^{-6} cm/sec). Since Caco-2 cells fail to express significant CYP3A4 activity under the culture conditions employed (24), the most likely explanation for the observed effect on drug transport is inhibition of P-glycoprotein activity, a known property of ketoconazole (27).

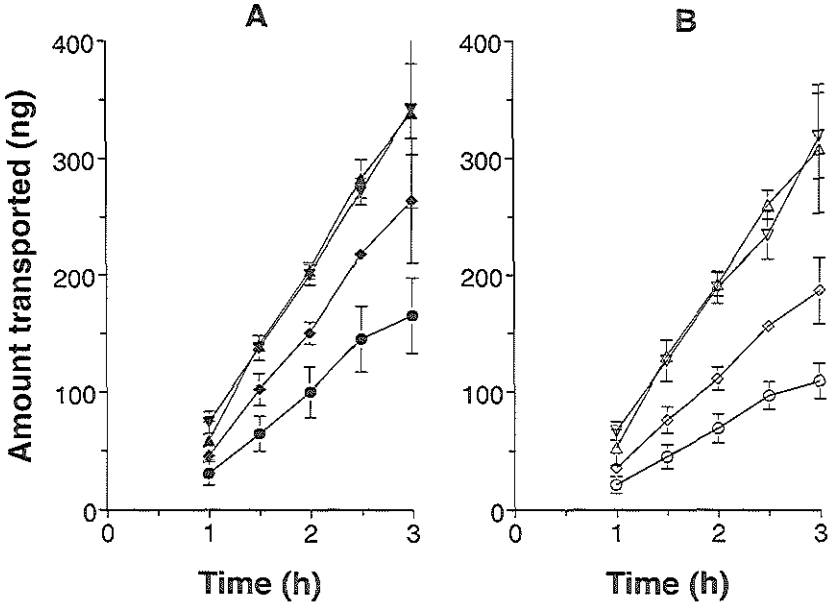

Figure 2. Transepithelial (apical to basolateral direction) transport of irinotecan (**A**) and SN-38 (**B**) across Caco-2 cells in the absence (circles) and presence of ketoconazole (lozenges), the P-glycoprotein/BCRP inhibitor GF120918 (pyramides), or ketoconazole plus GF120918 (triangles). Results are presented as mean values (symbol) ± SD (error bar).

DISCUSSION

This study shows that inhibition of CYP3A4 by the potent enzyme inhibitor, ketoconazole, results in a substantial pharmacokinetic interaction with CPT-11. The overall results indicate a significantly reduced exposure to the principal oxidative

metabolite APC by 87%, as well as highly increased (approximately 109%) circulating concentrations of the pharmacologically active metabolite SN-38. These data not only emphasize the need to consider the plausibility of kinetic interactions in the development of anticancer drugs, but also have a direct significant clinical relevance for chemotherapeutic treatment with irinotecan.

Clinically, one of the most important pathways of irinotecan elimination consists of an esterase-mediated hydrolysis of the bipiperidine moiety, leading to SN-38 (considered essential for antitumor activity) (7). Subsequently, UDP glucuronosyltransferase (UGT) 1A1 mediates a β-glucuronic-acid conjugation, forming SN-38G (7), a metabolite that may play a role as a precursor for hydrolysis by intraluminal glucuronidases to form SN-38 in the occurrence of irinotecan-induced diarrhea (28). The previous recognition that irinotecan is a substrate of CYP3A4 is a salient finding, since it makes the agent potentially subject to a host of enzyme-mediated drug interactions, even with commonly prescribed medication (18). For example, the prototypical CYP3A4 inhibitor troleandromycine inhibits the conversion of irinotecan into APC in vitro almost completely (18), which is consistent with our current in vivo findings (see http://www.drug-interactions.com/ for an updated CYP drug interaction table). In addition, both loperamide and racecadotril inhibit APC formation by more than 50%, whereas ondansetron causes inhibition by >25% (18), suggesting that some degree of interaction is to be expected with simultaneous administration of these agents with irinotecan.

The potential clinical implications of CYP3A4-mediated metabolism of irinotecan have until now received little more than cursory interest from both pharmacologists and oncologists, most likely because the contribution of this pathway to the overall elimination of irinotecan is rather low (10), and in view of the fact that oxidative metabolism of irinotecan is generally considered an efficient detoxification route (18). Previously, it was demonstrated that co-administration of irinotecan with another substrate of CYP3A4, cyclosporine, results in significantly reduced irinotecan clearance in both rodents and humans (29, 30). There was no change in the volume of distribution at steady-state (indicative for unchanged protein and tissue binding) and in the metabolic conversion of irinotecan to SN-38 due to the cyclosporine pretreatment,[?]implicating reduced biliary secretion of the parent drug as the potential cause for this interaction (29).

The current observation that inhibition of CYP3A4-mediated metabolism of irinotecan by ketoconazole leads to an induced esterase-mediated hydrolysis to form SN-38 was thus rather unexpected, and in order to discriminate between increased formation and reduced elimination of SN-38 as the principal mechanism underlying this phenomenon, several additional in vitro experiments were performed. By

measuring the total esterase activity in plasma of patients, ketoconazole was found to have no inducing effect on circulating enzyme levels that might explain the increase in relative exposure to SN-38. However, these data need to be interpreted with caution, as it has not yet been conclusively demonstrated that the plasma hydrolysis of the artificial substrate used (*o*-nitrophenyl acetate) is an accurate marker of irinotecan activation. Moreover, it is not known whether *o*-nitrophenyl acetate is a substrate for either of the two currently identified human carboxylesterases isoforms (hCE1 and hCE2) (31), or whether plasma enzyme activity correlates with hepatic activity, which may be more relevant to the plasma pharmacokinetics.

We found that ketoconazole had no effect on SN-38 biotransformation in human liver microsomes, in contrast to a previous observation suggesting prominent CYP3A4-mediated oxidation of SN-38 to a polar, currently unidentified compound (23). Our in vitro data obtained in the Caco-2 cell monolayers suggest that ketoconazole might interfere with active drug transport mediated by P-glycoprotein, which is consistent with previous observations that ketoconazole is a (poor) inhibitor of P-glycoprotein (27). In our patients, we observed that co-administration with ketoconazole had a marked effect on the fecal elimination of both APC and SN-38. However, the similarity of the terminal disposition phases in plasma of both metabolites between treatment courses indicates that the increased fecal excretion of SN-38 in the combination courses is unlikely related to diminished (P-glycoprotein-mediated) biliary secretion. Collectively, these findings suggest that the pharmacokinetic interference described here appears to be the result of inhibition of one of two competing enzymes involved in (hepatic) irinotecan metabolism, which results in shunting of parent drug to SN-38.

As mentioned previously, various classes of enzymes are involved in irinotecan metabolism, and variability in the expression of each of these will contribute to variability in drug handling between patients. In addition, this variability is further influenced by the recognition that polymorphic drug-metabolizing enzymes (e.g., UGT1A1) exist that can alter drug disposition (32). Recent studies have shown that determination of UGT1A1-gene promotor polymorphism (*UGT1A1*28*) may identify patients with altered SN-38 glucuronidation rates and greater susceptibility to irinotecan induced toxic effects (33, 34). In view of our current observation that CYP3A4-mediated metabolism of irinotecan might be more important than held previously, we have recently initiated a prospective trial to corroborate the usefulness of gene diagnosis of UGT1A1 in combination with CYP3A4 polymorphism prior to irinotecan chemotherapy. In addition, because CYP3A5 represents at least 50% of

the total hepatic CYP3A content in people polymorphically expressing CYP3A5, this isozyme may be the most important genetic contributor to interindividual and interracial differences in CYP3A-dependent drug clearance and in responses to many agents (35). In this context, it is of particular importance, however, that recent data indicate that the in vitro metabolism of irinotecan by Ad 293 cells or human liver microsomes expressing CYP3A5 was markedly different because, in contrast to kinetic studies performed in cells expressing CYP3A4, instead of APC a new metabolite was formed by de-ethylation of the camptothecin moiety (36). The production of this metabolite was totally absent from incubations with microsomes devoid of CYP3A5, and was almost completely prevented in vitro by the addition of ketoconazole, confirming the involvement of CYP3A isozymes. Importantly, the catalytic activity and the relative affinity of irinotecan for CYP3A5 were substantially weaker than those of CYP3A4 (36). This finding, as well as the polymorphic expression of CYP3A5 suggest that the de-ethylated metabolite plays a minor role in irinotecan disposition, and that effects of ketoconazole on CYP3A5 have no important clinical ramifications in this particular case.

Clinically we found that hematologic toxicity and non-hematologic toxicity between the treatment courses were very similar, in spite of the reduced irinotecan dose in the presence of ketoconazole, which might be explained by the increased exposure to SN-38. Previously, the idea of intentionally adding ketoconazole to systemic treatment with CYP3A4 substrate drugs (e.g. cyclosporine) for the purpose of decreasing toxicity and costs through a reduction in dosage regimens has been advanced (37). However, before taking advantage of the metabolic interaction between ketoconazole and irinotecan described here to supply the two drugs as a unique preparation for clinical use, a number of important questions needs to be solved. Most importantly, it is not yet known whether systemic circulating concentrations of SN-38 have any predictive ability toward antitumor activity. In fact, recent data from a study of irinotecan administered in combination with cyclosporin A (a competitive inhibitor of CYP3A4) and phenobarbital (an inducer of UGT1A1) suggest responses to treatment in patients with metastatic colorectal and esophageal cancer without any significant diarrhea, despite a very low exposure to SN-38 (38). This finding supports the hypothesis that intratumoral hydrolysis of irinotecan by esterases may be more important than plasma concentrations of SN-38 (39, 40). This suggests that the concept of using intentional CYP3A4-mediated interactions with irinotecan therapy may increase toxicity but not the overall antitumor activity.

In conclusion, ketoconazole considerably increased the plasma concentrations of the pharmacologically active irinotecan metabolite SN-38 relative to those

expected on the basis of dose, as a result of inhibition of CYP3A4-mediated biotransformation. With concomitant use of irinotecan and ketoconazole (or other potent substrates or inhibitors of CYP3A4), potentially fatal interactions are likely and extreme caution and substantial dose reductions should be employed if both drugs have to be administered together.

REFERENCES

1. Lazarou J, Pomeranz BH, Corey PN. Incidence of adverse drug reactions in hospitalized patients: a meta-analysis of prospective studies. J Am Med Assoc 279: 1200-1205, 1998
2. Ratain MJ. Drug combinations: dangerous liaisons or great expectations? Ann Oncol 10: 375-376, 1999
3. Sparreboom A, Loos WJ, de Jonge MJA, et al. J. Clinical trial design: Incorporation of pharmacokinetic, pharmacodynamic and pharmacogenetic principles. In: Baguley BC, Kerr DJ, editors. Anticancer Drug Development. Chapter 18, Philadelphia, (PA): Academic Press; 2002
4. Ingelman-Sundberg M, Oscarson M, McLellen RA. Polymorphic human cytochrome P450 enzymes: an opportunity for individualized drug treatment. Trends Pharmacol Sci 20: 342-349, 1999
5. Venkatakrishnan K, Von Moltke LL, Greenblatt DJ. Effects of the antifungal agents on oxidative drug metabolism: clinical relevance. Clin Pharmacokin 38: 111-180, 2000
6. Vanhoefer U, Harstrick A, Achterrath W, et al. Irinotecan in the treatment of colorectal cancer: clinical overview. J Clin Oncol 19: 1501-1518, 2001
7. Mathijssen RHJ, van Alphen RJ, Verweij J, et al. Clinical pharmacokinetics and metabolism of irinotecan (CPT-11). Clin Cancer Res 7: 2182-2194, 2001
8. Kehrer DFS, Yamamoto W, Verweij J, et al. Factors involved in prolongation of the terminal disposition phase of SN-38. Clin Cancer Res 6: 3451-3458, 2000
9. Kehrer DFS, Sparreboom A, Verweij J, et al. Modulation of irinotecan-induced diarrhea by co-treatment with neomycin in cancer patients. Clin Cancer Res 7: 1136-1141, 2001
10. Sparreboom A, de Jonge MJA, de Bruijn P, et al. Irinotecan (CPT-11) metabolism and disposition in cancer patients. Clin Cancer Res 4: 2747-2754, 1998
11. Sparreboom A, de Bruijn P, de Jonge MJA, et al. Liquid chromatographic determination of irinotecan and three major metabolites in human plasma, urine and feces. J Chromatogr B Biomed Sci Appl 712: 225-235, 1998
12. De Bruijn P, de Jonge MJA, Verweij J, et al. Femtomole quantitation of 7-ethyl-10-hydroxycamptothecine (SN-38) in plasma samples by reversed-phase high-performance liquid chromatography. Anal Biochem 269: 174-178, 1999
13. De Jonge MJA, Verweij J, de Bruijn P, et al. Pharmacokinetic, metabolic, and pharmaco-dynamic profiles in a dose-escalating study of irinotecan and cisplatin. J Clin Oncol 18: 195-203, 2000
14. Rivory LP, Haaz MC, Canal P, et al. Pharmacokinetic interrelationships of irinotecan (CPT-11) and its three major plasma metabolites in patients enrolled in phase I/II trials. Clin Cancer Res 3: 1261-1266, 1997

15. De Bruijn P, Kehrer DFS, Verweij J, et al. Liquid chromatographic determination of ketoconazole, a potent inhibitor of CYP3A4-mediated metabolism. J Chromatogr B Biomed Sci Appl 753: 395-400, 2001
16. Khanna R, Morton CL, Danks MK, et al. Proficient metabolism of irinotecan by a human intestinal carboxylesterase. Cancer Res 60: 4725-4728, 2000
17. Zor T, Selinger Z. Linearization of the Bradford protein assay increases its sensitivity: theoretical and experimental studies. Anal Biochem 236: 302-308, 1996
18. Haaz MC, Rivory LP, Riche C, et al. Metabolism of irinotecan (CPT-11) by human hepatic microsomes: participation of cytochrome P-450 3A and drug interactions. Cancer Res 58: 468-472, 1998
19. De Bruijn P, Verweij J, Loos WJ, et al. Determination of irinotecan (CPT-11) and its active metabolite SN-38 in human plasma by reversed-phase high-performance liquid chromatography with fluorescence detection. J Chromatogr B Biomed Sci Appl 698: 277-285, 1997
20. Yamamoto W, Verweij J, de Bruijn P, et al. Active transepithelial transport of irinotecan (CPT-11) and its metabolites by human intestinal Caco-2 cells. Anticancer Drugs 12: 419-432, 2001
21. Artursson P. Epithelial transport of drugs in cell culture. I. A model for studying the passive diffusion of drugs over intestinal absorptive (Caco-2) cells. J Pharm Sci 79: 476-482, 1990
22. De Bruin M, Miyake K, Litman T, et al. Reversal of resistance by GF120918 in cell lines expressing the ABC half-transporter, MXR. Cancer Lett 146: 117-126, 1999
23. Shepard DR, Ramirez J, Iyer L, et al. Metabolism of SN-38 by CYP3A4 and microsomes from human liver (HLM). Proc Am Soc Clin Oncol 18: 176a, 1999 (abstract)
24. Artursson P, Palm K, Luthman K. Caco-2 monolayers in experimental and theoretical predictions of drug transport. Adv Drug Deliv Rev 46: 27-43, 2001
25. Erlichman C, Boerner SA, Hallgren CG, et al. The HER tyrosine kinase inhibitor CI1033 enhances cytotoxicity of 7-ethyl-10-hydroxycamptothecin and topotecan by inhibiting breast cancer resistance protein-mediated drug efflux. Cancer Res 61: 739-748, 2001
26. Maliepaard M, Scheffer GL, Faneyte IF, et al. Subcellular localization and distribution of the breast cancer resistance protein transporter in normal human tissues. Cancer Res 61: 3458-3464, 2001
27. Choo EF, Leake B, Wandel C, et al. Pharmacological inhibition of P-glycoprotein transport enhances the distribution of HIV-1 protease inhibitors into brain and testes. Drug Metab Dispos 28: 655-660, 2000
28. Kehrer DFS, Soepenberg O, Loos WJ, et al. Modulation of camptothecin analogs in the treatment of cancer: a review. Anticancer Drugs 12: 89-105, 2001
29. Gupta E, Safa AR, Wang X, et al. Pharmacokinetic modulation of irinotecan and metabolites by cyclosporin A. Cancer Res 56: 1309-1314, 1996
30. Ratain MJ, Goh BC, Iyer L, et al. A phase I study of irinotecan (CPT-11) with pharmacokinetic modulation by cyclosporine A (CSA) and phenobarbital (PB). Proc Am Soc Clin Oncol 18: 202a, 1999 (abstract)
31. Humerickhouse R, Lohrbach K, Li L, et al. Characterization of CPT-11 hydrolysis by human liver carboxylesterase isoforms hCE1 and hCE2. Cancer Res 60: 1189-1192, 2000
32. Iyer L, King CD, Whitington PF, et al. Genetic predisposition to the metabolism of irinotecan (CPT-11). Role of uridine glucuronosyltransferase isoform 1A1 in the glucuronidation of its active metabolite (SN-38) in human liver microsomes. J Clin Investig 101: 847-854, 1998
33. Ando Y, Saka H, Ando M, et al. Polymorphisms of UDP-glucuronosyltransferase gene and

irinotecan toxicity: a pharmacogenetic analysis. Cancer Res 60: 6921-6926, 2000

34. Iyer L, Das S, Janisch L, et al. *UGT1A1*28* polymorphism as a determinant of irinotecan disposition and toxicity. Pharmacogenom J 2: 43-47, 2002
35. Kuehl P, Zhang J, Lin Y, et al. Sequence diversity in CYP3A promotors and characterization of the genetic basis of polymorphic CYP3A5 expression. Nat Genet 27: 383-391, 2001
36. Santos A, Zanetta S, Cresteil T, et al. Metabolism of irinotecan (CPT-11) by CYP3A4 and CYP3A5 in humans. Clin Cancer Res 6:2012-2020, 2000
37. Albengres E, Tillement JP. Cyclosporin and ketoconazole, drug interaction or therapeutic association? Int J Clin Pharmacol Ther Toxicol 30: 555-570, 1992
38. Ratain MJ, Innocenti F, Vogelzang NJ, et al. Modulation of irinotecan (CPT-11) toxicity and pharmacokinetics by cyclosporine and phenobarbital. Proc Am Soc Clin Oncol 20: 74a, 2001 (abstract)
39. Danks MK, Morton CL, Pawlik CA, et al. Overexpression of a rabbit liver carboxylesterase sensitizes human tumor cells to CPT-11. Cancer Res 58: 20-22, 1998
40. Guichard S, Terret C, Hennebelle I, et al. CPT-11 converting carboxylesterase and topoisomerase activities in tumour and normal colon and liver tissues. Br J Cancer 80: 364-370, 1999

ACKNOWLEDGEMENTS

We thank Drs. Sharyn Baker (The Sidney Kimmel Comprehensive Cancer Center at Johns Hopkins, Baltimore, MD) and Phil Potter (St. Jude Children's Research Hospital, Memphis, TN) for help with the plasma carboxylesterase assay; GlaxoSmithKline (Research Triangle Park, NC) for providing GF120918; and Drs. Walter Loos and Kees Nooter for their suggestions with regard to the manuscript.

Chapter Nine

Effects of St. John's Wort on Irinotecan Metabolism

Journal of the National Cancer Institute, 94: 1247-1249, 2002

Ron H.J. Mathijssen
Jaap Verweij
Peter de Bruijn
Walter J. Loos
Alex Sparreboom

Department of Medical Oncology, Erasmus MC - Daniel den Hoed
Rotterdam, The Netherlands

SUMMARY

St John's Wort (SJW), a widely used herbal product, has been implicated in drug interactions resulting from the induced expression of the cytochrome P450 CYP3A4 isoform. In this study, we determined the effect of SJW on the metabolism of irinotecan, a pro-drug of SN-38 and a known substrate for CYP3A4. Five cancer patients were treated with irinotecan (350 mg/m^2, intravenously) in the presence and absence of SJW (900 mg daily, orally for 18 days) in an unblinded, randomized crossover study design. The plasma levels of the active metabolite SN-38 decreased by 42% (95% confidence interval [CI] = 14% to 70%) following SJW cotreatment with 1.0 μM×h (95% CI = 0.34 μM×h to 1.7 μM×h) versus 1.7 μM×h (95% CI = 0.83 μM×h to 2.6 μM×h), P = .033, two-sided paired Student's t-test. Consequently, the degree of myelosuppression was substantially worse in the absence of SJW. These findings indicate that patients on irinotecan treatment should refrain from taking SJW because plasma levels of SN-38 were dramatically reduced, which may have a deleterious impact on treatment outcome.

INTRODUCTION

St John's Wort (SJW) has become one of the world's most popular herbal preparations, particularly among cancer patients (1) because of its alleged activity in mild to moderate forms of depression (2-4). Previous case reports and clinical investigations suggest that SJW induces the expression of the cytochrome P-450 enzyme system and drug-transporting proteins (5-8). Specifically, SJW was shown to directly induce the expression of the cytochrome P-450 CYP3A4 isoform in intestinal and hepatic cells and to induce the expression of MDR1 P-glycoprotein in intestinal cells (9-11). These observations might have profound clinical implications for patients with colorectal cancer receiving the chemotherapy agent irinotecan because the drug is, in part, eliminated *via* CYP3A4- and P-glycoprotein-mediated routes (12). Moreover, irinotecan, a topoisomerase I inhibitor, has a narrow therapeutic range, and the induction of CYP3A4 and P-glycoprotein by SJW might theoretically result in decreased systemic levels of the pharmacologically active metabolite SN-38, the consequence of which might be a loss of antitumor activity.

MATERIALS AND METHODS

We evaluated the potential of SJW to affect plasma concentrations of SN-38 in a group of cancer patients treated with irinotecan in an unblinded, randomized crossover

study design, with and without SJW coadministration. The clinical protocol was approved by the Erasmus MC Ethics Board, and all patients signed informed consent forms before study entry. Irinotecan was administered once every 3 weeks as a 90-minute continuous intravenous infusion at a dose of 350 mg/m^2. Fourteen days before the start of the first or second irinotecan administration, patients received one SJW tablet (300 mg; Bio Nutrition Health Products, Den Bosch, The Netherlands) three times a day (i.e., one tablet with each meal). The patients continued this co-medication while receiving the irinotecan therapy and stopped 4 days after irinotecan dosing. Patients were asked to abstain from alcohol, caffeine, grapefruit juice, other herbal dietary supplements and/or substances known to influence the expression of CYP3A4 for a period of 2 weeks before the first irinotecan administration up to 3 weeks after the second irinotecan administration. Blood sampling, drug analyses, and pharmacokinetic parameter calculations were performed as described (13, 14). Data are presented as mean value with 95% confidence intervals (CIs), and statistical calculations were performed on the Number Cruncher Statistical System version 5.X (J. L. Hintze, East Kaysville, UT).

RESULTS AND DISCUSSION

There were five evaluable patients: two men and three women, with a median age of 58 years (range, 54 to 66 years) and a median World Health Organization (WHO) performance score of 1 (range, 0 to 1) (http://www.who.int/home-page/). All five completed the study within the scheduled time without delay. Two patients had colorectal cancer, two had lung cancer, and one had sarcoma. Clinically, irinotecan-induced neutropenia, as measured by a decrease in the number of circulating neutrophils, was the most prominent side effect, and that the spectrum of side effects was unchanged by SJW. The degree of myelosuppression differed substantially between the treatment course with irinotecan alone and the combination course with irinotecan and SJW. At nadir, leukocyte and neutrophil counts decreased 56% (95% CI = 32% to 80%) and 63% (95% CI = 48% to 78%), respectively, during the course with irinotecan alone but decreased only 8.6% (95% CI = 0% to 29%) and 4.3% (95% CI = 0% to 20%), respectively, during the combination course with irinotecan and SJW.

We next measured the levels of the active irinotecan metabolite SN-38 and its CYP3A4-mediated detoxified metabolite 7-ethyl-10-[4-*N*-(5-aminopentanoic acid)-1-piperidino]-carbonyl-oxycamptothecin (APC). Compared with courses of irinotecan alone, the area under the curve (AUC) of SN-38 decreased by 42% (95% CI = 14%

to 70%) in the combination course with irinotecan and SJW from 1.7 μM×h (95% CI = 0.83 μM×h to 2.6 μM×h) to 1.0 μM×h (95% CI = 0.34 μM×h to 1.7 μM×h), $P = .033$, two-sided Student's *t*-test; Fig. 1 and Table 1.

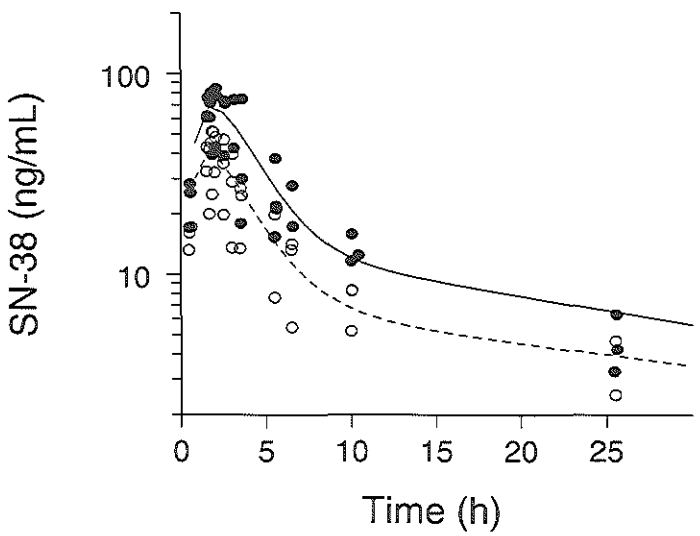

Figure 1. Effect of St. John's wort (SJW) on the plasma concentration of the active irinotecan metabolite SN-38 over time. The plasma concentration of SN-38 was measured over time as described (13, 14). Each data points represents an individual data time point of the plasma concentration of SN-38 measured in the absence (closed symbols; solid line) and presence (open symbols; dotted line) of SJW. The lines represent computer fits of the SN-38 concentration-time curves in the absence and presence of SJW, respectively.

Surprisingly, the AUC ratio of APC to irinotecan was also reduced by 28% (95% CI = 0% to 80%) in the combination course with irinotecan and SJW, although this reduction was not statistically significant. This result suggests that the induction of CYP3A4 expression results in the formation of presently unknown metabolites other than APC (15), as has been described previously (16) in pediatric high-grade glioma patients treated with irinotecan and CYP3A4-inducing anticonvulsants. Alternatively, the lack of effect on APC might be attributed to the fact that during both treatment

courses, patients were receiving dexamethasone. Dexamethasone is another known inducer of CYP3A4 expression and might already stimulate APC formation during the course without SJW co-treatment (17). In the liver, SN-38 can be metabolized to a glucuronic acid conjugate (SN-38G), a process which is catalyzed by uridine diphosphate glucuronosyltransferases (UGT). The rate of SN-38 glucuronidation (i.e., the AUC ratio of SN-38G to SN-38) was not influenced by SJW (Table 1), suggesting that increased glucuronidation through the induction of UGT was not contributing to the reduced SN-38 levels.

Table 1. Effect of St. John's wort (SJW) on irinotecan metabolism.

Parameter	Irinotecan [95% CI]	Irinotecan/SJW [95% CI]	$P^{\dagger}$
Irinotecan			
AUC (μM×h)	33 [5.0 to 60]	29 [6.6 to 52]	.14
CL (L/h)	36 [8.7 to 64]	40 [9.3 to 71]	.11
C_{max} (μM)	6.2 [4.8 to 7.5]	4.9 [1.3 to 8.5]	.35
SN-38[‡]			
AUC (μM×h)	1.7 [.83 to 2.6]	1.0 [0.34 to 1.7]	.033
C_{max} (μM)	0.19 [0.12 to 0.28]	0.11 [0.044 to 0.17]	.016
$t_{½(z)}$ (h)	26 [0 to 72]	20 [6.1 to 34]	.52
AUC ratios[‡]			
SN-38/irinotecan	0.054 [.036 to .073]	0.036 [.0054 to .067]	.054
SN-38G/SN-38	3.2 [2.6 to 3.8]	3.4 [2.6 to 4.3]	.33
APC/irinotecan	0.33 [0 to 0.97]	0.23 [0 to 0.55]	.31

Abbreviations: AUC = area under the plasma concentration versus time curve; APC = 7-ethyl- 10- [4-*N*-(5-amino-pentanoic acid) -1-piperidino]-carbonyloxycamptothecin; CI = confidence interval; CL = apparent clearance; C_{max} = peak plasma concentration; $t_{½(z)}$ = apparant half-life of the terminal disposition phase.

[†] Two-sided Student's *t*-test for matched pairs.

[‡] SN-38 is the active metabolite of irinotecan, also known as CPT-11; SN-38G is a detoxified metabolite of SN-38 that involves uridine diphosphate glucuronosyltransferase (UGT); APC is a detoxified metabolite of irinotecan that involves the CYP3A4 isoform of cytochrome P450.

Similar changes in SN-38 levels (peak plasma concentrations and AUCs) were noted among all patients, regardless of when they received SJW. The changes were, however, more pronounced for the three patients who received SJW during the second course of irinotecan than for those who received SJW during the first course. Previous work (18) has shown that the ability of SJW to induce CYP3A4 expression is dependent on the length of therapy, with no observable effects when given for 8 days or less. It has been hypothesized that this may be the result of the formation of an intermediate or slowly accumulating metabolite of the components of SJW [i.e., (pseudo)hypericin and hyperforin] with CYP3A4-inducing effects (19). Thus, one potential explanation for the schedule-dependent effects of SJW on irinotecan metabolism may be a prolonged effect of SJW on CYP3A4 expression with long-term administration regimens.

It has also been proposed that induction of MDR1 P-glycoprotein expression may be a component of the mechanism for interactions between several other drugs and SJW (11). Preclinical studies have shown that biliary transport of SN-38 is unchanged in mice lacking mdr1-type P-glycoprotein, which suggests no major role of MDR 1 P-glycoprotein in the elimination of SN-38 in patients (20). These observations, together with our current observation that the half-lives of SN-38 are unchanged in the presence and absence of SJW coadministration (Table 1), makes it unlikely that MDR1 P-glycoprotein is involved in the observed interaction. This is because a prominent role of MDR1 P-glycoprotein in the interaction would be associated with increased biliary transport of SN-38, resulting in a decreased half-life of SN-38 in plasma.

Overall, our findings suggest that irinotecan metabolism and toxicity are altered by SJW and that the two agents cannot be given safely in combination without compromising overall antitumor activity. We expect that the results presented here for irinotecan are representative of other anticancer drugs that are at least partial substrates for CYP3A4. This hypothesis is supported by recent observations that the pharmacokinetics of several commonly used agents, including taxanes [e.g., paclitaxel (21)] and camptothecines [e.g., irinotecan (22) and topotecan (23)], are altered in patients on anticonvulsants as a result of CYP3A4 induction, which leads to increased dose requirements to achieve similar pharmacologic effects. Until specific dosing guidelines are available, it is strongly recommended that patients receiving chemotherapeutic treatments with such agents refrain from taking SJW.

REFERENCES

1. Ernst E. A primer of complementary and alternative medicine commonly used by cancer patients. Med J Aust 174: 88-92, 2001

2. Fetrow CW, Avila JR, editors. Professional's handbook of complementary and alternative medicines. Springhouse (PA): Springhouse; 1999
3. Schrader E. Equivalence of St John's wort extract (Ze 117) and fluoxetine: a randomized, controlled study in mild-moderate depression. Int Clin Psychopharmacol 15:61-68, 2000
4. Stevinson C, Ernst E. Hypericum for depression. An update of the clinical evidence. Eur Neuropsychopharmacol 9: 501-505, 1999
5. Johne A, Schmider J, Brockmöller J, et al. Decreased plasma levels of amitriptyline and its metabolites on comedication with an extract from St. John's wort (*Hypericum perforatum*). J Clin Psychopharmacol 22: 46-54, 2002
6. Ruschitzka F, Meier PJ, Turina M, Lüscher TF, Noll G. Acute heart transplant rejection due to St John's wort. Lancet 355: 548-549, 2000
7. Johne A, Brockmöller J, Bauer S, Maurer A, Langheinrich M, Roots I. Pharmacokinetic interaction of digoxin with an herbal extract from St John's wort (Hypericum perforatum). Clin Pharmacol Ther 66: 338-345, 1999
8. Piscitelli SC, Burstein AH, Chaitt D, Alfaro RM, Falloon J. Indinavir concentrations and St John' s wort. Lancet 355: 547-548, 2000
9. Ernst E. Second thoughts about safety of St John's wort. Lancet 354: 2014-2016, 1999
10. Roby CA, Anderson GD, Kantor E, Dryer DA, Burstein AH. St John's Wort: Effect on CYP3A4 activity. Clin Pharmacol Ther 67: 451-457, 2000
11. Dürr D, Stieger B, Kullak-Ublick GA, et al. St John's Wort induces intestinal P-glycoprotein and hepatic CYP3A4. Clin Pharmacol Ther 68: 598-604, 2000
12. Mathijssen RHJ, van Alphen RJ, Verweij J, et al. Clinical pharmacokinetics and metabolism of irinotecan (CPT-11). Clin Cancer Res 7: 2182-2194, 2001
13. Sparreboom A, de Jonge MJA, de Bruijn P, et al. Irinotecan (CPT-11) metabolism and disposition in cancer patients. Clin Cancer Res 4: 2747-2754, 1998
14. Rivory LP, Haaz MC, Canal P, Lokiec F, Armand JP, Robert J. Pharmacokinetic interrelationships of irinotecan (CPT-11) and its three major plasma metabolites in patients enrolled in phase I/II trials. Clin Cancer Res 3: 1261-1266, 1997
15. Sai K, Kaniwa N, Ozawa S, Sawada JI. A new metabolite of irinotecan in which formation is mediated by human hepatic cytochrome P-450 3A4. Drug Metab Dispos 29: 1505-1515, 2001
16. Gajjar AJ, Radomski KM, Bowers DC, et al. Pharmacokinetics of irinotecan (IRN) and metabolites in pediatric high-grade glioma patients with and without co-administration of enzyme-inducing anticonvulsants. Proc Am Soc Clin Oncol 19:162a, 2000 (abstract)
17. Mc Cune JS, Hawke RL, LeCluyse EL, et al. In vivo and in vitro induction of human cytochrome P4503A4 by dexamethasone. Clin Pharmacol Ther 68:356-366, 2000
18. Markowitz JS, De Vane CL, Boulton DW, Carson SW, Nahas Z, Risch SC. Effect of St John's Wort (hypericum perforatum) on cytochrome P-450 2D6 and 3A4 activity in healthy volunteers. Life Sci 66:133-139, 2000
19. Burstein AH, Horton RL, Dunn T, Alfaro RM, Piscitelli SC, Theodore W. Lack of effect of St John's Wort on carbamazepine pharmacokinetics in healthy volunteers. Clin Pharmacol Ther 68: 605-612, 2000
20. Iyer L, Ramirez J, Shepard DR, et al. Biliary transport of irinotecan and metabolites in normal and P-glycoprotein-deficient mice. Cancer Chemother Pharmacol 49: 336-341, 2002
21. Chang SM, Kuhn JG, Rizzo J, et al. Phase I study of paclitaxel in patients with recurrent

malignant glioma: a North American Brain Tumor Consortium report. J Clin Oncol 16: 2188-2194, 1998

22. Friedman HS, Petros WP, Friedman AH, et al. Irinotecan therapy in adults with recurrent or progressive malignant glioma. J Clin Oncol 17: 1516-1525, 1999

23. Zamboni WC, Gajjar AJ, Heideman RL, et al. Phenytoin alters the disposition of topotecan and N-desmethyl topotecan in a patient with medulloblastoma. Clin Cancer Res 4:783-789, 1998

Chapter Ten

Irinotecan Disposition in Relation to Genetic Polymorphisms in ABC Transporters and Drug-Metabolizing Enzymes

Journal of Clinical Oncology, submitted

Ron H.J. Mathijssen[1]
Sharon Marsh[2]
Mats O. Karlsson[3]
Rujia Xie[3]
Sharyn D. Baker[4]
Jaap Verweij[1]
Alex Sparreboom[1]
Howard L. McLeod[2]

[1]Department of Medical Oncology, Erasmus MC - Daniel den Hoed
Rotterdam, The Netherlands

[2]Department of Medicine, Washington University School of Medicine
St. Louis, MO

[3]Department of Pharmaceutical Biosciences, Uppsala University
Uppsala, Sweden

[4]Division of Experimental Therapeutics, The Sidney Kimmel Comprehensive Cancer Center at Johns Hopkins, Baltimore, MD

ABSTRACT

Purpose: The objective of this study was to explore the relationships between irinotecan disposition and allelic variants of genes coding for ATP binding-cassette transporters and enzymes of putative relevance for irinotecan.
Patients and Methods: Irinotecan was administered to 65 cancer patients (32 males, 33 females; 63 European Caucasian, 2 Asian) as a 90-minute infusion (dose, 200-350 mg/m^2), and pharmacokinetic data were obtained during the first cycle. All patients were genotyped for variants in genes encoding MDR1 P-glycoprotein (ABCB1), multidrug resistance-associated proteins MRP-1 (ABCC1) and MRP-2 (cMOAT; ABCC2), breast cancer-resistance protein (ABCG2), carboxylesterases (CES1, CES2), cytochrome P450 isozymes (CYP3A4, CYP3A5), uridine diphosphate glucuronosyltransferase (UGT1A1), and a DNA-repair enzyme (XRCC1), which was included as a non-mechanistic control.
Results: Twenty genetic variants were found in 9 genes of putative importance for irinotecan disposition. The homozygous T allele of the ABCB1 1236 C>T polymorphism was associated with significantly increased exposure to irinotecan (P = .038) and its active metabolite SN-38 (P = .031). Pharmacokinetic parameters were not related to any of the other multiple-variant genotypes, although irinotecan clearance was slower in the two CYP3A4*3 carriers (P = .059). The extent of SN-38 glucuronidation was slightly impaired in homozygous variants of UGT1A1*28, although differences were not statistically significant (P = .22).
Conclusion: It is concluded that genotyping for ABCB1 1236 C>T may assist with dose optimization of irinotecan chemotherapy in cancer patients. Further investigation is required to confirm these findings in a larger population, and to assess relationships between irinotecan disposition and the rare variant genotypes, especially in other ethnic groups.

INTRODUCTION

The topoisomerase I inhibitor irinotecan (CPT-11) has a major role in the management of metastatic colorectal cancer (1), and has been approved either in combination with 5-fluorouracil and folinic acid in the first line treatment setting (2) or as monotherapy in the second line setting (3). In clinical use, irinotecan is subject to very substantial interindividual variability in pharmacokinetic behavior (4), treatment efficacy (5), and the occurrence of unpredictable, sometimes severe toxic side effects that might be life-threatening in some patients. Potential causes for such variability in drug effects include the pathogenesis and severity of the disease being treated, the

occurrence of unintended drug interactions [eg, with ketoconazole (6) and St. John's wort (7)], and impairment of hepatic (8, 9) and renal function (10), or both (11). Despite the potential importance of these clinical variables in determining drug effects, it is now recognized that inherited differences in the metabolism and excretion into the feces and urine can have an even greater impact on the efficacy and toxicity of drugs (12-15).

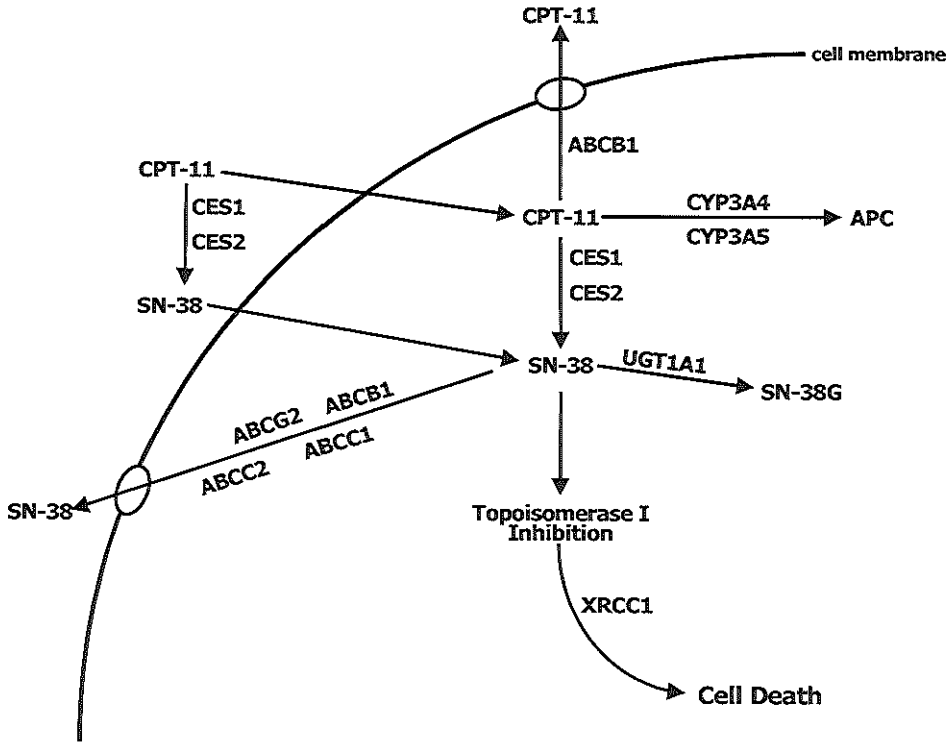

Figure 1. Pathway of genes with a putative role in regulating irinotecan disposition.

The metabolism of irinotecan is very complex, and involves several phase I and II metabolizing enzymes (Ref. 4; Fig. 1). In humans, the ester bond of irinotecan is cleaved by carboxylesterases to form the primary pharmacologically active metabolite 7-ethyl-10-hydroxycamptothecin (SN-38) (16), which is further conjugated by uridine diphosphate glucuronosyltransferases (UGT) to form an inactive β-glucuronic acid conjugate (SN-38G) (17). Another prominent pathway of irinotecan metabolism

consists of a cytochrome P450 (CYP) 3A4 and 3A5-mediated oxidation of the bipiperidine side-chain attached to the core structure (18), which results in the formation of a major metabolite identified as 7-ethyl-10-[4-N-(5-aminopentanoic acid)-1-piperidino]-carbonyloxy-camptothecin (APC) (19). The pharmacologic behavior of irinotecan is further complicated by the fact that its elimination pathways are partially mediated by membrane-localized, energy-dependent outward drug pumps that facilitate cellular efflux mechanisms (Ref. 20; Fig. 1). These proteins belong to the superfamily of ATP-binding cassette (ABC) transporters and include MDR1 P-glycoprotein (ABCB1; Ref. 21), multidrug resistance-associated protein (MRP1, ABCC1; Ref. 22) and its homologue MRP2 (also referred to as cMOAT or ABCC2; Ref. 23), and the breast cancer-resistance protein BCRP (also referred to MXR or ABCG2; Ref. 24). The aim of this study was to link genetic polymorphisms in enzymes and transporters involved in irinotecan elimination to interindividual differences in measures of drug exposure, in order to provide a stronger scientific basis for optimizing irinotecan therapy on the basis of each patient's genetic constitution.

PATIENTS AND METHODS

Patients and Treatment

Patients with a histologically-confirmed diagnosis of a malignant solid tumor for which there was no effective standard regimen and irinotecan was a reasonable treatment option were treated with a 90-minute intravenous infusion of irinotecan. The drug was given once every 3 weeks until progression of disease or dose-limiting toxicities appeared at a dose of 200-350 mg/m^2. All patients were treated between January 1997 and June 2001 at the Erasmus MC (Rotterdam, the Netherlands). Eligibility and exclusion criteria, premedication regimens, and protocols for treatment of drug-induced side effects (eg, diarrhea) were identical to those documented elsewhere (25). None of the patients received other drugs, dietary supplements or herbal preparations known to interfere with irinotecan pharmacokinetics. The clinical protocols, including blood sampling for the purpose of pharmacokinetic and pharmacogenetic analyses, were approved by the Erasmus MC Ethics Board, and all patients provided written informed consent prior to study entry.

Pharmacokinetic Data Analysis

Blood samples of approximately 5 ml were collected during the first cycle of treatment at the following time points: immediately prior to infusion; at 30 minutes after the start of the infusion; 5 minutes before the end of infusion; and at 10, 20 and 30 minutes, and 1, 1.5, 2, 4, 5, 8.5, 24, 32, and 48 hours after the end of infusion. In

37 of 65 patients, additional blood samples were taken at 56 hours, 196 hours (day 8), 360 hours (day 15) and 500 hours (day 21) after the end of infusion. Blood samples were handled as outlined (26), and concentrations of irinotecan and SN-38 were determined in all patients by reversed-phase high-performance liquid chromatography with fluorescence detection as described in detail elsewhere (27, 28). Concentrations of SN-38G and APC in plasma were measured in only 53 and 12 patients, respectively, because of limited sample supply that precluded an additional analysis on the same material.

Previously developed population pharmacokinetic models were used to predict the pharmacokinetic parameters of the lactone and carboxylate forms of the analytes (29). The considered parameters included clearance (CL), volume of distribution in the central compartment (V1), and the accumulated area under the plasma concentration-time curve (AUC). The latter parameter was simulated for irinotecan and its metabolites in all patients from time zero to 100 hours after start of infusion ($AUC_{0\text{-}100h}$) for a 90-minute intravenous infusion and a standard dose of 350 mg/m^2. This data analysis was performed using NONMEM version VI (S.L. Beal and L.B. Sheiner, San Francisco, CA). Metabolic ratios were calculated as described previously (30), and included the relative extent of conversion (REC; the AUC ratio of SN-38 to irinotecan), the relative extent of glucuronidation (REG; the AUC ratio of SN-38G to SN-38), and relative extent of metabolism (REM; the AUC ratio of APC to irinotecan). The REG in each individual patient was also calculated on the basis of the linear trapezoidal-rule AUC values from time zero to 24 hours after start of infusion, without extrapolation to infinity, with uniform weighting using non-compartmental analysis in WinNonlin version 3.0 (Pharsight Corp., Mountain View, CA), to allow for a comparative analysis with literature data.

Pharmacogenetic Data Analysis

Genomic DNA was extracted from 1 ml whole blood or plasma using the Gentra PureGene Blood Kit (Gentra, Minneapolis, MN) and the QIAamp DNA Blood midi kit (Qiagen Inc, Valencia, CA), respectively, following the manufacturers instructions, and was reconstituted in a buffer containing 10 mM Tris (pH 7.6) and 1 mM EDTA.

Single nucleotide polymorphisms and other genetic variations were identified from the literature or were mined using the publicly available SNP databases (31).

Variations in the ABCB1 (1236 C>T, 2677 G>A/T, and 3435 C>T), ABCC1 (23210 C>T and 34215 C>G), ABCC2 (156231 A>G), ABCG2 (828 T>C), CES1 (1509 A>T and 1592 A>C), CES2 (1703 C>T), CYP3A4 (*1B, *2 and *3), CYP3A5 (*3 and *6), UGT1A1 (*7 and *28), and XRCC1 (26304 C>T, 27466 G>A and 28152

G>A) genes were analyzed by polymerase chain reaction (PCR)-restriction fragment length polymorphism (RFLP) or by Pyrosequencing. XRCC1 variations were included as negative control genes. PCR for ABCB1 3435 C>T and UGT1A1*28 was carried out as previously described (32, 33). All other PCR primers were designed using Primer Express version 1.5 (ABI, Foster City, CA), and the Pyrosequencing primers were designed using the Pyrosequencing SNP Primer Design Version 1.01 software (http://www.pyrosequencing.com). RFLP sites were determined using Rebase (http://rebase.neb.com). The PCR primers, conditions, and restriction enzymes (NEB, Beverly, MA) used in the current study are listed in Table 1. PCR was carried out using Amplitaq Gold PCR master mix (ABI, Foster City, CA), 5 pmole of each primer, and 10-50 ng DNA isolated from whole blood or DNA from 1 μl undiluted plasma. Pyrosequencing was carried out as previously described (34) using the Pyrosequencing AB PSQ96 instrument and software (Uppsala, Sweden). RFLP results were analyzed by electrophoresis using 4% agarose (Promega Corporation, Madison, WI). The genotype was called variant if it differed from the Refseq consensus sequence for the single-nucleotide polymorphism (SNP) position (http://www.ncbi.nlm.nih.gov/LocusLink/refseq.html). Genotype-frequency analysis of Hardy-Weinberg equilibrium was carried out using Clump version 1.9 (http://www.mds.qmw.ac.uk/statgen/dcurtis/software.html; Ref. 35). Linkage was determined as a percentage of identical genotypes (wild type, heterozygous or variant) between SNPs in the same gene.

Statistical Considerations

All pharmacokinetic data are presented as mean values ± SD, unless stated otherwise. To relate pharmacokinetic parameters with each polymorphism, a non-parametrical Kruskal-Wallis test was used following a logarithmic transformation of the data because of skewed distribution. These statistical calculations were performed using SPSS version 9.0 (Paris, France) with an *a priori* cutoff of $P < .05$. To relate REG with the UGT1A1*28 polymorphism, a nonparametric-trend analysis was conducted using Stata version 7.0 (Stata Corp., College Station, TX), as described previously (39).

RESULTS

Patients and Pharmacokinetics

A total of 65 adult cancer patients (32 males and 33 females) with a median age of 53 years was enrolled onto this study (Table 2). The majority of patients was European Caucasian, the most prominent disease type was a gastrointestinal

Table 1. PCR primers, conditions, Pyrosequencing primers and restriction enzymes.

Polymorphism	Forward primer 5'-3'	Reverse primer 5'-3'
ABCB1 1236 C>T	*TGTGTCTGTGAATTGCCTTGAAG	CCTCTGCATCAGCTGGACTGT
ABCB1 2677 G>A/T	*ATGGTTGGCAACTAACACTGTTA	AGCAGTAGGGAGTAACAAAATAACA
ABCB1 3435 C>T	GAGCCCATCCTGTTTGACTG	*GCATGTATGTTGGCCTCCTT
ABCC1 14008 G>A	*GAGGGCACTTTGGGGCA	TCTTGAAGCGGAGGTCGTG
ABCC1 23210 C>T	GGTAAATTGAGGCTCGGTGG	*CCCCTCCACTTTGTCCATCTC
ABCC1 34215 C>G	GGGTGCATGTCCCACCTT	*CGTCTCGAGCCAGCAGCT
ABCC2 156231 A>G	GCAAGATCCAGGGGACTTGTC	CATCGTACAGTACACGAAGGTGAAA
ABCG2 828 T>C	CAGTTTATCCGTGGTGTGTCTGG	AAAGGACAGCATTTGCTGTGCT
CES1 1509 A>T	TGGACTTAATGGGGGACGTA	GCCATATGGAATCAGCCTTT
CES1 1592 A>C	CCCAAGACGGTGATAGGAGA	CCAGGAGAGGACAAAATTGC
CES2 1703 C>T	TGAATGAATGGCGAAGTGAA	GCCCAGAGTGACCCTCATAC
CYP3A4 –392 A>G	AGGACAGCCCATAGAGACAAGG	*ATCAATGTTACTGGGGAGTCC
CYP3A4 15713 T>C	AACAATCCACAAGACCCCTT	*ATCTTCAAATGTACTACAAATCACTGA
CYP3A4 23172 T>C	CCCACGTATGTACCACCCAGC	ATTAGGGTGTGACACAGCAAGA
CYP3A5 22893 G>A	*CCCACGTATGTACCACCCAGC	ATTAGGGTGTGACACAGCAAGA
CYP3A5 30597 G>A	*TCTTTGGGGCCTACAGCATG	AAAGAAATAATAGCCCACATACTTATTGAGAG
UGT1A1 $(TA)_n$	*GTCACGTGACACAGTCAAAC	TTTGTTCCTGCCAGAGGTT
UGT1A1 1456 T>G	TCTCCAGCCTTCACAAGGAC	ATTTCCCACCCACTTCTCAA
XRCC1 26304 C>T	CTTCTCCCTGCCTCTCCAC	CTACCCTCCTCCCTCAGAACC
XRCC1 27466 G>A	CCTGGATTGCTGGGTCTG	AGCCACTCAGCACCACTACC
XRCC1 28152 G>A	GCCCCTCAGATCACACCTAA	TCCCGCTCCTCTCAGTAGTC

Polymorphism	Annealing Temp (°C)	Product size (bp)	Pyrosequencing primer 5'-3'	Restriction enzyme
ABCB1 1236 C>T	65	148	GCACCTTCAGGTTCAG	
ABCB1 2677 G>A/T	50	207	TCATCTATTTAGTTTGACTC ACCTTC	
ABCB1 3435 C>T	60	250	GGTGGTGTCACAGGAAGA	
ABCC1 14008 G>A	62	214	ATAAGCCCAGGGTCA	
ABCC1 23210 C>T	64	197	CACCTTCTCCATCCC	
ABCC1 34215 C>G	64	257	GTCTCACACATGTGCACT	
ABCC2 156231 A>G	55	100		HhaI
ABCG2 828 T>C	55	136		MboII
CES1 1509 A>T	55	200		HaeIII
CES1 1592 A>C	55	180		MseI
CES2 1703 C>T	60	354		XhoI
CYP3A4 –392 A>G	55	116	CCATAGAGACAAGGGCA	
CYP3A4 15713 T>C	55	212	TTTGGATCCATTCTTTC	
CYP3A4 23172 T>C	60	160		NlaIII
CYP3A5 22893 G>A	65	176	CCAAACAGGGAAGAGA	
CYP3A5 30597 G>A	62	153	AGAAACCAAATTTTAGGAA	
UGT1A1 $(TA)_n$	50	100	AGGTTGGCCCTCTCCTA	
UGT1A1 1456 T>G	60	291		BsrI
XRCC1 26304 C>T	66	485		PvuII
XRCC1 27466 G>A	60	640		PvuI
XRCC1 28152 G>A	60	593		NciI

*biotinylated.

Table 2. Patient demographics.

Characteristic	No. of patients	Median (range)
Number of patients	65	
Males	32	
Females	33	
Age (years)		53 (34-75)
Body-surface area (m^2)		1.86 (1.29-2.36)
Performance score		1 (0-1)
Ethnicity		
European Caucasian	63	
Asian	2	
Tumor types		
Gastrointestinal	49	
(A)CUP	7	
Miscellaneous	9*	
Irinotecan dose		
200 – 230 mg/m^2	6	
250 – 300 mg/m^2	8	
350 mg/m^2	51	
Concomitant medication		
Cisplatin	3	
None	62	

Abbreviation: (A)CUP, (adeno-) carcinoma of unknown primary.
*pancreas (five), lung (two), cervix (two).

malignancy, and 62 of 65 individuals received single agent irinotecan (51 at a dose level of 350 mg/m^2). The observed plasma concentration-time profiles of irinotecan and its metabolites SN-38, SN-38G and APC were well predicted by our previously defined NONMEM models (29), as indicated by goodness-of-fit plots (data not shown). The individual and mean pharmacokinetic parameters of irinotecan and its metabolites are consistent with previous findings from patients on a similar regimen (reviewed in Ref. 4), showing extensive glucuronidation of SN-38 with wide interindividual variability (Table 3). All AUC ratios found in this group of patients were highly variable, with up to 6-fold, 22-fold and 15-fold difference between the lowest and highest values for REC, REG and REM, respectively (Table 3).

Table 3. Summary of pharmacokinetic parameters (n = 65).

Parameter	Mean ± SD	Range
Irinotecan		
CL lactone (L/h)	73.0 ± 19.9	31.1 - 109
AUC lactone (µg•h/mL)	5.73 ± 0.856	4.05 - 8.04
AUC total (µg•h/mL)	20.5 ± 7.07	10.4 - 46.1
SN-38		
CL(m) lactone (L/h)	1,264 ± 690.0	299.8 - 3,334
AUC total (ng•h/mL)	637 ± 336	216 - 1,746
SN-38G		
AUC total (µg•h/mL)*	4,455 ± 4,666	962 - 29,961
APC		
AUC total (µg•h/mL)**	4,569 ± 4,015	1,118 - 13,935
AUC ratios		
SN-38/CPT-11	0.032 ± 0.015	0.014 – 0.088
SN-38G/SN-38*	7.60 ± 5.88	1.70 - 37.45
APC/CPT-11**	0.21 ± 0.15	0.35 – 0.53

Abbreviations: n, number of patients studied; CL, clearance; AUC, area under the plasma-concentration time curve; CL (m), metabolic clearance.
*n = 53, **n = 12.

Genotyping

Twenty SNPs and 1 dinucleotide repeat were analyzed in 9 genes of putative relevance for irinotecan disposition (Fig. 1), and 1 gene likely to act downstream of topoisomerase I inhibition (ie, XRCC1; Ref. 36). XRCC1 was included as a control gene of unlikely significance to irinotecan disposition. All the SNPs in ABCC1, ABCC2, ABCG2, CES1 and CES2 represent novel data. These SNPs were described in databases but had not been previously validated. In 7 of the tested SNPs (ie, ABCC1 34215 C>G, ABCC2 156231 A>G, ABCG2 828 T>C, CES1 1703 C>T, CYP3A4*2, CYP3A5*6 and UGT1A1*7), no variants were observed. In the other polymorphisms studied, frequencies of the rarest alleles ranged from 0.01 to 0.47 (Table 4). The ABCB1 2677 G>A/T contains a tri-allelic SNP, with G at nucleotide 2677 found in the wild-type sequence, and with A or T at that position being the two possible variants. All genotype frequencies were found to be in Hardy-Weinberg equilibrium.

Table 4. Genotype and allele frequencies for the studied genes.

Polymorphism	Nomen-clature	Description	n	Genotype frequencies wt	het	var
ABCB1 1236 C>T*	n/a	G411G**	46	23	15	8
ABCB1 3435 C>T	n/a	E1143E	59	16	35	8
ABCB1 2677 G>A/T	n/a	A893T or S	53	12	23/4	13/1
ABCC1 14008 G>A	n/a	intron 27	64	32	27	5
ABCC1 23210 C>T	n/a	P154P	45	45	0	0
ABCC1 34215 C>G	n/a	intron 18	60	0	20	40
ABCC2 156231 A>G	n/a	intron 3	65	65	0	0
ABCG2 828 T>C	n/a	F208S	63	63	0	0
CES1 1509 A>T	n/a	L480F	64	64	0	0
CES1 1592 A>C	n/a	N509H	61	60	1	0
CES2 1703 C>T	n/a	L549L	57	56	1	0
CYP3A4 –392 A>G	CYP3A4*1B	Promoter	49	46	3	0
CYP3A4 15713 T>C	CYP3A4*2	S222P	39	39	0	0
CYP3A4 23172 T>C	CYP3A4*3	M445T	64	62	2	0
CYP3A5 22893 G>A	CYP3A5*3C	Splice variant	64	56	8	0
CYP3A5 30597 G>A	CYP3A5*6	Splice variant	63	63	0	0
UGT1A1 $(TA)_n$* **	UGT1A1*28	Promoter	58	34	22	2
UGT1A1 1456 T>G	UGT1A1*7	Y486D	62	62	0	0
XRCC1 26304 C>T	n/a	R194W	43	35	8	0
XRCC1 27466 G>A	n/a	R280H	62	60	2	0
XRCC1 28152 G>A	n/a	R399Q	57	25	27	5

Polymorphism	Allele frequencies (95% CI) p	q	r
ABCB1 1236 C>T*	0.66 (0.52-0.78)	0.34 (0.22-0.48)	
ABCB1 3435 C>T	0.57 (0.44-0.69)	0.43 (0.31-0.56)	
ABCB1 2677 G>A/T	0.48 (0.35-0.61)	0.47 (0.34-0.60)	0.05 (0.02-0.14)
ABCC1 14008 G>A	0.71 (0.59-0.81)	0.29 (0.19-0.41)	
ABCC1 23210 C>T	1.00	0.00	
ABCC1 34215 C>G	0.17 (0.1-0.28)	0.83 (0.72-0.90)	
ABCC2 156231 A>G	1.00	0.00	
ABCG2 828 T>C	1.00	0.00	
CES1 1509 A>T	1.00	0.00	
CES1 1592 A>C	0.99 (0.92-1)	0.01 (0-0.08)	
CES2 1703 C>T	0.99 (0.92-1)	0.01 (0-0.08)	
CYP3A4 –392 A>G	0.97 (0.88-0.99)	0.03 (0.01-0.12)	
CYP3A4 15713 T>C	1.00	0.00	
CYP3A4 23172 T>C	0.98 (0.91-1)	0.02 (0-0.09)	
CYP3A5 22893 G>A	0.94 (0.85-0.98)	0.06 (0.02-0.15)	
CYP3A5 30597 G>A	1.00	0.00	
UGT1A1 $(TA)_n$* **	0.78 (0.66-0.87)	0.22 (0.13-0.34)	
UGT1A1 1456 T>G	1.00	0.00	
XRCC1 26304 C>T	0.91 (0.79-0.96)	0.09 (0.04-0.21)	
XRCC1 27466 G>A	0.98 (0.91-1)	0.02 (0-0.09)	
XRCC1 28152 G>A	0.68 (0.55-0.79)	0.32 (0.21-0.45)	

Abbreviations: n, number of samples; Wt, Wild-type; Het, Heterozygous; Var, variation; n/a, information not available; VI, confidence intervals.

* number represents position in nucleotide sequence; ** number represents amino acid codon; *** p = 6 dinucleotide repeats, q = 7 dinucleotide repeats.

Complete genetic linkage was not seen between polymorphisms from within the same gene. SNPs in the ABCB1 gene (1236 C>T, 2677 G>A/T, and 3435 C>T) have been previously described to be in linkage with each other (37). In this study, ABCB1 3435 C>T shared 52% linkage with ABCB1 1236 C>T and 49% linkage with ABCB1 2677 G>A/T. ABCB1 1236 C>T shared 51% linkage with ABCB1 2677 G>A/T. Overall, 35% linkage was observed between the 3 ABCB1 SNPs. The 26% allele frequency for UGT1A1*28, a seven copy dinucleotide repeat polymorphism in the promotor region, was somewhat lower than the 38-40% reported in some previous studies (38, 39).

Table 5. Summary of genotype-phenotype associations.

Polymorphism	Phenotypic consequence*	*P*- value**
ABCB1 1236 C>T	Irinotecan total AUC increased	.038
	SN-38 total AUC increased	.031
	SN-38 lactone CL reduced	.015
ABCB1 3435 C>T	Irinotecan lactone AUC	.100
ABCB1 2677 G>A/T	Irinotecan lactone CL	.083
ABCC1 14008 G>A	SN-38 lactone CL	.127
ABCC1 34215 C>G	APC AUC	.345
CYP3A4*1B	SN-38 lactone CL	.213
CYP3A4*3	Irinotecan lactone CL	.059
CYP3A5*3C	Irinotecan carboxylate CL	.174
UGT1A1*28	SN-38G/SN-38 AUC ratio	.211

* Represents the best association (lowest *P*-value) between a given polymorphism (wild type *versus* heterozygous variant *versus* homozygous variant type patients) and a change in a pharmacokinetic parameter. **Kruskal-Wallis test following logarithmic transformation for data with a skewed distribution; except for ABCB1 1236 C>T, no statistically significant associations were found.

Genotype-Phenotype Associations

For the 9 polymorphisms in 5 genes in which variant alleles were observed, only one of the ABCB1 SNPs was associated with differences in irinotecan and SN-38 levels (Table 5). The systemic exposure to both irinotecan and SN-38, based on total drug concentrations, was significantly higher for patients with two variant alleles in

ABCB1 1236 C>T (ie, the TT allele) when compared to the patients with only one or no variant alleles. The mean AUC values for irinotecan and SN-38 were 25.5 ± 8.21 µg.h/ml *versus* 19.8 ± 6.81 µg.h/ml (P = .038) and 889 ± 445 ng.h/ml *versus* 604 ± 293 ng.h/ml (P = .031), respectively. Likewise, the metabolic clearance of the lactone form of SN-38 was significantly different between homozygous variants of this SNP and wild-type or heterozygous carriers (P = .015) (Table 5; Fig. 2). No statistically significant association was observed between the other variants in ABC-transporters and any of the studied pharmacokinetic parameters (Table 5).

Comparison of pharmacokinetic data in patients wild-type *versus* heterozygous for CYP3A4*3 (no homozygous patients for this allele were observed in the data set) suggested that the clearance of irinotecan lactone might be reduced and that the AUC might be increased in the heterozygotes, although these differences were not statistically significant (P = .059 and P = .070, respectively) (Fig. 3). Statistically significant differences were also not observed in pharmacokinetic parameters between variants in UGT1A1*28 (wild type > heterozygous variant > homozygous variant, P > .22) (Table 6).

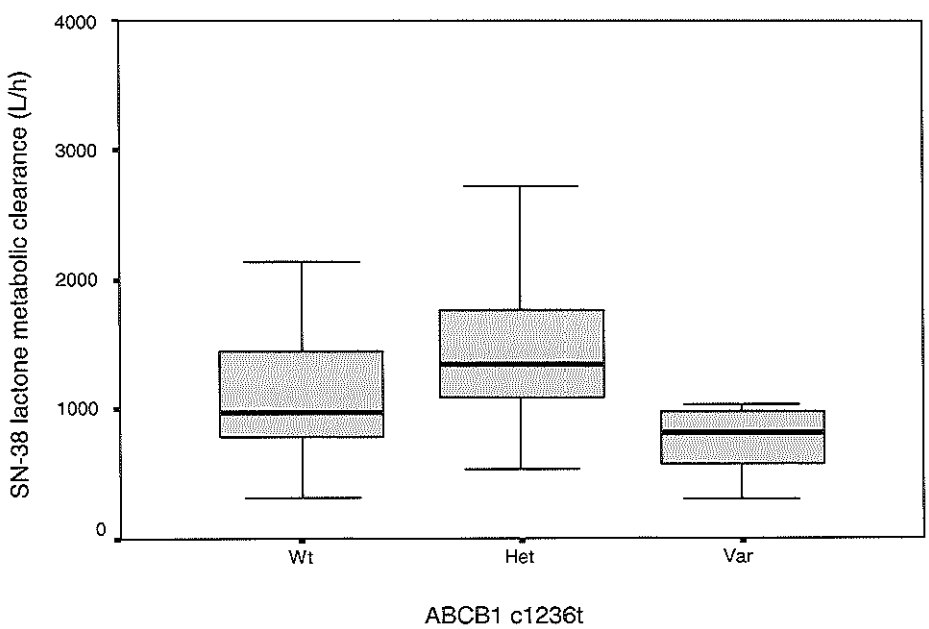

Figure 2. Single-nucleotide polymorphism ABCB1 1236 C>T in relation to the metabolic clearance of SN-38 lactone. Boxplots show the median, interquartile range and outliers of individual variables. *Abbreviations:* Wt, Wild type patient; Het, Heterozygous variant type patient; Var, Homozygous variant type patient.

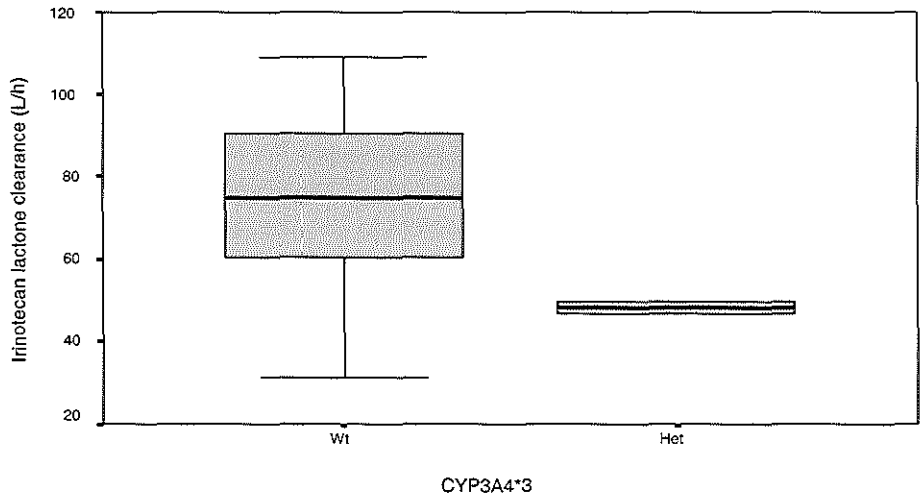

Figure 3. Single-nucleotide polymorphism CYP3A4*3 in relation to the clearance of irinotecan lactone. *Abbreviations:* Wt, Wild type patient; Het, Heterozygous variant type patient.

Table 6. Effect of UGT1A1*28 on the extent of SN-38 glucuronidation.

Genotype	Reference	n	AUC_{0-t} (24h) ratio* SN-38G/SN-38 mean ± SD (median)	AUC_{0-inf} (100h) ratio** SN-38G/SN-38 mean ± SD (median)
Wt	this study	32	7.6 ± 4.1 (6.6)	6.9 ± 3.5 (6.4)
	39	9	9.3 ± 11	n/a
Het	this study	19	7.1 ± 3.6 (6.6)	6.7 ± 3.2 (6.1)
	39	7	4.0 ± 1.7	n/a
Var	this study	2	2.2, 5.2 (3.7)	2.5, 4.6 (3.6)
	39	4	2.4 ± 1.1	n/a

Abbreviations: n, number of patients studied; AUC, area under the plasma concentration-time curve; Wt, Wild type patient; Het, Heterozygous variant type patient; Var, Homozygous variant type patient; n/a, information not available. *SN-38G/SN-38 AUC ratio based on nonparametric analysis of samples taken upto 24 h after irinotecan administration [trend analysis (Wt>Het>Var), P = .272]; **SN-38G/SN-38 AUC ratio based on NONMEM model [trend analysis (Wt>Het>Var), P = .300]; Iyer *et al.* (39) [trend analysis (Wt>Het>Var), P = .001].

DISCUSSION

The desire for better tools to individualize chemotherapy has led to new ways of evaluating patients. The observation that most chemotherapy agents have a high degree of variability in drug disposition has prompted the use of genetics to try and identify the meachanistic basis for this variation. Previous investigations have shown that pharmacogenetic testing may contribute to the individualization of drug treatment, and hence may have an increasing impact on enhanced drug safety and efficacy (12, 14, 15). In the present study, we assessed the relationships between disposition characteristics of the topoisomerase I inhibitor irinotecan and 21 allelic variants of 10 genes coding for various ABC transporters and drug-metabolizing enzymes in a group of 65 cancer patients.

The most relevant finding of this study was a significant association between the presence of the homozygous T allele of ABCB1 1236 C>T (located at exon 12) and increased exposure to both irinotecan and SN-38. This appears to be the first observation that this allelic variant is functionally polymorphic, in that it alters the activity of the encoded protein in relation to the wild-type and heterozygous sequences. ABCB1 1236 C>T is a synonymous cSNP located in codon 411 of the P-glycoprotein. It is unlikely that this variation directly affects P-glycoprotein expression, however, it may have an indirect effect such as altering RNA stability. Comprehensive analysis of all DNA variations in this gene is warranted to uncover the basis of the association between P-glycoprotein and irinotecan and SN-38 exposure.

Previously, Hoffmeyer *et al.* found an association between ABCB1 gene 3435 C>T (located at exon 26) and increased exposure to the P-glycoprotein substrate drug digoxin following oral administration (40). Although this SNP is also a silent polymorphism (ie, present in the amino acid coding region but not coding for an amino acid substitution), intestinal P-glycoprotein expression was significantly decreased, leading to increased absorption of the drug. More recently, a study was published that confirmed the functional importance of the ABCB1 3435 C>T polymorphism, although in this case the variant allele was associated with lower plasma concentrations of the anti-retroviral drugs nelfinavir and efavirenz (41). To explain this paradox, it was hypothesized that low levels of P-glycoprotein expression might be compensated for by overexpression of other ABC transporter proteins with affinity for these anti-retroviral drugs, and/or the induction of CYP3A isoforms (41). In our study, neither the ABCB1 3435 C>T nor the ABCB1 2677 G>A/T SNP was associated with altered plasma concentrations of irinotecan and/or its metabolites. The latter mutation leads to the replacement of Ala to Ser or Thr, but does not appear to result directly in an altered expression of P-glycoprotein (42, 43).

Recent investigations indicated that the metabolism of irinotecan is substantially influenced by a nucleotide polymorphism in the TATA-box sequences of UGT1A1. This gene encodes the enzyme UGT1A1 that is responsible for the glucuronidation of several compounds, including SN-38 (17). An extra (7th) TA-repeat [$A(TA)_7TAA$] in one allele results in approximately 70% reduction in transcriptional activity compared with wild type UGT1A1 [$A(TA)_6TAA$]. Inheritance of the promotor containing [$A(TA)_7TAA$] is one of the most common genotypes leading to Gilbert's syndrome (44), which is characterized by mild nonhemolytic, unconjugated bilirubinemia. Genetic abnormalities in UGT1A1 are also associated with the Crigler-Najjar hepatic syndromes with absent (type-I) or reduced (type-II) UGT1A1 activity (45, 46). As such patients cannot metabolize SN-38 adequately, they might be at increased risk for severe drug-related toxicities. Indeed, it has been suggested that screening for UGT1A1*28 prior to treatment might identify patients with lower SN-38 glucuronidation rates and greater susceptibility to irinotecan-induced hematological and non-hematological toxicities (39, 47, 48). Unfortunately, these results could not be confirmed in our study, although the study-settings were comparable. One reason for this discrepancy may be found in the allele-frequency of the variant allele in our population that was clearly lower than mentioned in literature for a normal Caucasian population (38). However, although differences in our study among genotypes were not statistically significant, an overall trend in reduced SN-38 glucuronidation rate (ie, REG) in homozygous variants of UGT1A1*28 could be observed (Table 6), particularly in the median values, both with pharmacokinetic data based on noncompartmental analysis or those based on the NONMEM population model. Furthermore, it is particularly noteworthy that one of the two patients with the variant allele in our study with data for REG was the only individual that experienced grade 4 diarrhea in the entire cohort. Clearly, further investigation is required to unambiguously define the association between genetic variation in UGT1A1 and irinotecan pharmacokinetics and pharmacodynamics.

Novel SNPs in ABCC1, ABCG2, CES1 and CES2 were identified and evaluated in this patient set. Due to the rapid expansion of SNP discovery and the present lack of overlap amongst the various SNP databases, it is possible that further functional polymorphisms in these genes are still to be described (31). Recent data also suggest that molecular determinants of SN-38 glucuronidation and irinotecan response might include common allelic variants of the hepatic UGT1A9 isozyme (49, 50). Consideration of these polymorphisms may eventually provide further refinement of the predictive strategies for irinotecan.

One might seriously question if our current findings already provide meaningful

tools for medical decision making in clinical practice. It is probably too simplistic to think that the complex metabolism of irinotecan can be predicted by screening for one or even a small number of genetic variants. Because every individual represents a combination of drug-metabolizer and transporter phenotypes, and given the large number of enzymes involved in irinotecan metabolism, it is apparent that some individuals are destined to have unusual reactions to this agent due to the coincidental occurrence of multiple genetic defects. Furthermore, it has been shown before that various physiologic and environmental factors are also involved in the way patients react to the irinotecan therapy (4). Besides the condition of the patient and measures of hepatic dysfunction, the role of co-medication and dietary supplements should not be underestimated. For example, sedatives, antiepileptic drugs and some corticosteroids, which are very commonly used among patients on chemotherapy treatment, can induce UGT1A1 (51, 52) and CYP3A4 activity (53, 54). In addition, co-administration of a wide variety of agents (eg, ketoconazole) can result in competitive inhibition of CYP3A4 activity (6), while recommended levels of the natural product St. John's wort significantly induce the activity of this enzyme (55), resulting in altered SN-38 concentrations in plasma (7). Therefore, the next step in predicting the pharmacokinetic and pharmacodynamic outcome of therapy would be by focusing on phenotyping strategies, as these combine both physiologic, environmental and genetic factors. Hopefully, these procedures will eventually lead toward individualized dosing of this drug. Trials implementing a strategy to phenotype total CYP3A4 expression by using the erythromycin-breath test and/or midazolam clearance as surrogate markers of hepatic activity prior to treatment with irinotecan are currently ongoing at our institute.

In conclusion, individuals homozygous for the T allele of ABCB1 1236 C>T appear to have altered irinotecan plasma concentrations in comparison with heterozygous and wild-type patients. Although this polymorphism does not completely explain the differences in irinotecan pharmacokinetics between patients, it may be of relevance in our aim to achieve individualized treatment strategies with this agent. Further investigation is required to confirm these findings in a larger population, and to assess relationships between irinotecan disposition and the rare variant genotypes, especially in other ethnic groups.

REFERENCES

1. Vanhoefer U, Harstrick A, Achterrath W, Cao S, Seeber S, Rustum YM. Irinotecan in the treatment of colorectal cancer: clinical overview. J Clin Oncol 19: 1501-1508, 2001
2. Saltz LB, Cox JV, Blanke C, et al. Irinotecan plus fluorouracil and leucovorin for metastatic colorectal cancer. Irinotecan Study Group. N Engl J Med 343: 905-914, 2000

3. Cunningham D, Falk S, Jackson D. Clinical and economic benefits of irinotecan in combination with 5-fluorouracil and folinic acid as first line treatment of metastatic colorectal cancer. Br J Cancer 86: 1677-1683, 2002
4. Mathijssen RHJ, van Alphen RJ, Verweij J, Loos WJ, Nooter K, Stoter G, Sparreboom A. Clinical pharmacokinetics and metabolism of irinotecan (CPT-11). Clin Cancer Res 7: 2182-2194, 2001
5. Garcia-Carbonero R, Supko JG. Current perspectives on the clinical experience, pharmacology, and continued development of the camptothecins. Clin Cancer Res 8: 641-661, 2002
6. Kehrer DFS, Mathijssen RHJ, Verweij J, de Bruijn P, Sparreboom A. Modulation of irinotecan metabolism by ketoconazole. J Clin Oncol 20: 3122-3129, 2002
7. Mathijssen RHJ, Verweij J, de Bruijn P, Loos WJ, Sparreboom A. Effects of St. John's wort on irinotecan metabolism. J Natl Cancer Inst: 94: 1247-1249, 2002
8. Van Groeningen CJ, van der Vijgh WJ, Baars JJ, Stieltjes H, Huibregtse K, Pinedo HM. Altered pharmacokinetics and metabolism of CPT-11 in liver dysfunction: a need for guidelines. Clin Cancer Res 6: 1342-1346, 2000
9. O'Reilly EM, Stuart KE, Sanz-Altamira PM, et al. A phase II study of irinotecan in patients with advanced hepatocellular carcinoma. Cancer 91: 101-105, 2001
10. Stemmler J, Weise A, Hacker U, Heinemann V, Schalhorn A. Weekly irinotecan in a patient with metastatic colorectal cancer on hemodialysis due to chronic renal failure. Onkologie 25: 60-63, 2002
11. Ong SY, Clarke SJ, Bishop J, Dodds HM, Rivory LP. Toxicity of irinotecan (CPT-11) and hepato-renal dysfunction. Anticancer Drugs 12: 619-625, 2001
12. McLeod HL, Evans WE. Pharmacogenomics: unlocking the human genome for better drug therapy. Annu Rev Pharmacol Toxicol 41: 101-121, 2001
13. Danesi R, De Braud F, Fogli S, Di Paolo A, Del Tacca M. Pharmacogenetic determinants of anti-cancer drug activity and toxicity. Trends Pharmacol Sci 22: 420-426, 2001
14. Relling MV, Dervieux T. Pharmacogenetics and cancer therapy. Nature Rev Cancer 1: 99-108, 2001
15. Innocenti F, Ratain MJ. Update on pharmacogenetics in cancer chemotherapy. Eur J Cancer 38: 639-644, 2002
16. Bencharit S, Morton CL, Howard-Williams EL, Danks MK, Potter PM, Redinbo MR. Structural insights into CPT-11 activation by mammalian carboxylesterases. Nat Struct Biol 9: 337-342, 2002
17. Hanioka N, Ozawa S, Jinno H, Ando M, Saito Y, Sawada J. Human liver UDP-glucuronosyltransferase isoforms involved in the glucuronidation of 7-ethyl-10-hydroxycamptothecin. Xenobiotica 31: 687-699, 2001
18. Santos A, Zanetta S, Cresteil T, et al. Metabolism of irinotecan (CPT-11) by CYP3A4 and CYP3A5 in humans. Clin Cancer Res 6: 2012-2020, 2000
19. Rivory LP, Riou JF, Haaz MC, et al. Identification and properties of a major plasma metabolite of irinotecan (CPT-11) isolated from the plasma of patients. Cancer Res 56: 3689-3694, 1996
20. Sugiyama Y, Kato Y, Chu X. Multiplicity of biliary excretion mechanisms for the camptothecin derivative irinotecan (CPT-11), its metabolite SN-38, and its glucuronide: role of canalicular multispecific organic anion transporter and P-glycoprotein. Cancer Chemother Pharmacol 42 Suppl: S44-S49, 1998
21. Iyer L, Ramirez J, Shepard DR, Bingham CM, Hossfeld DK, Ratain MJ, Mayer U. Biliary

transport of irinotecan and metabolites in normal and P-glycoprotein-deficient mice. Cancer Chemother Pharmacol 49: 336-341, 2002

22. Chen ZS, Furukawa T, Sumizawa T, Ono K, Ueda K, Seto K, Akiyama SI. ATP-Dependent efflux of CPT-11 and SN-38 by the multidrug resistance protein (MRP) and its inhibition by PAK-104P. Mol Pharmacol 55: 921-928, 1999
23. Chu XY, Kato Y, Niinuma K, Sudo KI, Hakusui H, Sugiyama Y. Multispecific organic anion transporter is responsible for the biliary excretion of the camptothecin derivative irinotecan and its metabolites in rats. J Pharmacol Exp Ther 281: 304-314, 1997
24. Nakatomi K, Yoshikawa M, Oka M, et al. Transport of 7-ethyl-10-hydroxycamptothecin (SN-38) by breast cancer resistance protein ABCG2 in human lung cancer cells. Biochem Biophys Res Commun 288: 827-832, 2001
25. De Jonge MJA, Sparreboom A, Planting AST, et al. Phase I study of 3-week schedule of irinotecan combined with cisplatin in patients with advanced solid tumors. J Clin Oncol 18: 187-194, 2000
26. Sparreboom A, de Jonge MJA, de Bruijn P, et al. Irinotecan (CPT-11) metabolism and disposition in cancer patients. Clin Cancer Res 4: 2747-2754, 1998
27. De Bruijn P, Verweij J, Loos WJ, Nooter K, Stoter G, Sparreboom A. Determination of irinotecan (CPT-11) and its active metabolite SN-38 in human plasma by reversed-phase high-performance liquid chromatography with fluorescence detection. J Chromatogr B Biomed Sci Appl 698: 277-285, 1997
28. De Bruijn P, de Jonge MJA, Verweij J, Loos WJ, Nooter K, Stoter G, Sparreboom A. Femtomole quantitation of 7-ethyl-10-hydroxycamptothecin (SN-38) in plasma samples by reversed-phase high performance liquid chromatography. Anal Biochem 269: 174-178, 1999
29. Xie R, Mathijssen RHJ, Sparreboom A, Verweij J, Karlsson MO. Clinical pharmacokinetics of irinotecan (CPT-11) and its metabolites: a population analysis. J Clin Oncol 20: 3293-3301, 2002
30. Rivory LP, Haaz MC, Canal P, Lokiec F, Armand JP, Robert J. Pharmacokinetic interrelationships of irinotecan (CPT-11) and its three major plasma metabolites in patients enrolled in phase I/II trials. Clin Cancer Res 3:1261-1266, 1997
31. Marsh S, Kwok P, McLeod HL. SNP databases and pharmacogenetics: great start but a long way to go. Hum Mutat: in press
32. Ameyaw MM, Regateiro F, Li T, et al. MDR1 pharmacogenetics: frequency of the C3435T mutation in exon 26 is significantly influenced by ethnicity. Pharmacogenetics 11: 217-221, 2001
33. Monaghan G, Ryan M, Seddon R, Hume R, Burchell B. Genetic variation in bilirubin UDP-glucuronosyltransferase gene promoter and Gilbert's syndrome. Lancet 347: 578-581, 1996
34. Ronaghi M. Pyrosequencing sheds light on DNA sequencing. Genome Res 11: 3-11, 2001
35. Sham PC, Curtis D. Monte Carlo tests for associations between disease and alleles at highly polymorphic loci. Ann Hum Genet 59: 97-105, 1995
36. Park SY, Lam W, Cheng YC. X-ray repair cross-complementing gene 1 protein plays an important role in camptothecin resistance. Cancer Res 62: 459-465, 2002
37. Kim RB, Leake BF, Choo EF, et al. Identification of functionally variant MDR1 alleles among European Americans and African Americans. Clin Pharmacol Ther 70: 189-199, 2001
38. Bosma PJ, Chowdhury JR, Bakker C, Gantla S, Boer A, Oostra BA. The genetic basis of the reduced expression of bilirubin UDP-glucuronosyltransferase 1 in Gilbert's syndrome. N Engl J Med 333: 1171-1175, 1995
39. Iyer L, Das S, Janisch L, et al. UGT1A1*28 polymorphism as a determinant of irinotecan

disposition and toxicity. Pharmacogenomics J 2: 43-47, 2002

40. Hoffmeyer S, Burk O, von Richter O, et al. Functional polymorphisms of the human multidrug-resistance gene: Multiple sequence variations and correlation of one allele with P-glycoprotein expression and activity *in vivo*. PNAS 97: 3473-3478, 2000
41. Fellay J, Marzolini C, Meaden ER, et al. Response to antiretroviral treatment in HIV-1-infected individuals with allelic variants of the multidrug resistance transporter 1: a pharmacogenetics study. Lancet 359: 30-36, 2002
42. Cascorbi I, Gerloff T, Johne A, et al. Frequency of single nucleotide polymorphisms in the P-glycoprotein drug transporter *MDR1* gene in white subjects. Clin Pharmacol Ther 69: 169-174, 2001
43. Mickley LA, Lee JS, Weng Z, et al. Genetic polymorphisms in MDR-1: a tool for examining allelic expression in normal cells, unselected and drug-selected cell lines and human tumors. Blood 91: 1749-1756, 1998
44. Kadakol A, Ghosh SS, Sappal BS, Sharma G, Chowdhury JR, Chowdhury NR. Genetic lesions of bilirubin uridine-diphosphoglucuronate glucuronosyltransferase (UGT1A1) causing Crigler-Najjar and Gilbert syndromes: correlation of genotype to phenotype. Hum Mutat 16: 297-306, 2000
45. Crigler JF Jr, Najjar VA. Congenital familial nonhemolytic jaundice with kernicterus. Pediatrics 10: 169-180, 1952
46. Sampietro M, Iolascon A. Molecular pathology of Crigler-Najjar type I and II and Gilbert's syndromes. Haematologica 84: 150-157, 1999
47. Ando Y, Saka H, Ando M, et al. Polymorphisms of UDP-glucuronosyltransferase gene and irinotecan toxicity: a pharmacogenetic analysis. Cancer Res 60: 6921-6926, 2000
48. Ando Y, Ueoka H, Sugiyama T, Ichiki M, Shimokata K, Hasegawa Y. Polymorphisms of UDP-glucuronosyltransferase and pharmacokinetics of irinotecan. Ther Drug Monit 24: 111-116, 2002
49. Tukey RH, Strassburg CP, Mackenzie PI. Pharmacogenomics of human UDP-glucuronosyltransferases and irinotecan toxicity. Mol Pharmacol 62: 446-450, 2002
50. Gagné J-F, Montminy V, Belanger P, Journault K, Gaucher G, Guillemette C. Common human *UGT1A* polymorphisms and the altered metabolism of irinotecan active metabolite 7-ethyl-10-hydroxycamptothecin (SN-38). Mol Pharmacol 62: 608-617, 2002
51. Gupta E, Wang X, Ramirez J, Ratain MJ. Modulation of glucuronidation of SN-38, the active metabolite of irinotecan, by valproic acid and phenobarbital. Cancer Chemother Pharmacol 39: 440-444, 1997
52. Ritter JK, Kessler FK, Thompson MT, Grove AD, Auyeung DJ, Fisher RA. Expression and inducibility of the human bilirubin UDP-glucuronosyltransferase UGT1A1 in liver and cultured primary hepatocytes: evidence for both genetic and environmental influences. Hepatology 30: 476-484, 1999
53. Friedman HS, Petros WP, Friedman AH, et al. Irinotecan therapy in adults with recurrent or progressive malignant glioma. J Clin Oncol 17: 1516-1525, 1999
54. Mc Cune JS, Hawke RL, LeCluyse EL, et al. In vivo and in vitro induction of human cytochrome P4503A4 by dexamethasone. Clin Pharmacol Ther 68: 356-366, 2000
55. Roby CA, Anderson GD, Kantor E, Dryer DA, Burstein AH. St John's Wort: effect on CYP3A4 activity. Clin Pharmacol Ther 67: 451-457, 2000

ACKNOWLEDGEMENTS

We would like to thank Christine Rose, Christi Ralph, Ranjeet Ahluwalia (St. Louis, MO), Peter de Bruijn and Wilfried Graveland (Rotterdam, the Netherlands) for their expert assistance.

Chapter Eleven

Discussion, Summary, and Future Perspectives

Although irinotecan has recently been registered for the first-line chemotherapeutic treatment of colorectal cancer, the unpredictability of serious side effects (neutropenia and diarrhea) remains a concern for many oncologists. In this thesis, we further elucidated the complex pharmacokinetic profile of the drug, which should lead to an improvement of the predictability of irinotecan tolerability.

In **chapter 2**, we review the (pre-) clinical research that has been done into the pharmacokinetics and metabolism of irinotecan, up to the year 2001. The drug's two most important routes of elimination have been described; i.e. the carboxylesterase-mediated pathway and the cytochrome P450-mediated route. This includes the involvement of many phase I and II enzymes and drug transporting proteins (like P-glycoprotein and the canalicular multispecific organic anion transporter; cMOAT).

Common pharmacokinetic parameters such as the plasma disposition, protein binding, and excretion have been discussed for irinotecan and its metabolites, along with several schedules and routes of administration of irinotecan. It was difficult to provide unequivocal pharmacokinetic-pharmacodynamic relationships, as the findings of such studies varied highly.

The last decade, irinotecan has been combined with several other anticancer drugs, in view of additive or synergistic antitumor effects in preclinical models. Here, we also reviewed combinations with platinum-analogs, taxanes and other agents.

One of the best pharmacokinetic parameters to decribe the exposure to a drug is the "area under the plasma concentration-time curve" (AUC). Unfortunately, up to now, 17 to 20 plasma samples were required to adequately calculate this parameter. In **chapter 3**, we developed limited sampling models, to predict the AUC out of only 3 samples (taken at 30min, 1h40min and 5h30min after the start of infusion). Univariate and multivariate regression analyses were employed to generate these models, using data from 24 patients. In another 24 patients, these models for both irinotecan and SN-38, and each total and lactone form, were validated. It was demonstrated that all the AUCs could be predicted sufficiently unbiased and precise. The implication of these models in clinical practice may enable PK sampling in an outpatient setting or in multi-institutional trials. Also, this procedure is more cost-effective for the hospital and convenient for patient, nurse and technician.

In **chapter 4**, irinotecan and SN-38 (both total and lactone forms), SN-38 glucuronide, APC, and NPC data of 70 patients were used to perform a population-analysis for this drug. The built mathematical models adequately describe the disposition characteristics of the drug. Generally, the compartmental models confirmed the pathways suggested from a traditional pharmacologic scope.

Meanwhile, these data refine our understanding of the clinical pharmacokinetics of the drug, like an assumed preferential formation of SN-38 and NPC out of the lactone form of irinotecan.

These models may be used to predict the most important pharmacokinetic parameters (like AUC, clearance, and volume of distribution) from measured plasma concentrations for irinotecan and its metabolites after various administration regimens of irinotecan.

Population pharmacokinetic models, built by the principles described in chapter 4, were used to predict irinotecan pharmacokinetics in 109 patients, which were sampled for irinotecan kinetics during one or two courses. In **chapter 5**, these pharmacokinetic outcomes were correlated with irinotecan's main toxicity, diarrhea. For the first time, a significant relationship between the AUCs of both irinotecan and SN-38 glucuronide and the grade of diarrhea could be described. Presumably, local re-activation of excreted SN-38 glucuronide into SN-38 by bacterial β-glucuronidases may be an explanation for this finding.

Recently, it was observed that SN-38 circulates for a longer period of time in the human body then previously thought. Hence, blood sampling based on a short time period (56 hours) can underestimate the SN-38 AUC substantially, and sampling up to 500 hours (3 weeks) was advised. In **chapter 6**, we studied the clinical relevance of this prolonged exposure. We found that the SN-38 concentrations circulating three weeks after an irinotecan infusion, were capable of inhibiting cell growth of several human tumor cell-lines *in vitro*. We also compared the SN-38 pharmacokinetics (based on a 56 hour and a 500 hour sampling time period) with pharmacodynamics. We used the percentage decrease in neutrophil count at nadir as a common pharmacodynamic parameter. Also, we introduced a new pharmacodynamic parameter, which described the decrease in blood-cell count during time. We showed that the pharmacokinetics based on 500 hours of sampling and the new pharmacodynamic parameter had the best pharmacokinetic/pharmacodynamic correlation. New limited sampling models were developed to predict the AUC of SN-38, based on prolonged sampling. This model, in which only 2 timed samples are required, enables to open up historic databases to retrospectively obtain information about SN-38-induced toxicities in patients treated with irinotecan. Currently, this limited sampling model is also applied in a multi-institutional trial.

For most anti-cancer drugs, including irinotecan, a dose is given to the patient which is based on the patient's body-surface area (BSA). Although there is lack of evidence of the clinical relevance of this procedure in adults, it was intended to

reduce the interindividual variability (IIV) in pharmacokinetics and result in less severe toxicities. In **chapter 7**, we studied the effect of BSA (and other body size measures) on the pharmacokinetics of irinotecan and SN-38 in 82 patients. The IIV in the clearance of irinotecan did not alter when the drug was dosed on BSA (IIV = 34.0%) or not (IIV = 32.1%). Also for SN-38, any other adjustment for body-size measures, did not effect pharmacokinetics in univariate and multiple regression analyses. Therefore, there is no rationale to dose irinotecan based on a body-size measure, and it is recommended to conduct a phase III study to prospectively compare BSA-based dosing and fixed dosing of this drug.

Anticancer drugs usually have narrow therapeutic margins. As cytochrome P450 (CYP) 3A4 is involved in the metabolism of irinotecan and this enzyme is susceptible to modulation by co-medication, we studied the effect of a potent CYP3A4 inhibitor on the pharmacokinetics of irinotecan in **chapter 8**. During a randomized, cross-over study, a total of 7 patients received one course of irinotecan (100 mg/m^2) combined with ketoconazole (200 mg orally for 2 days) and another course at the recommended dose of irinotecan (350 mg/m^2) without ketoconazole. With ketoconazole coadministration, the relative formation of APC was reduced with 87%, while the relative exposure to SN-38 increased with 109%. As irinotecan and SN-38 glucuronide concentrations did not change, we concluded that the inhibition of CYP3A4 by ketoconazole leads to a significantly increased formation of SN-38. Physisians should be warned that the simultaneous administration of CYP3A4 inhibitors and irinotecan may potentially result in fatal outcomes. Dosis reductions for irinotecan are indicated in case the patient has to use an effective CYP3A4 inhibitor.

In **chapter 9**, we studied the effect of a potent CYP3A4 inducer. As inhibition of CYP3A4 leads to higher levels of SN-38, we hypothesized that stimulation of this enzyme might do the opposite. St. John's wort (SJW), a very popular herbal product in the treatment of mild to moderate forms of depression, is known for its induction of CYP3A4. In a randomized cross-over setting, 5 patients were treated with irinotecan during 2 courses at a dose of 350 mg/m^2 intravenously. Prior to, during, and 4 days after one of these courses, patients received SJW orally 3 times a day at 300 mg. The AUC of SN-38 decreased by more than 40% as a result of SJW co-treatment, while the exposure to CPT-11 did not change. In addition, in the course following the combination treatment, this effect was still seen in the patients studied. Also, the degree of myelosuppression was substantially milder in the presence of SJW. As circulating levels of SN-38 are thought to be related with antitumor activity, these findings indicate that patients on irinotecan treatment should refrain from taking SJW.

In the chapters 7-9 we reported that BSA did not have an effect on irinotecan pharmacokinetics, and that co-medication did. The next step was to see if genetic differences between patients had an affect. In **chapter 10**, we studied single-nucleotide polymorphisms in irinotecan-metabolizing enzymes and ABC transporters in 65 patients. Subsequently, we compared these polymorphisms, one by one, with the pharmacokinetics of irinotecan and metabolites, using the population pharmacokinetic model described in chapter 4. Patients were genotyped for variants in P-glycoprotein, cMOAT, BCRP, carboxylesterases, cytochrome P450 isozymes and UGT1A1. A significant positive relation was found between the homozygous T-allele of P-glycoprotein and the exposure to irinotecan. Also, a negative trend was seen for the relation between mutants in CYP3A4*3 and irinotecan clearance. In addition, we found a lower glucuronidation in patients carrying an extra TA-repeat in the promotor area of the UGT1A1 gene in both alleles. Further investigation is required to confirm these findings and assess relationships between irinotecan disposition and other variant genotypes. The clinical relevance in other ethic groups remains uncertain.

As shown in this thesis, many factors are involved in irinotecan metabolism. Dose individualization for this drug should focus on strategies which combine both environmental influences and genetic factors. Currently, a phenotyping procedure for this drug is ongoing at the Erasmus MC – Daniel den Hoed. In this study, patients receive two noninvasive test-compounds; erythromycin and midazolam (also called "probes"), for the estimation of CYP3A4 activity in that specific individual at a specific moment in time. When this activity can be correlated with the pharmacokinetics of irinotecan, future patients can undergo these probe-tests to predict to which extent irinotecan will be metabolized in that individual, and thus can be dosed individually.

Finally, all important factors which influence and/or predict the PK of irinotecan (like co-medication, organ (dys-) function, patient's condition, clinically relevant genetic polymorphisms, and maybe even a body-size measure in extreme cases) should be taken into account in a formula with the aim to predict the PK of this drug with high reliability. Despite all our efforts, this probably cannot be achieved at this moment. But maybe in a near future, when most missing links in this puzzle are found, patients can be dosed more optimally, with positive effects for the antitumor activity.

Samenvatting en Conclusies

(Nederlandse versie voor niet ingewijden)

Het geneesmiddel irinotecan (ook wel CPT-11 genoemd) heeft het laatste decennium bewezen bij de meest actieve middelen tegen veel vormen van kanker te behoren. Het wordt momenteel als eerste keus medicament beschouwd bij de behandeling van niet-operabele dikke darm kanker. Helaas is het zeer lastig om de werking ervan bij een individuele patiënt te voorspellen. Sommige mensen reageren gunstig op de therapie, terwijl anderen er geen of nauwelijks baat bij hebben. Hetzelfde geldt voor de bijwerkingen van deze therapie (zoals diarree en een daling van de witte bloedcellen); sommige mensen hebben vrijwel geen klachten, terwijl bij anderen de bijwerkingen levensbedreigend kunnen zijn. In dit proefschrift hebben we belangrijke factoren, welke betrokken zijn bij de variatie in werking en bijwerkingen tussen patiënten, bestudeerd.

Nadat het geneesmiddel door middel van een infuus in de bloedbaan wordt gebracht, zal het zich door het lichaam verdelen. Zo kan het middel bij de tumor komen, maar ook bij gezonde weefsels, waardoor bijwerkingen optreden. Onder andere in de lever wordt irinotecan met behulp van zogenaamde "enzymen" deels omgezet in afbraakprodukten (metabolieten). Deze omzettings-produkten kunnen via de darmen en de nieren het lichaam verlaten. De beschrijving van de processen zoals verdeling door het lichaam, omzettingen en uitscheiding noemen we (farmaco-) kinetiek.

Na een inleiding (**hoofdstuk 1**) alwaar in het kort de historische ontwikkeling en het werkingsmechanisme van irinotecan wordt beschreven, volgt in **hoofdstuk 2** een overzicht van de belangrijkste farmacokinetische processen (voor zover nu bekend), betrokken bij het irinotecan metabolisme. Niet irinotecan zelf, maar één van de afbraakprodukten hiervan (genaamd SN-38) is actief tegen kanker. Alle andere gevormde metabolieten zijn niet actief, waardoor onze aandacht zich vooral richt op de kinetiek van SN-38.

Een van de meest gebruikte en belangrijkste farmacokinetische functies is de zogenaamde AUC. Met de AUC geven we de blootstelling (concentratie) van een medicijn gedurende de tijd weer. Aangezien de concentraties in het bloed voortdurend veranderen als gevolg van verdeling, afbraak en uitscheiding van irinotecan, moesten tot op heden vele bloedmonsters worden afgenomen om de AUCs van irinotecan en SN-38 goed te kunnen berekenen. In **hoofstuk 3** wordt beschreven hoe het met behulp van speciaal ontwikkelde wiskundige modellen mogelijk wordt om met slechts 3 bloedmonsters toch nauwkeurig een AUC te kunnen bepalen. Dit schept vele voordelen. Voor de patiënt wordt deelname aan een studie

met farmacokinetiek iets minder onplezierig, aangezien minder vaak geprikt hoeft te worden. Ook hoeft deze niet meer opgenomen te worden, maar kan poliklinisch behandeld worden. Voor verpleegkundige en analist betekent dit aanzienlijk minder werk, waardoor ook de werkdruk en de kosten kunnen afnemen.

De ontwikkeling en het gebruik van modellen hebben we doorgetrokken in **hoofdstukken 4 en 5**. Omdat patiënten (zoals eerder beschreven) zeer gevarieerd op de therapie met irinotecan reageren en het tot op heden zeer moeizaam lukte een verband met werking en bijwerkingen te leggen, bestond de behoefte aan een geheel nieuwe aanpak van dit probleem. Alle kinetiek gegevens van 70 patiënten, behandeld met irinotecan, werden verzameld. In samenwerking met wiskundigen van de universiteit van Uppsala (Zweden) werden zogenaamde populatie-modellen voor irinotecan en metabolieten ontwikkeld, zoals beschreven in het vierde hoofdstuk. Deze modellen geven vanuit een alternatieve benadering (namelijk met behulp van wiskundige patronen, in plaats van het medische gedachtengoed) weer hoe het metabolisme van dit medicijn plaatsvindt in een grote groep mensen (populatie). In het vijfde hoofdstuk worden deze modellen toegepast en wordt een sterke relatie gelegd tussen een eerder nauwelijks relevant geacht afbraakprodukt van irinotecan, genaamd SN-38G, en het voorkomen van diarree bij patiënten.

Inmiddels is bekend geworden dat SN-38 langer in de bloedbaan van de patiënt verblijft dan eerder werd aangenomen. Wat de klinische relevantie hiervan is wordt weergegeven in **hoofdstuk 6**. Verschillende cellijnen (dit zijn gekweekte kankercellen) werden in het laboratorium blootgesteld aan SN-38 gedurende een periode van 3 weken. Zelfs bij een continue blootstelling aan zeer lage concentraties SN-38 (welke in de bloedbaan van een gemiddelde patiënt circuleren na 3 weken), blijken kankercellen nog steeds gevoelig te zijn voor deze metaboliet. Oftewel, indien deze experimenten met gekweekte cellen representatief zijn voor een gezwel bij de patiënt, werkt SN-38 maar liefst 3 weken lang! Mogelijk is dit een verklaring waarom irinotecan zo effectief is in tegenstelling tot veel andere anti-kanker middelen welke veel kortdurender, of alleen bij hogere concentraties, werkzaam zijn.

Van oudsher bestaat de gedachte dat grotere mensen een hogere dosis chemotherapie kunnen verdragen dan kleinere mensen. Dit zou dan kunnen komen omdat grotere mensen sneller het medicijn kunnen afbreken en uitscheiden dan kleinere mensen. In medische termen noemen we dit het "klaren" van het medicament. Door te doseren op het lichaamsoppervlakte van de patiënt (welke wordt berekenend uit diens lengte en gewicht) zou een ieder een gepaste en veilige dosis toegediend krijgen. De aanbevolen dosis van irinotecan wordt tot op heden ook op deze wijze weergegeven; deze is namelijk gesteld op 350 mg/m^2 per 3 weken. Een goed onderbouwd onderzoek naar deze gedachte is echter nooit gedaan! In **hoofdstuk 7** hebben we bestudeerd of het doseren per lichaamsoppervlak bijdraagt

aan het verkleinen van de verschillen in klaring tussen de patiënten. Het bleek dat sommige kleine mensen (dus met een klein lichaamsoppervlak) in staat waren tot een snelle klaring van irinotecan, terwijl anderen dat niet waren. Hetzelfde gold voor grote mensen. De oude gedachte is dus onjuist gebleken en het doseren op lichaamsoppervlak is daarom niet zinvol. Zolang geen betere doseringsstrategieën worden uitgevonden, raden wij een vaste dosering van 600 mg per 3 weken voor iedere patiënt (klein of groot, dik of dun) aan.

Als het lichaamsoppervlak geen rol speelt bij de wijze waarop patiënten op hun irinotecan-chemotherapie reageren, wat zijn dan wel belangrijke factoren? Zoals eerder genoemd wordt irinotecan via enzymen omgezet in metabolieten. De vorming van SN-38 (de actieve metaboliet) is ook afhankelijk van enzymen en deze spelen dus mogelijk een belangrijke rol. Een van de betrokken enzymen wordt CYP3A4 genoemd. Dit enzym blijkt minder goed of juist beter te gaan werken onder invloed van andere medicijnen. In **hoofdstuk 8** hebben we onderzocht wat er gebeurt wanneer irinotecan gecombineerd wordt met ketoconazol. Ketoconazol is een anti-schimmel medicament waarvan bekend is dat het de werking van CYP3A4 kan remmen. Het bleek dat deze combinatie leidde tot een enorme stijging van de actieve metaboliet SN-38. Hiermee is een belangrijk bewijs geleverd dat de activiteit van CYP3A4 een cruciale rol speelt bij het metabolisme van irinotecan. Bovendien dienen we te waarschuwen voor het gedachtenloos combineren van irinotecan met ketoconazol (of andere CYP3A4 remmers), aangezien ernstige bijwerkingen kunnen ontstaan als gevolg van de stijging van SN-38 concentraties.

In **hoofdstuk 9** onderzochten we de combinatie van irinotecan met een zeer veel gebruikt "alternatief" geneesmiddel tegen depressies, genaamd St. Jan's kruid. Uit eerdere studies met St. Jan's kruid, waarin het werd gecombineerd met andere geneesmiddelen werd gevonden dat ook St. Jan's kruid de werking van CYP3A4 kan beïnvloeden. Juist vanwege het grote gebruik van St. Jan's kruid onder kanker-patiënten zagen we het hierdoor als een noodzaak om de combinatie van het kruid met irinotecan te onderzoeken. Uit onze resultaten bleek dat de concentraties van SN-38 in het bloed met meer dan 42% daalden, wanneer deze twee middelen gecombineerd werden. Bovendien houdt het effect een behoorlijke tijd aan; zelfs 3 weken na het stoppen van St. Jan's kruid. Mensen dienen dus gewaarschuwd te worden voor de combinatie van dit "natuurlijke" (en zonder recept verkrijgbare) middel en dit anti-kanker middel, want de therapie wordt mogelijk geïnactiveerd door het gebruik van St. Jan's kruid.

De werking van enzymen wordt niet alleen bepaald door co-medicatie, maar kan ook het gevolg zijn van genetische aanleg. Bij een grote groep patiënten namen we genetisch materiaal (DNA) af om relevante genetische afwijkingen (variaties of polymorfismen genoemd) aan te tonen en deze te relateren aan hun irinotecan-

kinetiek (**hoofdstuk 10**). Er bleken enkele goede relaties te zijn tussen bepaalde genetische variaties en het irinotecan-metabolisme. Een voorbeeld hiervan is het enzym UGT1A1, wat betrokken is bij de afbraak van SN-38. Wanneer een afwijking in het genetisch materiaal behorende bij dit enzym bestaat, werkt het enzym minder goed. Hierdoor wordt SN-38 slechter afgebroken, waardoor hogere concentraties SN-38 in het bloed komen. Nog dramatischer zou het zijn wanneer dit enzym totaal niet meer werkt, waardoor SN-38 haast niet meer omgezet zou kunnen worden en dit tot zeer ernstige bijwerkingen kan leiden.

Uit de laatste 3 hoofdstukken leerden we dat CYP3A4-beïnvloedende co-medicatie en genetische aanleg een belangrijkere invloed kunnen hebben op de irinotecan-kinetiek. Momenteel voeren we een studie in het Erasmus MC uit, waarbij we al voor het toedienen van de chemotherapie de werking van CYP3A4 in een individuele patiënt te weten proberen te komen. Daarbij dienen we de patiënt een onschuldig middel toe dat, net als irinotecan, via CYP3A4 wordt omgezet. Wanneer er een goed verband blijkt te bestaan tussen de kinetiek van dit onschuldige middel en de kinetiek van irinotecan, kunnen we in de toekomst het onschuldige middel als een soort "test" geven om te zien hoe de patiënt op de irinotecan-chemotherapie zal gaan reageren. Op deze wijze houden we rekening met zowel de co-medicatie als de genetische aanleg van die individuele patiënt en wordt de kinetiek, en daarmee de mogelijkheid van ongewenste neveneffecten, beter voorspelbaar.

Met hoofdstuk 10 zijn we aanbeland in een nieuw tijdvak, waarbij het belang van de genetische achtergrond van een individu steeds centraler wordt. Ook de titel van dit proefschrift, "Van klinische farmacokinetiek naar farmacogenetica", refereert hier aan. Waarschijnlijk zullen in de toekomst steeds meer rechtstreekse verbanden tussen genetische variaties en kinetiek worden gevonden en mogelijk kan ook een direct verband met anti-kanker werking worden aangetoond. Door rekening te houden met de genetische basis van een patiënt en belangrijke co-factoren kan gezocht worden naar een individuele en optimale doserings-strategie van het meest ideale medicament. Een optimist ziet de voordelen voor de toekomstige patiënt.

List of co-authors

R.J. van Alphen, MD (Robbert)
Resident in Internal Medicine
Department of Internal Medicine
M.C.R.Z.-Clara
Rotterdam, the Netherlands

S.D. Baker, PharmD (Sharyn)
Assistent Professor of Oncology
Division of Experimental Therapeutics
The SKCCC at Johns Hopkins
Baltimore, MD, USA

P. de Bruijn, BSc (Peter)
Technician
Department of Medical Oncology
Erasmus MC-Daniel den Hoed
Rotterdam, the Netherlands

M.J.A. de Jonge, MD, PhD (Maja)
Medical Oncologist
Department of Medical Oncology
Erasmus MC-Daniel den Hoed
Rotterdam, the Netherlands

M.O. Karlsson, PhD (Mats)
Professor of Pharmacometrics
Department of Pharm. Biosciences
Uppsala University
Uppsala, Sweden

D.F.S. Kehrer, MD, PhD (Diederik)
Medical Oncologist
Department of Internal Medicine
IJsselland Hospital
Capelle a/d IJssel, the Netherlands

W.J. Loos, PhD (Walter)
Scientist
Department of Medical Oncology
Erasmus MC-Daniel den Hoed
Rotterdam, the Netherlands

S. Marsh, PhD (Sharon)
Research Associate
Division of Molecular Oncology
Washington Univ. School of Medicine
St. Louis, MO, USA

H.L. McLeod, PharmD (Howard)
Associate Professor of Medicine
Division of Molecular Oncology
Washington Univ. School of Medicine
St. Louis, MO, USA

K. Nooter, PhD (Kees)
Head, Laboratory of Drug Resistance
Department of Medical Oncology
Erasmus MC-J.N.I.
Rotterdam, the Netherlands

A. Sparreboom, PhD (Alex)
Head, Laboratory of Pharmacology
Department of Medical Oncology
Erasmus MC-Daniel den Hoed
Rotterdam, the Netherlands

G. Stoter, MD, PhD (Gerrit)
Professor of Medical Oncology
Head, Dept. of Medical Oncology
Erasmus MC-Daniel den Hoed
Rotterdam, the Netherlands

J. Verweij, MD, PhD (Jaap)
Professor of Medical Oncology
Head, Div. of Experim. Chemotherapy
Erasmus MC-Daniel den Hoed
Rotterdam, the Netherlands

R. Xie, PhD (Rujia)
Senior Clinical Pharmacology Scientist
Clinical Pharmacology Unit
Pharmacia Singapore
Singapore

Curriculum Vitae

De auteur van dit proefschrift werd op 9 augustus 1974 geboren te Ulvenhout (voormalige gemeente Nieuw-Ginneken). In 1993 behaalde hij het VWO diploma aan het Onze Lieve Vrouwe Lyceum te Breda, waarna met de studie Biologie aan de Universiteit Utrecht zijn studententijd werd gestart. Een jaar later behaalde Ron zijn propedeuse, maar toch leek hem een carriére in de plantenfysiologie of oecologie niet het meest ideale toekomstbeeld. Vandaar dat in 1994 de overstap naar de studie geneeskunde aan de Erasmus Universiteit te Rotterdam werd gemaakt. In 1998 volgde het doctoraalexamen na een stage van een half jaar in de Rotterdamse Daniel den Hoed kliniek. In het laboratorium voor experimentele chemotherapie en farmacologie van de afdeling interne oncologie (hoofd Prof. dr G. Stoter) werden hem onder de bezielende leiding van dr A. Sparreboom en Prof. dr J. Verweij de kneepjes van het "research"-vak bijgebracht. Na het afronden van de co-schappen in 2000, ging Ron zijn pas behaalde artsexamen in praktijk brengen in het Medisch Centrum Rijnmond-Zuid (MCRZ), locatie Clara, te Rotterdam, bij de afdeling interne geneeskunde (opleider dr A.F. Grootendorst). Echter, de behoefte aan het doen van onderzoek bleef bestaan, waardoor werd gezocht naar een mogelijkheid om klinisch werk te combineren met onderzoek. Via een zogenaamde AGIKO-constructie (welke mogelijk werd gemaakt door Prof. dr H.A.P. Pols, opleider interne geneeskunde aan het Erasmus MC te Rotterdam), kon vorig jaar worden gestart met een promotie-onderzoek waarvan dit proefschrift het resultaat is. In januari 2003 zal hij vervolgens starten met zijn opleiding tot internist in het MCRZ locatie Clara, waarna de opleiding zal worden voortgezet binnen het Erasmus MC. Het zal niemand verbazen dat Ron een voorkeur heeft ontwikkeld voor de oncologie en daarvan zijn interne aandachtsgebied hoopt te kunnen maken.

Publications

1. Sparreboom A, de Jonge MJA, de Bruijn P, Brouwer E, Nooter K, Loos WJ, van Alphen RJ, **Mathijssen RHJ**, Stoter G, Verweij J. Irinotecan (CPT-11) metabolism and disposition in cancer patients. Clin Cancer Res 4: 2747-2754, 1998
2. **Mathijssen RHJ**, van Alphen RJ, de Jonge MJA, Verweij J, de Bruijn P, Loos WJ, Nooter K, Vernillet L, Stoter G, Sparreboom A. Sparse-data set analysis for irinotecan and SN-38 pharmacokinetics in cancer patients co-treated with cisplatin. Anticancer Drugs 10: 9-16, 1999
3. De Jonge MJA, Verweij J, de Bruijn P, Brouwer E, **Mathijssen RHJ**, van Alphen RJ, de Boer-Dennert MM, Vernillet L, Jacques C, Sparreboom A. Pharmacokinetic, metabolic, and pharmacodynamic profiles in a dose-escalating study of irinotecan and cisplatin. J Clin Oncol 18: 195-203, 2000
4. **Mathijssen RHJ**, van Alphen RJ, Verweij J, Loos WJ, Nooter K, Stoter G, Sparreboom A. Clinical pharmacokinetics and metabolism of irinotecan (CPT-11). Clin Cancer Res 7: 2182-2194, 2001
5. **Mathijssen RHJ**, Verweij J, de Jonge MJA, Nooter K, Stoter G, Sparreboom A. Impact of body-size measures on irinotecan clearance: Alternative dosing recommendations. J Clin Oncol 20: 81-87, 2002
6. **Mathijssen RHJ**, Sparreboom A, Dumez H, van Oosterom AT, de Bruijn EA. Altered metabolism of irinotecan (CPT-11) in a patient receiving phenytoin. Anticancer Drugs 13: 139-140, 2002
7. **Mathijssen RHJ**, Loos WJ, Verweij J, Sparreboom A. Pharmacology of topoisomerase I inhibitors irinotecan (CPT-11) and topotecan. Curr Cancer Drug Targets 2: 103-123, 2002
8. **Mathijssen RHJ**, Verweij J, Loos WJ, de Bruijn P, Nooter K, Sparreboom A. Irinotecan pharmacokinetics-pharmacodynamics: the clinical relevance of prolonged exposure to SN-38. Br J Cancer 87: 144-150, 2002
9. Kehrer DFS, **Mathijssen RHJ**, Verweij J, de Bruijn P, Sparreboom A. Modulation of irinotecan metabolism by ketoconazole. J Clin Oncol 20: 3122-3129, 2002

10. Xie R, **Mathijssen RHJ**, Sparreboom A, Verweij J, Karlsson MO. Clinical pharmacokinetics of irinotecan (CPT-11) and its metabolites: population-modeling analysis. J Clin Oncol 20: 3293-3301, 2002
11. **Mathijssen RHJ**, Verweij J, de Bruijn P, Loos WJ, Sparreboom A. Effects of St. John's wort on irinotecan metabolism. J Natl Cancer Inst 94: 1247-1249, 2002
12. Xie R, **Mathijssen RHJ**, Sparreboom A, Verweij J, Karlsson MO. Clinical pharmacokinetics of irinotecan (CPT-11) and its metabolites in relation with diarrhea. Clin Pharmacol Ther 72: 265-275, 2002
13. **Mathijssen RHJ**, Marsh S, Karlsson MO, Xie R, Baker SD, Verweij J, Sparreboom A, McLeod HL. Irinotecan disposition in relation to genetic polymorphisms in ABC transporters and drug-metabolizing enzymes. Submitted

Abstracts and Poster Presentations

1. Xie R, **Mathijssen RHJ**, Sparreboom A, Karlsson MO. Clinical pharmacokinetics of irinotecan (CPT-11) and its metabolites. PAGE #16, 2001
2. Kehrer DFS, **Mathijssen RHJ**, Verweij J, de Bruijn P, Sparreboom A. Inhibition of CYP3A4 during irinotecan (CPT-11) chemotherapy can result in potentially fatal outcomes. Clin Cancer Res #407, 3735S-3736S, 2001
3. **Mathijssen RHJ**, Verweij J, Kehrer DFS, Sparreboom A. Irinotecan (CPT-11) pharmacokinetics-pharmacodynamics: the clinical relevance of prolonged SN-38 circulation. Clin Cancer Res #414, 3737S, 2001
4. Xie R, **Mathijssen RHJ**, Sparreboom A, Karlsson MO. Population pharmacokinetics of CPT-11 and its metabolites SN-38 and SN-38 glucuronide in relation to diarrhea. Am Soc Clin Pharmacol Ther #MPI-92, 2002
5. **Mathijssen RHJ**, Loos WJ, Verweij J, de Bruijn P, Sparreboom A. Differential distribution and red blood cell partitioning of irinotecan (CPT-11) and SN-38 in cancer patients. Proc Am Assoc Cancer Res #1048, 43: 209, 2002
6. **Mathijssen RHJ**, Verweij J, de Bruijn P, de Jonge MJA, Sparreboom A. Modulation of irinotecan (CPT-11) metabolism by St. John's wort in cancer patients. Proc Am Assoc Cancer Res #2443, 43: 492, 2002
7. Sparreboom A, Marsh S, **Mathijssen RHJ**, Verweij J, McLeod HL. Irinotecan (CPT-11) disposition in relation to single-nucleotide polymorphisms (SNPs) of

ABC transporters and drug-metabolizing enzymes. Proc Am Soc Clin Oncol #331, 21: 83a, 2002

8. **Mathijssen RHJ**, Xie R, McLeod HL, Verweij J, Palmer PA, Karlsson MO, Sparreboom A. Pharmacokinetic and pharmacogenetic analysis of irinotecan (CPT-11) given in combination with R115777. EORTC-NCI-AACR #133, 2002

Oral Presentations

1. Modulation of irinotecan (CPT-11) metabolism by St. John's wort in cancer patients. Minisymposium, 93rd Am. Assoc. Cancer Res. Annual Meeting, San Francisco, CA, April 8, 2002

Dankwoord

- In de eerste plaats wil ik mijn moeder danken. Met ongelooflijk veel moed en kracht heb je je ziekte gedragen. Je strijd heeft als een rode draad door de afgelopen twee jaar gelopen en het zal me er elke dag weer aan doen herinneren waarom ik dit werk doe.
- Prof. dr Jaap Verweij en dr Alex Sparreboom; wat heb ik ontzettend veel aan jullie te danken. Misschien een open deur, maar ik respecteer jullie beiden zeer; zowel persoonlijk als wetenschappelijk. Natuurlijk was jullie prettige wijze van werken niet geheel onbekend voor me, maar toch heeft het me nog aangenaam verrast. Jullie hebben werkelijk wetenschappelijk vuur en ik denk dat er een vonk is overgeslagen. Ondanks de soms massale hoeveelheid werk heb ik zeer genoten van mijn promotie-onderzoek. (Ik weet dat dit eigenlijk niet zo hoort te zijn, maar daarvoor houd ik jullie mede verantwoordelijk!) Alex, wat vind ik het jammer dat je naar de States bent gegaan. Ik hoop desondanks dat we de komende jaren nog veel samen kunnen blijven werken; misschien kan ik dan nog eens iets terug doen wat enigszins in verhouding staat tot hetgeen jij voor mij gedaan hebt.
- Prof. dr Gerrit Stoter en Prof. dr Huib Pols. Zonder jullie was deze opleidings-constructie nooit tot stand gekomen. Ik hoop dat ik de komende jaren met net zoveel plezier mijn opleiding tot internist kan voltooien, om daarna in het oude vertrouwde nest tot oncoloog te kunnen worden opgeleid.
- Dr Kees Nooter; bedankt voor al je adviezen bij elke lab-bespreking. En met name bij de GLP-operatie zullen we je hulp nog hard nodig hebben!
- Prof. dr Mats Karlsson, dr Rujia Xie, dr Howard McLeod, dr Sharon Marsh, and dr Sharyn Baker; I am really thankful that I got the chance to work with you. I have learned a lot from you, and hope that our recent collaborations form the basis for new projects.
- Prof. dr Ernst de Bruijn; je zult bij het lezen van dit proefschrift wel één specifiek onderwerp missen. Geen probleem; ik ben het niet vergeten. Er wordt aan gewerkt!
- Ing. Peter de Bruijn; mijn irino-maatje. Het spijt me dat ik je de afgelopen jaren met zoveel meetwerk heb opgezadeld. En dan geduldig op de uitslag wachten; nee, ho maar! Zonder jou had mijn promotie nooit in dit tempo kunnen verlopen.
- Dr Walter Loos. Dankzij jou zal ik secuur op het juiste aantal significante getallen in een tabel blijven letten! Je morele ondersteuning voor de persconferentie en presentatie in San Francisco heeft me ook goed gedaan.

- Ing. Desiree van Boven-van Zomeren; de vrolijke noot van het lab. Het zal duidelijk zijn dat me dat wel aanstaat. Dr Alessandra Felici, mi dispiace per il brutto tempo che hai trovato in Olanda, ma spero che tu sia stata bene qui! Marine Goffinet, je voudrais te remercier pour le travail énorme de saisie informatique que je t'aie demandé de réaliser.
- Dr Maja de Jonge, dank voor alle hulp bij onder andere de protocollen. Voor je adviezen met betrekking tot de ziekte van mijn moeder blijf ik je eeuwig dankbaar. Het betekent meer voor me dan je misschien beseft.
- Alle senior-, junior-internisten en longartsen voor het includeren van patiënten en sowieso voor de gezellige tijd. Dr Diederik Kehrer en dr Hans Gelderblom; dankzij jullie krijgen congressen altijd weer een speciaal cachet.
- Carla Hartman, drs. Agnes Klaren, Leny van Doorn, Miranda Frijters, Hans van der Meulen en Tatjana Pronk. Ik wil jullie danken voor het instrueren van de patiënten en het uitvoeren van al mijn gedachtenkronkels. Met name het organiseren van de fenotyperings-studie moet een ware crime zijn!
- Bimla Sital, je zal heel wat kilometers afgelopen hebben in het kader van de kinetiek. (Dank mij maar, want ik zorg er indirect voor dat je in conditie blijft).
- Afdeling B1 en behandelcentrum: verpleging, secretaressen en patiënten; zonder jullie inzet is het goed uitvoeren van een kinetiek-studie onmogelijk.
- Dr Sjaak Burgers, dr Wim van den Berg, Jan Francke, Trinet Rietveld, drs. Frederike Engels en Dirk Buijs. Ook jullie zijn (zonder het te beseffen) onmisbare schakels geweest in mijn onderzoeken.
- Marijke Westerhout-Kersten en Kerstin van der Veen, hoeveel dagen zullen jullie niet hebben gevuld met het opzoeken en aanvragen van artikelen voor mij?
- Datamanagers; dankzij jullie ordening was het mogelijk om eens wat jaartjes terug in de tijd te gaan voor oude gegevens. Anders zou al deze mooie informatie definitief verloren zijn gegaan.
- Overige commissieleden; ik wil u hartelijk danken voor het plaatsnemen in mijn promotie-commissie.
- Vrienden. Robbert van Alphen; vijf jaar geleden wilde jij naar de Daniel. Pieter ter Borg, je was de eerste uit onze groep die met promotie-onderzoek startte na het arts-examen. Normaal ben ik niet zo volgzaam zoals jullie weten, maar ik ben blij dat ik jullie in deze wel gevolgd ben. Niet meer dan logisch dus, dat ik jullie gevraagd heb paranimf te willen zijn. Ook Iris Waanders, Laura de Jong, Annemarie de Nijs en Bhartie ter Borg-Sewradj; jullie hebben het afgelopen jaar maar weer eens bewezen echte vrienden te zijn.
- Papa, Claudia, Alvarez en familie; zonder een hechte band zou deze tijd ondraaglijk zijn geweest. Samen helpen we elkaar er wel doorheen.